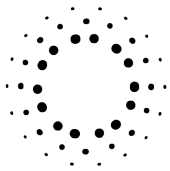

IFT - UNESP
INSTITUTO DE FÍSICA TEÓRICA

M. Sc. Thesis IFT–D.009/22

Modelling Vaccination
In An Ongoing Epidemics of SARS-CoV-2

Leonardo Souto Ferreira

Advisor

Roberto André Kraenkel

Co-Advisor

Renato Mendes Coutinho

August, 2022

Ferreira, Leonardo Souto
F383m Modelling vaccination in an ongoing epidemics of SARS-CoV-2 / Leonardo Souto Ferreira. – São Paulo, 2022
209 f.

Dissertação (mestrado) – Universidade Estadual Paulista (Unesp), Instituto de Física Teórica (IFT), São Paulo
Orientador: Roberto André Kraenkel
Coorientador: Renato Mendes Coutinho

1. COVID-19 (Doença). 2. Vacinação. 3. Modelos matemáticos. I. Título

Sistema de geração automática de fichas catalográficas da Unesp. Biblioteca do Instituto de Física Teórica (IFT), São Paulo. Dados fornecidos pelo autor(a).

Dedico esta dissertação à memória de
meu avô, Oswaldo,
minha avó, Celi,
e a minha família

Agradecimentos

Agradeço a meus pais, André e Anabela, minhas irmãs, Marina e Luiza, e minha namorada, Satyabhama, pelo apoio emocional e financeiro nesses tempos sombrios.

Agradeço a meus orientadores, Roberto e Renato, e aos meus colegas de grupo, Carol, Otavio, Rafael, Silas, Vítor e Tatiana, pelas sempre interessantes discussões e ideias mirabolantes.

Agradeço a meus amigos Adolfo, Anthony, Alisson, Barbosa, Sanson, Chico, Café, Diogo, Franck, Greg, Gauche, Gabriel, Hamilton, Heloíse, Helcinho, Igor, Ibarra, Juarez, Jung, João Böger, João Pering, Kevin, Krick, Kill, Muryel, Portilho, Rômulo, Tirelli, Thiago, Tadeu, Valéria e Zé, por ajudarem a manter a minha (in)sanidade mental nestes tempos de pandemia.

Agradeço ao "Anarchic College", Flavinha, Marcelo Borges, Marcelo Gomes, Paulo Inácio, Oswaldo e Leo Bastos, por todo o aprendizado que me propiciaram durante nossas conversas da madrugada.

Agradeço ao Observatório COVID-19, em especial a Maria Amélia, Flávia Ferrari, Verônica, Juliano e Márcia Castro, por me mostrarem o valor da interdisciplinaridade.

Agradeço ao grupo de modelagem da COVID-19 no Brasil, em especial aos professores Cristiana, Ricardo, Suzi e José Alexandre, por orientarem e ensinarem a conversar com tomadores de decisão na saúde pública do Brasil, e aos colegas Gabriel Berg e Gabriel Müller, pelas frutíferas colaborações nos trabalhos desenvolvidos.

Por fim, agradeço à CAPES, por fornecer uma bolsa de Mestrado que me permitiu trabalhar sem me preocupar com renda, ao CoMo consortium, por financiar o custo de publicação de um dos trabalhos, e ao CNPq, por financiar o projeto "Modelagem da Dinâmica de Transmissão da COVID-19 no Brasil" via Processo #402834/2020-8 (pedido de propostas MCTIC/CNPq/FNDCT/MS/SCTIE/Decit N° 07/2020).

"I simply wish that, in a matter which so closely concerns the wellbeing of the human race, no decision shall be made without all the knowledge which a little analysis and calculation can provide."

Daniel Bernoulli, *1760.*

"Things you have now, things you've lost. People who're near by, people who've gone far away. No matter what you choose, truth is, both regret and reluctance are going to follow you around. You just have to make sure you don't make excuses to yourself down the road."

Berserk, by Kentaro Miura, *2016.*

"Mankind's greatest fear is Mankind itself. - Gendo Ikari"

Neon Genesis Evangelion, by Hideaki Anno, *1995.*

Resumo

A pandemia de SARS-CoV-2 representou um grande desafio para a Saúde Pública em todo o mundo. O vírus se espalhou por quase todos os países e causou mais de 500 milhões de casos e 6 milhões de mortes até os dias de hoje (2022-04-20). No entanto, devido a investimentos maciços e fortes colaborações internacionais, várias vacinas contra a COVID-19 estavam disponíveis até o final de 2020. Isto levantou questões sobre como estas vacinas deveriam ser alocadas neste cenário de alta demanda e estoque escasso.

Este trabalho contribui para esta discussão, desenvolvendo vários modelos relacionados à vacinação COVID-19. Primeiro fornecemos uma revisão da COVID-19 no Brasil, seguida por uma introdução à modelagem matemática de epidemias, com ênfase nos modelos de vacinação. Em seguida, mostramos três aplicações desta teoria às estratégias de vacinação contra a COVID-19 no Brasil.

Como a maioria das vacinas desenvolvidas foram projetadas com uma implementação de duas doses de vacinação, uma das questões levantadas foi o intervalo ideal para cada vacina neste cenário de escassez de doses. Para responder a isto, desenvolvemos um modelo de equações diferenciais com atraso acoplado a um modelo de otimização para alocar entre a primeira e a segunda dose sem exigir reservas de doses. Concluímos que, se a eficácia da primeira dose em relação à segunda for inferior a 50%, a melhor estratégia para reduzir as mortes é inocular a segunda dose o mais rápido possível, enquanto se a eficácia relativa for superior a 50%, a estratégia depende fortemente da taxa de produção de doses de vacina ao longo do tempo. Se a taxa de produção for baixa, a melhor estratégia é retardar o máximo possível, enquanto que se a taxa de produção for maior, a estratégia ótima depende da eficácia relativa. Mostramos também que a janela de tempo ideal entre as doses não depende do número de reprodução efetivo da doença, mas este tem um papel na magnitude das mortes evitadas pela vacinação.

À medida que a pandemia avançava e a variante Gama emergia no Brasil, as recomendações precisaram ser revisitadas. Desenvolvemos um modelo de vacinação estático de tempo discreto para avaliar a melhor estratégia para alocar doses de AZD1222 (AstraZeneca/Oxford/Fiocruz) com as novas estimativas de efetividade da vacina. Primeiro descobrimos que, em uma implementação baseada na idade, pelo menos 80% de um grupo etário mais velho deveria ser vacinado

antes de disponibilizar as vacinas para os indivíduos mais jovens, tendo mortes adicionais em geral, caso contrário. Em seguida, mostramos que o intervalo entre doses de AZD1222 deve ser reduzido de 12 para 8 semanas em uma epidemia dominada pela Gama e em um cenário ideal de disponibilidade de doses. Entretanto, mostramos que esta mudança de política só teria um efeito mensurável se o número de doses aumentasse em pelo menos 50% da quantidade suprida pelo governo brasileiro até o final de 2021.

No final de 2021, as vacinas infantis foram aprovadas pela Agência Nacional de Vigilância Sanitária (ANVISA) ao mesmo tempo em que a variante Delta estava sendo substituída pela variante Ômicron no Brasil. Desenvolvemos, então, um modelo dinâmico de duas linhagens em tempo discreto com reinfecção para avaliar o impacto da vacinação infantil (5 a 11 anos) em um cenário de substituição de variantes no Brasil. Estimamos que cerca de 2,4 mil internações e 180 mortes de crianças poderiam ser evitadas com o número de doses adquiridas pelo governo brasileiro, com um efeito indireto de redução de quase 10 mil internações e 1,5 mil mortes em todas as faixas etárias, entre meados de janeiro e abril de 2022. Mostramos também que o impacto da vacinação de crianças mais que duplica em uma implementação ótima (e alcançável) de 1 milhão de doses inoculadas por dia, com 5,4 mil internações e 410 mortes evitadas em crianças, com um efeito indireto de 26,5 mil internações e 4,2 mil mortes pela COVID-19 evitadas em todas as faixas etárias, evidenciando a necessidade de aumentar o número de doses supridas pelo governo brasileiro.

Continuamos com uma introdução básica à modelagem estatística Bayesiana e uma visão geral da relativamente nova Integrated Nested Laplace Approximation (INLA). Em seguida, continuamos a desenvolver um modelo estatístico usando o INLA para estimar o impacto inicial da vacinação contra a COVID-19 no Brasil. Realizando uma análise contrafactual de um modelo autorregressivo com covariáveis de cobertura de vacinação explícitas, estimamos que a vacinação evitou diretamente cerca de 167 mil hospitalizações e 76 mil mortes pela COVID-19 no Brasil na faixa etária de alto risco de 60+ anos até o final de agosto de 2021. Ao deslocar a implementação da vacinação 4 e 8 semanas antes, estimamos que estes números aumentariam para 219 mil internações e 101 mil mortes, e 268 mil internações e 124 mil mortes, respectivamente, evidenciando o impacto se o planejamento e a aquisição de vacinas adequadas tivessem sido feitos pelo governo brasileiro.

Terminamos este trabalho com algumas observações sobre o uso de modelagem matemática na saúde pública no Brasil.

Palavras Chaves: COVID-19; Vacinação; Modelos compartimentais; Otimização Linear; Equações com atraso; INLA.

Áreas do conhecimento: Matemática; Matemática Aplicada; Epidemiologia Matemática. Probabilidade e Estatística; Probabilidade e Estatística Aplicada.

Abstract

The SARS-CoV-2 pandemic represented a great challenge for Public Health around the world. The virus has spread to almost all countries in the world and caused more than 500 million cases and 6 million deaths to this day (2022-04-20). Yet, due to massive investments and strong international collaborations, several COVID-19 vaccines were available by the end of 2020. This sparkled questions on how these vaccines should be allocated in this scenario of high demand and scarce stock.

This work contributes to this discussion by developing several models related to COVID-19 vaccination. We first provide a review of COVID-19 in Brazil, followed by an introduction to mathematical modelling to epidemics, with an emphasis on vaccination models. We then show three applications of this theory to vaccination strategies against COVID-19 in Brazil.

As most vaccines developed were designed with a two-dose vaccination rollout, one of the questions raised was the optimal interval for each vaccine in this scenario of scarcity of doses. To answer this, we develop a delay differential equations model coupled with an optimization model to allocate between first and second doses without requiring reserves of doses. We conclude that, if the effectivity of the first dose compared to the second one is lower than 50%, the best strategy to reduce deaths is to inoculate the second dose as fast as possible, whereas if the relative effectivity is higher than 50%, the strategy is strongly dependent on the production rates of vaccine over time. If the production rate is low, the best strategy is to delay as much as possible, whereas if the production rate is higher, the optimal strategy is dependent on the relative effectivity. We also show that the optimal time window between doses is not dependent on the effective reproduction number of the disease, but it has a role in the magnitude of deaths averted by vaccination.

As the pandemic progressed and the Gamma variant emerged in Brazil, the recommendations needed to be revisited. We developed a discrete-time static vaccination model to assess the best strategy to allocate doses of AZD1222 (AstraZeneca/Oxford/Fiocruz) with the new estimates of vaccine effectiveness. We first found that, following an age-based rollout, at least 80% of an older age group should be vaccinated before making vaccines available to younger individuals,

having additional overall deaths otherwise. We then proceed to show that the interval between doses of AZD1222 should be reduced from 12 to 8 weeks in a Gamma dominated epidemic and in an ideal scenario of availability of doses. However, we show that this change in policy would only have a measurable effect if the number of doses increases by at least 50% of the quantity procured by the Brazilian government until the end of 2021.

At the end of 2021, child vaccines were approved by the Brazilian National Agency of Sanitary Vigilance (ANVISA) at the same time that the Delta variant was being substituted by the Omicron variant in Brazil. We then developed a two-strain discrete-time dynamic model with reinfection to assess the impact of children (5 to 11 years old) vaccination in a scenario of variant substitution in Brazil. We estimate that around 2.4 thousand hospitalizations and 180 deaths of children could be averted with the number of doses procured by the Brazilian government, with an indirect effect of reducing almost 10 thousand hospitalizations and 1.5 thousand deaths in all age groups, between mid-January and April 2022. We also show that the impact of vaccinating children more than doubles in an optimal (and achievable) rollout of 1 million doses inoculated per day, with 5.4 thousand hospitalizations and 410 deaths averted in children, with an indirect effect of 26.5 thousand hospitalizations and 4.2 thousand deaths by COVID-19 averted in all age groups, evidencing the necessity of increasing the number of doses procured by the Brazilian government.

We continue with a basic introduction to Bayesian statistical modelling and an overview of the relatively new Integrated Nested Laplace Approximation (INLA). We then proceed to develop a statistical model using INLA to estimate the early impact of vaccination against COVID-19 in Brazil. By doing a counterfactual analysis of an autoregressive model with explicit vaccination coverage covariates, we estimated that the vaccination directly averted around 167 thousand hospitalizations and 76 thousand deaths by COVID-19 in Brazil in the high risk age group of 60+ years old until the end of August 2021. By shifting the vaccination rollout by 4 and 8 weeks earlier, we estimated that these figures would increase to 219 mil hospitalizations and 101 thousand deaths, and 268 thousand hospitalizations and 124 thousand deaths, respectively, evidencing the impact if proper planning and vaccine procurement were done by the Brazilian government.

We end this work with some remarks regarding the usage of mathematical modelling in public health in Brazil.

Keywords: COVID-19; Vaccination; Compartmental models; Linear optimization; Delay equations; INLA.

Research Areas: Mathematics; Applied Mathematics; Mathematical Epidemiology. Probability and Statistics; Applied Probability and Statistics.

Contents

Chapter 1

Introduction

This work aims to develop mathematical and statistical models to assess optimal strategies of vaccination against COVID-19 in Brazil. We first introduce the situation of the COVID-19 pandemic in Brazil, then we introduce the basic concepts involving mathematical and statistical modelling of epidemics. We then show four studies developed by the author of this thesis (and colleagues) regarding vaccination strategies in Brazil.

Severe Acute Respiratory Syndrome Coronavirus 2 (SARS-CoV-2) is a novel betacoronavirus discovered in late December 2019, in Wuhan, China [1]. It causes the Coronavirus Disease 2019 (COVID-19) and is responsible for the ongoing pandemic declared on March 11, 2020, by the World Health Organization (WHO) [2]. It has spread to almost all countries in the world and caused more than 500 million cases and 6 million deaths to this day (2022-04-20) [3]. The virus bears great genomic similarity with SARS-CoV and MERS-CoV [4], the viruses that were responsible by the Severe Acute Respiratory Syndrome (SARS) [5] and Middle East Respiratory Syndrome (MERS) [6] outbreaks, respectively. The origin of SARS-CoV-2 is believed to be a zoonotic spillover from bat coronaviruses, due to the remarkable genomic similarity. However, conclusive evidence is still required due to considerable gaps in the phylogenetic tree of the betacoronaviruses [7].

SARS-CoV-2 is a spherical coronavirus with diameter between 80 and 160 nm. The surface is covered with spike (S), membrane (M) and envelope (E) proteins [8] (Fig. 1.1). The coronavirus genome comprises a single-stranded positive-strand RNA ranging from 26 Kb to 32 Kb in length [4]. The list of symptoms of COVID-19 include, but are not limited to: cough, fever, fatigue, rhinorrea and/or nasal congestion, headache, fatigue, myalgia and loss of sense of smell and/or taste [9]. An infection can evolve to a severe form of the disease, with symptoms including: pneumonia with hypoxemia, Severe Acute Respiratory Infection (SARI), encephalopathy, myocardial injury, heart failure, coagulation dysfunction and acute kidney injury [10]. The acute form of COVID-19 generally begins with an incubation, yet infectious, period that lasts around 6.4 days (95% Credible Interval:

2.1-11.1 days) [11], then followed by a time to recovery that goes from 2 up to 6 weeks [12]. However, many individuals can show post-infection (also called long COVID) symptoms that include fatigue, dyspnea, cardiac abnormalities, cognitive impairment, sleep disturbances, symptoms of post-traumatic stress disorder, muscle pain, concentration problems, and headache [13]. Also, a considerable number of individuals do not show symptoms at all, while still being infectious, hampering containment strategies against COVID-19 [14]. The severity of the disease varies per person, but is strongly correlated with the presence of comorbidities and older age [15].

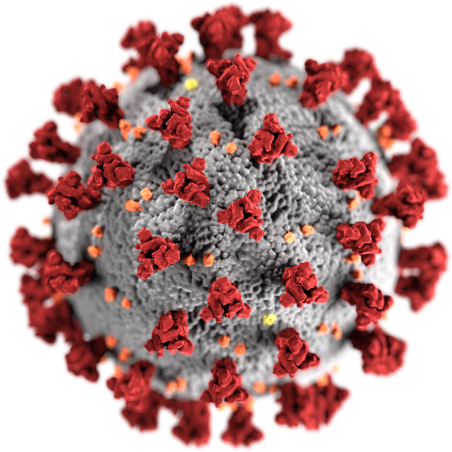

Figure 1.1: SARS-CoV-2 model. Color legend: gray – membrane; red – spike glycoprotein (S); yellow – envelope (E) protein; orange – membrane (M) protein. 3D model comissioned by the Centers for Disease Control and Prevention. Available as Creative Commons.

In the first days of the pandemic, it was believed that the main route of transmission of SARS-CoV-2 was by contact with wild animals or ingestion of raw food, since the early cases were linked to the Huanan Food Market in Wuhan [16]. However, with a case of COVID-19 in a person that have had not travelled to China, human-to-human transmission was confirmed in January, 23 of 2020 [17, 18]. Yet, due to a century-old dogma regarding routes of disease transmission [19], the WHO guidelines for preventing infections during the pandemic were strongly based on the assumption that human-to-human COVID-19 spreading occurs through large ($> 100\mu m$) droplets, usually generated in coughs or sneezes, that would then rapidly fall in the air. An infection would then happen by touching contaminated surfaces or objects, followed by touching exposed mucous parts such as eyes and mouth. This led to recommendations that included periodical surface disinfection, hand cleaning and 1-meter distancing in indoor situations, re-

stricting mask usage to infected individuals and persons in close contact with them [20]. But, with increasing evidence of super-spreading events and long-range transmission [21, 22, 23, 24], it was concluded that COVID-19 is airborne-transmitted [25]. Airborne spreading occurs by the dispersal of smaller droplets, also called *aerosols*, capable of floating in the air by hours, that are then inhaled by the exposed individual. Besides coughing and sneezing, aerosol particles can also be produced by actions such as talking or simply breathing, also explaining asymptomatic and incubating individuals being able to spread the disease as well [26]. This then required an update of the recommended non-pharmaceutical interventions[1] that included well-fit high-grade (N95/PFF2) mask usage, adequate indoor ventilation, isolation of infected individuals and air filtering [26]. It is important to notice that this shift in paradigm is still underway, with implications in other diseases such as Influenza and SARS [19], and it took almost two years into the pandemic for the WHO to explicitly state that airborne transmission is possible in their guidelines [27].

Even though SARS-CoV-2 has a lower mutation rate compared to other viruses such as the Influenza virus, its high attack rate in the population allowed it to accumulate mutations by recombination and copying error [28], and, as the strains of the virus further diverges from the original, lineages are created. If a SARS-CoV-2 lineage has mutations that are known to confer epidemiologic advantages such as transmissibility or immune escape, and is identified as causing significant community transmission or suggesting an emerging risk to global public health, it receives the denomination of a Variant of Interest (VOI). If this variant is also associated with significant increase in transmissibility, virulence, severity, immune escape, or reduced effectiveness of public health and social measures, it is designated as a Variant of Concern (VOC). To this day, five SARS-CoV-2 lineages have received the VOC denomination. Following WHO (and PANGO) lineage nomenclature, they are: Alpha (B.1.1.7), Beta (B.1.351), Gamma (P.1), Delta (B.1.617.2), and Omicron (B.1.1.529) [29].

The Alpha variant was first detected in the United Kingdom around September 2020 and is acknowledged to be the first VOC to appear. It is estimated to have around 50% greater transmissibility and increased mortality by 1.1 to 1.8 times compared to the strains circulating at the time [30, 31]. No increased immune escape was found [32]. The Beta variant was first detected in South Africa around

[1] In Brazil, most of the recommendations kept related to hand cleaning and temperature assessment, leading to a pejorative term called “teatro do alquingel".

September 2020. Besides having similar transmissibility to Alpha variant (as they have similar mutations), this VOC posed a problem to public health due to increased risk of reinfection and immune escape from vaccines [33, 34, 35, 36]. The Gamma variant emerged around November 2020, in Brazil [37]. It is known to have from 1.7 up to 2.8 times higher transmissibility than the circulating variants in Brazil at the time [38, 39, 40], and increased capability of reinfection [38, 41], with some studies documenting vaccines having reduced effectiveness against this variant compared to the original one [42, 43]. The Delta variant originated around December 2020, in India. It is known to have considerably higher transmissibility compared to previous VOCs (up to 167% higher compared to Alpha VOC) [44, 35], and increased hospital admission rate [45]. It is also considered to have some immune escape against vaccines due to some breakthrough infections [46, 47]. Finally, the Omicron variant stands out by having a strong immune escape from vaccines and higher reinfection rate compared to previous variants [48, 49, 50, 51, 52]. Even though it possesses lower severity, its shorter serial interval is capable of increased hospital burden due to overflow of patients [53, 54].

Once the SARS-CoV-2 genome was made available in early January 2020, several manufacturers started vaccine development [18]. The development of vaccines starts with pre-clinical research, testing the vaccine's capacity of eliciting immune response and its safety in animals that have similar respiratory tract (in the case of COVID-19 vaccines) to humans, such as the rhesus macaque [55, 56]. If the results are good enough, the manufacturer starts human trials. The phase I is responsible for assessing the initial safety of the vaccine, testing in small groups of humans. Phase II clinical trials then assess safety in a larger number of humans, also assessing immune response by often comparing with individuals that have not received the vaccine. Finally, phase III clinical trial focuses on assessing the efficacy of the vaccine in protecting individuals against the disease outcomes, while also being capable of further studies in safety [57].

To accelerate the vaccine research, most manufacturers opted to proceed with simultaneous Phase I/II and II/III trials. This, together with staggering amounts of money invested and the fact that COVID-19 incidence was very high, increasing the statistical power of the evaluations, allowed multiple vaccines to be finished around the last quarter of 2020. Nowadays, we already have 10 different vaccines approved for emergency use by the WHO, and 38 vaccines approved by at least one country [57]. The 10 approved vaccines have used very different manufacturing platforms [58]. NVX-CoV2373 [59] (also Nuvaxovid, by Novavax) and

NOVAVAX (same formulation of NVX-CoV2373, by Serum Institute of India) use the protein subunit platform. This consists of directly injecting specific proteins from the virus that will elicit an immunogenic response. In the case of SARS-CoV-2, the Spike and M proteins are the most used. BNT162b2 [60] (also Comirnaty, from Pfizer/BioNTech) and mRNA-1273 [61] (also Spikevax, from Moderna) both use the mRNA platform. This consists in producing synthetic mRNA that codifies production of certain parts of the virus (in this case, the S protein), involved in a lipid coat, that is then absorbed by the cells and start replicating the part codified in the mRNA, eliciting immune response. Ad26.COV2.S [62] (by Janssen), AZD1222 [63] (also Vaxrevia, by AstraZeneca/Oxford/Fiocruz) and Covishield (same formulation of AZD1222, by Serum Institute of India) use the viral vector platform. This consists in using a different virus to transport the genetic information of the original virus (in this case a non-replicating adenovirus), that is absorbed by the cell and start producing the S protein (in the case of COVID-19), without reproduction capabilities. Finally, BBV152 [64] (also Covaxin, by Bharat Biotech), BBIBP-CorV [65] (also Covilo, by Sinopharm) and CoronaVac [66] (by Sinovac) use the inactivated virus platform. This consists in injecting the entire virus, that was rendered inactivated by some procedure that can be chemical or by heat, for example. Except for Ad26.COV2.S, all vaccines used a two-dose rollout plan.

Following the declaration Public Health Emergency of International Concern (PHEIC) by the WHO in January, 30th of 2020 [67], Brazil declared COVID-19 a Public Health Emergency of National Concern (PHENC) in February, 3rd of 2020, to coordinate a response to the threat that would come [68]. The first case of COVID-19 in Brazil was confirmed in February, 27th of 2020 [69], and the first death was confirmed in March, 12th of 2020 [70]. The epidemic started in the major metropolitan areas in the Southeast region of Brazil that had international flight connections. The disease then spread to other regions in the country through an interiorization process, leaving little synchronicity between the first waves in each state [71]. How harsh the spreading of COVID-19 was in each state bears strong correlation with precariousness of the health system and the capacity to enact stringent measures in each place [72]. By the end of October, Brazil had already reached around 500 thousand hospitalizations and 150 thousand deaths by COVID-19 (Figs. 1.2 and 1.3) [73].

Around November 2020, Manaus (Amazonas state), a place that already had experienced a harsh number of hospitalizations and deaths in the first wave, was

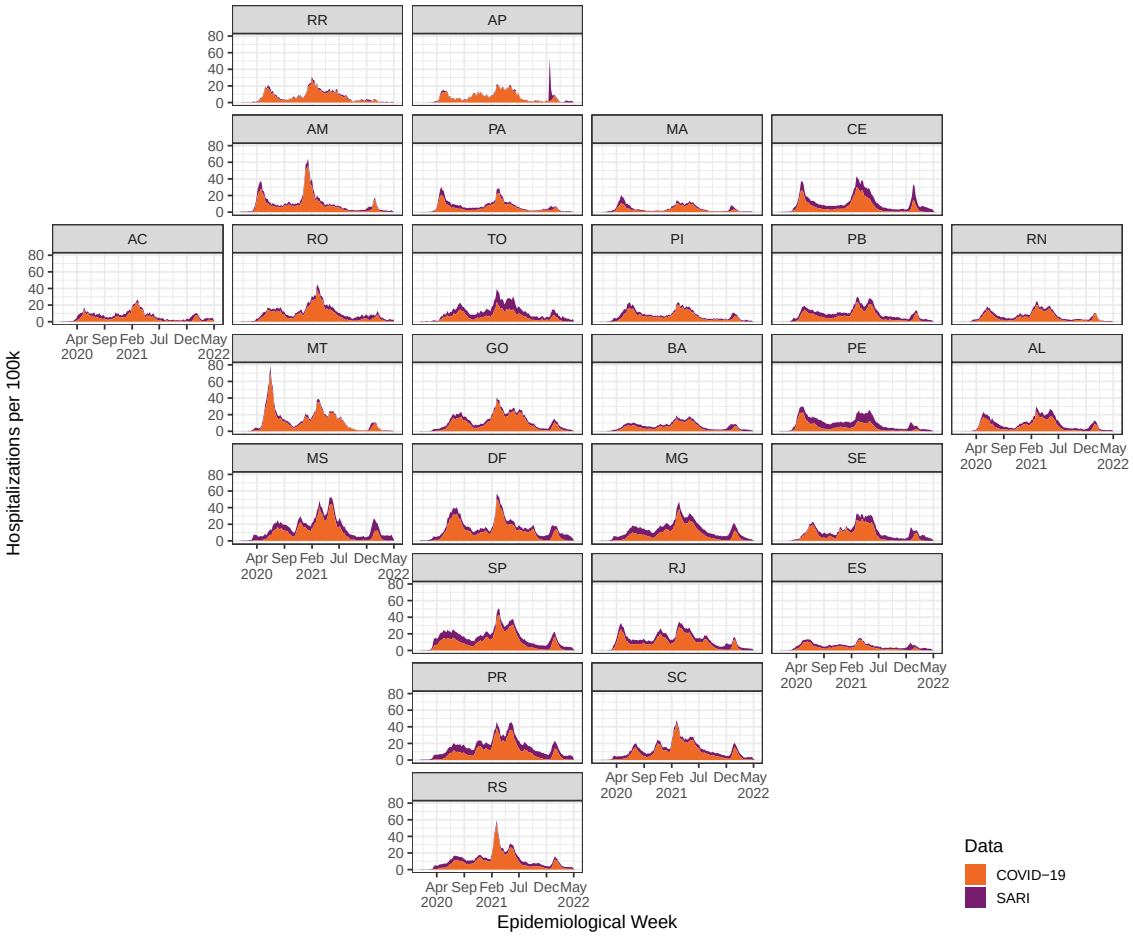

Figure 1.2: Weekly hospitalizations by date of first symptoms per 100k individuals by Severe Acute Respiratory Infection (SARI) and COVID-19, per state. SARI hospitalizations include COVID-19 hospitalizations. Last four weeks should be ignored due to notification delay. Source: SIVEP-Gripe [73, 74]. Developed by the author.

seeing a surge in cases despite having an estimated prevalence of COVID-19 of around 75% at the time [37, 38]. This surge in cases was caused by the appearance of Gamma (P.1) variant (Fig. 1.4), that led to an even worse wave in the state, with its peak around January 2021. The Gamma variant spread quickly in the country, leading to a synchronized wave in the other states around March 2021, that led the Brazilian health system to the brink of collapse, with around 1.7 million hospitalizations and 500 thousand deaths by the end of June 2021 [74]. The Gamma variant was then replaced by the Delta variant, but Brazil has not experienced another surge in cases (except for Rio de Janeiro state) and this was

correlated to the considerable vaccine coverage[2] and previous infections in the country. The last COVID-19 wave to date happened with the introduction of the Omicron variant around December 2021 in the country, leaving Brazil with a total of 2,030,468 hospitalizations and 637,638 deaths by COVID-19 until 2022-05-18 [74].

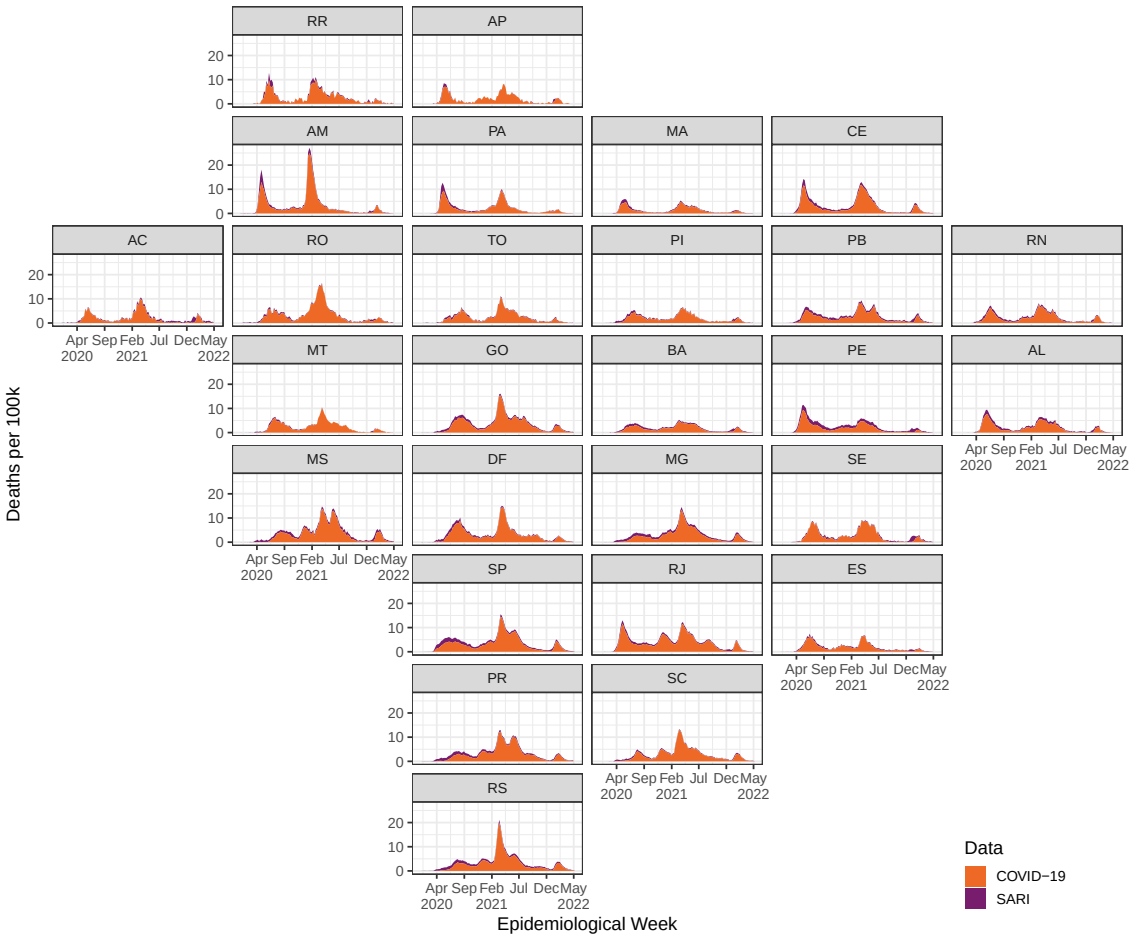

Figure 1.3: Weekly deaths by date of death per 100k individuals by Severe Acute Respiratory Infection (SARI) and COVID-19, per state. SARI deaths include COVID-19 deaths. Last four weeks should be ignored due to notification delay. Source: SIVEP-Gripe [73, 74]. Developed by the author.

The vaccination in Brazil started with the approval of CoronaVac and AZD1222 vaccines for emergency use in January, 17th of 2021 [76]. The criteria established by the National Agency of Sanitary Vigilance (ANVISA) for emergency use included Phase I/II/III studies in the country and at least 50% of efficacy (and at least 30%

[2] Around 97% and 57% individuals with one and two doses, respectively, in the 60+ age group, by the end of June 2021.

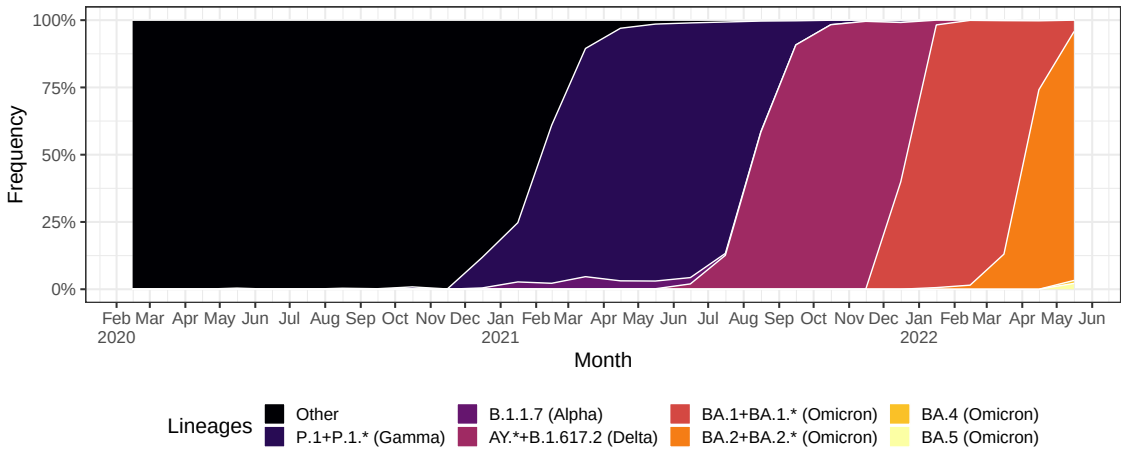

Figure 1.4: Frequency of SARS-CoV-2 variants in Brazil over time, simplified to consider only VOC. Source: [75]. Developed by the author.

in the lower bound) in the primary outcome of the studies [77]. Besides these vaccines, Ad26.COV2.S was later approved in March, 31st of 2021 [78]. AZD1222 and Ad26.COV2.S also received final registration in March, 13th and April, 5th of 2021, respectively [79, 80]. Another vaccine that is used in Brazil is BNT162b2, that received direct final registration in February, 23rd of 2021 [81]. CoronaVac and BNT162b2 are also authorized for usage in children and adolescents, with the first being used in at least 6-year-olds and the latter being used in at least 5-year-olds (though with a different formulation from the adult vaccine) [82, 83, 84].

The first months of vaccination against COVID-19 in Brazil were at a very low pace. In a country known to vaccinate around a million individuals daily in previous campaigns [85], between January and March, Brazil vaccinated around 300 thousand individuals each day (Fig. 1.5). Since the country already had a strong capillarity of the Brazilian's Unified Health System (SUS), this slowness is attributed to the shortage of vaccine doses. This shortage was not only caused by the low availability of doses in the international market, but also due to low rate of procurement of vaccines by the federal government [86]. The vaccine uptake increased to around 850 thousand between April and June, still below the full capacity of the system. Yet, in a study done by us (also described in Chapter 7), we were able to show that the vaccines were crucial to avoid an even greater disaster in the management of the pandemic in Brazil. Nevertheless, the impact of vaccination could have been better if vaccines were deployed earlier. The vaccine uptake increased steadily until August 2021, reaching an average of 1.7 million doses per day. The number of daily doses inoculated have been falling since

then, only having a surge of vaccine search due to the appearance of the Omicron variant in the country (Fig. 1.5). Even though Brazil reached a good coverage of vaccination nationwide, it has a considerable heterogeneity, with states in the North and Northeast regions with noticeably lower coverage (Fig. 1.6). Also, the country struggles to reach a high coverage of individuals protected with booster doses that came to be necessary due to waning of vaccine protection and higher immune escape of variants such as Omicron.

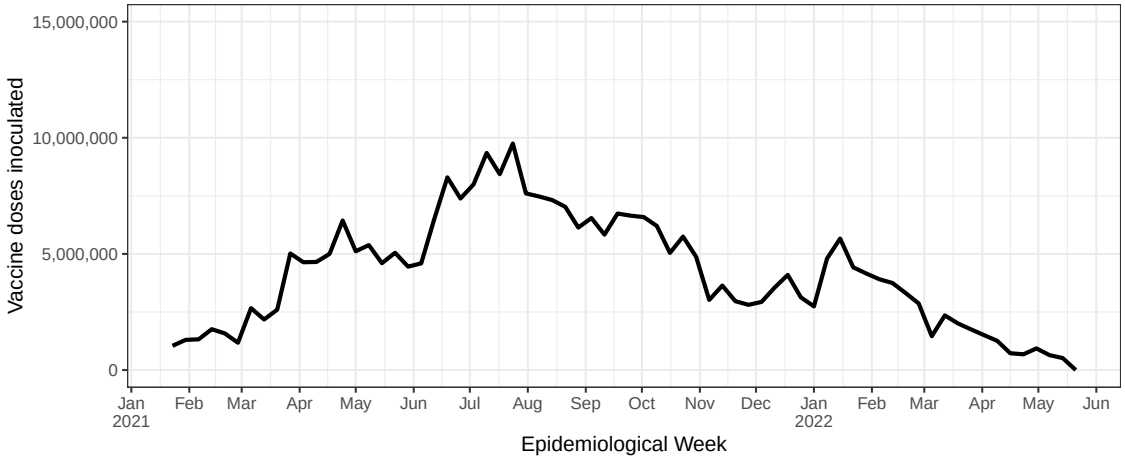

Figure 1.5: Weekly COVID-19 vaccine uptake in Brazil. Last four weeks should be ignored due to notification delay. Source: SI-PNI [87]. Developed by the author.

The epidemiological data about COVID-19 in Brazil comes mainly from two publicly available databases. SIVEP-Gripe contains anonymous microdata about Severe Acute Respiratory Infection (SARI) cases in Brazil [73, 74]. An individual is first characterized as having an Influenza-like Illness (ILI) if they present at least two of the following symptoms or signals: fever (even if referred), chills, sore throat, headache, cough, runny nose, smell disturbances or taste disturbances. An individual with SARI is a person with ILI who has: dyspnea/respiratory discomfort or persistent chest pressure or pain or O_2 saturation less than 95% on room air or bluish coloration (cyanosis) of the lips or face. Additionally, if an individual with SARI has a positive COVID-19 test, or anosmia (olfactory dysfunction) or acute ageusia (gustatory dysfunction) without other pre-existing cause, or contact with a confirmed case of COVID-19 prior to the appearance of symptoms, or some specific changes in results of image exams, they should be considered a severe case of COVID-19 [88]. Since the 2011 H1N1 pandemic, it is compulsory to notify any case of SARI in the SIVEP-Gripe database, and, since the COVID-19 pandemic, it has been used to monitor the hospitalizations and

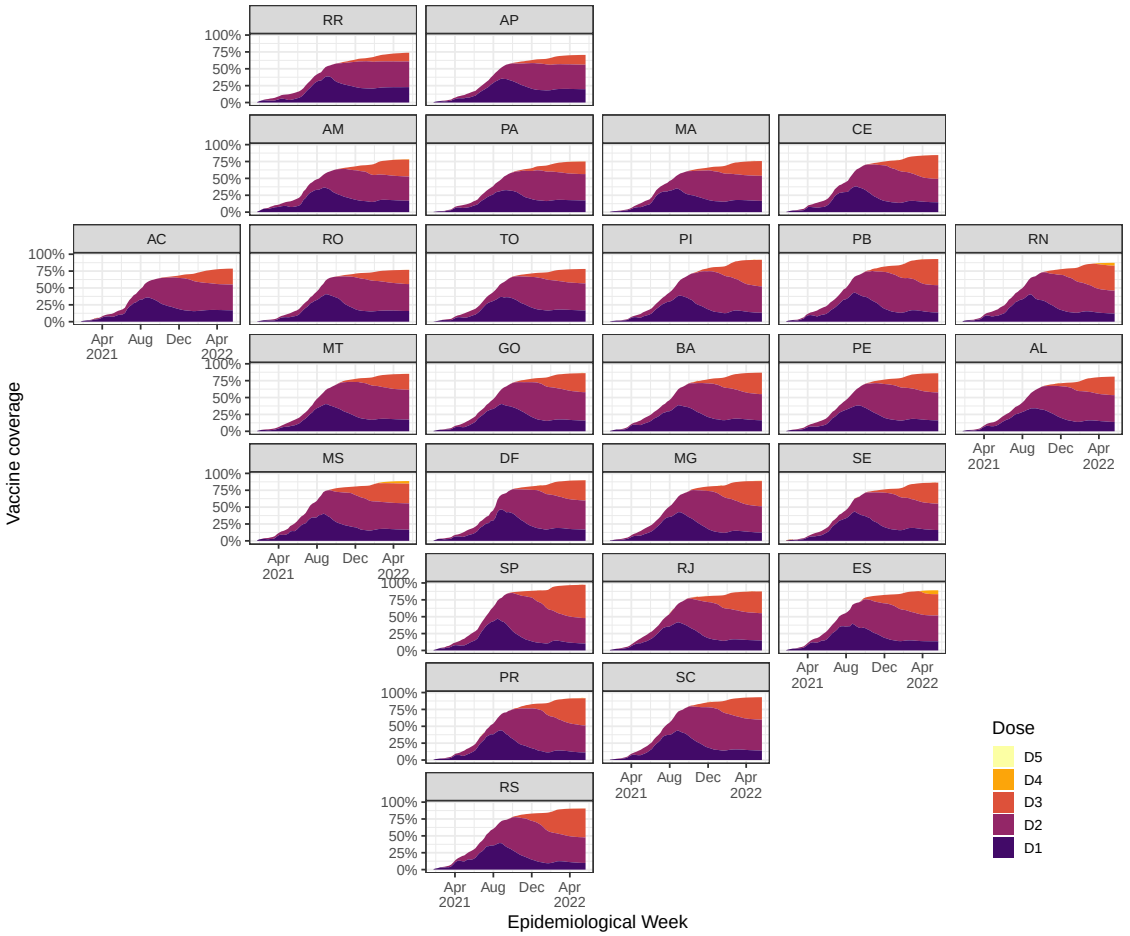

Figure 1.6: COVID-19 vaccine coverage in Brazil, by number of doses and state. Source: SI-PNI [87]. Developed by the author.

deaths due to COVID-19 in Brazil (See Figs. 1.2 and 1.3). The Information System of the National Immunization Plan (SI-PNI) contains anonymous microdata about COVID-19 vaccine doses inoculated in Brazil, being able to provide coverage estimates in almost all geographical arrangements in Brazil, requiring, however, high computational resources due to the database size (150 GB+) [87]. Additionally, one could consider the usage of the e-SUS VE database to analyze COVID-19 confirmed ILI cases in Brazil [89, 90, 91]. However, due to the lower reporting rate[3] correlated with weaker symptoms than SARI makes this database unusable in general applications. For this reason, we only consider severe cases of COVID-19 and vaccination rates in this work.

Due to the necessity to expedite planning during the COVID-19 pandemic, mathematical and statistical modelling has been used extensively to this day.

[3]This database is also a bit of a mess.

Some early mathematical models were used to estimate the impact of unmitigated epidemics throughout the world, evidencing the necessity to consider stringent measures to contain the spread of the disease [92], whereas some statistical models were used to apply corrections in the number of reported cases due to notification delays [93]. Other models considered the usage of specific non-pharmaceutical interventions such as lockdown or school closure to suggest routes of disease containment [94, 95, 96, 97]. Some models considered socio-economic inequalities to illustrate disparities of COVID-19 burden in these populations [98, 99]. Strategies concerning the usage of mass testing to optimally isolate individuals were also considered [97, 100]. With the emergence of SARS-CoV-2 variants, multiple-strain models were used retroactively to estimate parameters of importance that would then be used to forecast the impact of these variants in disease spread [30, 38, 39, 40, 51].

As the pandemic further progressed, the possibility of having vaccines available in early 2021 motivated a myriad of models studying vaccination strategies [101]. Matrajt et al. [102] have shown that, in a scenario of vaccination prior to the epidemic dynamics, it is generally better to prioritize high-risk individuals (i.e., older individuals) if the vaccine effectiveness (VE) is low, whereas if VE is high enough, it might be better to prioritize high-transmissibility individuals (i.e., 20-49 years old). This result was further confirmed by Bubar et al. [103], that considered vaccination rollout occurring concomitantly to the epidemic dynamics. In their model, if the primary outcome is reducing the number of deaths, vaccinating older individuals is preferred, but if the spreading velocity is low enough or the vaccination rollout is fast enough, it may be preferable to vaccinate highly mobile individuals. Wagner et al. [104] shows that combatting COVID-19 should be a combined effort between the countries. Vaccine hoarding by richer countries leads to higher burden and non-elimination of the disease, and to avoid that, these countries should share vaccine doses with places with lower monetary power.

In this work, we aim to contribute to the discussion of strategies of vaccination against COVID-19, specially focused on the scenario of Brazil. In Chapter 2, we introduce the main techniques in mathematical modelling of diseases, with a focus on vaccination models. In Chapter 3, we develop a delay differential equations model to assess the best interval between doses during a vaccination rollout. In Chapter 4, we develop a discrete time model to assess the impact of AZD1222 vaccination strategies during the Gamma wave in Brazil. In Chapter 5, we study the impact of children vaccination with BNT162b2 in an Omicron

wave in Brazil, analyzing the difference in outcome due to different rollouts. In Chapter 6, we introduce the basic concepts of Bayesian statistical modelling and the Integrated Nested Laplacian Approximation. Finally, in Chapter 7, we develop a statistical model to assess the early impact of the vaccination rollout in Brazil, also estimating how many hospitalizations and deaths could be additionally avoided if the vaccination had started earlier.

Chapter 2

Mathematical Models in Epidemiology

2.1 Introduction

The first known model of epidemics is attributed to Daniel Bernoulli, published in 1766 [105]. He developed a static (i.e., constant force of infection) model for smallpox inoculation. He was able to derive an equation for the life expectancy with and without the presence of smallpox in the population, and also derived the age-dependent prevalence of the disease. The first dynamic models would not be developed until the 20th century, with the seminal works by Hamer and Ross [106, 107], where they studied measles and malaria disease dynamics, and Kermack and McKendrick [108, 109, 110], where they studied the basic conditions for an epidemic to occur.

In this chapter, we describe the basic mathematical tools for epidemic modelling, with a focus on models of vaccination.

2.2 Compartmental models

One basic assumption that the modeler can make is to assume that the population being studied is homogenous with respect to some characteristic of importance. This allows them to categorize the population into some boxes, traditionally called *compartments*. Let us see some examples of these models.

2.2.1 The SIR model

The most famous model in epidemic modelling is the Susceptible-Infectious-Recovered (SIR) model (Fig. 2.1), by Kermack and McKendrick [108]. It is known for its ability to describe most short-term directly transmissible disease dynamics, such as measles and influenza, for example. It assumes that infectious individuals have an equal probability of infecting any susceptible individuals on what is called the *well-mixed* assumption. This leads to modelling the transmission as obeying

the law of mass action, i.e., being proportional to the product of susceptible and infectious individuals [111]. In real life scenarios, this does not necessarily hold, as much of the transmission is done by super-spreading events or individuals, with some individuals being naturally more mobile than others or having different susceptibility or infectiousness. It also assumes life-long protection from reinfection. While this is generally true for diseases such as measles and smallpox, this does not hold for diseases such as malaria. The other important assumption is that the probability of transferring between compartments (recovering, for example) is exponentially distributed [112]. Considering that the population in each compartment can vary continuously, we arrive at:

$$\frac{dS}{dt} = -\beta \frac{I}{N} S \tag{2.1}$$

$$\frac{dI}{dt} = \beta \frac{I}{N} S - \mu I \tag{2.2}$$

$$\frac{dR}{dt} = \mu I \tag{2.3}$$

where β is the probability of infection upon contact rate per unit of time, μ is the (exponentially distributed) recovery rate, and $N = S + I + R$, is the total population.

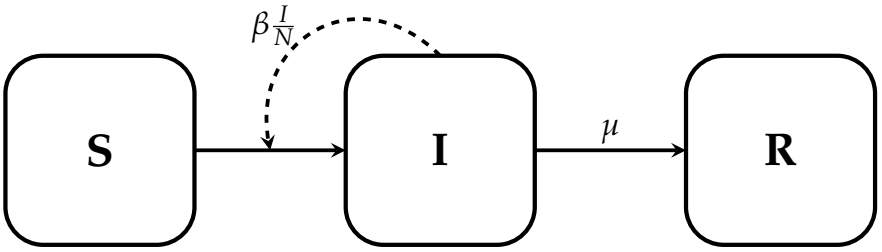

Figure 2.1: SIR model diagram. The black arrows denote the evolution of the individuals between the compartments, and the dashed arrow denotes the transmission dynamics. The S box denotes the susceptible individuals, the I box denotes the infectious individuals, and the R box denotes the recovered individuals.

2.2.2 The Basic Reproduction Number

We can easily simplify these equations by dividing both sides by N, where each compartment is the proportion of individuals in the total population:

$$\frac{ds}{dt} = -\beta is \tag{2.4}$$

$$\frac{di}{dt} = \beta is - \mu i \tag{2.5}$$

$$\frac{dr}{dt} = \mu i \tag{2.6}$$

The criteria for having an outbreak happening is that $\frac{di}{dt} > 0$ (i.e., the number of cases growing). This implies that the proportion of susceptible must be higher than a threshold given by:

$$s > \frac{\mu}{\beta} = \frac{1}{R_0} \tag{2.7}$$

where $R_0 = \frac{\beta}{\mu}$ is called the *basic reproduction number*.

Notably, as $0 \leq s \leq 1$, this implies that R_0 not only have to be a positive number, but for an outbreak also be capable to occur, it has to be greater than 1. Since β describes the probability of being infected upon contact rate per unit of time, and $1/\mu$ is the mean time to recovery, then the mean number of secondary cases caused by a single individual within their infectious period is given by $\beta\frac{1}{\mu}$, which is equal to R_0. Thus, if $R_0 < 1$, the transmission would not be able to sustain itself and the outbreak would not happen.

Whilst R_0 is the number of secondary infections per infection during the initial period of the epidemic, as the dynamics evolves, the number of susceptible individuals reduces and the infected individuals are not able to transmit the disease efficiently. We can then define the *effective reproduction number* as:

$$R_t = \frac{\beta}{\mu}\frac{S}{N} = \frac{\beta}{\mu}s \tag{2.8}$$

which is the mean number of individuals an infected individual is expected infect if a proportion s of individuals are susceptible at the time. While $R_t > 1$ the number of active cases is able to grow, if $R_t < 1$ the active cases (here represented by the I compartment) would start to fall. Therefore, $R_t = 1$ defines the peak of the outbreak (Fig. 2.2).

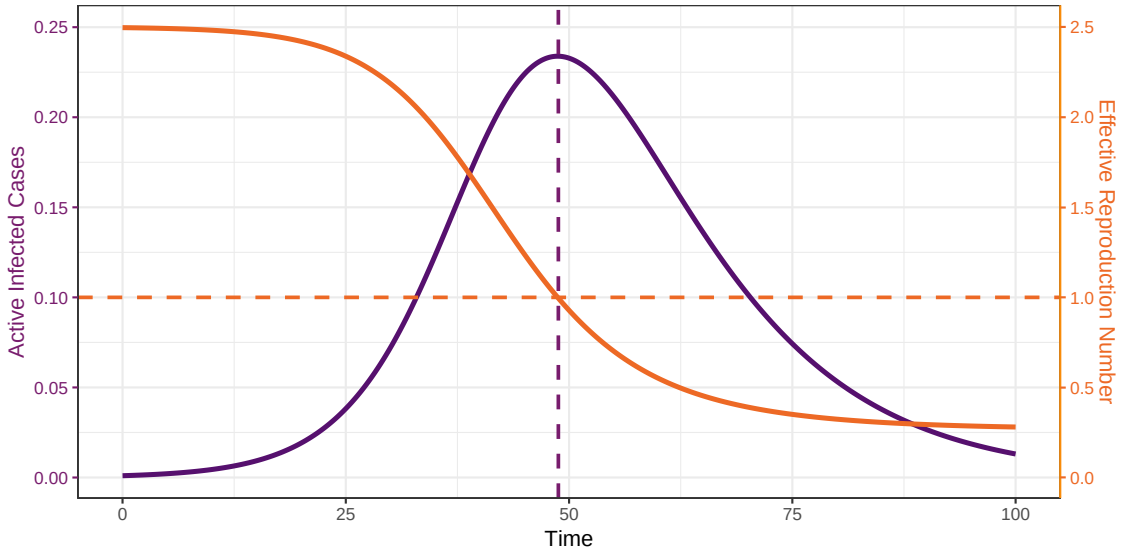

Figure 2.2: Active infected cases (purple, left axis) and effective reproduction number (orange, right axis) as a function of time. $\beta = 0.25$, $\mu = 1/10$, $s(0) = 0.999$, $i(0) = 0.001$, $r(0) = 0$. Notice that the peak of active cases happens at the same time as R_t is equal to 1.

2.2.3 The Final Epidemic Size

A counter-intuitive result from the Kermack-McKendrick model is that some people might not be infected at the end of the epidemic. This happens because the mechanism that ends the epidemic is not the complete depletion of susceptibles, but the inability of the infectious individuals to infect other individuals before they recover.

We can calculate the *final epidemic size* Z first by computing $\frac{di}{ds}$, as follows:

$$\frac{di}{ds} = \frac{di}{dt}\frac{dt}{ds} = \frac{\beta si - \mu i}{-\beta si} = -1 + \frac{1}{R_0 s} \tag{2.9}$$

By separation of variables, one can find:

$$i(t) = i_0 + s_0 - s(t) + \frac{1}{R_0} \ln\left(\frac{s(t)}{s_0}\right) \tag{2.10}$$

At the end of the epidemics in $t \to \infty$, $i(\infty) = i_\infty = 0$ and $s(\infty) = s_\infty$. We can define our final epidemic as $Z = s_0 - s_\infty$, wielding:

$$0 = i_0 + Z + \frac{1}{R_0} \ln\left(\frac{s_0 - Z}{s_0}\right) \tag{2.11}$$

Isolating Z inside the logarithm, we can find an implicit equation for the final epidemic size:

$$Z = s_0 \left(1 - e^{-R_0(Z+i_0)}\right) \tag{2.12}$$

In the limit of $i_0 \ll 1$ and $s_0 \approx 1$, this reduces to:

$$Z = 1 - e^{-R_0 Z} \tag{2.13}$$

These equations can be solved explicitly using the Lambert's W function [113], leading to:

$$Z = s_0 + \frac{1}{R_0} W\left[-R_0 s_0 e^{-R_0(i_0+s_0)}\right] \tag{2.14}$$

and

$$Z = 1 + \frac{1}{R_0} W\left[-R_0 e^{-R_0}\right] \tag{2.15}$$

respectively.

Considering Eq. 2.15, since $-R_0 e^{-R_0} \geq -1/e$ if $R_0 \geq 1$, this implies that $W\left[-R_0 e^{-R_0}\right] \geq -1$ if $R_0 \geq 1$. Therefore:

$$Z = 1 + \frac{1}{R_0} W\left[-R_0 e^{-R_0}\right] \geq \frac{1}{R_0}(R_0 - 1) = 1 - \frac{1}{R_0} \tag{2.16}$$

Notably, as $1 - 1/R_0$ is the number of recovered individuals at the peak of the outbreak, the difference $Z - (1 - 1/R_0)$ is the number of individuals that get infected after the peak, a phenomenon called *overshoot* (Fig. 2.3). This is important because during the COVID-19 pandemic many researchers and media outlets publicized $1 - 1/R_0$ as the estimated final burden of the epidemic, wielding the value of $\approx 60\%$ of recovered individuals for an $R_0 \approx 2.5$, whereas the true value should be $\approx 89\%$, much bigger than the former value. This happened due to a confusion with an expression related to the necessary vaccine coverage for an epidemic not to happen, that we will discuss in the following sections.

2.2.4 Discrete-time SIR Model

We can build an equivalent discrete time SIR model. Considering that θ is the average number of infectious contacts per susceptible per day, given by:

$$\theta = \frac{\beta I}{N} \tag{2.17}$$

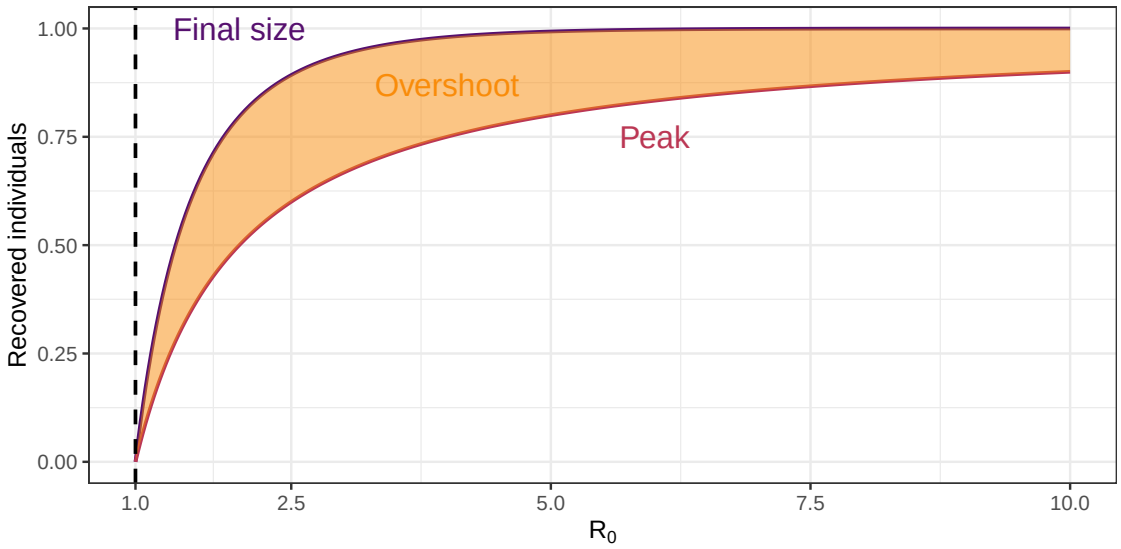

Figure 2.3: The number of recovered individuals at each stage of the outbreak as a function of R_0 in a SIR model. The dark orange line describes the number of recovered individuals at the peak of the outbreak, whereas the purple line describes the final size of the epidemic. The light orange shaded area describes the difference between the two values, i.e., the overshoot.

which can be used as the parameter of a Poisson distribution that models the probability of n successful contacts in a day [114]:

$$P(n) = e^{-\theta}\frac{\theta^n}{n!} \tag{2.18}$$

but since only a successful contact is necessary to infect a single susceptible, the probability of a single individual not being infected in a day is given by:

$$P(0) = e^{-\theta} = e^{-\frac{\beta I}{N}} \tag{2.19}$$

Remembering that we considered an exponentially distributed recovery rate μ, the probability of an infected individual not recovering in a day is given by $e^{-\mu}$, and, naturally, the probability of recovering is $\hat{\mu} = 1 - e^{-\mu}$. Our discrete-time SIR model is, then [114]:

$$S^{t+1} = e^{-\frac{\beta I}{N}} S^t \tag{2.20}$$

$$I^{t+1} = \left(1 - e^{-\frac{\beta I}{N}}\right) S^t + (1 - \hat{\mu}) I^t \tag{2.21}$$

$$R^{t+1} = R^t + \hat{\mu} I^t \tag{2.22}$$

The basic reproduction number of this model is then given by:

$$R_0 = \frac{\beta}{\hat{\mu}} \tag{2.23}$$

which is pretty similar to the expression for the continuous-time model. However, if we use the values from Fig. 2.2, which are: $\beta = 0.25$, and $\mu = 1/10$, the reproduction number yields approximately 2.63 instead of 2.5. This happens because the probability of not being infected in an iteration is equivalent to considering that the number of infectious individuals is constant between $[t, t+1]$ in the continuous-time model and integrating dS/dt. We will show how to compute the basic reproduction number in discrete-time models in section 2.3.

Discrete time models are useful because they can easily be modified to consider stochasticity in the dynamics, whereas with continuous-time models it is not so trivial.

2.2.5 The SEIR model and other modifications

Naturally, one can extend the assumptions underlying the model to better describe the dynamics of the disease. A disease can have a period prior to the infectious phase that does not show symptoms, the incubation period. This compartment is usually called Exposed, thus the model being named Susceptible-Exposed-Infected-Recovered (SEIR) model (Fig. 2.4). The individual in the Exposed compartment can also be infectious, usually with reduced transmissibility. We arrive to:

$$\frac{dS}{dt} = -\beta \frac{\rho E + I}{N} S \tag{2.24}$$

$$\frac{dE}{dt} = \beta \frac{\rho E + I}{N} S - \gamma E \tag{2.25}$$

$$\frac{dI}{dt} = \gamma E - \mu I \tag{2.26}$$

$$\frac{dR}{dt} = \mu I \tag{2.27}$$

where ρ denotes the relative transmissibility of the exposed individual compared to the infected individual, and γ denotes the incubation rate.

Remembering that R_0 denotes the mean number of infections caused by a single infectious individual, we can infer the basic reproduction number of the SEIR model. An individual stays exposed with mean time $1/\gamma$ and has a probability of

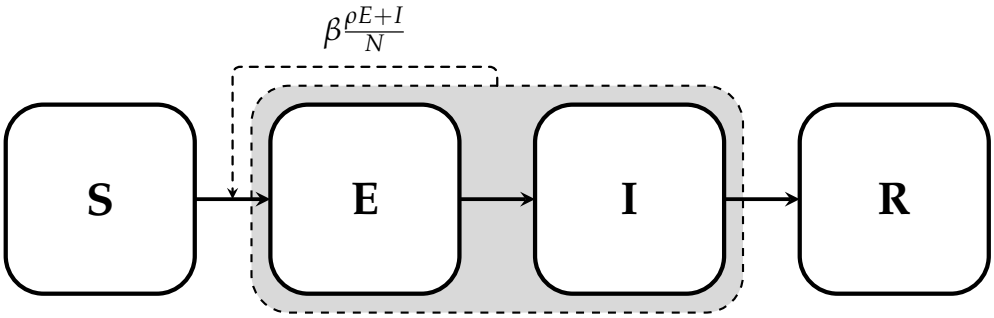

Figure 2.4: SEIR model diagram. The black arrows denote the evolution of the individuals between the compartments, and the dashed arrow denotes the transmission dynamics. The gray box encircles the transmissible compartments. The S box denotes the susceptible individuals, the E box denotes the exposed individuals, the I box denotes the infected individuals, and the R box denotes the recovered individuals.

infecting someone during this period given by $\beta\rho$, whereas during the infectious period $1/\mu$ their probability is given by β. Since we need to consider the entire interval that they can infect, we arrive at:

$$R_0 = \rho\frac{\beta}{\gamma} + \frac{\beta}{\mu} \tag{2.28}$$

Of course, this line of thinking only works in the simplest models. In section 2.3, we will present a procedural approach to the problem of estimating R_0.

Another basic modification one can consider is that the immunity conferred by the infection is not maintained forever. This is modelled by a Susceptible-Infected-Recovered-Susceptible (SIRS) model (Fig. 2.5), with equations given by:

$$\frac{dS}{dt} = -\beta\frac{I}{N}S + \omega R \tag{2.29}$$

$$\frac{dI}{dt} = \beta\frac{I}{N}S - \mu I \tag{2.30}$$

$$\frac{dR}{dt} = \mu I - \omega R \tag{2.31}$$

where ω is the waning immunity rate. This type of model has some interesting results, including that it may have a stationary solution where $I \neq 0$, thus characterizing an endemic disease. It can also be reduced to a model without immunity (the SIS model) if we set $\omega \to \infty$.

Some diseases can have multiple strains competing with each other. The

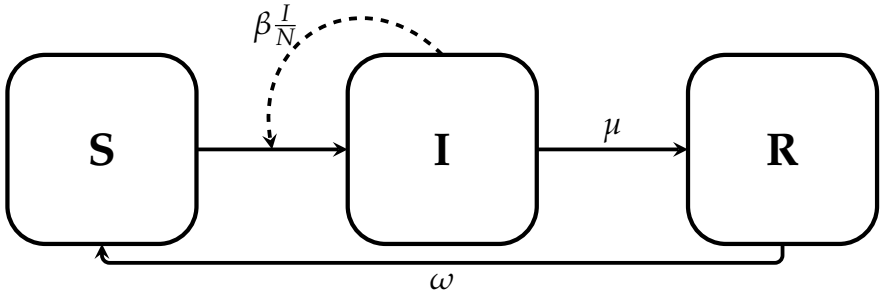

Figure 2.5: SIRS model diagram. The black arrows denote the evolution of the individuals between the compartments, and the dashed arrow denotes the transmission dynamics. The S box denotes the susceptible individuals, the I box denotes the infected individuals, and the R box denotes the recovered individuals.

simplest conceivable model is the two-strain SIR model where they share the same pool of susceptible individuals and an infection by any of them confer life-long immunity to both strains. Another possibility is having reduced immunity against the same strain and *cross immunity* against the other one. This immunity relationship can be encoded in a relative infectiousness matrix given by:

$$\rho = \begin{pmatrix} \rho_{1,1} & \rho_{1,2} \\ \rho_{2,1} & \rho_{2,2} \end{pmatrix} \tag{2.32}$$

where $\rho_{i,j}$ denotes an $i-$recovered individual being reinfected by the j strain.

The equations of this model are given by:

$$\frac{dS}{dt} = -\beta_1 \frac{I_1}{N} S - \beta_2 \frac{I_2}{N} \tag{2.33}$$

$$\frac{dI_1}{dt} = \beta_1 \frac{I_1}{N} S + \rho_{1,1}\beta_1 \frac{I_1}{N} R_1 + \rho_{2,1}\beta_1 \frac{I_1}{N} R_2 - \mu_1 I_1 \tag{2.34}$$

$$\frac{dI_2}{dt} = \beta_2 \frac{I_2}{N} S + \rho_{1,2}\beta_2 \frac{I_2}{N} R_1 + \rho_{2,2}\beta_2 \frac{I_2}{N} R_2 - \mu_2 I_2 \tag{2.35}$$

$$\frac{dR_1}{dt} = \mu_1 I_1 - \rho_{1,1}\beta_1 \frac{I_1}{N} R_1 - \rho_{1,2}\beta_2 \frac{I_2}{N} R_1 \tag{2.36}$$

$$\frac{dR_2}{dt} = \mu_2 I_2 - \rho_{2,1}\beta_1 \frac{I_1}{N} R_2 - \rho_{2,2}\beta_2 \frac{I_2}{N} R_2 \tag{2.37}$$

where β denotes the daily probability of infection per infectious contact and μ is the recovery rate. The numerical index denotes the strain.

One can readily derive the basic and effective reproduction numbers of each strain:

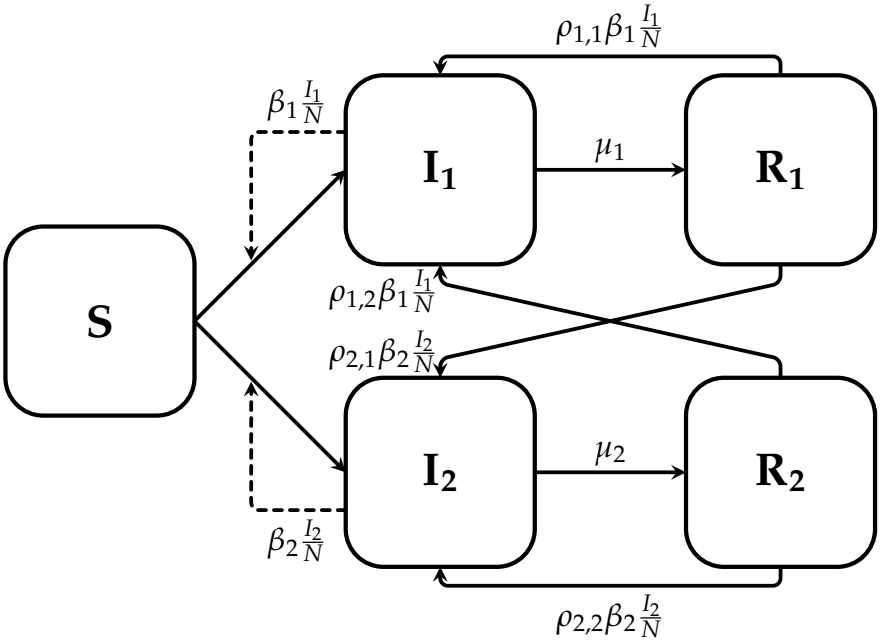

Figure 2.6: Two-strain SIR model diagram. The black arrows denote the evolution of the individuals between the compartments, and the dashed arrow denotes the transmission dynamics. The S box denotes the susceptible individuals, the I box denotes the infected individuals, and the R box denotes the recovered individuals. The subscripts denote the strains.

$$R_{0,1} = \frac{\beta_1}{\mu_1} \tag{2.38}$$

$$R_{t,1} = \frac{R_{0,1}}{N}(S + \rho_{1,1}R_1 + \rho_{2,1}R_2) \tag{2.39}$$

$$R_{0,2} = \frac{\beta_2}{\mu_2} \tag{2.40}$$

$$R_{t,2} = \frac{R_{0,2}}{N}(S + \rho_{1,2}R_1 + \rho_{2,2}R_2) \tag{2.41}$$

This type of model is important to study invasion by a new variant, such as done when Gamma invaded the original strain in Brazil [38], and leads to non-trivial solutions such as a strain with lower infectiousness invading a population because its immune escape is high enough to dominate when the prevalence of disease is high enough. Notice, however, that this type of model is only suited for short-term modelling due to the fact that being reinfected by a strain makes the individual lose the immunological memory from the previous infection. In Chapter 5, we develop a discrete-time two-strain model to study the impact of

vaccinating children against the Omicron variant.

Finally, these models can also assume subcompartments to consider age stratification, as individuals may have different contact rates and risks in outcome due to age. This is the case of COVID-19, and we develop age stratified and multiple disease severity compartment models in chapters 3, 4 and 5.

2.3 The Next Generation Matrix method

In this section we will derive a general method to compute the basic (and effective) reproduction number and the associated growth rate following the development by Driessche and Watmough [115] and Allen and Van Den Driessche [116]. The section will be separated in continuous and discrete-time models as they have slightly different procedures.

2.3.1 Continuous-time models reproduction number and growth rate

Let us start with the simplest, the SIR model. The first step is to separate the set of compartments in two groups x and y, the infectious and non-infectious groups, respectively. This implies in $x = \{I\}$ and $y = \{S, R\}$ for the SIR model. The second step is to separate each equation in the x set in the parts responsible to generate new infections $\mathcal{F}$ and to transition between compartments $\mathcal{V}$. In the case of SIR model:

$$\begin{aligned}\frac{dI}{dt} &= \mathcal{F}[I,(S,R)] - \mathcal{V}[I,(S,R)] \\ &= \beta\frac{SI}{N} - \mu I \\ \mathcal{F} &= \beta\frac{SI}{N} \\ \mathcal{V} &= \mu I\end{aligned}$$

As we aim to estimate the cases generated by a single individual at the start of the epidemic, we can linearize the model in the disease-free equilibrium, i.e.,

S, R = constant, and $I = 0$. This leads us to:

$$\left.\frac{d\mathcal{F}}{dI}\right|_{I=0} = F = \beta\frac{S}{N} \tag{2.42}$$

$$\left.\frac{d\mathcal{V}}{dI}\right|_{I=0} = V = \mu \tag{2.43}$$

As we want to estimate the cases from a single individual, we solve $\frac{dI}{dt}$ considering that $F = 0$. Giving us:

$$I(t) = \int_0^t \frac{dI}{dt}dt = -\mu\int_0^t Idt = I_0 e^{-\mu t} \tag{2.44}$$

we can take $I_0 = 1$ as we are considering a single individual.

The cases generated by this single individual can then be computed as:

$$R_t = \int_0^\infty FI(t)dt = \int_0^\infty \beta\frac{S}{N}e^{-\mu t}dt = \beta\frac{S}{N}\int_0^\infty e^{-\mu t}dt = \frac{\beta}{\mu}\frac{S}{N} \tag{2.45}$$

If we assume that the disease is newly invading, i.e., $S = N$, we have:

$$R_0 = \frac{\beta}{\mu} \tag{2.46}$$

Now let us consider a model with an arbitrary number of compartments, with n disease compartments and m nondisease compartments. This leads to $x \in \mathbb{R}^n$ and $y \in \mathbb{R}^m$ describing the disease and nondisease populations, respectively. Again, separating the model in the parts that generates new infections and the parts of the disease progression, we have:

$$\frac{dx_i}{dt} = \mathcal{F}_i(x,y) - \mathcal{V}_i(x,y), \qquad i = 1,\ldots,n \tag{2.47}$$

$$\frac{dy_j}{dt} = g_j(x,y), \qquad j = 1,\ldots,m \tag{2.48}$$

we then linearize the model around $(0, y_0)$, with:

$$[F]_{i,j} = F_{i,j} = \left.\frac{\partial\mathcal{F}_i}{\partial x_j}\right|_{(0,y_0)} \tag{2.49}$$

$$[V]_{i,j} = V_{i,j} = \left.\frac{\partial\mathcal{V}_i}{\partial x_j}\right|_{(0,y_0)} \tag{2.50}$$

with F and V being written as matrices.

The disease compartments equations then reads:

$$\frac{dx}{dt} = (F - V)x \tag{2.51}$$

We want, again, to solve $\frac{dx}{dt}$ in the absence of secondary infections, giving:

$$x(t) = e^{-Vt}x_0 \tag{2.52}$$

where the exponential of a matrix is given by the Taylor series:

$$e^A = I + A + \frac{A^2}{2} + \frac{A^3}{3!} + \dots$$

Now, integrating the secondary cases caused by an individual, we have:

$$\int_0^\infty Fe^{-Vt}x_0 dt = FV^{-1}x_0 \tag{2.53}$$

The matrix FV^{-1} is called the *next generation matrix* and R_0 is given by:

$$R_0 = \rho(FV^{-1}) \tag{2.54}$$

where $\rho(K)$ is the *spectral radius* of a matrix K, which is the maximum modulus of the eigenvalues of K. If K is irreducible, then $\rho(K)$ is a simple eigenvalue. If K is reducible, it can have multiple positive eigenvalues, generally related to multiple strains in the model. Naturally, we can compute R_t by considering other than purely susceptible populations in y_0. For a more complete discussion on the requirements of the model for this approach be valid, please refer to [115].

Finally, we can compute the growth rate of cases, which is simply the spectral radius of the Jacobian of the system, that we have already computed as $\mathbb{J} = F - V$, wielding:

$$r = \rho(F - V) \tag{2.55}$$

Furthermore, the eigenvector related to the dominant eigenvalue can be used as the proportion of individuals in each disease compartment, allowing to start a simulation mid-outbreak. We show some use cases in chapters 3 and 5.

Example: The SEIR model

Let us consider a more concrete example. We first separate the model in disease and non-disease compartments, giving $x = (E, I)$ and $y = (S, R)$. Remembering the equations (2.24)-(2.27), we have:

$$\mathcal{F}_E = \beta \frac{\rho E + I}{N} S \tag{2.56}$$

$$\mathcal{F}_I = 0 \tag{2.57}$$

$$\mathcal{V}_E = \gamma E \tag{2.58}$$

$$\mathcal{V}_I = -\gamma E + \mu I \tag{2.59}$$

yielding:

$$F = \begin{pmatrix} \beta\rho\frac{S}{N} & \beta\frac{S}{N} \\ 0 & 0 \end{pmatrix} \tag{2.60}$$

$$V = \begin{pmatrix} \gamma & 0 \\ -\gamma & \mu \end{pmatrix} \tag{2.61}$$

The next generation matrix is then given by:

$$FV^{-1} = \begin{pmatrix} \beta\frac{S}{N}\left(\frac{\rho}{\gamma} + \frac{1}{\mu}\right) & \frac{\beta}{\mu}\frac{S}{N} \\ 0 & 0 \end{pmatrix} \tag{2.62}$$

if we solve the eigenvalue problem of this matrix, we find:

$$\lambda_1 = \beta\frac{S}{N}\left(\frac{\rho}{\gamma} + \frac{1}{\mu}\right), \lambda_2 = 0 \tag{2.63}$$

Knowing that all parameters are positive, and using that $S = N$, we find:

$$R_0 = \rho\frac{\beta}{\gamma} + \frac{\beta}{\mu} \tag{2.64}$$

as expected.

The Jacobian of this system is given by:

$$J = \begin{pmatrix} \rho\beta\frac{S}{N} - \gamma & \beta\frac{S}{N} \\ \gamma & -\mu \end{pmatrix} \tag{2.65}$$

where the dominant eigenvalue can be computed by standard procedures.

2.3.2 Discrete-time models reproduction number and growth rate

We can develop an equivalent expression of R_0 and r for discrete-time models. We again separate the model in disease (x) and nondisease (y) compartments. Focusing on disease compartments, the equations related to them can be separated in parts related to generating new infections $(\mathcal{F})$ and parts related to transitioning between the disease compartments $(\mathcal{T})$, as done before. By assuming the disease-free equilibrium, we can linearize the model, wielding [116]:

$$x_{t+1} = (F + T)x_t \tag{2.66}$$

where $F + T$ is the Jacobian of the model. Notice the change in signal compared to the continuous-time expression.

The matrix T can be interpreted as the probabilities of transitioning between compartments and, as the sum of probabilities are at maximum 1, this implies in:

$$\sum_{i=1}^{n} T_{i,j} \leq 1, \forall\, j \in (1, \ldots, n) \tag{2.67}$$

where n is the number of disease compartments.

If we assume that there is no permanent infection, i.e., an individual always recovers or dies, this implies that $\lim_{k\to\infty} T^k x_0 = 0$ or, equivalently, $\lim_{k\to\infty} T^k = 0$. With this, we can say that:

$$\rho(T) < 1 \tag{2.68}$$

If we consider a starting number x_0 of infectious individuals, the number of secondary cases caused by them is given by:

$$Qx_0 = F(\mathbb{I}x_0 + Tx_0 + T^2x_0 + T^3x_0 + \ldots) \tag{2.69}$$

where $\mathbb{I}$ denotes the identity matrix.

Each power k of T multiplied by x_0 denotes the number of individuals that

have not recovered/died at iteration k and thus generates $FT^k x_0$ more secondary cases.

Our next generation matrix Q is then:

$$Q = F(\mathbb{I} + T + T^2 + T^3 + \dots) \tag{2.70}$$
$$= F(1 - T)^{-1} \tag{2.71}$$

where the second expression is possible because (2.68) is valid [117].

Then the basic reproduction number for discrete-time models is simply:

$$R_0 = \rho(Q) \tag{2.72}$$

and, again, R_t can be computed by considering y_0 different from completely susceptible population.

Instead of giving the growth rate of the system, the dominant eigenvalue of the Jacobian of a discrete time model gives the expansion rate. Thus, we need to log-transform the eigenvalue:

$$r = \ln(\rho(\mathbb{J})) \tag{2.73}$$

2.4 Vaccination models

Let us finish this chapter by talking about some basic models of vaccination, as this will be relevant throughout the text.

2.4.1 Pre-outbreak vaccination and the Herd Immunity Threshold

The simplest way to treat vaccination is by assuming that all individuals in a SIR model will be vaccinated prior to a disease outbreak, as usually occurs with the early Influenza vaccination in Brazil. Let us first assume that a vaccinated individual is completely protected from the disease. This essentially implies in removing the vaccinated population V from the pool of susceptibles, and R_t at the start of the outbreak may be calculating accordingly:

$$R_t(V) = \frac{\beta}{\mu}\left(1 - \frac{V}{N}\right) = R_0\left(1 - \frac{V}{N}\right) \tag{2.74}$$

When $R_t(V) \leq 1$, the outbreak does not start. This condition is fulfilled when:

$$\frac{V}{N} \geq 1 - \frac{1}{R_0} \tag{2.75}$$

and this vaccinated fraction threshold is called the *Herd Immunity Threshold* (HIT), a concept that literally comes from early bovine vaccination studies. This concept was borrowed during the COVID-19 pandemic to refer to immunization through infection, but ignored that for a person to be immunized in this way, the outbreak have to occur, leading to all the side effects related to COVID-19 infection, including life-long disabilities and death. It also ignored the overshoot effect discussed earlier, as R_t would only be 1 at the peak of the epidemic, meaning that it would still have to go all the way down the curve of active cases, which may lead to a difference up to 30% in the total number of cases, which is around 60 million individuals additionally infected when looking to the Brazilian population. Finally, it also has not considered the successive reinfections that SARS-CoV-2 is causing nowadays, showing that this strategy of containment is fundamentally flawed.

Even though some vaccines may have really high efficacy with long-lasting immunity, most vaccines have partial efficacy against infection. Assuming that the vaccine blocks infections at a proportion ε, R_t may be rewritten as:

$$R_t(V, \varepsilon) = \frac{\beta}{\mu}\left(1 - \varepsilon\frac{V}{N}\right) = R_0\left(1 - \varepsilon\frac{V}{N}\right) \tag{2.76}$$

The Herd Immunity Threshold is then given by:

$$\frac{V}{N} = \left(1 - \frac{1}{R_0}\right)\frac{1}{\varepsilon} \tag{2.77}$$

This also implies that if $\varepsilon < 1 - 1/R_0$, the outbreak would occur even if the entire population were vaccinated. Fig. 2.7 denotes the necessary vaccination coverage as function of R_0 and vaccine effectivity.

2.4.2 Vaccination in ongoing epidemics

We can now consider models of vaccination with ongoing epidemics, which adds a new level of complexity related to the vaccination rollout. How we interpret a partial effectivity is also something to consider. Here we show two ways to consider single dose vaccination in a SIR model. Chapter 3 shows a way to treat

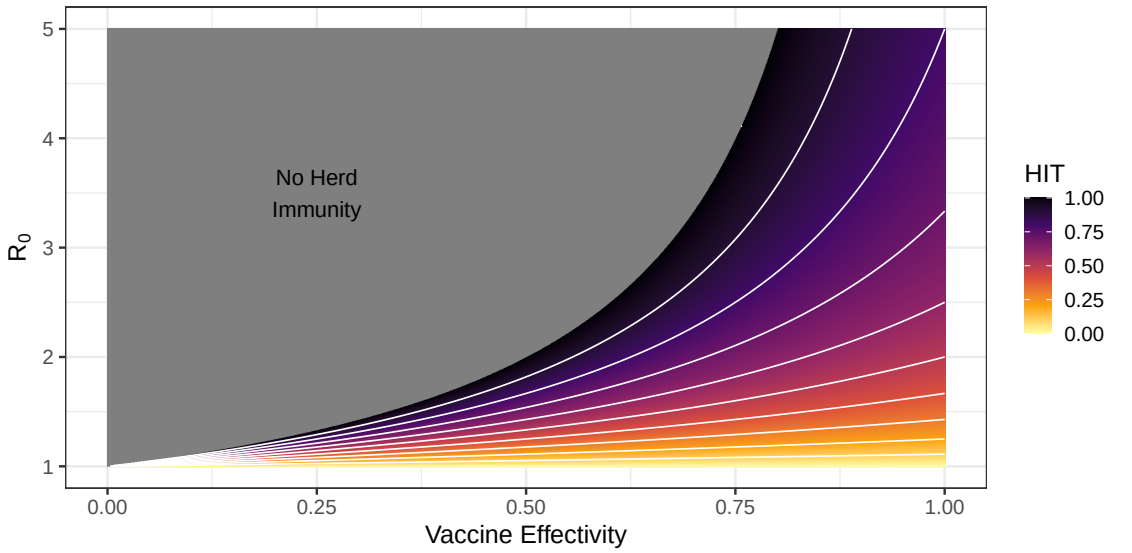

Figure 2.7: Herd Immunity Threshold as function of R_0 and vaccine effectivity. The gray area denotes combinations of values where HIT is not achievable, white lines denote equal-valued HIT in 0.1 bins.

two-dose vaccination in a COVID-19 scenario.

2.4.2.1 The "leaky" model

Let us assume that a vaccine acts only in reducing the number of infections, but other parameters such as recovery time are kept equal to non-vaccinated individuals. Let also assume that seropositive individuals are not vaccinated, as we consider life-long immunity from infection. Effectivity can then be modelled as partially reducing the probability of infection. This leads to a leaky vaccination model (Fig. 2.8):

$$\frac{dS}{dt} = -\beta\frac{I + I_v}{N}S - v(t) \tag{2.78}$$
$$\frac{dI}{dt} = \beta\frac{I + I_v}{N}S - \mu I \tag{2.79}$$
$$\frac{dR}{dt} = \mu I \tag{2.80}$$
$$\frac{dS_v}{dt} = -(1-\varepsilon)\beta\frac{I + I_v}{N}S_v + v(t) \tag{2.81}$$
$$\frac{dI_v}{dt} = (1-\varepsilon)\beta\frac{I + I_v}{N}S_v - \mu I_v \tag{2.82}$$
$$\frac{dR_v}{dt} = \mu I_v \tag{2.83}$$

where ε is the vaccine effectivity and $v(t)$ is the vaccination rate.

$v(t)$ can either be modelled as a simple exponential rate, meaning that the number of new vaccinated individuals goes down as the rollout progress, or can be modelled as an actual number of vaccines being inoculated per unit of time, but in the latter case the modeler must take care to avoid possible negative population in the susceptible compartment.

Notice that we replicated infected and recovered compartments for vaccinated individuals, but as we assumed that the vaccine only acts as reducing infections, we could transfer new vaccinated infections to the same infected compartment.

2.4.2.2 The "all-in" model

Whilst the leaky model assumes that everyone vaccinated receives partial protection from vaccine, the "all-in" model assumes that a part of the vaccinated population receives full protection, while the rest receives no protection. This leads to (Fig. 2.9):

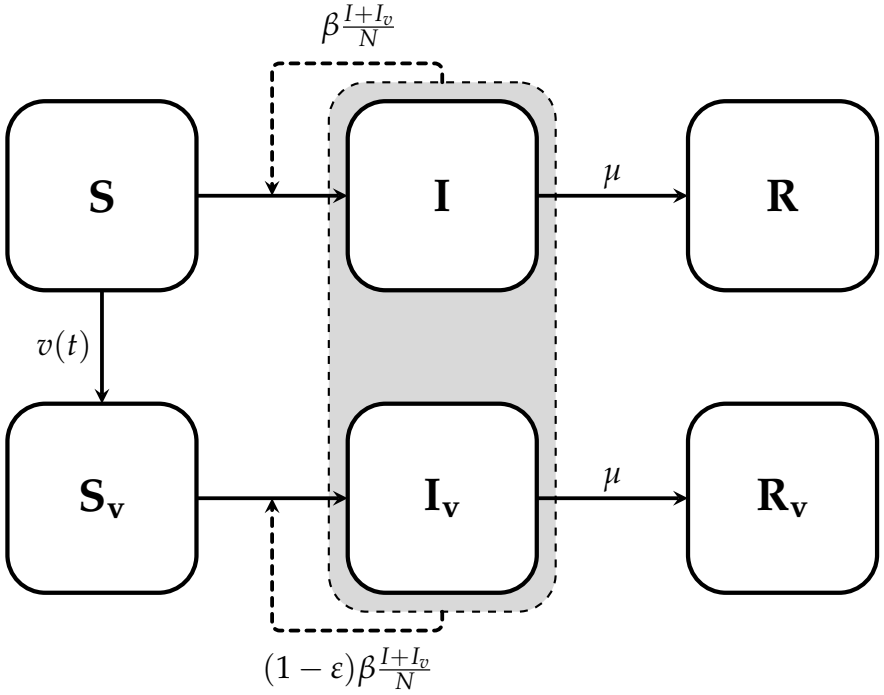

Figure 2.8: Leaky vaccination SIR model diagram. The black arrows denote the evolution of the individuals between the compartments, and the dashed arrow denotes the transmission dynamics. The gray box encircles the transmissible compartments. The S box denotes the susceptible individuals, the I box denotes the infected individuals, and the R box denotes the recovered individuals. The subscripts denote the vaccination status.

$$\frac{dS}{dt} = -\beta\frac{I+I_v}{N}S - v(t) \tag{2.84}$$
$$\frac{dI}{dt} = \beta\frac{I+I_v}{N}S - \mu I \tag{2.85}$$
$$\frac{dR}{dt} = \mu I \tag{2.86}$$
$$\frac{dV}{dt} = \epsilon v(t) \tag{2.87}$$
$$\frac{dS_v}{dt} = -\beta\frac{I+I_v}{N}S_v + (1-\epsilon)v(t) \tag{2.88}$$
$$\frac{dI_v}{dt} = \beta\frac{I+I_v}{N}S_v - \mu I_v \tag{2.89}$$
$$\frac{dR_v}{dt} = \mu I_v \tag{2.90}$$

Whilst it is interesting to develop many ways to model vaccination, it is a bit

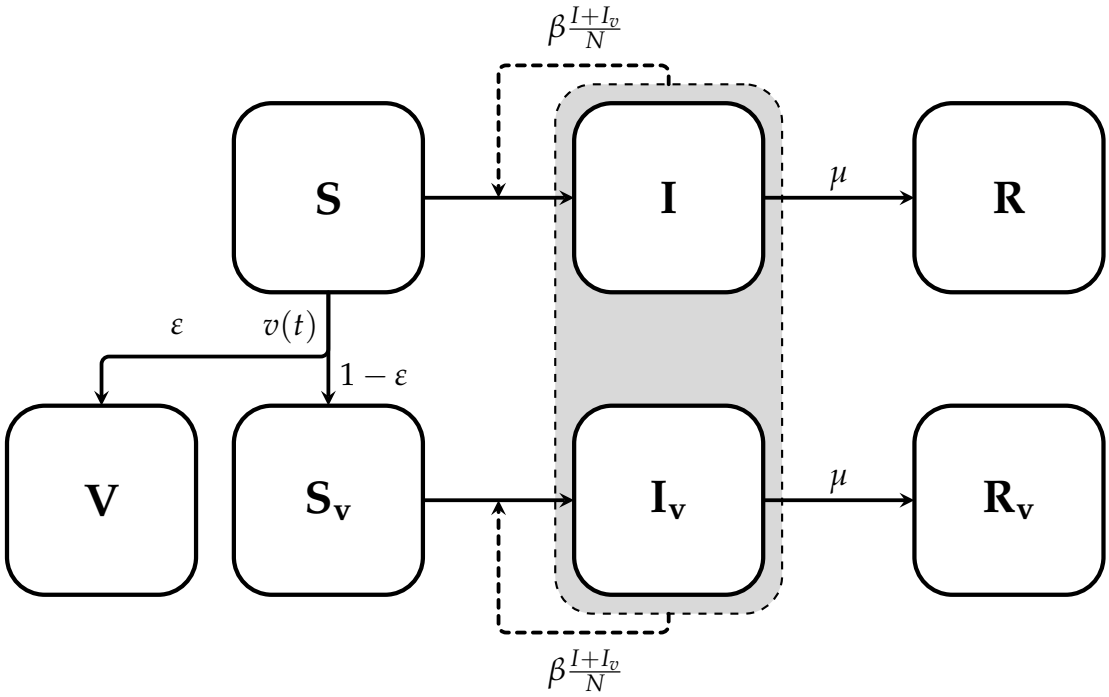

Figure 2.9: All-in vaccination SIR model diagram. The black arrows denote the evolution of the individuals between the compartments, and the dashed arrow denotes the transmission dynamics. The gray box encircles the transmissible compartments. The S box denotes the susceptible individuals, the I box denotes the infected individuals, the R box denotes the recovered individuals, and the V compartment denotes the fully protected vaccinated individuals. The v subscripts denote the vaccinated and unprotected compartments.

harder to understand breakthrough infections in the “all-in" framework. It also gets even more complicated when we study two-dose vaccination rollouts, as it would imply full protection with a single dose in some cases, while having no protection with both doses for others. Adding to that, Bubar et al. [103] have shown that the two frameworks have almost no difference from the standpoint of vaccination strategies. We then adopt the “leaky” framework in our vaccination models in the following chapters.

Chapter 3

Assessing the best time interval between doses in a two-dose vaccination regimen to reduce the number of deaths in an ongoing epidemic of SARS-CoV-2

This work was done by Leonardo Souto Ferreira[1,2], Otavio Canton[1,2], Rafael Lopes Paixão da Silva[1,2], Silas Poloni[1,2], Vítor Sudbrack[1,2,3], Marcelo Eduardo Borges[2,4], Caroline Franco[1,2,5], Flavia Maria Darcie Marquitti[2,6], José Cássio de Moraes[2,7], Maria Amélia de Sousa Mascena Veras[2,7], Roberto André Kraenkel[1,2] and Renato Mendes Coutinho[2,4] and it was published at *PLOS Computational Biology* in March 2022 at [118]. The author of this thesis was the first author in the article and has developed the model, software, formal analysis, investigation, and writing. The other authors also contributed during all phases of production.

Abstract

The SARS-CoV-2 pandemic is a major concern all over the world and, as vaccines became available at the end of 2020, optimal vaccination strategies were subjected to intense investigation. Considering their critical role in reducing disease burden, the increasing demand outpacing production, and that most currently approved vaccines follow a two-dose regimen, the cost-effectiveness of delaying the second dose to increment the coverage of the population

[1]Instituto de Física Teórica, Universidade Estadual Paulista, São Paulo, Brazil.
[2]Observatório COVID-19 BR, São Paulo, Brazil.
[3]Department of Ecology and Evolution, University of Lausanne, Lausanne, Switzerland.
[4]Centro de Matemática, Computação e Cognição, Universidade Federal do ABC, Santo André, Brazil.
[5]Big Data Institute, Li Ka Shing Centre for Health Information and Discovery, Nuffield Department of Medicine, University of Oxford, Oxford, United Kingdom.
[6]Instituto de Física 'Gleb Wataghin' and Instituto de Biologia, Universidade Estadual de Campinas, Campinas, Brazil.
[7]Faculdade de Ciências Médicas da Santa Casa de São Paulo, São Paulo, Brazil.

receiving the first dose is often debated. Finding the best solution is complex due to the trade-off between vaccinating more people with lower level of protection and guaranteeing higher protection to a fewer number of individuals. Here we present a novel extended age-structured SEIR mathematical model that includes a two-dose vaccination schedule with a between-doses delay modelled through delay differential equations and linear optimization of vaccination rates. By maintaining the minimum stock of vaccines under a given production rate, we evaluate the dose interval that minimizes the number of deaths. We found that the best strategy depends on an interplay between the vaccine production rate and the relative efficacy of the first dose. In the scenario of low first-dose efficacy, it is always better to vaccinate the second dose as soon as possible, while for high first-dose efficacy, the best strategy of time window depends on the production rate and also on second-dose efficacy provided by each type of vaccine. We also found that the rate of spread of the infection does not affect significantly the thresholds of the best window, but is an important factor in the absolute number of total deaths. These conclusions point to the need to carefully take into account both vaccine characteristics and roll-out speed to optimize the outcome of vaccination strategies.

3.1 Introduction

As the implementations of SARS-CoV-2 vaccination programs evolve in several countries around the world, governments must decide how to allocate doses among the population during the epidemic, usually prioritizing the most at-risk groups, such as healthcare workers, people with comorbidities, and older adults. In a context of limited vaccine supply, an optimized dose allocation strategy is critical to effectively immunize the population whilst achieving the best reduction in hospitalizations and deaths. On this basis, some countries considered partially protecting a greater percentage of the population by administering the first dose more widely at the expense of delaying second doses, and thus having less fully vaccinated individuals [119, 120, 121].

Vaccination programs can have different goals, depending on the context and characteristics of both the disease and the available vaccines. The immunization program against Covid-19 has focused on reducing the burden of hospitalizations and deaths, which is justified given the risk of health care system collapse and the lack of vaccine supplies to quickly reach the high coverage required to substantially reduce infections. Another strong argument for that strategy is that many of the

current vaccines are highly effective against hospitalization and death, but not in preventing new infections. For instance, AZD1222 (Oxford/AstraZeneca) has shown an efficacy of 86% (95% CI: 53-96%) against hospitalization [122], but 59.9% (95% CI: 35.8-75.0%) effective against new infections measured by nucleic acid amplification-positive tests [123]; for CoronaVac (Sinovac) this contrast is even starker with 83.7% (95% CI: 58.0-93.7%) efficacy against severe cases but only 50.7% (95% CI: 35.9-62.0%) for mild symptomatic cases as outcome [124]. Even BNT162b2 (Pfizer/BioNTech), which showed high efficacy against infections in the first trials [125] may provide a lower protection against new variants, as exemplified by the variant B.1.617.2 (also known as Delta) [126]. In this context, vaccination programs in many countries have prioritized the groups most at risk of developing severe disease, namely high exposure individuals (*e.g.*, health care professionals), people with aggravating conditions, and older adults [127, 128].

Mathematical models in epidemiology have been widely used to assess optimal vaccination strategies for a variety of communicable diseases [129, 130, 131, 132, 133]. In a previous study on influenza viruses, [134] explored how two different vaccination strategies (single dose or two dose) could be integrated into pandemic control plans of a limited vaccination supply. They conclude that the best strategy depends on the level of partial protection introduced by a single dose, but the study is limited to pre-pandemic vaccination scenario and does not capture vaccination roll-out during a pandemic.

Mass vaccination strategies have been proposed as the main approach to tackle the spread of SARS-CoV-2, complementing or replacing non-pharmaceutical interventions (NPIs). SIR-like models have pointed to the possibility of securely relaxing NPIs months after vaccination campaigns, depending on the rate of vaccination, as shown by [135]. The same work also suggests that, given a low roll-out rate scenario, one-dose strategies allow safe relaxation of NPIs sooner if the first dose corresponds to more than 80% of the vaccination protection (vaccination parameters based on BNT162b2). Although one-dose vaccination allows earlier relaxation of NPIs, it requires a slower transition to pre-pandemic levels for more vaccines to be delivered. The one-dose scheme is modelled as an effectively weaker vaccine, with no second doses being considered in the long run.

In this work, we aim to find the best time-window between doses under different scenarios of relative efficacy of the first dose and infection rate in the population. We assess these scenarios for the three most used vaccine platforms, namely inactivated virus, viral vector of adenovirus, and mRNA-based vaccines.

Given that most vaccination protocols requires a second dose, we introduce a mathematical model that rigorously describes a two-dose vaccination scheme and optimal allocation of vaccines through delay differential equations. We explore the consequences of different strategies regarding the time-window between the two vaccine doses. The distribution of available vaccines for the first and second dose is optimized for each between-doses time interval, assuming a constant production rate. The partial protection offered by single-dose vaccination compared to double-dose vaccination is controlled by a single relative efficacy parameter. The best strategy, considering time interval between doses for the vaccine type, is defined based on the lowest total number of deaths in the range of time analyzed. We find that the best strategy depends on the interplay between the vaccine production rate and the single-dose relative efficacy, with the effective reproduction number being an important factor for the reduction of deaths.

3.2 Methods

To investigate the impact on total hospitalizations and mortality of delaying the second dose in a two-dose vaccination roll-out during an ongoing epidemic, we built a model that takes into account the severity of the disease, age classes (the main risk factor for severity and death), and vaccination status.

Our model consists of an **SEIR** model extended to account for asymptomatic, severe/hospitalized, and deceased individuals, thus being named **SEAIHRD**, corresponding to susceptible, pre-symptomatic, asymptomatic, mildly symptomatic, severely symptomatic/hospitalized, recovered, and deceased classes respectively. Each epidemiological class comprises three age classes, namely children and teenagers (0-19), adults (20-59), and older adults (60+) classes. To account for vaccinated individuals with one or two doses, we have duplicated this set of classes for individuals who received one dose and two doses, which have different epidemiological parameters, as discussed below. The model structure is shown in Fig 3.1 and the model equations are presented in Appendix A.

The demographic characteristics of the population were based on the State of São Paulo, Brazil. The basic epidemiological parameters come from current literature and are detailed in Appendix A.2. The daily contact rates between age classes are based on the matrices projected by [136], from which we use the Brazilian all-locations average for simplicity, reducing the age compartments using the same approach as in [38] (Supplementary material, section 3).

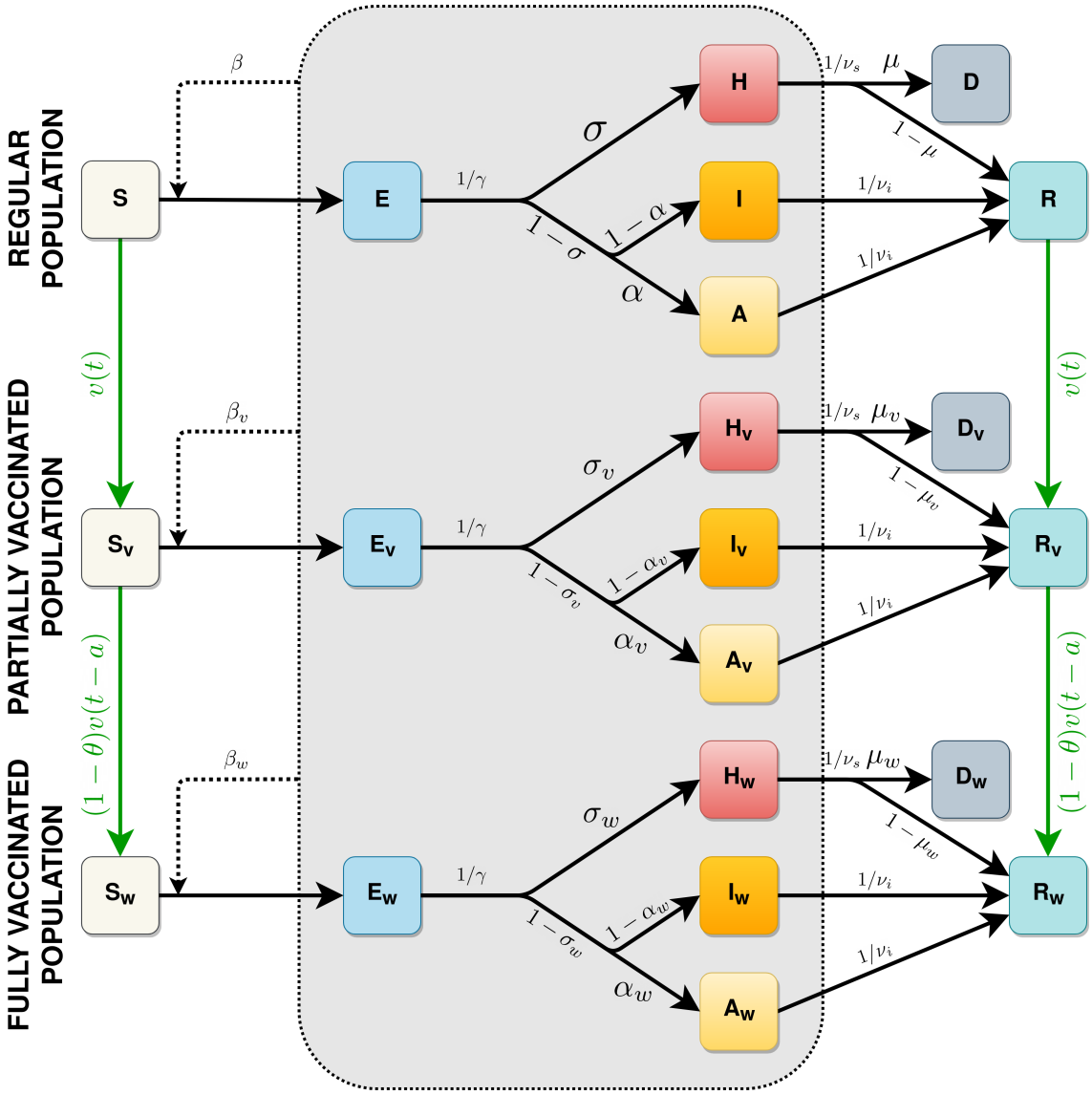

Figure 3.1: Diagram representing the full model structure. Subscripts v and w indicate the first- and second-dose vaccinated classes, respectively. Black arrows indicate transitions between epidemiological stages, green arrows indicate vaccination. All classes pictured inside the gray box are infectious. Because epidemiological progressions happen at time-scales shorter than those related to vaccine effects, infectious classes are not vaccinated in the model.

We assume a "leaky" vaccination effect, in which vaccinated individuals receives partial protection, in contrast to the "all-in" model where part of the vaccinated individuals receives full protection. [103] has shown that the outcome of these models do not differ substantially, and the leaky model is simpler to understand and to implement.

The main parameters that describe the vaccination dynamics are the vaccine's protective effect against (i) acquiring the disease, (ii) developing symptoms, (iii) developing severe symptoms (i.e., leading to hospitalization), and (iv) death. We present our analysis using sets of parameters that represent three types of vaccine developed for Sars-Cov-2; inactivated virus (CoronaVac, from Sinovac), adenovirus-based vaccine (AZD1222, from AstraZeneca-Oxford) and mRNA (BNT162b2, from Pfizer-BioNTech). The parameters for each vaccine are shown in Table 3.1.

Table 3.1: Parameters related to vaccine efficacy.

Parameter	Description	CoronaVac	AZD1222	BNT162b2
$E_{\beta,w}$	Observed efficacy against infectious contact given second dose	0.00[a]	0.599 [123]	0.90 [137]
$E_{\alpha,w}$	Observed efficacy against clinical symptoms given second dose	0.50 [124]	0.813 [123]	0.94 [137]
$E_{\sigma,w}$	Observed efficacy against hospitalization given second dose	0.83 [124]	0.900[b]	0.87 [137]
$E_{\mu,w}$	Observed efficacy against death given second dose	0.95[b]	0.950[b]	0.98[b]
$\epsilon_{\beta,w}$	Protection against infectious contact with second dose	0.000	0.599	0.900
$\epsilon_{\alpha,w}$	Protection against clinical symptoms given second dose	[0.499, 0.498, 0.494]	[0.533, 0.533, 0.537]	[0.402, 0.415, 0.494]
$\epsilon_{\sigma,w}$	Protection against hospitalization of infected individual given second dose	0.830	0.750	-0.300
$\epsilon_{\mu,w}$	Protection against death of hospitalized cases given second dose	0.706	0.500	0.846

[a] Assumed. There is no data available yet.
[b] Assumed. The value reported had no statistical significance.

The observed efficacies are obtained from trials or effectiveness studies. The parameters of protection are calculated through the method explained in Appendix A.2.1.

As the required parameters may not be available in the studies for each vaccine, specially regarding the efficacy of a single dose, we simplify the problem by assuming that the efficacy for each outcome is proportional to the efficacy after the second dose by a fixed ratio, called *relative efficacy of the first dose*. This is a key parameter influencing the model outcome: if it is too small it is better to vaccinate the second dose sooner, but the opposite should be expected if the efficacy with one dose is as large as with two doses. Thus, we vary this parameter over all reasonable values (0-100%).

As the efficacy related to a specific outcome can be caused by a multiplicative effect of efficacy related to another outcome, (for example, lower number of deaths caused by a lower number of hospitalizations), we translate mathematically the observed efficacies that come from field studies to the parameters used in the mathematical model, as described in Appendix A.2.1. The values of parameters used in the model are given in Table 3.1. Notice that this mathematical translation

makes the protection against clinical symptoms age-dependent, and also makes the protection against hospitalization for BNT162b2 negative. The latter case occurs because the efficacy against hospitalization is lower than the efficacy against infectious contact, but when the parameters of protection are multiplied as in the model's equations (Appendix A.1) the value of efficacy is recovered.

Since we aim to study vaccination roll-out during an ongoing epidemic, we set the initial conditions for recovered and infectious populations using estimated values from hospitalization data. The procedure follows closely the one presented in [38], and is described in Appendix A.3. We use epidemiological and demographic data from the state of São Paulo, Brazil, although we do not expect the results to change substantially from one region to another.

We do not explicitly implement non-pharmaceutical interventions in our study, opting instead to model different scenarios by fixing the initial value of the effective reproduction number R_t. Thus, we computed R_t using the method of Next Generation Matrix (for details, see Appendix A.3) and chose the value of probability of infection per contact (β) that yields the desired value of R_t at the beginning of the simulation. We vary this initial R_t between 0.9 and 1.4, accounting for potentially more transmissible variants [38, 138] or increased contact rates due to less rigid non-pharmaceutical interventions.

The distribution of vaccines follows the priority of age groups: first older adults, then adults, and at last children and teenagers [128]. We assume that serological tests are not performed before vaccination, therefore vaccination does not depend on the individual's previous serological status. Thus, susceptible and recovered individuals are vaccinated proportionally to the compartment's population size. Severe and symptomatic individuals do not receive doses while infectious due to noticeable infection. We also exclude pre-symptomatic and asymptomatic from vaccination, since it would lead to unrealistic immediate benefits and there is a window between the date of vaccination and the start of protective effects. Recovered individuals are assumed to be completely immune and, since we fix our simulation interval at 300 days, we consider that the effects of waning immunity can be negligible. Likewise, we ignore aging dynamics, since it would be relevant only at much longer time scales.

Our model specifies that the time between first and second doses (a) is fixed for all individuals, which leads to a delay differential equation formulation. In contrast, constant rate models, where individuals receive the second dose at a fixed rate with an exponential distribution of times, would imply that some of

them immediately receive the second dose and lead to incorrect average times between doses when vaccination rates fluctuate over time. We also allow for a proportion θ of individuals that take the first but not the second dose, representing abandonment; this value is fixed at 0.1 throughout our simulations (in the case of CoronaVac vaccine phase 3 trial, the rate of abandonment was 0.16 [139]).

To optimally allocate the vaccination, keeping the number of stocked vaccines as low as possible while ensuring that second doses are available, we solve a delayed optimization problem that is described in the following section. After minimizing the vaccine stock for the different time interval between doses, we calculate the number of deaths each vaccine type and time interval produces, and we choose the time window for each vaccine by considering the one with the lowest number of deaths, and this is considered the best window.

3.2.1 Optimizing vaccination roll-out

We write a dynamical equation for the vaccine stock $V(t)$ assuming a constant production (or deployment) rate p and a varying withdrawal rate is given by the vaccination rate $v(t)$, which can be chosen, that is, it is the control variable. We impose that a constant fraction $\theta' = 1 - \theta$ of the people who take the first dose will receive the second one after a period a, so we must be careful that the total vaccination rate is the sum of both first and second dose vaccination rates and it is limited to a maximum rate of vaccination v_{max}, but the control variable is the vaccination rate of first doses only. We also assume that there's an initial stock of vaccines V_0. The equation for $V(t)$ then is:

$$\begin{cases} \dfrac{dV}{dt} & = p - v(t) - \theta' v(t-a) \\ V(0) & = V_0\,, \qquad v(t) = 0 \,\forall\, t < 0 \end{cases} \tag{3.1}$$

We note already that we can solve this equation, obtaining

$$V(t) = V_0 + pt - \int_0^t v(t')dt' - \theta' \int_0^{t-a} v(t')dt' \tag{3.2}$$

We define the optimization problem by stating the objective function to be minimized and the restrictions that the solution must obey. Since we want to use vaccine doses as quickly as possible, a reasonable goal is to minimize the stock of vaccines $V(t)$. With that, we impose that the total vaccination rate is limited by a certain maximum value, and of course, it is positive; also, the vaccine stock $V(t)$ is

always positive. Finally, we must ensure that in the period after the simulation ends ($t > T$) there will be enough doses left to use as second doses on those who have already taken the first dose.

These considerations lead to the following optimization problem:

$$\begin{aligned} \min_f J &= \int_0^T V(t)dt \\ \text{subject to } & v(t) \geq 0 \\ & v(t) + \theta' v(t-a) \leq v_{max} \\ & V(t) \geq 0 \\ & V(T) \geq \theta' \int_{T-a}^{T} v(t')dt' - pa \end{aligned} \tag{3.3}$$

Solution

We can solve the problem defined by Eqs. (3.2, 3.3) using linear programming. This is feasible because the objective function and all constraints are linear functions of the control variable v and state variable V and, as Eq.(3.2) shows, V is linear on the control variable.

We first discretize the time in n intervals of length $\Delta t = \frac{T}{n}$, each interval ending at t_i, $i = 1, \ldots, n$, and assume that the control function will be constant over each interval (that is, a step function), with values $\vec{x} = (v(t_1), v(t_2), \ldots, v(t_n))$. Eq.(3.2) then becomes

$$V(t_i) = V_0 + pt_i - \sum_{j=1}^{i} x_j - \theta' \sum_{j=1}^{i-\hat{a}} x_j \,, \tag{3.4}$$

and we seek to minimize the objective function (given by Eq.(3.3), up to a constant) that is a linear function of $\vec{x}$, subject to the (linear) restrictions.

The discrete version of the problem becomes:

$$\begin{aligned}
&\min_{\vec{x}} J = \min_{\vec{x}} -\sum_{j=1}^{n}\left[\sum_{i=1}^{j} x_i + \theta' \sum_{i=1}^{j-\hat{a}} x_i\right] \\
&\text{subject to } \vec{x} \geq 0 \\
&\qquad x_i + \theta' x_{i-\hat{a}} \leq v_{max} \text{ , for } i = 1, \ldots, n \\
&\qquad \sum_{i=1}^{j} x_i + \theta' \sum_{i=1}^{j-\hat{a}} x_i \leq V_0 + pt_i \text{ , for } j = 1, \ldots, n \\
&\qquad (1+\theta') \sum_{i=1}^{n} x_i \leq V_0 + p(t_n + a) \text{ ,}
\end{aligned} \tag{3.5}$$

where $\hat{a} = \frac{a}{\Delta t}$ (chosen so that $\hat{a}$ is integer), and, to simplify notation, x_i is taken to be zero over values of i below 1.

These conditions can readily be written in matrix form and solved using standard linear programming algorithms. We implemented them in R using the package `lpSolve` [140] to solve the linear programming problem.

Finally, to assess which conditions is best to employ a longer (up to 12 weeks) or shorter (at least 3 weeks) interval between first and second doses, we simulate the model and compute the total number of deaths across all ages and vaccination status at the end of a period of 300 days, choosing as the best strategy of window the one that has the lowest number of deaths. We performed this comparison by varying the relative efficacy of the first dose and also the parameters related to the current rate of infection (R_t) and vaccine production rate.

3.3 Results

The optimal vaccine roll-out with time between doses of 3 and 12 weeks is shown in Fig 3.2. We can see that for reasonable parameters of production and vaccination rate for São Paulo State, the vaccine stock can be kept close to zero (i.e. all doses can be used immediately) after about 30 days after the beginning of vaccination when using a time interval of 3 weeks. For the time interval of 12 weeks, the stock is kept close to zero during the first stage of the first dose vaccination, but doses need to be stored to be used as second-doses for a small time window. In both cases, we see a pattern of alternating stages of first and second dose vaccination, while optimally keeping the stock of vaccines close to zero.

By varying the initial values of R_t for a fixed production rate (Fig 3.3), we see

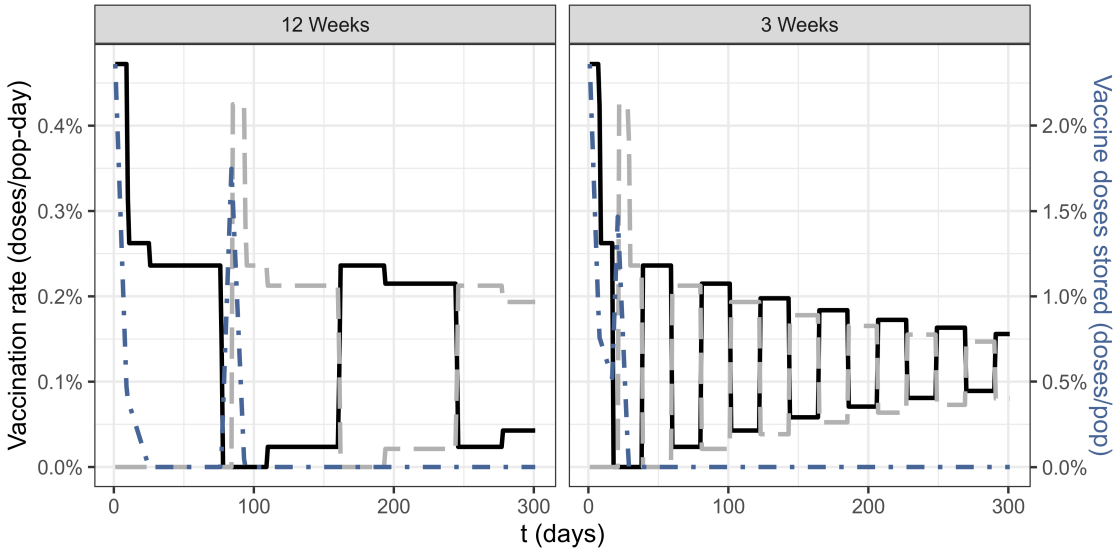

Figure 3.2: Vaccination rate as a function of time for first (solid, black) and second doses (dashed, grey) – scale is given by the left y-axis. Number of stored vaccine doses as function of time (dot-dashed, blue), scale in the right y-axis. Taking into account 3 or 12 weeks (panels) as separation between doses. $V_0 = 2.83\%$ of population in doses, $\rho(t) = 0.23\%$ of population in doses/day, $v_{max} = 0.45\%$ of population in doses/day.

that longer periods between the first and second doses led to a lower number of deaths when the relative efficacy of the first dose alone is higher than approximately 60%, whereas smaller time intervals are better if the relative efficacy is lower than approximately 50%, and intermediary periods are the best interval between doses if the relative efficacy is between 50% and 60%. It is also important to note that the value of initial R_t does not substantially affect the value of relative efficacy where transitions between best time windows occur, but is an important factor in the absolute value of deaths.

Since our results show that the best time window is not strongly dependant on the value of R_t, we fixed this value at 1.1 and varied the relative efficacy and production rate. Then, we compare the best window relative to the reduction in deaths for several time window intervals (Fig 3.4). The result is computed by simulating a coarse grid of values and then linearly interpolating a finer mesh. For all vaccines, relative efficacy of the first dose below approximately 45% indicates that regardless of the vaccine production rate, the best strategy to reduce mortality is to complete the two-dose scheme 3 weeks after the initial dose. If the production rate is low (approximately below 0.2% of doses/population-day), increasing the relative efficacy above 45% rapidly shifts the best time window to increasingly

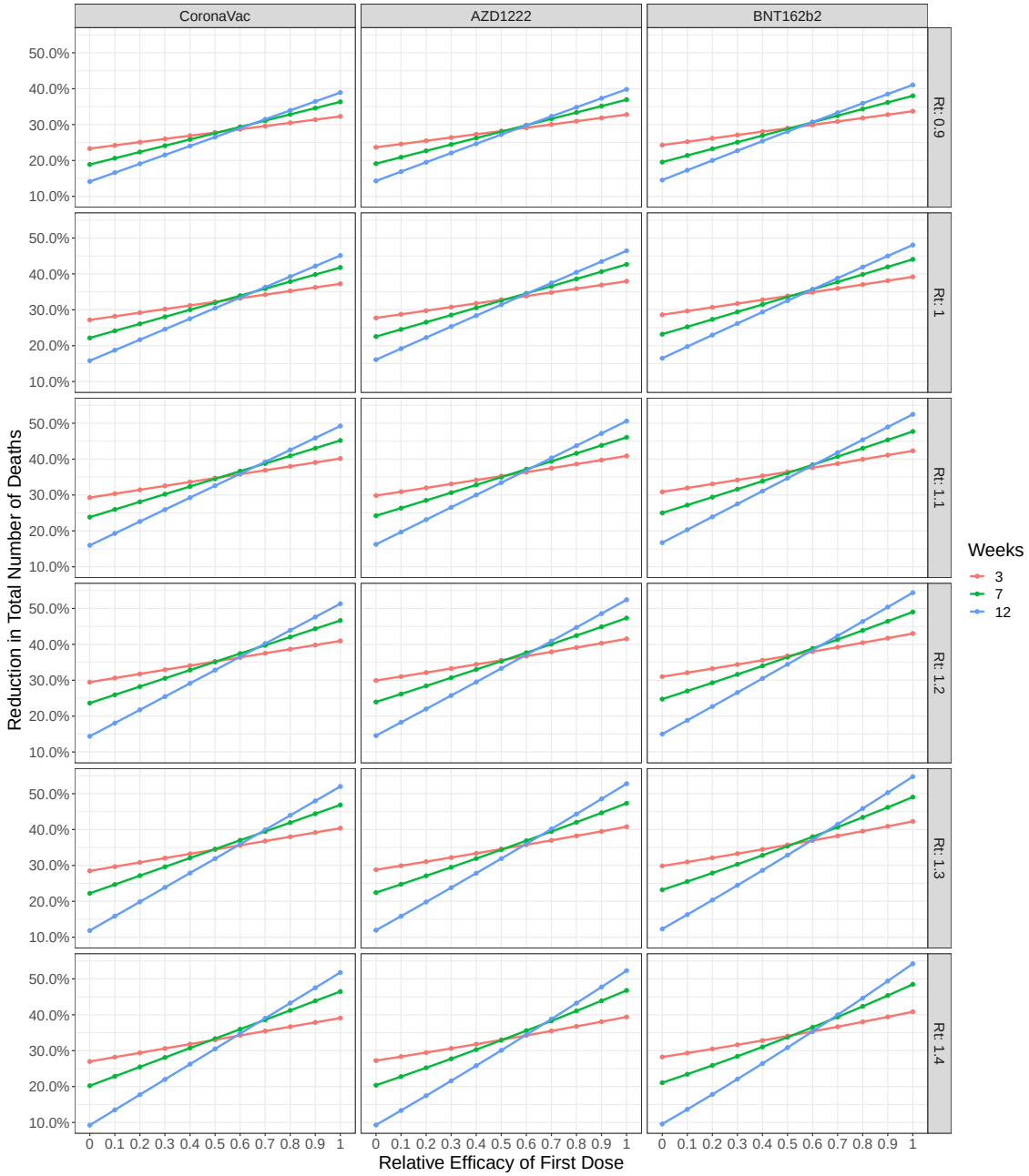

Figure 3.3: Reduction in total number of deaths as function of the first dose relative efficacy, considering three time windows between doses: 3,7 and 12 weeks (colors); varying vaccine type (columns); and effective reproduction number at the start of simulation (rows). $V_0 = 2.83\%$ of population in doses, $\rho(t) = 0.23\%$ of population in doses/day, $v_{max} = 0.45\%$ of population in doses/day.

larger periods, and converges to the maximum interval of 12 weeks. However, on this same range for the relative efficacy of the first dose, increasing the production rates results in a non-linear transition to shorter time-windows.

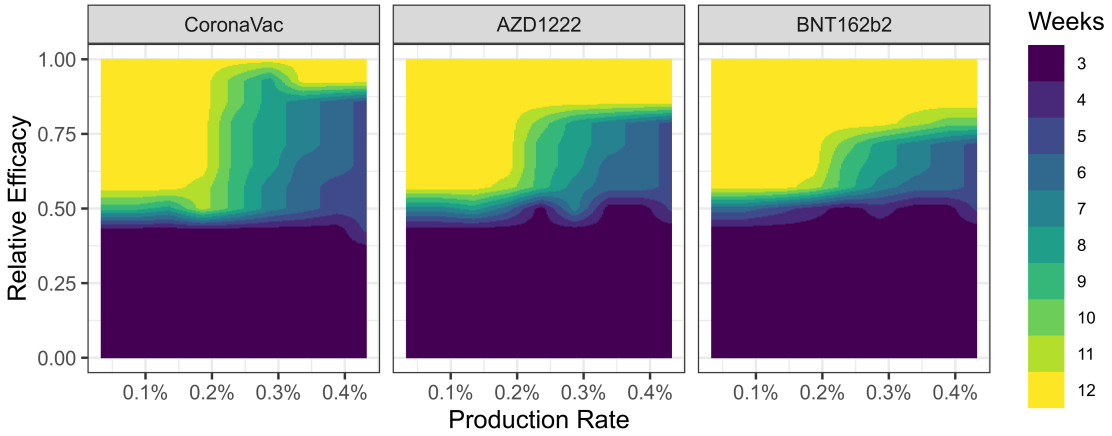

Figure 3.4: Best window (color) for reduction of deaths as function of production rate (x axis) and relative efficacy of first dose (y axis). Each panel represents a different vaccine with the respective second dose parameters. The initial R_t is 1.1, V_0 is set to zero, vaccination rate limited to approximately 0.45% of population in doses per day.

Although it is expected that the best time window should always increase with higher relative efficacy, and decrease with higher production rate, the latter hypothesis is sometimes violated in the simulations (Fig 3.4). Despite that, the general pattern is largely unaltered.

3.4 Discussion

Our model evaluates the best time windows between first and second doses for individuals in a context of limited vaccine supply in the ongoing COVID-19 pandemic. We found that the time window that best reduces the mortality depends on the interplay between two key parameters: vaccine production rate and the relative efficacy of the first dose. Within the simulated regimes with low single-dose efficacy, the resulting best strategy consistently relied on allocating the available doses to complete the two-dose scheme at the shortest time possible to provide the vaccine's maximum protection and minimize the mortality of the population. However, when the first dose presents a higher level of relative efficacy and vaccine supply is restricted, the best strategy relied on prioritizing the allocation of doses to increase the proportion of the population receiving the

first dose, resulting in a longer interval between doses to effectively allocate the use of the limited vaccine supply. Further, this interval is shortened by increasing the vaccine supply, as it progressively alleviates the conflict on dose allocation. Given that the effective reproduction number has little effect when considering the best window between doses, this further ensures the applicability of our results to other locations.

Another important parameter that varies across vaccines is the protection against infection, *i.e.* reduction in susceptibility, after the second dose, with values of 0, 0.6 and 0.9 for CoronaVac, AZD1222 and BNT162b2 respectively (See table 3.1). This difference allows for larger delays with lower relative efficacy of the first dose, even with similar protection against deaths (0.95, 0.95, 0.98, in the same order) simply by avoiding new infections.

Given the key role of the efficacy of the first dose in deciding the best strategy to reduce mortality, it is worth considering the best available knowledge for the vaccines evaluated in this study. Preliminary results of the effectiveness of the inactivated virus vaccine CoronaVac in Chile have shown that the first-dose efficacy of that vaccine is substantially lower before the second dose vaccination, with effectiveness against symptomatic infection being 17.2% (95% CI: 15.8–18.6%) [141]. This result, together with previous studies concerning inactivated virus vaccines showing that the protection against infectious contact is likely to be low [142, 143], suggests that the safest strategy concerning the second dose of CoronaVac is a three-week interval, the shortest recommended, to achieve the largest reduction in the number of deaths.

In the case of the adenovirus-based AZD1222 vaccine, [123] estimated 76.7% (95% CI: 47.0-89.8%) for the efficacy against symptoms 21 days after the first dose. Albeit this estimate provides reasonably high values, the small number of events results in great uncertainty on this estimate, reflected in its wide confidence intervals. [144] corroborates those results with effectiveness against having a positive RT-PCR test of 64% after 21 days (95% CI: 59–68%) in a study in the UK, but without differentiating between AZD1222 and BNT162b2. Using this value as a proxy of first dose efficacy compared to the efficacy against symptoms post second-dose, the relative efficacy would be around 80%, which, according to our results, would suggest that delaying the second dose can be an effective strategy, especially in lower production rates. The efficacy post second-dose using a window less than 6 weeks is substantially lower (55.1%, 95% CI: 33.0-69.9%) when compared to 12 weeks (81.3%, 95% CI: 60.3-91.2%) [123], providing another

argument in support of delaying the second dose of AZD1222.

For the mRNA vaccine BNT162b2, [144] have shown that its effectiveness is very high 21 days after the first dose (78%, 95% CI: 72-83%), results corroborated by a study conducted by the [119], from the UK. With these values, together with very high post second-dose efficacy against infectious contacts, our model results entail that postponing the second dose is the best strategy. However, as this is the first known vaccine using the mRNA platform, it would be advisable to postpone the second dose only after studies assuring the efficacy of such vaccine in these conditions, as pointed out by [145].

Vaccines developed to have more than one dose usually benefit from increased interval between doses, presenting stronger immunogenic response with larger intervals [146]. Thus, by using the same efficacy of the second dose for any interval between doses, our results might have been biased, favoring shorter time intervals as the best strategies. Therefore, a more complete evaluation of best strategy would require efficacy information for any of the intervals studied. Due to the emergency situation vaccines were tested in their trials, few experiments were designed to analyse different time interval between doses (yet, check some data available in [123] for AZD1222 and [124] for CoronaVac). Future works can re-evaluate the choice of the best interval between doses when these data become available, especially if the immunogenic response and efficacy increases non-linearly with time interval.

Previous studies that have evaluated the best strategies for vaccination for COVID-19 have focused on the interplay between vaccination and non-pharmaceutical interventions [103, 147, 148]. More recently, some agent-based models estimated the reduction in deaths and infections if postponing the second dose: [149] found that delaying the second dose for BNT162b2 and mRNA-1273 (from Moderna) is usually the best strategy until it reaches peak values for longer intervals; [150] found that the results are even better in the scenarios of low vaccine production rates. We confirm these initial results and extend the analysis to more combinations of first dose efficacy and production rates, and also consider more types of vaccine. Our model also accounts for optimal allocation of vaccination rates of first and second doses, an issue not addressed in those works.

Using a differential equations formulation, [151] compared the strategies of “hold back" (storing half of the vaccines to guarantee the second dose) and “release" (vaccinating as much as first doses possible, while minimizing the backlog of second dose vaccination) and found that first dose efficacy is essential when

deciding for the best vaccine protection coverage if delaying the second dose. Their results agree with ours but it has the limitation of not guaranteeing that the mean period with single-dose protection is preserved in a varying vaccination rate, which is only possible using a more complex formulation, such as delay differential equations as used here. They also argue that, while the "release" strategy enables better allocation of vaccines, in a real-world situation the implementation of such strategy is too complicated to manage. While we agree that this strategy adds a complication factor, we also believe that stock optimization models such as the one developed in this study could be linked to vaccination databases and, as the vaccination roll-outs to tackle the SARS-CoV-2 pandemic were centralized by the national health systems, thus allowing more efficient allocation of vaccines.

Throughout this study, we assumed that post second-dose efficacies do not depend on the time-window between doses, although evidence suggests that this is not the case for AZD1222 vaccine [123]. This simplifying assumption probably leads to a slight underestimation of the benefits of increasing the lag between doses for this vaccine. We have also assumed that first dose efficacy is constant over time, when in reality it builds up over approximately 2 weeks and wanes later on [144, 152]. This can be addressed using agent-based models [149], or age-of-infection models in a differential equations formulation, but that would greatly increase the complexity of the algorithm. This difficulty is also present when trying to compare model parameters to first dose efficacy in observational studies, as only the period after 14 days is usually considered, leaving a very short period in which events can occur. The impact of this on our conclusions can go in either direction: for shorter time windows, the efficacy in the model should be lower than the observed one, since for most of the time – the first 14 days – protection is virtually non-existent; while for longer time windows the same happens, that is, model parameters should be below measured efficacies due to waning effects of the vaccine. We currently do not have enough details of the profile of the immunological response over time to settle the issue definitively, yet we expect the pattern of the results to hold, given that we cover every possibility of relative efficacy and thus this can be compared to averaged values in time of the efficacy of the first dose.

In summary, we developed a novel approach to assess the best conditions to delay the second dose of three different vaccine platforms for COVID-19. Our approach consisted of using a SEIR-like model coupled with a delay differential equation vaccination model and optimization of vaccine stock. We found that the

first dose efficacy relative to post second dose efficacy is an essential parameter when defining the best window between doses, but the vaccine production rate in each country can be also decisive. Finally, we also found that those results have little dependence on the current epidemic situation at the start of the simulation. Further research in this theme would include non-constant production rate in the optimization scheme, together with starting such model in an ongoing vaccination roll-out, as well as considering lower efficacy in different age bins and other dose prioritization schemes.

Chapter 4

Modelling optimal vaccination strategies against COVID-19 in a context of Gamma variant predominance in Brazil

This work was done by Leonardo Souto Ferreira[1,2], Gabriel Berg de Almeida[3], Lorena Mendes Simon[4], Silas Poloni[1,2], Ângela Maria Bagattini[5], Marcelo Eduardo Borges[2,6], Michelle Quarti Machado da Rosa[5], José Alexandre Felizola Diniz Filho[2,4], Ricardo de Souza Kuchenbecker[7], Suzi Alves Camey[8], Roberto André Kraenkel[1,2], Renato Mendes Coutinho[2,4], and Cristiana Maria Toscano[5], and an older version is available as a preprint at *MedRxiv* in March 2022 at [153], and is undergoing review at the date of writing. The author of this thesis was the first author in the article and has developed the model, software, formal analysis, investigation, and writing. The other authors also contributed during all phases of production.

Abstract

Introduction: Brazil experienced moments of collapse in its health system throughout 2021, driven by a timid initial vaccination strategy against Covid-19, combined with the emergence of variants of concern (VOC).

[1]Instituto de Física Teórica, Universidade Estadual Paulista, São Paulo, Brazil.
[2]Observatório COVID-19 BR, São Paulo, Brazil.
[3]Departamento de Doenças Infecciosas, Escola de Medicina de Botucatu, Universidade Estadual Paulista, Botucatu, Brazil.
[4]Departamento de Ecologia, Programa de Pós-graduação em Ecologia e Evolução, Universidade Federal de Goiás, Goiânia, Brazil.
[5]Instituto de Patologia Tropical e Saúde Pública, Universidade Federal de Goiás, Goiânia, Brazil.
[6]Centro de Matemática, Computação e Cognição, Universidade Federal do ABC, Santo André, Brazil.
[7]Programa de Pós-graduação em Epidemiologia, Universidade Federal do Rio Grande do Sul, Porto Alegre, Brazil.
[8]Instituto de Matemática e Estatística, Universidade Federal do Rio Grande do Sul, Porto Alegre, Brazil.

Objectives: To support decision-makers in immunization policy makers in the context of limited vaccine availability, and evolving variants over time, we evaluate optimal strategies for Covid-19 vaccination in Brazil in 2021, when vaccination was rolled out during Gamma variant predominance.

Methods: Using a discrete-time epidemic model we estimate Covid-19 deaths averted, considering currently Covid-19 vaccine products and doses available in Brazil; vaccine coverage by target population; and vaccine effectiveness estimates. We considered a 5-month time horizon, from early August to end of December 2021. Optimal vaccination strategies considered included varying dose intervals from 8-12 weeks, and coverage levels to be achieved prior to expanding vaccination to younger target populations. Dose availability required over time to allow implementation of optimal strategies was also estimated through modelling.

Results: Differently than what has been implemented by several local policy makers, recovering vaccination coverage rates in high-risk groups in order to reach coverages of at least 80% results in higher population impact than expanding vaccination to younger groups when vaccine coverages are not-optimal. Reduction of dose interval from 12 to 8 weeks results in fewer COVD-19 deaths, but is only feasible to be implemented if accompanied by an increase in vaccine supply of at least 50% in the coming six-months in Brazil.

Conclusion: Covid-19 immunization strategies should be tailored to local vaccine product availability and supply over time, circulating variants of concern, and vaccine coverage in target population groups. Modelling can provide valuable and timely evidence to support implementation of vaccination strategies tailored to the local context, yet following international and regional technical evidence-based guidance.

4.1 Introduction

By the end of 2021, Brazil had reached over 600,000 deaths due to COVID-19, ranking second in the world for the absolute number of COVID-19 deaths [154]. Brazil's first COVID-19 case was identified in March 2020, and the first wave of the epidemic on a national level peaked in July and lasted until October 2020, when more than 5 million confirmed cases and at least 150,000 deaths had been registered [155]. The downward trend that lasted 16 weeks ceased in late November 2020, when a new rise in cases and deaths was observed [37]. This coincides with the detection of new variants of concern (VOC) in the country,

challenging Brazil's Universal Health Care System (SUS) and the government's public response. As the fifth-largest world's country, Brazil presented multiple and different epidemic curves according to the transmission of SARS-CoV-2 between regions in 2020, progressively reaching countryside smaller cities and developing a national synchronization process between 2020 and 2021 where epidemics caused by VOC including Delta and Gamma were important drivers of sustainable viral transmission in the population. The Gamma variant (P1 lineage or GR/501Y.V3), first identified in Brazil [37], spread throughout the country before the national vaccination campaign that started in January 2021, resulting in numerous surges throughout the country. In the tenth epidemiological week (EW) of 2021, there was an impressive number of 40,797 hospital admissions at a national level, representing a 2-fold increase when compared to the worst week of the epidemic in 2020 (EW 28) [156].

Brazil's COVID-19 national vaccination rollout started in late January 2021, following the prioritization strategy recommended by the World Health Organization (WHO) [157], initially targeting health care professionals, older adults, and people with comorbidities. Vaccination pace started and progressed slowly from January to March 2021, restricted by limited vaccine availability in the country. The average number of daily doses administered was around 200,000, much smaller than the daily doses of influenza administered during national campaigns in previous years. Only after April did the daily number of vaccines administered reached 700 thousand [158]. COVID-19 vaccines registered and in use in Brazil include AZD1222 (AstraZeneca/Oxford/Fiocruz), a viral vector platform vaccine, in a 2-dose primary schedule initially administered with 8-weeks dose-interval; BNT162b2 (Pfizer/BioNTech), a two-dose mRNA vaccine, also initially administered with 8-weeks dose-interval; CoronaVac (Sinovac/Butantan), a 2-dose inactivated virus vaccine, administered with a 4-weeks dose-interval; and Ad26.COV2.S (Janssen) a single dose viral vector vaccine.

National vaccination rollout and strategy were determined in a context of high first-dose efficacy against the original wild-type virus strain [159, 160, 125]. With the emergence of new VOCs and amid an intense second wave of the pandemic, in late August 2021, the Brazilian Ministry of Health (MoH) opted to extend the dose interval of 2 of the available vaccines at the time (AZD1222 and BNT162b2 vaccines) to 12 weeks, following WHO recommendations [161, 162]. The objective was to increase the number of vaccinated high-risk individuals with at least one dose, thus increasing the population-level impact in the context of limited global

vaccine supply.

Differently than what would be expected in a country with a robust National Immunization Program, COVID-19 vaccination in Brazil has faced several obstacles. These included lack of national coordination and support to evidence-based decision-making, inconsistent vaccine supply and availability over time, limited social communication strategies, and the widespread misinformation about vaccine safety and efficacy in social networks. In addition, the anti-vax movement in the country has been gaining strength during the pandemic. From the operational point of view, COVID-19 vaccination rollout was fragmented, with different vaccination strategies being adopted at state and municipal levels due to lack of central coordination. As such, vaccines were progressively made available to adults without comorbidities, by age, irrespective of vaccine coverage levels reached in priority risk populations. One critical point is that, in this age-based strategy, a minimum coverage goal set by age group was not established before the vaccine was made available for younger groups. This progression was based on a temporal criterion of vaccination campaign (for example, a one-week period designated for each age group), varying by state and municipality.

To support decision-makers in immunization policymakers in the context of limited vaccine availability, and evolving variants over time, we evaluate optimal strategies for COVID-19 vaccination in Brazil in 2021, when vaccination was rolled out during Gamma variant predominance.

We specifically aim to address three programmatic questions: a) what should be the vaccination coverage of an age group before starting vaccination in a subsequent younger group?; b) What should be the ideal interval between doses of AZD1222 vaccine that would result in the greatest impact (considering intervals between 8 and 12 weeks), assuming available vaccine supply over time?; and finally, c) what is the minimum number of AZD vaccine doses to be made available over time that will allow the implementation of the optimal interval between doses?

4.2 Methods

The following COVID-19 vaccines registered for use and introduced in Brazil were considered: AZD1222 (AstraZeneca/Oxford/Fiocruz), CoronaVac (Sinovac/Butantan) and BNT162b2 (Pfizer/BioNTech). Since our goal is to estimate optimal strategies considering the interval between vaccine doses, we have not

included the Ad26.COV2.S vaccine in the model, as this is a single dose vaccine, and given the very small number of individuals that received or will receive this vaccine (4.5 million people out of 211 million people, representing less than 2% of the population).

4.2.1 Data inputs and sources

We obtained the number of vaccinated individuals from Brazil's National Immunization Program Information System (SI-PNI) (up to Sept 8th, 2021) which contains anonymized information of each vaccinated individual in Brazil, including vaccine product, dose, vaccination date, and age of vaccine recipient [158].

We considered the number of vaccine doses procured by the Brazilian MoH and anticipated to be delivered until the end of 2021 [158]. The time-horizon considered was 5 months, from Aug 9th to Dec 31st, 2021, as this was the period for which data on vaccine dose availability was available. Since the number of doses is projected by month or quarter, we assume a constant rate of vaccine delivery or production (for locally produced vaccines), distribution and administration rates in each time interval considered in the model (See Appendix B.2). We then estimated the number of individuals who would receive one or two vaccine doses by product, for each age group, during the study time-horizon, as well as the time elapsed since receipt of the first-dose at each point in time. These data were inputted to the model, further described in the next section.

4.2.2 Model structure and assumptions

We developed a simplified discrete-time disease transmission model, in which we assumed a constant probability of infection. Infection transmission dynamics are encoded in a transition matrix that provides the proportion of individuals moving through model compartments daily [163]. Model structure is an extended SEIR compartmental model [164], accounting also for asymptomatic, hospitalized, and deceased individuals, thus described as SEAIRHD [118]. The model is structured in 10-year age subgroups. The structure is replicated for vaccine product (AZD1222, CoronaVac, and BNT162b2), and dose (first and second dose), with vaccines then modelled simultaneously (see Figure 4.1).

To estimate the number of vaccine doses that should be allocated for the first or second dose, we use a modified version of the dose optimization model developed previously and described in further detail elsewhere [118], that accounts

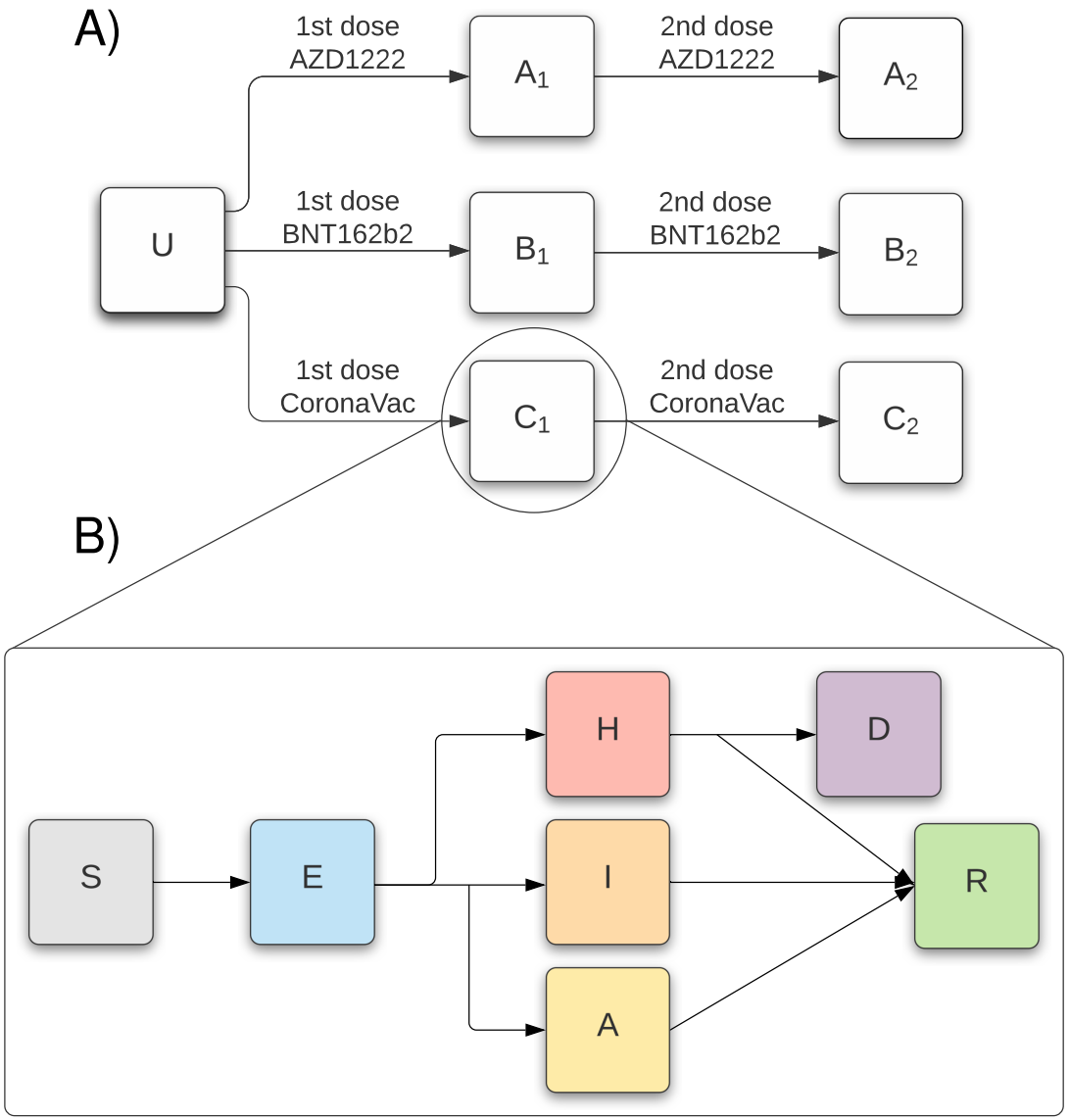

Figure 4.1: Model Structure. The first diagram (A) describing vaccination pathways. U accounts for unvaccinated individuals; A, B, and C accounts for individuals vaccinated with AZD1222, BNT162b2, and CoronaVac, respectively. The subscripts account for the first (1) or second (2) dose. The second diagram (B) describes the infection pathways. A susceptible (S) individual is transferred to a pre-symptomatic (or exposed, E) compartment after infection. After the incubation period, the individual evolves to an asymptomatic (A), mild (I), or severe (H) infection. The individual eventually recovers (R) or dies (D), if severe.

for varying vaccine production and deployment rates, as well as individuals vaccinated with only one dose (see further details on the Appendix B.1.3). This optimization model calculates the number of first or second doses administered

by day, given a pre-specified production rate and dose interval, minimizing the number of doses that should be kept in stock while guaranteeing that individuals receive the second dose in a timely manner.

We assumed a single model for the whole country. We also assume that after initially targeting high-risk populations, vaccination rollout was expanded over time, following a decreasing age-prioritization strategy. We considered the number of administered doses by vaccine, over time, as being proportional to the total number of doses of each vaccine made available at the time of vaccination. We considered that the vaccination rate in each age group is proportional to the unvaccinated population in this group (more details in Appendix B.1.4).

We limited the analysis of optimal inter-dose time interval (and the required dose supply) to AZD1222 for the following reasons: 1) there is no evidence to support the use of CoronaVac vaccine in a longer interval than the recommended four weeks; 2) BNT162b2 vaccine used in Brazil, differently than AZD1222 and CoronaVac, is imported and not produced locally, and as such, there is no possibility of expanding production and distribution capacity. Further, at the time of our modelling, there was no data on BNT162b2 effectiveness against the Gamma variant. Also, we considered 8–12-week intervals between doses, as per recommendation of current guidelines [162].

4.2.3 Model parameters and scenarios considered

We considered four scenarios of infection probability: very low, low, medium, and high (assuming SARS-CoV-2 infection probability, including asymptomatic infection, of 0.0001, 0.0025, 0.005, and 0.01, respectively).

Since Brazil does not have systematic serological inquiries, the exact SARS-CoV-2 prevalence in the population at the time of modelling was unknown. We assumed the percentage of recovered individuals at the start of the simulation period drawing from a uniform distribution ranging from 40% to 60%, based on existing seroprevalence estimates [165, 166].

Vaccine effectiveness estimates were obtained from the literature, considering the best available evidence. Effectiveness estimates for CoronaVac, AZD1222, and BNT162b2 vaccines stratified by age, outcome, and vaccine dose were considered, and presented in Tables B.1, B.2, and B.3, respectively. We considered estimates reported by Cerqueira-Silva et al. [43], who evaluated AZD1222 and CoronaVac effectiveness in Brazil during Gamma predominance, in a retrospective cohort of

more than 60 million individuals. Considering available evidence, we assumed CoronaVac effectiveness against SARS-CoV-2 infection to be zero, as it is an inactivated vaccine [142]. We draw the values of the effectiveness of the vaccines from the Beta distributions that obey the confidence interval of each estimate.

Each scenario of the infection probability and vaccination strategy considered are simulated with the same values of seroprevalence and vaccine effectiveness, thus ensuring comparability of strategies. Each scenario was run using 500 combinations of values for each result shown in the next section.

4.3 Results

Results are presented below considering three programmatic questions addressed by our modelling.

4.3.1 What should be the vaccination coverage of an age group before starting vaccination in a subsequent younger group?

We calculated the excess number of COVID-19 deaths resulting from initiating vaccination in a younger age group given a specific coverage threshold in the older group was achieved, compared to that resulting from only initiating vaccination once the older age group was fully vaccinated. As shown in Figure 2, the lower the vaccination coverage reached in older age groups, the greater the estimated excess of deaths, regardless of the probability of infection. Furthermore, vaccine coverage of at least 90% is necessary for a minimal excess of deaths to be reached, varying from 10.57 (95%CI: 10.60-13.43) to 620.21 (95%CI: 617.35-774.56), depending on the probability of infection. Nevertheless, starting vaccination in a younger age group when at least 80% vaccination coverage had been reached in older age groups resulted in a third of excess COVID-19 deaths compared to starting vaccination when only 40% coverage had been reached, as shown in Fig. 4.2 below. The magnitude of the impact varies by probability of infection, being smaller when the probability of infection is lower. The estimates for all values of threshold are presented in the Appendix B.3.

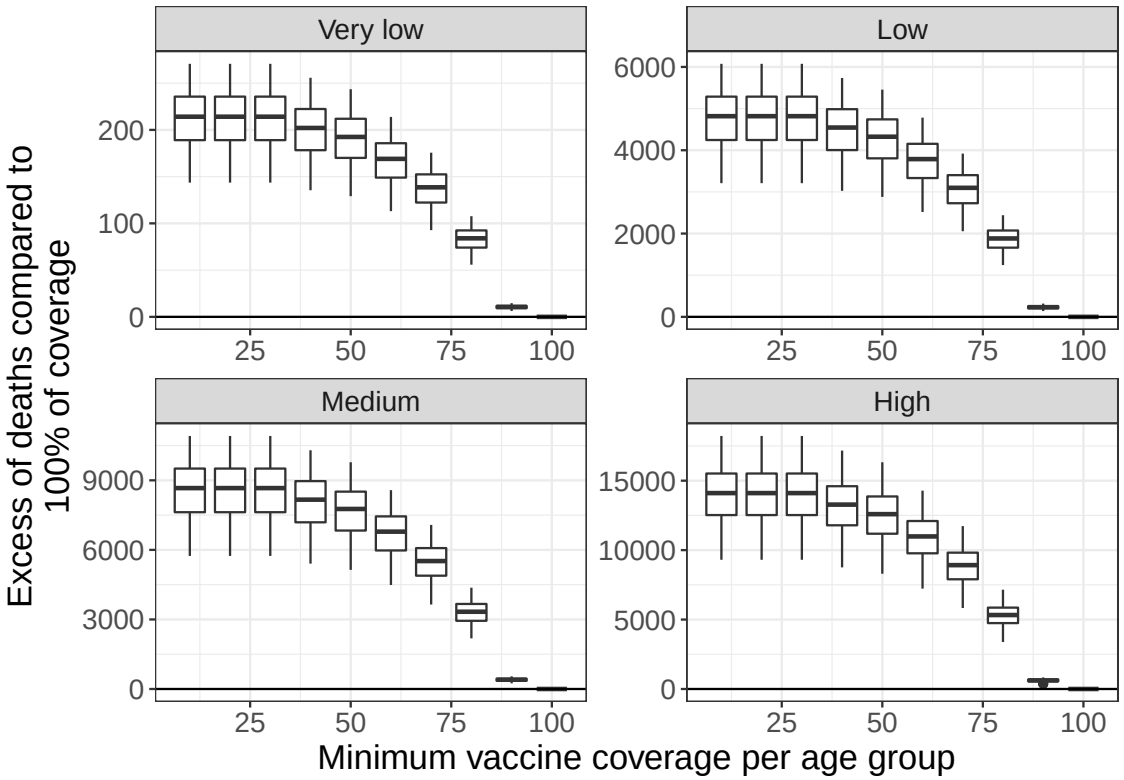

Figure 4.2: COVID-19 number of excess deaths (median and interquartile ranges) (y-axis) by minimum 2-dose coverage threshold (x-axis) reached before initiating vaccination of younger age groups, stratified by the probability of infection (panels), given by very low, low, medium, and high (with numerical values 0.0001, 0.0025, 0.0050, and 0.0100, respectively) values.

4.3.2 What should be the ideal interval between doses of AZD1222 vaccine that would result in the greatest impact (considering intervals between 8 and 12 weeks), assuming available vaccine supply over time?

Although the results of our model show that 90% vaccine coverage rate is the minimal coverage required in older age groups before expanding vaccination to younger age groups, in order to reduce excess deaths to minimum levels, we consider a conservative estimate of 80% as a feasible target. We then estimated the difference of COVID-19 deaths estimated when considering AZD1222 vaccine schedules with different dose intervals (8, 9, 10, and 11 weeks) compared to the standard initially recommended 12-week interval (Fig. 4.3). We assumed a setting without limitation of AZD1222 vaccine supply, i.e., we ran the model

assuming a number of doses up to ten times higher than the number of AZD1222 doses currently and projected to be made available during the study time-horizon. We found that the lower dose-interval of 8 weeks leads to a greater reduction in the number of COVID-19 deaths, varying from 99.56 (95%CI: 64.17-133.82) deaths averted in the lower probability of infection scenario to 9,126.66 (95%CI: 5,941.56-12,298.09) in a scenario of a high probability of infection. All estimates are presented in the Appendix B.3.

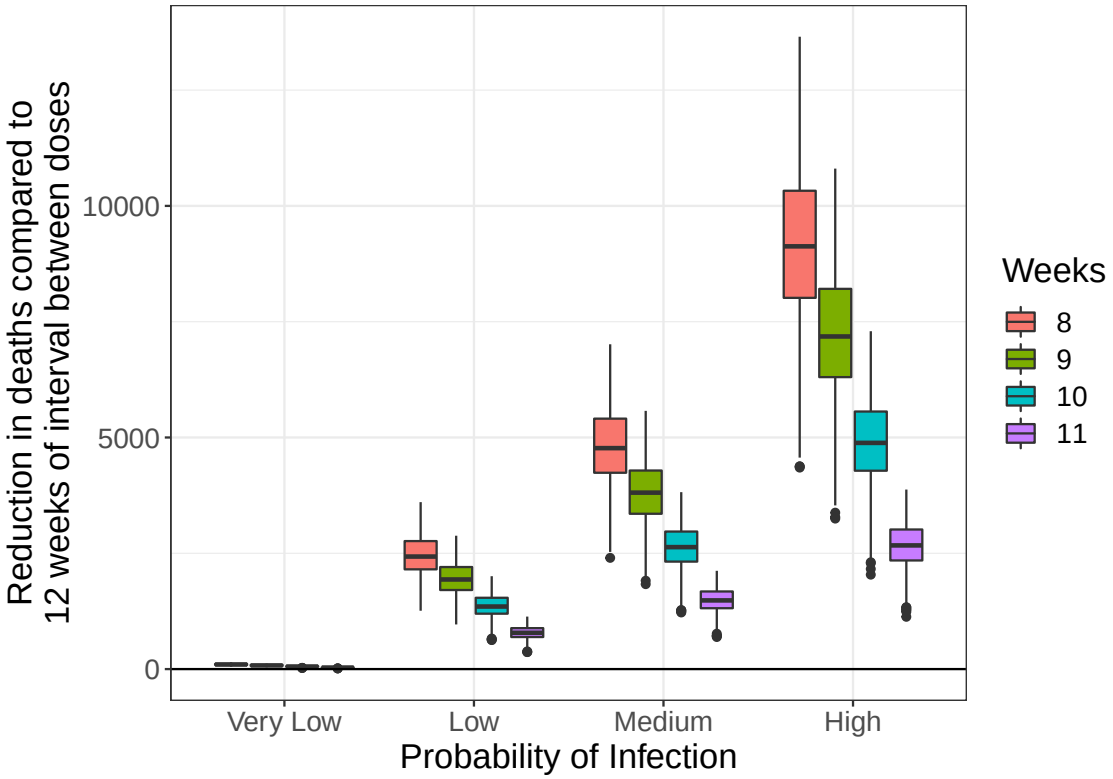

Figure 4.3: COVID-19 deaths averted (median and interquartile ranges) (y-axis) by different dose intervals (color) compared to 12 weeks, stratified by the probability of infection (x-axis), under the scenario of no limitation of AZD1222 vaccine supply. The probabilities of infection are given by very low, low, medium, and high (with numerical values 0.0001, 0.0025, 0.0050, and 0.0100, respectively) values.

This result leads to whether the strategy of using a lower dose-interval for AZD1222 would be effective considering the currently projected vaccine supply (until the end of 2021). We observe that vaccine supply over time is a bottleneck to the strategy of dose-interval reduction, as the reduction in deaths is negligible regardless of the probability of infection, in the scenario of the current vaccine supply (Fig. 4.4).

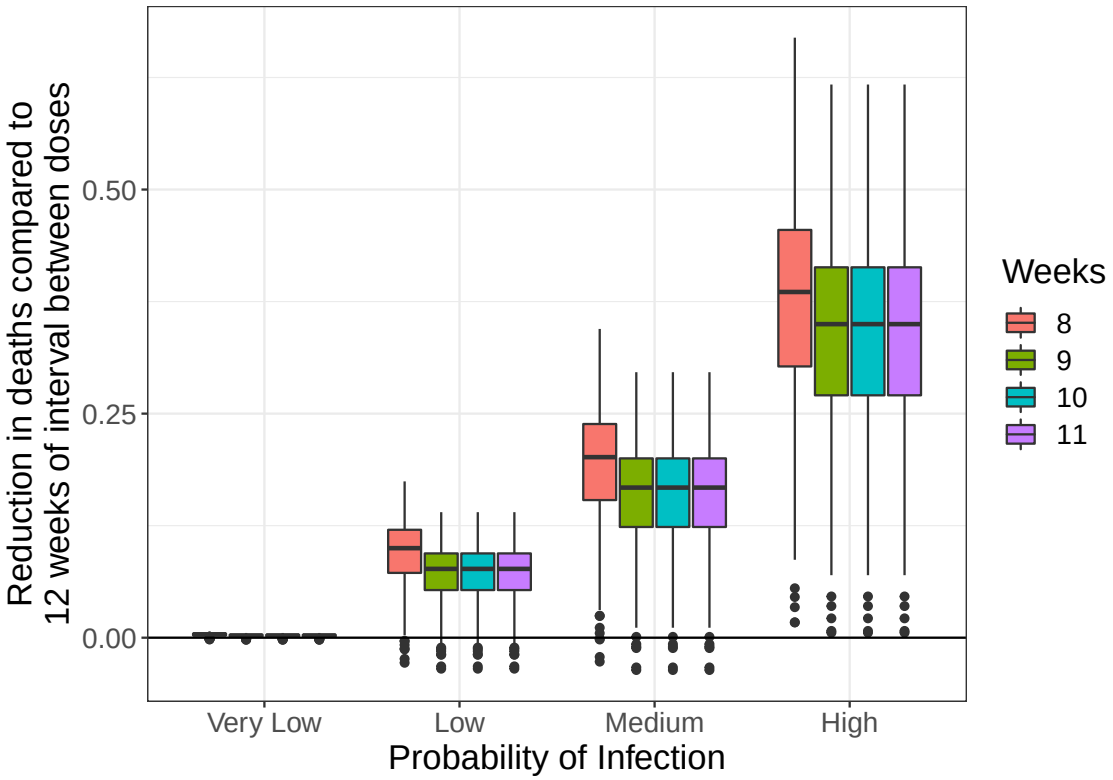

Figure 4.4: Reduction in deaths (in median percentage and interquartile ranges) (y-axis) by different dose-intervals (color) compared to 12 weeks, stratified by the probability of infection (x-axis), under the scenario of the currently projected AZD1222 vaccine supply. The probabilities of infection are given by very low, low, medium, and high (with numerical values 0.0001, 0.0025, 0.0050, and 0.0100, respectively) values.

4.3.3 What is the minimum number of AZD vaccine doses to be made available over time that will allow the implementation of the optimal interval between doses?

Considering the different dose-intervals for the AZD1222 vaccine, we estimate that the number of vaccine doses administered needs to be increased by at least 50% to avoid supply bottlenecks and allow for an impact on Covid-19 deaths reduction to be observed (Fig. 4.5). When comparing these estimates to the ones presented in Figure 4.3, we can observe the different population impact of the strategy when considering a scenario in which enough vaccine doses are available to meet the entire demand and a scenario in which an insufficient number of vaccine doses is available to meet the demand (Fig. 4.4), thus requiring an increase in vaccine supply (Fig. 4.5). Even with a 100% increase in vaccine supply, the

impact of reducing the time between doses to 8 weeks is reduced to at least about one-fifth of the maximum potential impact (reduction from 9,126.66 (95%CI: 5,941.56-12,298.09) to 2018.58 (95%CI: 1,167.27-2,823.14) deaths averted in the scenario of a high probability of infection). A higher increase in vaccine supply was not considered, as we assumed this was not a feasible scenario.

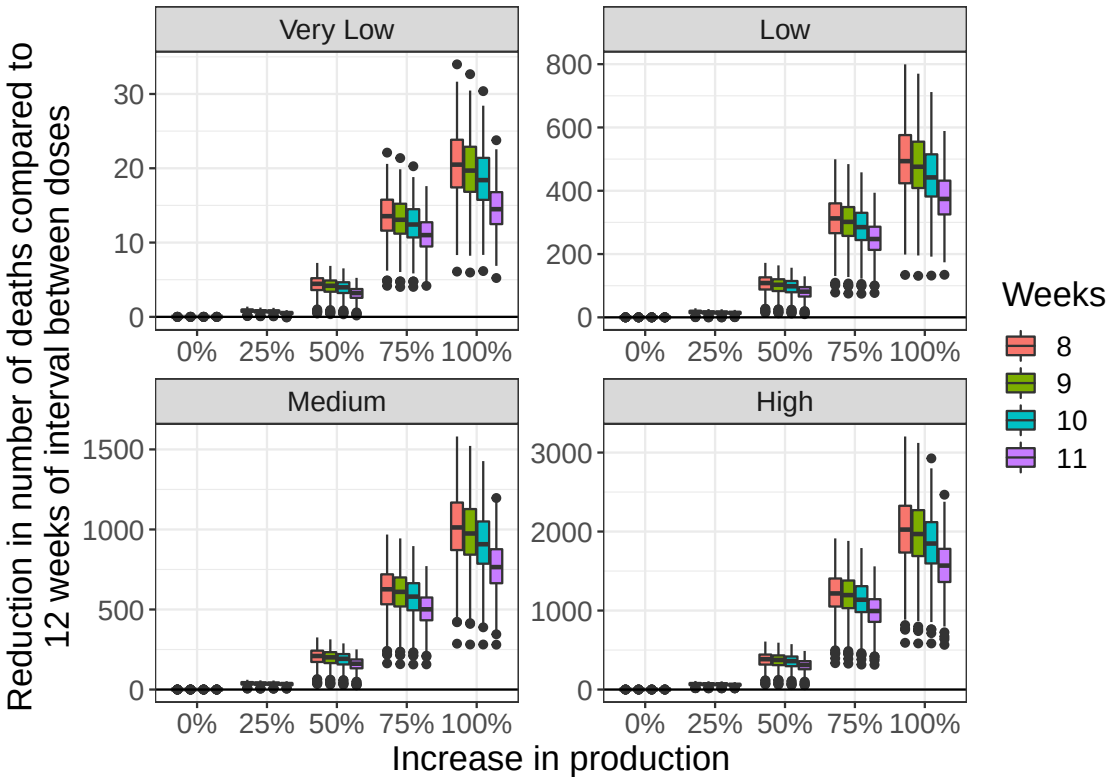

Figure 4.5: Covid-19 deaths averted (median and interquartile ranges) (y-axis) when considering lower dose-intervals (color) compared to 12 weeks, by per cent increase in AZD1222 vaccine supply (when compared to current projections) (x-axis), stratified by the probability of infection (panels), given by very low, low, medium, and high (with numerical values 0.0001, 0.0025, 0.0050, and 0.0100, respectively) values.

4.4 Discussion

Our findings support that, in order to reach higher impact in the context of gamma variant predominance in Brazil, Covid-19 vaccine coverage rates in high-risk groups should be maximized, reaching a minimum of 80% 2-dose coverage before expanding vaccination to populations of younger age. We further demonstrate that, assuming vaccine effectiveness estimates against the Gamma variant,

reducing the inter-dose interval from 12 to 8 weeks for AZD1222 ensures the highest reduction in Covid-19 deaths independently of infection transmission rates, reaching up to 10 thousand deaths in the high transmission scenario.

Routine monitoring and evaluation of disease transmission dynamic and local epidemiology are required and of utmost importance during a pandemic, and should guide formulation, implementation and adjustments of public health policies. The emergence of new variants of concern (VOC), such as the Gamma variant [167] first identified in Brazil in late 2020, can pose additional challenges to public policymaking. Being flexible and rethinking strategies has been mandatory in the context of the pandemic, particularly in settings as Brazil, a large and diverse country, where many were the challenges faced for mitigating Covid-19 and efficiently rolling out its national Covid-19 vaccination strategy [168].

Considering the available evidence at the time of significant protection with one-dose against the original wild virus strain, Brazil and many other countries prioritized the administration of one vaccine dose to the greatest number of people, ensuring some protection, and spacing out the second dose for the maximum period of time stipulated by the manufacturers (i.e. 12 weeks). With the predominance of a new variant, this assumption no longer held true, as protection conferred by one dose against the Gamma variant was not adequate.

In addition, the eagerness to reach a higher number of vaccinated individuals quickly led many states and municipalities to expand vaccination to younger age groups, beyond the priority target population, including early on younger populations. This was done without defining a priori a minimum coverage to be reached in the priority groups prior to expanding vaccine to other groups, which, as we demonstrate, result in reduced population impact of vaccination.

In the context of scarce global-level vaccine supply, it is crucial to ensure that at-risk individuals are adequately and timely protected against Covid-19. Since our model limits to age-stratified populations, ignoring other groups such as pregnant women and immunosuppressed individuals, we can only measure the effect of different thresholds of older individuals' coverage before making vaccine doses available to younger individuals. Ensuring a good vaccine coverage of older individuals (at least 90% of coverage) reduces the number of Covid-19 deaths considerably, as expected. However, more important than that, even assuming lower coverages (lower than 80%) as a threshold generates a sharp increase in the number of additional averted deaths compared to vaccinating the whole population of older individuals beforehand. Thus, the first strong

recommendation we provided to policymakers based in our model results, is that it is necessary to resume efforts to achieve minimum coverage of 80% in older age groups, and only then should vaccination be expanded to younger age groups. This calls for urgent measures from government policymakers, including social mobilization and communication campaigns, in addition to active search of unvaccinated individuals.

Structured in 1973 at the end of the smallpox eradication initiative, The Brazilian National Immunization Program (PNI) represents a robust public health intervention, providing, free of charge, vaccines incorporated into the routine immunization schedule to all populations through its publicly-funded SUS [169]. Managed by the Federal Government, together with States and Municipalities, decentralized and with good capillarity, achieved by more than 36 thousand vaccination rooms throughout 5,570 Brazilian municipalities, the PNI has historically been able to deliver massive amounts of vaccines in immunization campaigns and get to hard-to-reach populations. Assuming that Brazil is perfectly capable of rescuing unvaccinated older people, given the country's brilliant history concerning vaccination planning and implementation, acceptance by the population, and especially the capillarity of the health system, we can advance on other issues we modelled.

An important issue raised by our results is that the optimal impact of reducing the interval between doses is not (nearly) achievable given the available vaccine supply at the time of modelling (i.e., the projected number of doses to be distributed in Brazil in the following 6 months). Without increasing vaccine supply, reducing the inter-dose interval would result in lack of dose availability to be administered as the second to a significant proportion of the eligible to receive their second dose (ie. after 8 weeks of receipt of the first dose) population. This bottleneck can result in damage to the immunization program and its credibility.

In order to achieve a noticeable impact of changing the interval between doses of AZD1222, an increase of at least 50% of the current vaccine supply, in terms of number of available doses, is required, independently of the transmission level of the epidemic. This is very useful information, particularly to support vaccine procurement and purchase, but in Brazil mostly to improve production capacity locally, as Brazil's AZD1222 producer Fiocruz-Biomanguinhos is upgrading its factory from filling doses to in-loco full vaccine production. This would, in principle, enable the production of four monthly lots of doses instead of the currently produced three lots. Although our result suggests that increasing vaccine avail-

ability by 100% would result in the most significant impact, we did not model such increase as we assumed it to be unrealistic. Thus, one more strong recommendation based on our results can be made: decreasing the interval between doses of AZ vaccines from 12 to 8 weeks can be highly beneficial, only if adequate vaccine supply is available, and in Brazil this represented a 100% increase in vaccine availability by the end of 2021.

This recommendation is important to reinforce the need for increasing and sustaining local vaccine availability and sustainable supplies, and demonstrate that the country cannot let down its guard in the fight against the pandemic. Vaccine supply and vaccination policy may change depending on vaccine effectiveness data, infection transmission, new VOC and local epidemiology, among others. This is further reinforced by the emergence of the Omicron VOC, predominant in Brazil since early 2022, against which a third dose of vaccine has been demonstrated to be required to maintain protection against severe disease [170].

Mathematical modelling has been extensively used to assist policymakers during the Covid-19 pandemic. The range of issues evaluated through modelling include, but is not limited to, school reopening [97], the effects of lockdown and social distancing measures [171], and, of course, the impact of vaccination and identification of best vaccination strategies. Moore et al. [172] have shown that vaccinating older age groups should be prioritized to minimize the number of future deaths or years of life lost in the UK. The same results were found by Bubar et al. [103] when considering the number of deaths as the outcome. However, assuming the use of a highly effective vaccine against infection, vaccinating younger and thus more mobile population resulted in the higher reduction of infection in the population. Some agent-based models have been used to assess the effects of delaying the second dose of mRNA-based vaccines, showing that in the context of Alpha VOC predominance, delaying up to 12 weeks would have significant impact in reducing Covid-19 deaths [150, 149].

Our results are in agreement with those reported by Silva et al. [173] who also estimated that 8-week inter-dose interval would result in reduced ICU admissions using a hypothetical scenario on the number of vaccine doses. Our work further improves on Silva et al. by, first, considering realistic and not hypothetical vaccine supply over time. Second, considering real-life national immunization strategy in which all three vaccines are modelled simultaneously, further optimizing the allocation of doses by vaccine in the ongoing vaccination program. Third, using the most up-to-date and best quality evidence from the literature as vaccine

effectiveness parameters against Gamma VOC.

Ferreira et al. [118] also demonstrated that first dose efficacy and available number of vaccine doses are important parameters when considering the optimal interval between doses, whereas varying values of infection transmission (effective reproduction number) did not impact estimates. This was also observed in our study, supporting our choice of using various scenarios with fixed probabilities of infection over the time horizon of the study. This rendered modelling simpler and allowed for better timeliness of modelling and communication of results to decision makers and policymakers in Brazil.

Covid-19 vaccination strategies should be tailored to local vaccine product availability and supply over time, circulating variants of concern, and vaccine coverage in target population groups. Simpler modelling approaches can provide valuable and timely evidence to support implementation of vaccination strategies tailored to the local context, yet following international and regional technical evidence-based guidance. These strategies should be continuously monitored and adjusted over time.

Chapter 5

Modeling the impact of child vaccination (5 to 11 y) on overall COVID-19 related hospitalizations and mortality in a context of Omicron variant predominance and different vaccination coverage paces in Brazil

This work was done by Gabriel Cardozo Müller[1], Leonardo Souto Ferreira[2,3], Felipe Ernesto Mesias Campos[3,4], Marcelo Eduardo Borges[3,5], Gabriel Berg de Almeida[6], Silas Poloni[2,3], Lorena Mendes Simon[7], Ângela Maria Bagattini[8], , Michelle Quarti Machado da Rosa[8], José Alexandre Felizola Diniz Filho[3,7], Roberto André Kraenkel[2,3], Renato Mendes Coutinho[3,5], Suzi Alves Camey[9,10], Ricardo de Souza Kuchenbecker[1,10], and Cristiana Maria Toscano[8]. This work is not publicly available yet, but is undergoing review at the date of writing. The author of

[1]Programa de Pós-graduação em Epidemiologia, Faculdade de Medicina, Universidade Federal do Rio Grande do Sul, Porto Alegre, Brazil.
[2]Instituto de Física Teórica, Universidade Estadual Paulista, São Paulo, Brazil.
[3]Observatório COVID-19 BR, São Paulo, Brazil.
[4]Programa de Pós-Graduação em Ecologia, Instituto de Biociências, Universidade de São Paulo, São Paulo, Brazil
[5]Centro de Matemática, Computação e Cognição, Universidade Federal do ABC, Santo André, Brazil.
[6]Departamento de Doenças Infecciosas, Escola de Medicina de Botucatu, Universidade Estadual Paulista, Botucatu, Brazil.
[7]Departamento de Ecologia, Programa de Pós-graduação em Ecologia e Evolução, Universidade Federal de Goiás, Goiânia, Brazil.
[8]Instituto de Patologia Tropical e Saúde Pública, Universidade Federal de Goiás, Goiânia, Brazil.
[9]Instituto de Matemática e Estatística, Universidade Federal do Rio Grande do Sul, Porto Alegre, Brazil.
[10]Hospital de Clínicas de Porto Alegre, Porto Alegre, Brazil.

this thesis shares first-authorship with Gabriel Cardozo Müller in the article and has developed the model, software, formal analysis, investigation, and writing. Gabriel has done the literature review, investigation, and writing. This work was reproduced with permission. The other authors also contributed during all phases of production.

Abstract

Background: Developing countries have experienced significant COVID-19 disease burden. With the emergence of new variants, particularly Omicron, disease burden in children has increased. When the first COVID-19 vaccine was approved for use in children aged 5-11 years of age, very few countries recommended vaccination due to limited risk–benefit evidence for vaccination of this population. In Brazil, ranking second in global COVID-19 death toll, childhood COVID-19 disease burden increased significantly in early 2022. This prompted a risk-benefit assessment of the introduction and scaling-up of COVID-19 vaccination of children.

Methods: To estimate the potential impact of vaccinating children aged 5 to 11 years with mRNA based COVID-19 vaccine in the context of Omicron dominance, we developed a discrete-time SEIR-like model stratified in age groups, considering a three month time horizon. We considered three scenarios: No vaccination, slow, and optimal vaccination pace. In each scenario we estimated the potential reduction in total COVID-19 cases, hospitalizations, deaths, hospitalization costs, and potential years of life lost, considering the absence of vaccination as the base-case scenario.

Findings: We estimated that vaccinating at an optimal pace could prevent, between mid-January and April 2022, about 26,000 COVID-19 hospitalizations, and 4,200 deaths in all age groups; of which 5,400 hospitalizations and 410 deaths in children aged 5 to 11 years.

5.1 Introduction

COVID-19 had a great impact in developing countries, especially in Brazil, which holds the second largest number of COVID-19 related deaths worldwide [71]. Due to its large territorial extension, Brazil's COVID-19 epidemic was characterized by regional epidemic curves after the introduction of new variants of concern (VOC), culminating with a large nationwide synchronized wave caused by Gamma VOC in mid-2021 [71]. In December 2021 the Omicron variant was

detected in Brazil, leading to an exponential increase in infections and causing a very high number of cases in all age groups as of early 2022 [174].

The Omicron variant is characterized by a large number of mutations in the spike protein, which explains its high capability of transmission and reinfection [174]. Moreover, these mutations have conferred the capacity to partially escape from immune response [175]. Omicron has a higher reinfection rate compared to the Delta variant, being also capable of infecting vaccinated individuals and causing disease in those partially vaccinated [174, 176]. As a result, considering that a third (booster) vaccine dose can significantly lower these rates, booster vaccination has been recommended to further protect against Omicron.

There is even greater concern about the impact of Omicron on children. For children aged between 5 and 11 years, 6,877 hospitalizations and 308 deaths by COVID-19 have been registered in Brazil since the beginning of the pandemic until February 7, 2022 [177, 73, 74]. Children can be considered natural reservoirs of SARS-CoV-2 and its variants7, usually presenting mild or asymptomatic disease. Nevertheless, a higher transmission rate of Omicron infections among children has been documented, resulting in a sharp increase in COVID-19 hospitalizations in this age group in many countries. In the United States [178] and in many Brazilian states [179], this increase has resulted in a more significant disease burden in children than in any other previous moments of the pandemic.

Vaccination against COVID-19 in Brazil was initiated in January 2021 targeting priority groups including elderly and healthcare professionals, and was later extended for all adults. Vaccination of teenagers aged 12 to 17 began in September 2021. More recently, in December 2021, results of randomized clinical trials evaluating the efficacy of the vaccine against COVID-19 in children 5 to 11 years old demonstrated its efficacy and safety, estimating an effectiveness greater than 90% in reducing hospitalizations and deaths by COVID-19 in children [180, 181].

Vaccination in children aged 5 to 11 started in January 2022, after the Brazilian Health Regulatory Agency (ANVISA) approved Pfizer's mRNA vaccine (BNT162b2) for this age group. Despite the recommendation of specialized societies, vaccination started amid intense social controversy fueled by misinformation campaigns. The vaccination campaign also faced many operational difficulties and meager mass media campaigns of mobilization and communication about the importance of vaccinating children. These are among the many reasons which may account for the slow pace of vaccination in this age group, reaching national average coverage with first dose of only 22.7% by March 15th, 2022 [87]. Coverage

levels in the different Brazilian states is very heterogeneous, varying 3.7% up to 46.0% at the time [87].

To evaluate the impact of vaccination against COVID-19 in children aged 5 to 11 years in the epidemiological dynamics of SARS-CoV-2 in Brazil, we conducted a modelling simulation study to estimate how many COVID-19 hospitalizations, deaths, and potential years of life lost could be averted, as well as the financial savings resulting from averted hospitalizations resulting from childhood vaccination. Moreover, we estimated the additional benefits of a child vaccination campaign that reaches an optimal pace compared to the currently observed pace of childhood vaccine administration in Brazil at the time of modelling.

5.2 Methods

5.2.1 Data used in the model

Anonymized information of individuals' vaccine status from the Information System of the National Immunization Program (SI-PNI) of Brazil and the Influenza Epidemiological Surveillance System (SIVEP-Gripe) were used to calibrate the model. SI-PNI yielded vaccine coverage rates by age group, dose type, and vaccine type by each one of the 27 states and federative unit of the country. The following population age sub-groups were considered: 1-4, 5-11, 12-17, 18-29, 30-39, 40-49, 50-59, 60-69, 70-79, 80-89, and 90+ years. We computed the coverage of vaccinated individuals according to dose (first, second, and booster doses) and vaccine product (BNT162b2, AZD1222, and CoronaVac), by state and age group. The population size for each age sub-group was estimated based on population projections made by the Brazilian Institute of Geography and Statistics [177]. SIVEP-Gripe provided numbers of confirmed COVID-19 cases, hospitalizations, and deaths in Brazil over time and by state. The time series data extracted from this database, extracted in January 26th, 2022, were corrected by nowcasting estimates in order to minimize the effects of delays in notification [182].

To estimate the potential costs averted due to COVID-19 hospitalizations prevented by vaccination, we considered the average reimbursement cost of hospitalizations (considering both regular and intensive care hospitalization costs for children and adults) obtained from the Brazilian Hospital Information System (SIH-DATASUS) [183] for November and December 2021. The average reimbursement values weighted by macro-region was obtained in Brazilian Reais (BRL) and

then converted to International Dollars (Int$) considering the 2021 purchasing power (4102.37 Int$/hospitalization, 1 Int$ = 2.53 BRL).

5.2.2 Model structure

We developed a SEIR-like model in discrete-time and stratified in age groups, considering the following scenarios of vaccine administration in this age group: i) No vaccination; ii) Slow vaccination pace (current), considered as 250,000 vaccines doses administered per day nationally; iii) Optimal vaccination pace, considered as 1 million doses administered per day. The current vaccination pace was estimated considering information shared by the Ministry of Health and reported by the press on the number of vaccine doses distributed weekly by the National Immunization Program to the states and federative unit. We assumed that the doses were evenly distributed over time. The optimal vaccination pace considered the true vaccine administration capacity of the National Immunization Program, based in previous child vaccination campaigns in the country. In this scenario, higher vaccine coverage rates could be reached earlier.

For the remaining population age groups (adolescent, adults, and elderly), we considered vaccine coverage per dose and vaccine product, by state obtained from SIPNI at 2022-01-02. In these groups, we assumed a fixed vaccine coverage rate during the 3-month time horizon, to explicitly estimate the incremental impact of child vaccination over the existing vaccination strategies targeting other age groups.

The SEIR model used is constituted of the following compartments (Figure 1b): Susceptibles (S), Exposed and infective (E), Asymptomatics (A), mild Symptomatics (I), Hospitalized (H), Recovered (R) and Deaths (D) due to COVID-19. We assume that Exposed individuals have reduced infectiousness in comparison to symptomatic individuals due to the incubation period, whereas Hospitalized individuals have reduced infectiousness due to isolation. We assume that Asymptomatic individuals have the same infectiousness as Symptomatics. We model the contacts of individuals between different age groups using the contact matrices estimated for the Brazilian population and our infection model in discrete-time (for a complete description please see Appendix C.1). This structure simulates all the conditions of clinical and infectious progression possible relative to a SARS-CoV-2 infection. This structure is replicated considering vaccination, with each compartment using the corresponding parameters of vaccine effectiveness, by

dose, against different endpoints for each one of the vaccine products in use in the country (BNT162b2, AZD1222,and CoronaVac), by age group as shown in Figure 5.1.

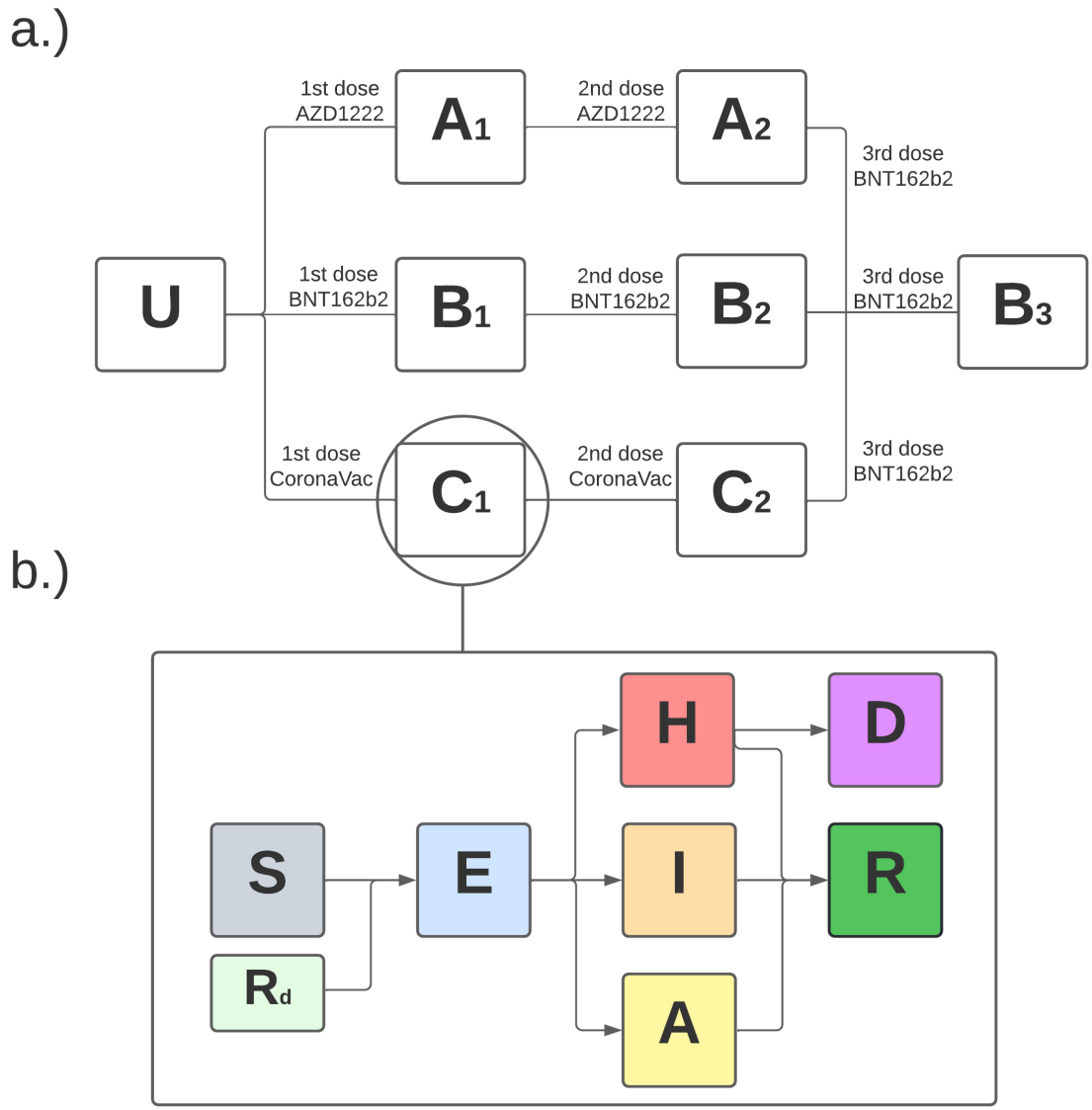

Figure 5.1: Model structure. Schematic compartmental structure of model, with each compartment replicated for each vaccine product and dose. For more information, please see the Model section in Methods. a. Structure replication for each vaccine product and dose b. General compartmental structure of model.

Our model considers a 90-day time horizon, between January 2022 and April 2022,period in which we model disease transmission and occurrence and hence estimated impact of children vaccination. During this period, Omicron is the dominant circulating variant; individuals previously infected are assumed to be

Recovered individuals at the beginning of the simulation having been infected mainly by Gamma and Delta variants. Equations are described in the Appendix C.1.

5.2.3 Model parameters

The effectiveness of the various vaccine products used in Brazil and the effectiveness of BNT162b2 vaccine in children aged 5 to 11 years, by dose, for each endpoint and age-group, were obtained through a literature review (see SM Figures 1-4). Vaccine effectiveness (VE) against infection were based on the studies by the New York State Department of Health [184] (for age group 5 to 11 years), Powell et al. [185] (for 12 to 18 age group), and, for other ages, the studies by Andrews et al. [176], Tseng et al. [186] or Willett et al. [187]. VE estimates against COVID-19 hospitalization and death considered were those reported by Barnard et al. [188], from UK Health Security Agency [189], and Young-Xu et al. [190].

We assumed no effectiveness of inactivated Sinovac's vaccine (CoronaVac) against Omicron infection. For other outcomes, (COVID-19 hospitalization and deaths), considering the limited available evidence, we assumed a reduction of 50% in effectiveness when compared to the estimated effectiveness of this vaccine against these outcomes for other variants [43].

Point estimate and corresponding 95% confidence intervals of each vaccine effectiveness estimates were considered, when available. These values were used to parametrize a Beta distribution and then imputed to the model. We then sample each parameter a thousand times to provide a combination of effectiveness samples. In addition, we sample an assumed distribution of Recovered individuals with a mean of around 70% of the population (see Appendix C). Even though we do not have prevalence estimates for each state of the country, seroprevalence estimates from blood donors in selected cities prior to vaccination and Gamma VOC epidemic wave shows that prevalence rates in the country were already high prior to the introduction of Omicron VOC, supporting our assumptions [191].

To account for the heterogeneity in disease dynamics, we fit the number of weekly new COVID-19 hospitalizations in each state to an exponential function to estimate the hospitalization growth rate. We then sample the growth rate assuming a normal distribution with deviance from the fitting procedure.

Finally, considering vaccine effectiveness parameters, initial prevalence at start of simulation and hospitalization growth rate, we compute the corresponding basic

reproduction number (R0) of Omicron infection using the Next Generation Matrix (NGM) method, adjusting the growth rate estimated from secondary surveillance data to the growth rate of the Jacobian of the model [116]. Using the eigenvector associated with the largest eigenvalue of the Jacobian (i.e. the growth rate), we compute the proportion of individuals each compartment, also accounting for variation due to age groups, as described in the Appendix C.2.

5.2.4 Impact estimation and sensitivity analysis

Children vaccination impact was estimated in terms of COVID-19 hospitalizations and deaths averted, as well as resulting averted costs of hospital admissions, and potential years of life lost (YLL) averted. For this estimate, COVID-19 deaths which would occur without childhood vaccination were considered, and the average age of death due to COVID-19 in each age sub-group was subtracted from the average life expectancy at birth in Brazil (76 years [177]), and then multiplied to the total death count of each age group.

These outcomes were estimated for a period of 3 months after the start of vaccination (time horizon of the analysis). Thus, after estimating and projecting the expected number of hospitalizations and deaths from COVID-19, by age group, for each scenario, we estimated the avoided number of hospitalizations and deaths resulting from the vaccination of children between 5 and 11 years. We measured both the impact of vaccination for the population aged 5 to 11 years (direct effects of vaccination) and all other age groups (indirect effects of vaccination).

In order to account for variation and uncertainty on the main parameter values of the model, we conducted sensitivity analysis (Table C.3).

5.3 Results

In Figure 5.2 and Table 5.1, we present the estimated averted events by age group, considering the two vaccination pace scenarios. In the three-month period of analysis, vaccinating children at the (current) slow pace of vaccination has the potential to prevent 1,450 deaths (95%CI: 805 – 2,360) and 9,704 hospitalizations (95%CI: 6,329 – 14,237) from COVID-19 for all age groups (Table 5.1). When we consider only the direct impact of the vaccine on children aged 5 to 11 years in the scenario of a slow vaccination pace, we found an impact of 180 avoided deaths (95%CI: 170 - 190) and 2,389 avoided hospitalizations (95%CI: 2,253 - 2,553) (Table

5.1).

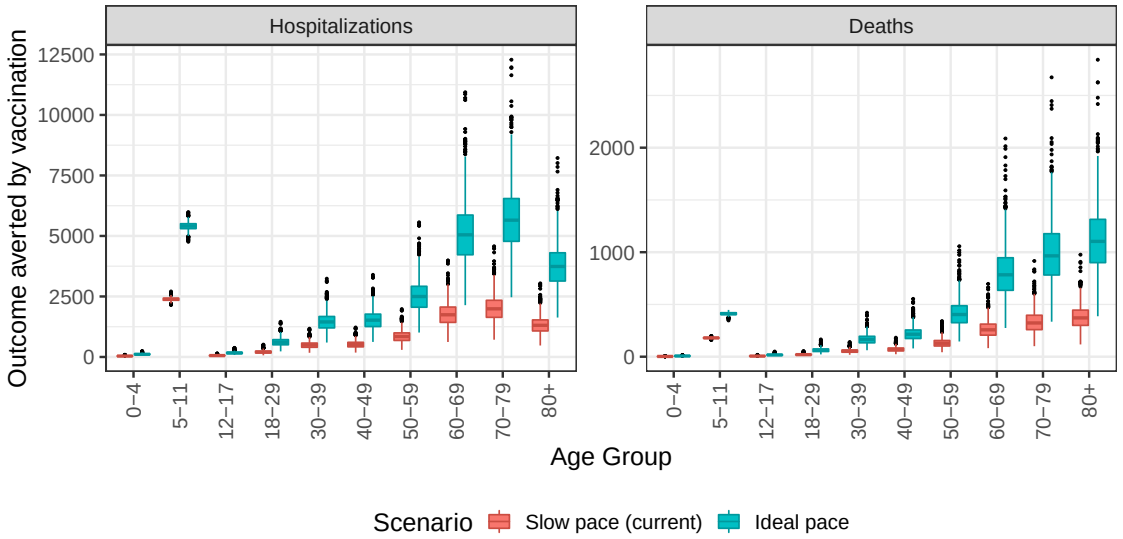

Figure 5.2: Boxplot of the number of events (hospitalization and deaths from COVID-19) preventable by vaccination against COVID-19 in children, by age group and vaccination pace.

Table 5.1: Outcomes Prevented per Scenario. Total events prevented (zero vaccination subtracted by each scenario), per outcome, expressed in thousands of events. Results were expressed as mean and 95% Confidence Interval.

Outcome	Age group	Vaccination at slow pace	Vaccination at optimal pace
Hospitalization	All	9.7 (6.33-14.24)	26.56 (17.76-38.39)
Death	All	1.45 (0.8-2.36)	4.25 (2.38-6.89)
Hospitalization	5-11	2.39 (2.25-2.55)	5.4 (5.07-5.74)
Death	5-11	0.18 (0.17-0.19)	0.41 (0.38-0.44)

Considering vaccination at an optimal pace, with the administration of 1 million doses per day of vaccines against COVID-19 to children between 5 and 11 years old, the impact would be much higher, avoiding a total of 4,251 COVID-19 deaths (95%CI: 2,380 – 6,894) and 26,560 hospitalizations (95%CI: 17,759 – 38,391) (Table 1). If the speed of vaccination proceeded at optimal pace, it would be possible to avoid 412 deaths (95%CI: 385 – 437) and 5,403 hospitalizations (95%CI: 5,070 – 5,744) due to COVID-19 only in children aged between 5 and 11 years (Table 5.1).

Regarding the cost analysis, the hospitalizations avoided in all age groups would result in a cost reduction of Int$ 39,812,206 (95%CI: 22,208,828 – 25,521,822)

considering vaccination at a slow pace, reaching Int$ 57,920,893 (95%CI: 54,922,182 – 62,430,000) for an optimal vaccination pace (Table 5.2). Considering only the reduction in costs related to averted hospitalizations in children aged 5 to 11 years, vaccination at an optimal pace could lead to a reduction in costs in the amount of Int$ 22,232,244 (95%CI: 21,751,540 – 23,313,930) (Table 5.2). In addition, we estimated a total of 24,750 (95%CI: 18,690 – 33,338) YLL prevented by a slow pace of vaccination (with 12,232 (95%CI: 11,548 – 12,952) YLL reduction corresponding to the direct effect) and a larger effect of 66,568 (95%CI: 48,659 – 92,291) YLL could be prevented in an optimal pace (also observing a prevention of 27,982 (95%CI: 26,161 – 29,711) YLL on age group 5-11 years) (Table 5.3).

Table 5.2: Averted costs by vaccination scenario and age group.

Age group	Vaccination at slow pace (in Million Int$)	Vaccination at optimal pace (in Million Int$)
All	39.81 (25.97-58.41)	108.98 (72.86-157.5)
0-4	0.4 (0.22-0.65)	1.17 (0.7-1.8)
5-11	24.79 (23.38-26.5)	56.08 (52.62-59.62)
12-17	0.62 (0.34-1.00)	1.76 (1.08-2.7)
18-29	2.16 (1.12-3.56)	6.46 (3.54-10.43)
30-39	5.18 (2.74-8.42)	15.25 (8.63-24.06)
40-49	5.44 (2.85-8.85)	16.02 (9.1-25.24)
50-59	8.93 (4.65-14.63)	26.4 (14.72-41.95)
60-69	18.43 (9.75-30.14)	53.33 (30.9-83.77)
70-79	20.98 (11.2-34.09)	59.79 (35.3-93.06)
80+	13.79 (7.33-22.49)	39.41 (22.89-61.71)

Table 5.3: Potential years of life lost averted by vaccination scenario and age group.

Age group	Vaccination at slow pace	Vaccination at optimal pace
All	24,750 (18,690-33,338)	66,568 (48,659-92,291)
5-11	12,232 (11,548-12,952)	27,982 (26,162-29,712)

Model estimates were robust and did not vary significantly in sensitivity analysis (Table C.3).

5.4 Discussion

Significant impact of COVID-19 vaccination in children was estimated in Brazil shortly after Omicron VOC introduction, and during the initial increase and

epidemic wave caused by this VOC in early 2022 in the country.

The comparison of the two vaccination scenarios reinforces that timing and efficiency of COVID-19 vaccination in children counts, with an optimal pace of vaccination resulting in a reduction of COVID-19 hospitalizations and deaths in the order of three times higher, when compared to slow pace of vaccination. The total number of hospitalizations and deaths preventable by vaccination in a period of three months in children between 5 and 11 years old has the same order of magnitude as the total number of COVID-19 deaths (308) and hospitalizations (6,877) that occurred in this age group during the entire COVID-19 pandemic, from February 2020 to February 2022, in Brazil [73, 74].

Assuming an estimated 20 million of children in Brazil, we estimated a total of 4,250 prevented hospitalizations in six months, a higher estimative than the one reported by the US CDC study that estimated the benefits for every million doses of Pfizer-BioNTech COVID-19 vaccination in children 5-11 years of age using two incidence scenarios: scenario A "recent epidemiology data" from the week ending on September 9th, 2021 and scenario B "pandemic average data" assuming an average for the entire pandemic through the week ending on October 16th, 2021. Prevented COVID-19 and hospitalization cases were estimated as, respectively, 58,204 and 226 in scenario A and 18,549 and 80 in scenario B [178]. Such difference may be because CDC estimates were based on an epidemiological scenario previous to the introduction of VOC Omicron.

The United Kingdom Joint Commission on Vaccination and Immunization (JCVI) estimated that children vaccination might prevent 98 hospitalizations for every million administered doses in 20 weeks, and thus 1,760 hospitalizations in the period. In contrast, JCVI considered higher protection post-infection and a lower vaccine effectiveness as parameters to modeling. In addition, they also report a small indirect effect on hospitalizations and deaths as a result of childhood vaccination, a finding very similar to our results. In relation to indirect effects (i.e prevention of deaths and hospital admissions on adults), we hypothesized that it could be related to the proportion of people vaccinated with booster doses, (since this effect is greater in federative units with lower proportions of booster dose Supp. Fig 5,6) and found a moderate/weak, non-significant correlation between indirect impact and 3rd dose coverage in the 27 states in Brazil (Fig. C.7). Even so, an indirect effect on hospitalizations of a child vaccination strategy for influenza was found in mathematical modelling studies [192].

The economic impact was also significant, albeit underestimated as it con-

sidered only averted hospitalization costs. Furthermore, since the reimbursement value paid by the National Health System to hospitals, obtained from SIH-DATASUS was considered to estimate averted costs, the cost of each hospitalization is also underestimated, as reimbursed costs have been demonstrated to be much lower than real costs of hospitalizations using micro-costing methodology, especially in patients with SARI due to COVID-19. For example, Miethke-Morais et al. [193] estimated the average cost of one COVID-19 hospitalization at Int$ 12,000 (equivalent to US$), a value much higher than the reimbursed value of Int$ 4102·37 we considered in our estimates.

Our study has several limitations. First, in order to assess the effects of vaccinating children, we assumed that the vaccination coverage in adults remained constant throughout our simulations. Although this assumption may lead to an increased number of expected hospitalizations and deaths for these age groups, incorporating increasing vaccine coverage in adults would not qualitatively alter our results, and imply only minor quantitative changes in our estimates. Since the end of 2021, the pace of vaccination in adults has significantly decreased, especially in older age groups, the population at greater risk of hospitalization and death [87]. From January 2022, the majority of the population from this age group willing to adhere to the vaccination campaign have already been vaccinated with 3 doses. For older adults (more than 60 years), booster shots were since October 202112. Furthermore, adults below 60 years who received the second or booster doses between January and March 2022 would have a lower risk of developing severe disease [176, 189]. Thus, a small increase in the vaccination coverage for these groups for the analyzed period would likely have little impact in our estimates and main conclusions.

Second, the impact estimated by our model considers only a fixed period of time. The decision to assess the impact for a short-term period relies on the understanding that the longer the projection time of the epidemiological dynamics, the greater the uncertainty [194]. In addition, high disease burden in children would likely occur during a period of intense circulation and epidemic wave of the newly introduction and predominance of the Omicron VOC, which is not expected to last more than 3 months, as it was later demonstrated. However, limiting the estimation for a 3-month period does not capture the benefit of vaccinating children in the context of continuing transmission of COVID-19 as the most plausible scenario includes the persistence of transmission in different locations and populations, albeit at endemic level [195]. Although there is great uncertainty

regarding transmission rates in the medium and long-term, even the maintenance of endemic levels of transmission can present a continuous risk to the health of children, in addition to the risk of new epidemic waves and increased levels of transmission due to the eventual introduction of new variants [195] or untimely relaxation of adherence to NPIs [196].

Thus, we conclude that vaccination in the 5-11 age group has significant potential to reduce the impact of the Omicron variant in terms of hospitalizations, deaths and associated costs. The impact of vaccination can be significantly greater if the vaccination pace is higher, achieving faster vaccination of this population and higher vaccine coverage in a shorter period. Childhood vaccination can result in significant impact and should be introduced, particularly in settings with intense viral circulation in this age group, and after having achieved high vaccine coverage rates in priority groups for vaccination.

Chapter 6

Introduction to Statistical Modelling

6.1 Introduction to Bayesian Statistics

Frequentist analysis assumes that the procedure for testing hypotheses should be repeating controlled experiments that eventually wields true values in the long run. The Bayesian statistical framework, on the other hand, assumes that the scientist already have some hypotheses prior to accessing data. The strength of their belief in the said hypotheses are translated to *prior* probabilities for each hypothesis [197].

Bayesian statistics presupposes that the likelihood of data being explained by a given set of parameters should alter our prior knowledge about the probable values of such parameters, updating our beliefs as more data is available, giving our *posterior* knowledge (or distribution). Such statement is translated by Bayes' Theorem [198], as follows:

$$\text{posterior} \propto \text{likelihood} \times \text{prior} \tag{6.1}$$

or, in a more mathematical way:

$$\pi(\boldsymbol{\theta}|\mathbf{y}) = \frac{\pi(\mathbf{y}|\boldsymbol{\theta})\pi(\boldsymbol{\theta})}{\pi(\mathbf{y})} \tag{6.2}$$

The above equation states that the conditional probability $\pi(\boldsymbol{\theta}|\boldsymbol{y})$ of $\boldsymbol{\theta}$ (our set of parameters) given our set of data $\mathbf{y}$ is true, is equal to the likelihood $\pi(\mathbf{y}|\boldsymbol{\theta})$ of our data $\mathbf{y}$ be explained by our set of parameters $\boldsymbol{\theta}$ multiplied by the prior probability $\pi(\boldsymbol{\theta})$ of our parameters $\boldsymbol{\theta}$ (how much we believe that our values of parameters are good beforehand). This is then normalized by the marginal probability distribution of our data set $\mathbf{y}$, that is given by:

$$\pi(\mathbf{y}) = \int \pi(\mathbf{y}|\boldsymbol{\theta})\pi(\boldsymbol{\theta})d\boldsymbol{\theta} \tag{6.3}$$

Notice that if $\pi(\mathbf{y}|\boldsymbol{\theta})$ and $\pi(\boldsymbol{\theta})$ are properly defined, it leads to $\int \pi(\boldsymbol{\theta}|\mathbf{y})d\boldsymbol{\theta} = 1$, thus defining a probability distribution of $\boldsymbol{\theta}$ values.

Due to the fact that in most practical uses Eq. (6.3) is too complex to be solved analytically, the usual approach is to do Bayesian inference through computational techniques. The most common technique used is the so-called *Markov Chain Monte Carlo* (MCMC). It uses the Markov Chain property of only depending on the current state of system to guess the next step in the solution. It also uses the same Monte Carlo process very common in statistical mechanics (such as Ising-like models) of using a quantity of interest to decide if it should accept the next step or not. In statistical mechanics, the objective is usually minimizing energy in the system, whereas in Bayesian inference is maximizing the posterior conditional probability.

In Section 6.2 we describe the simplest methods of MCMC for the sake of learning, whereas in Section 6.3 we describe an approximation used to speed up computation, that is actually used to study some scenarios of vaccination against COVID-19 in Brazil in Section 7.

6.2 The Metropolis and Metropolis-Hastings algorithms

The *Metropolis* and *Metropolis-Hastings* algorithms come from the idea of sequentially updating the posterior density distribution of parameters $\boldsymbol{\theta}$ following a rule of jumping between states in parameter space, and accepting the new state based on maximization of the conditional probability of the parameter state. Our posterior distribution would then be simply the collection of accepted states $\boldsymbol{\theta}^t$ generated by the successive jumps between states.

Let $\boldsymbol{\theta}^t$ be our current parameter state in iteration t, we then need to define a jumping rule between states $\mathbf{J}(\boldsymbol{\theta}^{t+1}|\boldsymbol{\theta}^t)$. In the case of Metropolis algorithm, such rule must be symmetric (i.e. $\mathbf{J}(\boldsymbol{\theta}_a|\boldsymbol{\theta}_b) = \mathbf{J}(\boldsymbol{\theta}_b|\boldsymbol{\theta}_a)$) to guarantee convergence, whereas in the case of Metropolis-Hastings this condition can be relaxed. An example of $\mathbf{J}$ could be:

$$\mathbf{J}(\boldsymbol{\theta}^{t+1}|\boldsymbol{\theta}^t) = \mathrm{N}(\boldsymbol{\theta}^t, \mathbf{Q}^{-1})$$

where N denotes a multivariate normal distribution centered around the current parameter state and $\mathbf{Q}$ is a precision matrix.

A naive approach to the Metropolis algorithm can be described as follows:

1. At the start of the simulation, provide an initial condition $\boldsymbol{\theta}^0$, or sample it

from an initial distribution $p_0(\boldsymbol{\theta})$ (not necessarily equal to the prior distribution).

2. For $t \in (1, \ldots, n)$, where n is the number of iterations wanted:

   (a) Sample a proposal $\boldsymbol{\theta}^*$ from $\mathbf{J}(\boldsymbol{\theta}^*|\boldsymbol{\theta}^{t-1})$.

   (b) Compute the ratio of conditional probabilities r as:

$$r = \frac{\pi(\boldsymbol{\theta}^*|\mathbf{y})}{\pi(\boldsymbol{\theta}^{t-1}|\mathbf{y})} = \frac{\pi(\mathbf{y}|\boldsymbol{\theta}^*)\pi(\boldsymbol{\theta}^*)}{\pi(\mathbf{y}|\boldsymbol{\theta}^{t-1})\pi(\boldsymbol{\theta}^{t-1})} \tag{6.4}$$

   (c) set $\boldsymbol{\theta}^t$ as:

$$\boldsymbol{\theta}^t = \begin{cases} \boldsymbol{\theta}^*, \text{ if a sample from Unif}(0,1) \leq \min(r,1) \\ \boldsymbol{\theta}^{t-1}, \text{ otherwise} \end{cases} \tag{6.5}$$

   (d) save $\boldsymbol{\theta}^t$.

Notice that if $r \geq 1$, the step increases the conditional probability, and therefore is always accepted, whereas if $r < 1$, the acceptance depends stochastically on the ratio of the conditional probabilities.

This simple approach, however, can lead to strong dependence on initial conditions and too much correlation between samples of the posterior probabilities. We can enhance the algorithm with additional steps to ensure convergence of the posterior distribution:

- To guarantee that the model can converge to a single region of the parameter state, more than one run, here called *chain*, should be considered, generally with over-dispersed initial conditions to cover a reasonable region of the parameter space. If some chains do not converge to the same region, adding more iterations would make then converge eventually (to see proof of convergence of the methods, check [199]);

- Since the algorithm works sequentially, the initial values of parameters could be a considerable part of the posterior distribution. To reduce this dependency on initial conditions, we discard a few of the initial values (usually half of the iterations), maintaining only the values that already converged to the final posterior distribution. The iterations discarded are usually called *burn-in* iterations.

- Finally, to reduce correlation between iterations due to the Markov property, it is usual to only save every other kth iteration of the chain. This process is called *thinning*.

If n_{ch} is the number of chains, n_{it} the number of iterations per chain, n_{bu} the number of burn-in iterations and n_{th} the size of the thinning process, the number of samples that our posterior distribution have is then given by:

$$N_{sa} = \frac{n_{it} - n_{bu}}{n_{th}} n_{ch} \tag{6.6}$$

More details on how to assess convergence and quality of the results can be seen in [199].

The metropolis algorithm can be summarized as follows:

1. For every chain, provide an initial condition $\boldsymbol{\theta}^0$, or sample it from an initial distribution $p_0(\boldsymbol{\theta})$ (not necessarily equal to the prior distribution).
2. For $t \in (1, \ldots, n_{it})$:
   (a) Sample a proposal $\boldsymbol{\theta}^*$ from $\mathbf{J}(\boldsymbol{\theta}^*|\boldsymbol{\theta}^{t-1})$.
   (b) Compute the ratio of conditional probabilities r as:
   $$r = \frac{\pi(\boldsymbol{\theta}^*|\mathbf{y})}{\pi(\boldsymbol{\theta}^{t-1}|\mathbf{y})} = \frac{\pi(\mathbf{y}|\boldsymbol{\theta}^*)\pi(\boldsymbol{\theta}^*)}{\pi(\mathbf{y}|\boldsymbol{\theta}^{t-1})\pi(\boldsymbol{\theta}^{t-1})} \tag{6.7}$$
   (c) set $\boldsymbol{\theta}^t$ as:
   $$\boldsymbol{\theta}^t = \begin{cases} \boldsymbol{\theta}^*, \text{ if a sample from Unif}(0,1) \leq \min(r,1) \\ \boldsymbol{\theta}^{t-1}, \text{ otherwise} \end{cases} \tag{6.8}$$
   (d) if $\text{mod}(t|n_{th}) = 0$ and $t > n_{bu}$, save $\boldsymbol{\theta}^t$.
3. Then, the final posterior distribution is the combination of all $\boldsymbol{\theta}^t$ saved from each chain.

In principle, the only difference between Metropolis and Metropolis-Hastings algorithms is in the calculation of the ratio of probabilities r as:

$$r = \frac{\pi(\boldsymbol{\theta}^*|\mathbf{y})/\mathbf{J}(\boldsymbol{\theta}^*|\boldsymbol{\theta}^{t-1})}{\pi(\boldsymbol{\theta}^{t-1}|\mathbf{y})/\mathbf{J}(\boldsymbol{\theta}^{t-1}|\boldsymbol{\theta}^*)} = \frac{\pi(\mathbf{y}|\boldsymbol{\theta}^*)\pi(\boldsymbol{\theta}^*)/\mathbf{J}(\boldsymbol{\theta}^*|\boldsymbol{\theta}^{t-1})}{\pi(\mathbf{y}|\boldsymbol{\theta}^{t-1})\pi(\boldsymbol{\theta}^{t-1})/\mathbf{J}(\boldsymbol{\theta}^{t-1}|\boldsymbol{\theta}^*)} \tag{6.9}$$

This allows asymmetric jumping rules and speed up computation by allowing larger jumps more frequently. Notice also that if $\mathbf{J}$ is symmetric, we recover the Metropolis algorithm.

Nowadays, much more efficient MCMC algorithms are available, such as the No U-Turn Sampler (NUTS) [200], available in `RStan` [201]. However, as models increase in complexity, requiring bigger number of iterations to reach convergence, it might take too long to give the expected results. In this scenario, some alternatives to MCMC were proposed considering approximations in the distributions used. One example of this is the Integrated Nested Laplacian Approximation (INLA) [202, 203], that we present in the next section.

6.3 Integrated Nested Laplacian Approximation

Before we delve into the details of INLA, we need to revisit some definitions and learn others. Our likelihood function can be rewritten in a more explicit way, following the notation from [202, 203], as:

$$\pi(\mathbf{y}|\mathbf{x},\boldsymbol{\theta}) = \prod_{i=1}^{n} \pi(y_i|\eta_i(\mathbf{x}),\boldsymbol{\theta}) \tag{6.10}$$

where $\mathbf{y} = (y_1,\ldots,y_n)^T$ is our dataset, also called the *response* vector, $\mathbf{x} = (x_1,\ldots,x_n)^T$ is the *latent* field (the parameters we want to infer), $\boldsymbol{\theta} = (\theta_1,\ldots,\theta_m)^T$ is our set of *hyperparameters*, and $\eta_i(\mathbf{x})$ is the i-th linear predictor that connects the data to the latent field (i.e. our model). This new notation separates our set of parameters in two. The first one is called latent (i.e. hidden) in the sense that we can not measure their values directly from data, and we must use a mathematical model to infer them. The second set refers to additional parameters that are not part of the model, but part of the prior distributions used in the analysis (the variance of a normal distribution, for example).

A Structured Additive Regression Model (SARM) assumes that our observations y_i belong to an exponential family, with mean μ_i linked to a structured additive predictor η_i through a link function $g(\cdot)$, where $g(\mu_i) = \eta_i$. The predictor η_i can be written as:

$$\eta_i = \alpha + \sum_{j=1}^{n_f} f^{(j)}(\mathbf{u}_{ji}) + \sum_{k=1}^{n_\beta} \beta_k z_{ki} + \epsilon_i \tag{6.11}$$

where α is the intercept, $f^{(j)}$ are unknown functions of the covariates $\mathbf{u}$, β_k are linear predictors of the covariates z_k, and ϵ_i are random unstructured covariates [202]. The presence of $f^{(j)}$ adds great flexibility to this type of model, as they include Generalized Additive Models (GAM) and Autoregressive (AR) models as subsets, for example.

The Integrated Nested Laplacian Approximation restricts the possibilities of SARM to Gaussian Latent Models (GLM). This subset assumes that the prior distributions of the latent field $\mathbf{x} = \{\alpha, \{f^{(j)}\}, \{b_k\}\}$ are restricted to the Gaussian family:

$$\mathbf{x}|\boldsymbol{\theta} \propto \mathrm{N}(\boldsymbol{\mu}(\boldsymbol{\theta})|\mathbf{Q}^{-1}(\boldsymbol{\theta})) \tag{6.12}$$

i.e. our latent field $\mathbf{x}$ subject to hyperparameters $\boldsymbol{\theta}$ is *explained* by a multivariate normal (thus Gaussian) distribution with mean $\boldsymbol{\mu}$ and precision matrix $\mathbf{Q}$ described in terms of our hyperparameters. The hyperparameters also need to be supplied with a prior distribution, also called *hyperprior*[1]:

$$\boldsymbol{\theta} \propto \pi(\boldsymbol{\theta}) \tag{6.13}$$

Our posterior distribution is then rewritten as:

$$\begin{aligned}\pi(\mathbf{x}, \boldsymbol{\theta}|\mathbf{y}) &\propto \pi(\boldsymbol{\theta})\pi(\mathbf{x}|\boldsymbol{\theta}) \prod_{i=1}^{n} \pi(y_i|\eta_i(\mathbf{x}), \boldsymbol{\theta}) \\ &\propto \pi(\boldsymbol{\theta})|\mathbf{Q}(\boldsymbol{\theta})|^{1/2} \exp\left[-\frac{1}{2}\mathbf{x}^{\mathbf{T}}\mathbf{Q}(\boldsymbol{\theta})\mathbf{x} + \sum_{i=1}^{n} \log\{\pi(y_i|\eta_i(\mathbf{x}), \boldsymbol{\theta})\}\right]\end{aligned} \tag{6.14}$$

where the first term in the right-hand side is the prior distribution of the hyperparameters, the first part in the exponential is the prior distribution of the latent field, taking into consideration that it has to be described by a multivariate normal distribution, and the last term is a simple exponentiation of the likelihood.

INLA requires the latent field $\mathbf{x}$ to be not only Gaussian, but also a (sparse) Gaussian Markov Random Field (GMRF) [204]. A field having the Markov property implies that x_i and x_j are conditionally independent[2] given other parameters in $\mathbf{x}_{-ij}$, for a considerable amount of $\{i, j\}$ pairs. For a Gaussian field, this also implies that the covariance matrix (the inverse of the precision matrix $\mathbf{Q}$) has zeroes in the conditionally independent pairs, thus having great sparsity that

[1] notice the hierarchical nature of INLA modelling.

[2] Random variables A and B are *conditionally independent* given C if $\pi(A|B, C) = \pi(A|C)$.

provides a high speed up in computation[3]. Furthermore, the GMRF condition allow us to describe the density distribution of a random field $\mathbf{z}$ as:

$$\pi(\mathbf{z}) = (2\pi)^{-n/2}|\mathbf{Q}|^{1/2}\exp\{-\frac{1}{2}(\mathbf{z}-\boldsymbol{\mu})^T\mathbf{Q}(\mathbf{z}-\boldsymbol{\mu})\} \tag{6.15}$$

where n is the dimension of $\mathbf{z}$ and $\boldsymbol{\mu}$ is the mean.

Our quantities of interests are the posterior marginal distributions of the parameters. These are given by:

$$\pi(x_i|\mathbf{y}) = \int \pi(x_i|\boldsymbol{\theta},\mathbf{y})\pi(\boldsymbol{\theta}|\mathbf{y})d\boldsymbol{\theta} \tag{6.16}$$

$$\pi(\theta_j|\mathbf{y}) = \int \pi(\boldsymbol{\theta}|\mathbf{y})d\boldsymbol{\theta}_{-j} \tag{6.17}$$

where the negative subscript $-j$ denotes "all *but* j".

As we can see, both equations depend on calculating $\pi(\boldsymbol{\theta}|\mathbf{y})$, and this is our first step. Starting from the identity:

$$\pi(\boldsymbol{\theta}|\mathbf{y}) = \frac{\pi(\mathbf{x},\boldsymbol{\theta}|\mathbf{y})}{\pi(\mathbf{x}|\boldsymbol{\theta},\mathbf{y})} \tag{6.18}$$

The GMRF condition allow us to write $\pi(\mathbf{x}|\boldsymbol{\theta},\mathbf{y})$ as [205]:

$$\pi(\mathbf{x}|\boldsymbol{\theta},\mathbf{y}) \propto \exp\left[-\frac{1}{2}\mathbf{x}^\mathbf{T}\mathbf{Q}(\boldsymbol{\theta})\mathbf{x} + \sum_{i\in\mathcal{L}} g_i(x_i)\right] \tag{6.19}$$

where $g_i(x_i) = \log\{\pi(y_i|x_i,\boldsymbol{\theta})\}$. We can then do a second order approximation of $g_i(x_i)$ around the mode $\mu_i^{(0)}$:

$$g_i(x_i) \approx g_i(\mu_i^{(0)}) + b_i x_i - \frac{1}{2}c_i x_i^2 \tag{6.20}$$

where c_i and b_i depend on $\boldsymbol{\mu}^{(0)}$. In multidimensional expression, this yields:

$$\tilde{\pi}_G(\mathbf{x}|\boldsymbol{\theta},\mathbf{y}) \propto \exp\left(-\frac{1}{2}(\mathbf{x}-\boldsymbol{\mu}(\boldsymbol{\theta}))^T(\mathbf{Q}(\boldsymbol{\theta}) + \mathrm{diag}(\mathbf{c}))(\mathbf{x}-\boldsymbol{\mu}(\boldsymbol{\theta}))\right) \tag{6.21}$$

where G denotes that this is a *Gaussian approximation* of the conditional probability, $\boldsymbol{\mu}$ is the mode of $\pi(\mathbf{x}|\boldsymbol{\theta},\mathbf{y})$. The vector $\mathbf{c}$ comes from the second order expansion around the peak of $\sum\log\pi(y_i|x_i,\boldsymbol{\theta})$ [205]. This expression also preserves the

[3]Further details on why this condition speeds up everything, refer to [205, 202].

Markov condition of the GMRF, thus keeping the problem computationally feasible [202].

This can then be used to approximate the marginal distribution of the hyperparameters as:

$$\tilde{\pi}(\boldsymbol{\theta}|\mathbf{y}) \propto \left.\frac{\pi(\mathbf{x},\boldsymbol{\theta}|\mathbf{y})}{\tilde{\pi}_G(\mathbf{x}|\boldsymbol{\theta},\mathbf{y})}\right|_{\mathbf{x}=\mathbf{x}^*(\boldsymbol{\theta})} \tag{6.22}$$

where $\mathbf{x}^*(\boldsymbol{\theta})$ is the mode of $\mathbf{x}$ for each $\boldsymbol{\theta}$. This is the *Laplace approximation* of the marginal posterior, as done in Tierney and Kadane [206]. To obtain $\tilde{\pi}(\theta_j|\mathbf{y})$ we can simply integrate over all θ's but j, as in equation (6.25), and this is a good enough approximation to the marginal of the hyperparameters.

To compute $\pi(x_i|\boldsymbol{\theta},\mathbf{y})$, we could simply integrate over all $\mathbf{x}_{-i}$. However, this fails to capture the skewness of the distribution, not being able to properly model more complex situations [205]. This is fixed by Rue, Martino, and Chopin [202] by computing the Gaussian approximation of $\pi(\mathbf{x}_{-i}|x_i,\boldsymbol{\theta},\mathbf{y})$ first. We then compute the Laplace approximation of the conditional $\pi(x_i|\boldsymbol{\theta},\mathbf{y})$ as:

$$\tilde{\pi}(x_i|\boldsymbol{\theta},y) \propto \left.\frac{\pi(\mathbf{x},\boldsymbol{\theta}|\mathbf{y})}{\tilde{\pi}_{GG}(\mathbf{x}_{-i}|x_i,\boldsymbol{\theta},\mathbf{y})}\right|_{\mathbf{x}_{-i}=\mathbf{x}^*_{-i}(x_i,\boldsymbol{\theta})} \tag{6.23}$$

where $\tilde{\pi}_{GG}$ is the Gaussian approximation to $\pi(\mathbf{x}_{-i}|x_i,\boldsymbol{\theta},\mathbf{y})$ at the mode $\mathbf{x}^*_{-i}$ of each $(x_i,\boldsymbol{\theta})$.

We then finally have the *nested* approximations of the marginals:

$$\tilde{\pi}(x_i|\mathbf{y}) = \int \tilde{\pi}(x_i|\boldsymbol{\theta},\mathbf{y})\tilde{\pi}(\boldsymbol{\theta}|\mathbf{y})d\boldsymbol{\theta} \tag{6.24}$$

$$\tilde{\pi}(\theta_j|\mathbf{y}) = \int \tilde{\pi}(\boldsymbol{\theta}|\mathbf{y})d\boldsymbol{\theta}_{-j} \tag{6.25}$$

Substituting (6.23) into (6.24) would, in principle, solve all our problems. However, computing $\tilde{\pi}_{GG}$ is still computationally expensive and requires further approximations. We will not delve into these approximations as this is not the focus of this work, but they are available, together with an explanation of the numerical implementation of INLA, in the seminal paper of Rue, Martino, and Chopin [202].

For a more practical approach to INLA, the reader might want to see the books Gomez-Rubio [207] and Moraga [208] for a tutorial approach to INLA modelling and a focus on spatial analysis, respectively. In the next section, we show a counterfactual analysis of vaccination rollout against COVID-19 in Brazil using INLA.

Chapter 7

Estimating the impact of implementation and timing of COVID-19 vaccination program in Brazil: a counterfactual analysis

This work was done by Leonardo Souto Ferreira[1,2], Flavia Maria Darcie Marquitti[2,3], Rafael Lopes Paixão da Silva[1,2], Marcelo Eduardo Borges[2,4], Marcelo Ferreira da Costa Gomes[2,5], Oswaldo Gonçalves Cruz[2,5], Roberto André Kraenkel[1,2], Renato Mendes Coutinho[2,4], Paulo Inácio Prado[2,6], and Leonardo Soares Bastos[2,5], and it was made available as a preprint at *MedRxiv* in December 2021 at [209], and is undergoing review at the date of writing. The author of this thesis was the first author in the article and has developed the model, software, formal analysis, investigation, and writing. The other authors also contributed during all phases of production.

Abstract

Background: The vaccines developed in 2020-2021 against the SARS-CoV-2 virus were designed to prevent severity and deaths due to COVID-19. However, estimates of the effectiveness of vaccination campaigns in achieving these goals remain a methodological challenge. In this work, we developed a

[1]Instituto de Física Teórica, Universidade Estadual Paulista, São Paulo, Brazil.
[2]Observatório COVID-19 BR, São Paulo, Brazil.
[3]Instituto de Física 'Gleb Wataghin' and Instituto de Biologia, Universidade Estadual de Campinas, Campinas, Brazil.
[4]Centro de Matemática, Computação e Cognição, Universidade Federal do ABC, Santo André, Brazil.
[5]Fundação Oswaldo Cruz, Programa de Computação Científica, Grupo de Métodos Analíticos em Vigilância Epidemiológica, Rio de Janeiro, Brazil.
[6]Instituto de Biociências, Universidade de São Paulo, São Paulo, Brazil.

Bayesian statistical model to estimate the number of deaths and hospitalisations avoided by vaccines in older adults in Brazil.

Methods: We fit a linear model to predict the number of deaths and hospitalisations in older adults as a function of vaccination coverage and of casualties in younger adults. We then used this model to perform counterfactual analysis, simulating alternative scenarios without vaccination or with earlier vaccination roll-out. We estimated direct effects of COVID-19 vaccination by computing the difference between hypothetical and realised scenarios.

Results: We estimated that more than 165 thousand individuals above 60 y.o. were not hospitalised due to COVID-19 in the first seven months of the vaccination campaign. An additional contingent of 100 thousand hospitalisations could have been avoided if vaccination had started earlier. We also estimated that more than 75 thousand lives were saved by vaccination in the period analysed for the same age group, and that additional 48 thousand lives could have been saved had the Brazilian Government started the vaccination programme earlier.

Conclusions: Our estimates provide a lower bound for vaccination impacts in Brazil, demonstrating the importance of preventing suffering and loss of the older adults Brazilians. Once vaccines were approved, an early vaccination roll-out could have saved many more lives, especially when facing a pandemic.

7.1 Introduction

Since March 15, 2020, the SARS-CoV-2 has been declared in community transmission in Brazil. During the first year of the pandemic, the epidemic spread fast in Brazil but with different timings and burdens between regions, because of regional differences in health assistance, income and local mitigation policies [210, 71]. On top of that, by January of 2021, Brazil's epidemics saw a strong increase in the number of notified cases and deaths due to SARS-CoV-2, specially in the northern region [71]. The new burst quickly spread to the rest of the country, synchronizing the waves in each region, reducing by the end of May. This wave was later associated with the appearance of the VOC P.1, also known as Gamma, whose emergence was estimated as November of 2020 in Manaus [211, 37]. Brazil also had community transmission of Alpha VOC. However, it was not capable of overcoming Gamma, because the latter was found more transmissible and with

a potential immunity escape [38, 40, 37]. Gamma variant was eventually substituted by the Delta variant in relative frequency, although the majority of Brazilian COVID-19 cases and deaths in 2021 occurred during the Gamma dominance [75]. The country did not suffer another marked increase in cases and deaths during the rest of 2021 as other countries, and such difference is attributed to the vaccination campaign in Brazil.

Brazil has an outstanding history of successful government policies for mass vaccination, including coordinated vaccination campaigns at country level, effective communication strategies, free availability of doses, and the capillarity of the Brazilian's Unified Health System (SUS). For instance, in 2010, the SUS was able to vaccinate 89 millions individuals [212, 85] in response to the 2009 H1N1 influenza pandemic. However, due to several funding cuts and widespread misinformation, the following vaccination campaigns could not surpass the coverage objectives. [213]. The COVID-19 vaccination campaign in Brazil suffered from poor coordination and logistics at the federal level [214], which delayed and slowed down the pace of vaccine roll-out. Vaccination eventually started on January 17, 2021, first covering institutionalized people, native Brazilians, and health professionals. After that, the vaccination roll-out was structured considering age groups, from older to younger individuals, in an at-risk basis [128, 215]. Currently, Brazil has 88.9% and 66.7% of the total population with one and two doses, respectively by the date of December 22, 2021 [87], with an ongoing campaign of booster inoculation. This coverage surpasses richer countries that had earlier availability of vaccines.

However, information about the effectiveness of the current vaccination campaign was in preventing hospitalizations and deaths countrywide, the main purpose of the developed vaccines, still lacks a proper estimation. The only estimates available are for the São Paulo State, the most populous State with the highest GDP in Brazil [216]. Around 24 thousand hospitalizations and 11 thousand deaths have been averted by vaccination in São Paulo state in the age group of 65+ between February 8 and May 28 of 2021, reducing hospitalization costs in US$ 287 millions [216]. Thus, our objective is to expand these figures for the whole country, also accounting for other possible scenarios of vaccination roll-out.

We developed a statistical model to predict the number of deaths and hospitalizations by COVID-19 in age group of older adults from the time series of deaths and cases in younger age groups. The model considers the reduction in relative risks of older age groups as vaccine coverage progressed in this population over

time. We then used the estimated effect of vaccine coverage on reducing relative risks in a counterfactual analysis to estimate the direct effect of vaccination in averting hospitalizations and deaths by COVID-19 in Brazil. Since the model directly accounts for vaccination, we could also provide estimates for the potential number of hospitalizations and deaths averted if vaccines were available earlier to the population. The analysis was conducted considering the age group of adults above 60 years old with a time series that runs until August 28, 2021.

7.2 Methods

7.2.1 Data

The weekly count of hospitalizations and deaths due to COVID-19 notified as Severe Acute Respiratory Infection (SARI) in each age group was obtained from the Influenza's Epidemiological Surveillance Information System (SIVEP-Gripe [73, 74, 217]), extracted on October 18, 2021. This database is publicly available by the Brazilian National Health System. No ethical approval is needed according to the National Ethical Commission (CONEP) of the National Health Council, Resolution Number 510 of April 7, 2016. Shortly after the pandemic onset in Brazil, the anonymized data was published with all the individual cases notified by health care units, and municipal and state health secretariats. We filtered the dataset to keep only the cases that were hospitalized or died due to SARI associated with COVID-19. The association with COVID-19 was filtered based on the case classification field (CLASSI_FIN), plus all cases with a positive RT-PCR test for SARS-CoV-2 regardless of classification. All cases were aggregated by the state of residence. For the weekly count of hospitalized cases, the date of reference is based on symptoms onset. We used the date of death as reference for the weekly number of deaths. The vaccination data was extracted from the National immunization Plan Information System (SIPNI) [87], extracted on November 6, 2021, which includes location, date, type of vaccine, dose (1st, 2nd, 3rd) of vaccine, and age of every person vaccinated against COVID-19 in Brazil. For the SIPNI, we considered the state of vaccine application instead of the state of residence of the individual, as the latter is not always available; although people can be vaccinated in cities other than the one they reside, the difference in numbers is negligible at the state level.

7.2.2 Statistical model

We built a Bayesian statistical model to infer and predict the number of hospitalizations and deaths due to COVID-19 in age classes above 60 y.o. (60+) as a linear function of both the number of hospitalizations and deaths in the 20-29 age class and the vaccine coverage in each age class. We used the coverage of second dose (counting after 14 days from inoculation) of each vaccine v ={AZD1222, CoronaVac, BNT162b2}, produced by AstraZeneca/Oxford/Fiocruz, Sinovac/Butantan and Pfizer/BioNTech, respectively, from the SI-PNI [87]. Aside from these three vaccines, Ad26.COV2.S (Janssen) was also used in Brazilian territory. However, we considered that the number of inoculated doses was too low to have statistical significance in this analysis. The model is given by:

$$\begin{aligned} Y^{(t)} &\sim \text{Normal}(\mu^{(t)}, \sigma), \quad \sigma > 0, \quad t = 1, 2, \dots \\ \mu^{(t)} &= \beta_0 + \beta_1 X^{(t)} + \sum_v \beta_v X^{(t)} c_{Y,v}^{(t)} + \gamma^{(t)}, \end{aligned} \tag{7.1}$$

where $Y^{(t)}$ denotes the number of hospitalizations or deaths at time t expected in the age group being studied, $X^{(t)}$ the number of hospitalizations or deaths at time t of the age group being used as reference, $c_{i,v}^{(t)}$ denotes the coverage of vaccine v in age group i at time t, and $\gamma^{(t)}$ for $t = 1, 2, \dots$ represents temporal Gaussian random effects, modelled as a first-order autoregressive process, AR(1), as the following

$$\begin{aligned} \gamma^{(t)} &\sim \text{Normal}(\rho\gamma^{(t-1)}, \phi), \quad \phi > 0, \quad |\rho| < 1, \quad t = 2, 3 \dots \\ \gamma^{(1)} &\sim \text{Normal}\left(0, (\phi(1-\rho^2))^{-1}\right), \end{aligned} \tag{7.2}$$

where ρ is a temporal correlation and ϕ is the random effects precision.

The model assumes a linear relationship between Y and X in absence of vaccination. The third term in Equation 7.1 expresses that, when vaccination is present, the difference between X and Y is linearly related to the coverage of each vaccine (notice that a different β is fitted to each vaccine). Finally, the latter term of Eq. 7.1 accounts for temporal dependence among hospitalizations or deaths.

Finally, our prior distributions are given (in terms of precision) by:

$$\begin{aligned} p(\beta_0) &\propto 1, \\ \beta_1 &\sim \text{Normal}(0, 0.001), \\ \beta_v &\sim \text{Normal}(0, 0.001), \\ \sigma &\sim \text{Gamma}(1, 0.00001), \end{aligned} \tag{7.3}$$

and the prior distributions of the AR(1) random effects (following the notation of [202]) are given by:

$$\begin{aligned} \kappa = \phi(1-\rho^2) &\sim \text{Gamma}(2, 100) \\ \theta = \log\left(\frac{1+\rho}{1-\rho}\right) &\sim \text{Normal}(0, 0.15). \end{aligned} \tag{7.4}$$

The inference is made using the integrated nested Laplace approximation (INLA) approach [202, 203] implemented in R [218]. The models are fitted independently for each age group of older adults (categorized here as 60-69, 70-79 and 80+) and Brazilian State using 20-29 age group as the reference one (X) between March 1, 2020, and August 29, 2021. The posterior trajectories of fitted and simulated time series are drawn from 1,000 samples for each simulation set and added to generate an aggregated posterior sample to the whole country, providing a 95% Credible Interval (hereafter, 95% CI).

To estimate the effect of vaccination, we set the coverage values to zero and predicted the number of hospitalizations and deaths expected in the absence of the explanatory variables of coverage. Then, we compare the cumulative number of hospitalizations and deaths of this hypothetical trajectory with their equivalent when observed vaccine coverage is considered from January 1, 2021 up to August 29, 2021. We also estimated the effect of vaccination on COVID-19 dynamics if vaccines were available earlier in 2021. To make this, we created two counterfactual scenarios of earlier vaccination by keeping the same pace and shifting the time series of observed vaccine coverage to start four and eight weeks earlier. These counterfactual scenarios are repeated for each age target age group, considering the same amount of vaccines were available in these earlier starting scenarios. To keep the time series until August 29, 2021, in these hypothetical scenarios, we used the four and eight following weeks in the observed time series.

7.3 Results

In Fig. 7.1, the observed time series (dark orange curve and dots) and the estimated series without vaccination (light orange curve) present similar trajectories until May for 60-79 y.o, and until March-April for the age class of more than 80 y.o (80+). The curves by state are presented in the Appendix D. We also present the similarity between the fitted model and the observed data in Fig. D.1. The overlap of these curves shows that the risk of hospitalizations and deaths in the target groups relative to the reference group was little affected during the period when vaccine coverage was still small. Therefore, the model provides a realistic estimate of the reduction of relative risks of casualties in the target groups as coverage increases (see Figs. D.2 and D.3).

The vaccination was not able to suppress the wave of hospitalization cases due to the Gamma variant, which occurred from late January 2021 [40] to late March 2021 [42]. Although for 60-79 y.o., the estimates of deaths have no difference compared to the observed deaths during the Gamma wave, the vaccines decreased the fatal cases for those who were vaccinated earlier (80+) and who likely had a more robust immunity when the Gamma VOC hit. After, vaccination shows a decisive role to preclude the next wave of the deaths and hospitalizations cases at the time of the introduction of the Delta VOC, which occurred in Brazil between May 2021 and July 2021.

If the vaccination roll-out started four weeks earlier, it would have reduced even more hospitalizations and deaths than it actually did in the group 80+ during the Gamma wave (Fig. 7.2). It would also have affected the number of deaths in the 70-79 age group, decreasing its number during the Gamma wave. When we consider vaccine deployment of eight weeks earlier, the number of deaths would be reduced by approximately 45%, 50%, and 40% of the observed number that occurred during the peak of Gamma wave in the 60-69, 70-79, and 80+ age groups, respectively.

If we compare the cumulative number of hospitalizations and deaths between January 1, 2021, and August 29, 2021, with the counterfactual scenario without vaccination, we estimate that the vaccination against COVID-19 directly accounts for reducing at least 166,780 (95% CI: 157,198-176,309) hospitalizations, and 76,503 (95% CI: 71,832-80,714) deaths in the older adults age group. These figures increase to 219,006 (95% CI: 205,903-232,651) and to 101,416 (95% CI: 95,079-107,091), respectively, if we assume that the same vaccination started 4 weeks earlier. Finally,

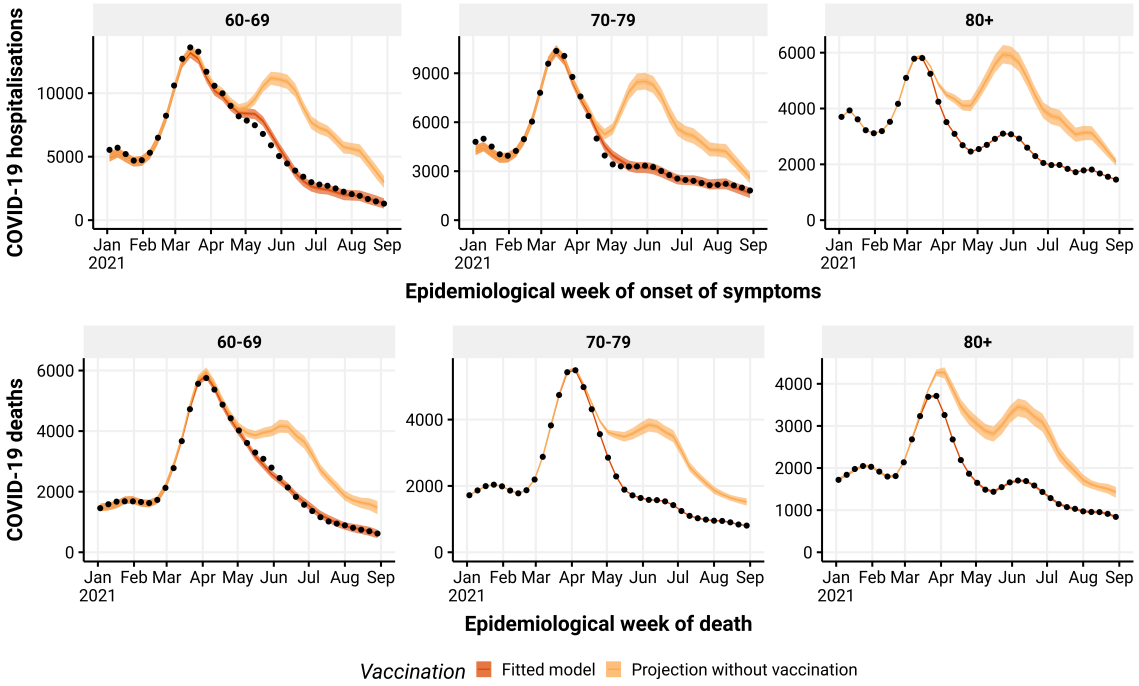

Figure 7.1: Estimated number of hospitalizations (top) and deaths (bottom) by epidemiological week with (dark orange) or without (light orange) vaccination roll-out, by age group (panels). The observed number of hospitalizations and deaths are given by the black dots.

if the vaccination was started 8 weeks earlier, the number of hospitalizations and deaths averted would increase to 268,614 (95% CI: 248,858-289,034) and 124,962 (95% CI: 116,573-132,234), respectively (see Table 7.1). The small overlap between the probability distribution curve of the hypothetical four weeks earlier scenario and the curve of the realized scenario illustrates how significant the avert would be in the number of deaths and hospitalizations by starting vaccination earlier (Fig. 7.3) for all the age groups studied. The difference between the realized and the eight weeks earlier hypothetical scenario is even more remarkable, evidenced by the little overlap between the distributions for the different age groups.

7.4 Discussion

In this work, we used a Bayesian model approach to estimate the number of hospitalizations and deaths in the older adults population (above 60 y.o.) due to COVID-19 in Brazil, under three different scenarios of vaccination roll-outs: the re-

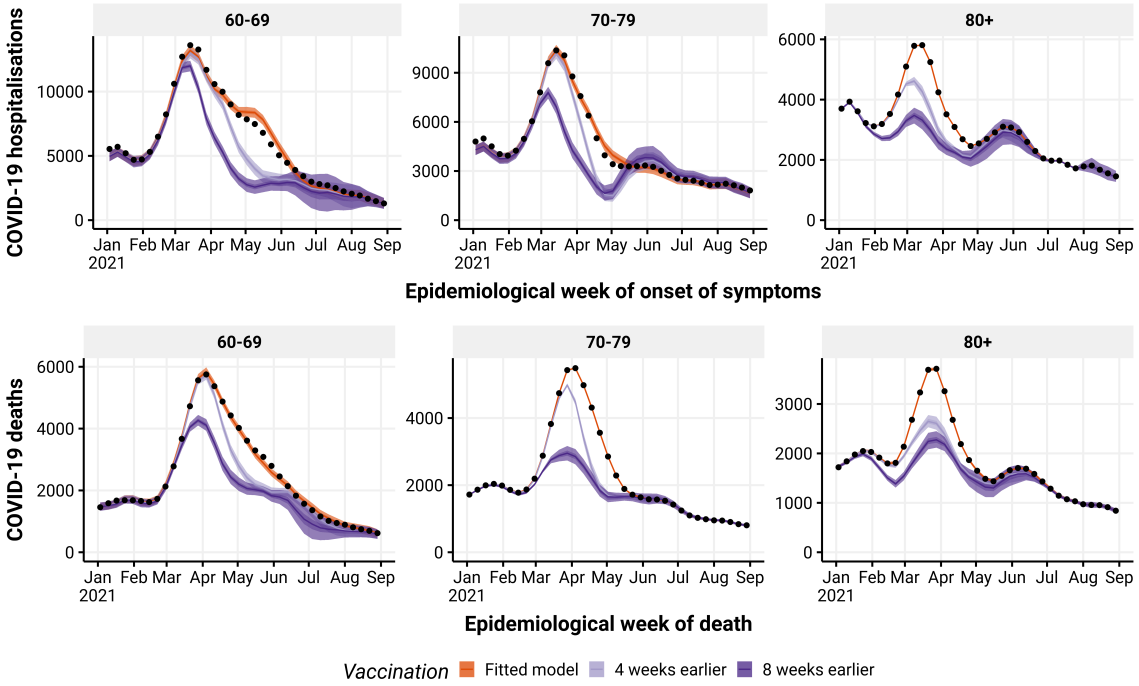

Figure 7.2: Estimated number of hospitalizations (top) and deaths (bottom) due to COVID-19 by epidemiological week with the realized (dark orange), 4 (light purple) and 8 (dark purple) weeks earlier vaccination roll-out, by age group (panels). The observed number of hospitalizations and deaths are given by the black dots. Check legend for gray scale.

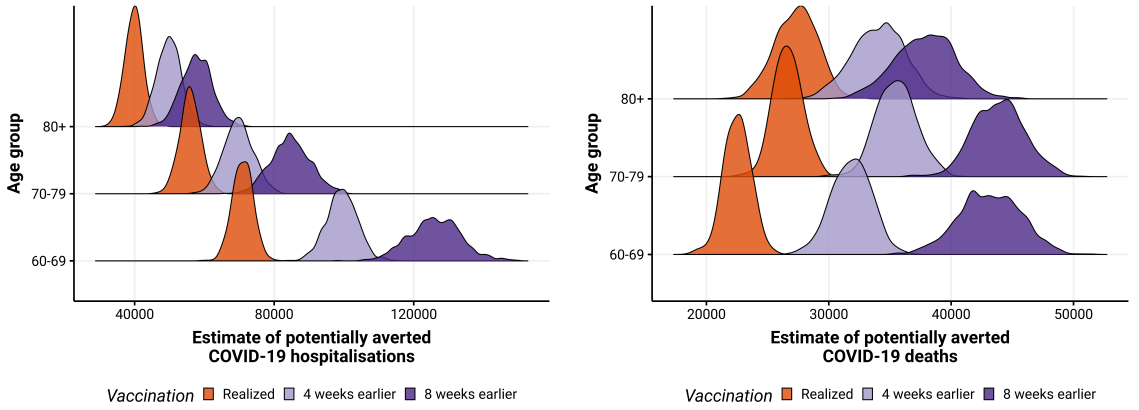

Figure 7.3: Posterior distribution of hospitalizations (left) and deaths (right) due to COVID-19 potentially averted by vaccination between January 1, 2021, and August 29, 2021, by age group, with the realized (dark orange), 4 (light purple) and 8 weeks earlier (dark purple) vaccination roll-out. Check legend for grey scale.

Table 7.1: Estimated reductions in hospitalizations/deaths by age group and vaccine roll-out. 60+ is the aggregate of the all age groups of older adults.

Outcome	Age Group	Vaccine roll-out	Estimated reduction (95% CI)
Hospitalizations	60+	Realized	166,780 (157,198–176,309)
		4 weeks earlier	219,006 (205,903–232,651)
		8 weeks earlier	268,614 (248,858–289,034)
	60-69	Realized	70,987 (65,238–76,641)
		4 weeks earlier	99,425 (90,605–107,850)
		8 weeks earlier	126,102 (111,585–141,016)
	70-79	Realized	55,957 (50,158–61,945)
		4 weeks earlier	69,774 (61,846–78,351)
		8 weeks earlier	84,721 (74,065–96,134)
	80+	Realized	39,837 (34,861–44,874)
		4 weeks earlier	49,806 (43,109–56,685)
		8 weeks earlier	57,791 (49,327–66,424)
Deaths	60+	Realized	76,503 (71,832–80,714)
		4 weeks earlier	101,416 (95,079–107,091)
		8 weeks earlier	124,962 (116,573–132,234)
	60-69	Realized	22,518 (20,370-24,564)
		4 weeks earlier	31,849 (28,648–34,863)
		8 weeks earlier	43,158 (38,122–47,858)
	70-79	Realized	26,637 (24,440–29,027)
		4 weeks earlier	35,518 (32,511–38,783)
		8 weeks earlier	43,916 (39,993–48,055)
	80+	Realized	27,348 (23,830–30,440)
		4 weeks earlier	34,049 (29,765–38,110)
		8 weeks earlier	37,888 (32,962–42,515)

alized one; starting immunizations four weeks earlier; and starting immunizations eight weeks earlier. These numbers were compared to a putative scenario with no vaccination. By assuming that the risks in the target group (older adults) relative to a reference group (20-29 age group) decrease as vaccination coverage increases, we accurately fit the decrease in the number of hospitalizations and deaths in the target group.

We estimated that vaccination in Brazil averted hospitalizations due to COVID-19 of more than 165 thousand individuals above 60 y.o. between January and August 2021, a decrease of 35% compared to the scenario with no vaccination. Furthermore, if we consider the mean cost of US$12,000.00 per admission in hospital [193], Brazil saved about US$ 2 billion in health care as a direct effect of vaccination, which is equivalent to what the country spent on vaccination in the same period (US$ 2.2 billion, [219]). An additional 100 thousand more individuals

above 60 y.o. would not have been hospitalized if the immunization had started eight weeks earlier. We also estimate that more than 75 thousand lives of older adults were saved in the period analyzed, a 35% decrease in deaths that would occur between March and August in the scenario without vaccination. A further 48 thousand lives would have been saved if the Brazilian Government started the immunization eight weeks earlier, *i.e.* at least 20% of the actual deaths in 60+ y.o. individuals during the period analyzed could be avoided. It is important to notice that, although the Brazilian vaccination campaign was officially started in January 18, 2021 [128], second dose coverage in the population above 80 y.o. only reached the level of about 50% nationwide by the end of March [87]. For those of $60-69$ y.o., it only reached above 50% by the end of the first semester [87]. Since those age groups were mostly vaccinated with CoronaVac [43, 87], with an interval of $2-4$ weeks between doses at that time, the 4 and 8 weeks earlier vaccination scenarios are not unrealistic ones, since population level impacts are only significant after at least a significant part of the target population is immunized.

In the next paragraphs, we discuss three points that allow us to state that our estimates are a lower bound for the saved lives in the most critical period of COVID-19 epidemic in Brazil: (i) our model estimates only the direct effects of vaccination, therefore no herd immunity and no secondary morbidity or mortality effects were considered; (ii) we performed analysis considering only the most vulnerable age population (60+), which accounts for the 42.5% of hospitalizations and 62.8% of deaths in Brazil during the period analyzed; and (iii) we considered exactly the same pace of vaccination in our hypothetical earlier roll-out scenarios that was performed, which is very slow if compared to the speed capacity and organization Brazil had during previous mass vaccinations [212, 85].

Vaccination can reduce hospitalizations and deaths via three main (direct and indirect) effects: reducing the severity of the disease in infected individuals; reducing the susceptibility to infection of vaccinated individuals; and reducing the transmission potential of vaccinated individuals that do get infected, mostly by shortening the period during which viral shedding is high [220, 221, 222]. Our counterfactual scenarios assumed that vaccination affected hospitalization and death only in the target age group (60+), but not in the reference age group (20-29 y.o.), since this age group remained unvaccinated in the period studied. This assumption means that we did not account for the curbing of infections caused by reducing susceptibility and transmission.

Population effects, such as those affecting the transmission, are not included

here, and therefore this model is always expected to underestimate figures of averted hospitalizations and deaths. Another factor we did not consider is that, with fewer hospitalizations, the healthcare system would provide better services and potentially increase the survival of individuals with severe COVID-19. High healthcare burden substantially affected in-hospital mortality, especially during peaks and in regions with fragile health infrastructure [71]. Ignoring this effect also leads to an underestimation of the vaccination effect on deaths.

Our estimates are restricted to age groups over 60 y.o. We made this choice for two main reasons: the National immunization Plan prioritized an order of vaccination from older age groups towards younger age groups, so that for the period analyzed, most of the vaccination effort had been directed towards these age groups. Vaccination of younger age groups by age criterion (excluding health workers, individuals with certain medical conditions, among others), in turn, only started after July in most states. The second reason is that age groups above 60 y.o. represent the highest risk of hospitalization and mortality, accounting for 42.5% of hospitalizations and 62.8% of deaths in Brazil during the period analyzed. Therefore, the choice to focus on these age groups reduces the estimates on the number of averted hospitalizations and casualties since it is also affected by the age pyramid distribution in each state.

Another hypothetical scenario, not analyzed here, is considering a different pace of vaccination, compatible with the Brazilian capacity to organize mass vaccinations. In the past, Brazil was capable of making the oral immunization of nearly 20 million children against polio in a single day [223, 224]. In the 2010 mass vaccination against Influenza, Brazil vaccinated more than 80% of the target group, corresponding to 89 million people, during the seasonal campaign [212, 85]. Recent local and national experiences with yellow fever vaccination [225] also indicate the country has the organization and structure to make fast massive campaigns to control epidemics, which, for a variety of reasons, was not the case with the COVID-19 vaccination. Brazil vaccinated 250,000 doses per day between February and March 2021, passing to an average of 500,000 doses per day in the period between April and May 2021, and reaching a pace of above 1 million doses per day only in June 2021 [87]. If the Brazilian government had used all its capacity to organize the COVID-19 campaign, one could expect more significant reduction in deaths and hospitalizations than the figures estimated in this work.

On the other tail of age groups (children), Brazil faces a similar problem to the one analyzed here. The BNT162b2 pediatric vaccine was approved by the

Brazilian Health Regulatory Agency (ANVISA) in December 16, 2021 [84], and the starting date of the pediatric vaccination was a month later – officially in January 14, 2022 [226, 154] in a slow rate of delivery. Contradictorily, Brazil has high pediatric hospitalization and mortality from COVID-19. For the 5-11 age group the COVID-19 was the cause of 3302 and 3317 hospitalizations in 2020 and 2021 (until November 29, 2021), respectively [73, 74], whereas 156 and 142 deaths occurred in 2020 and 2021 (until November 29, 2021), respectively, as a consequence of COVID-19 [73, 74]. Additionally, deaths due to SARI consequences were 450 and 292 in 2020 and 2021 (until November 29, 2021), respectively [73, 74]. In order to compare the magnitude of these figures related to SARI, one can look at the leading mortality cause of children in the 5-9 age group in Brazil: disregarding external causes (such as violence), nervous system diseases and neoplasms, the greatest cause of mortality between 2015 and 2019 was the sum of all respiratory system diseases, which in average caused 283 deaths per year [227]. These numbers put evident importance of the role COVID-19 alone is playing in child mortality.

Based on the results presented in this work, in which we observe the direct effect of lives saved, comparing to a scenario with no vaccination, we can say, in advance, that postponing children's vaccination led to avoidable suffering and deaths. Therefore, future studies similar to ours will be needed to estimate the number of children's lives Brazil has sacrificed due to unexplained delays.

Chapter 8

Conclusion

Public Health faced an unprecedented challenge to mitigate the SARS-CoV-2 pandemic. However, with the advance of mathematical and computational techniques, the researchers were able to deliver expedite results with the ability of impacting public policies around the world. In Brazil, we had the opportunity of contributing to this through the studies displayed in this work.

Whilst in the work presented in Chapter 3 we developed a general framework for preparing vaccination strategies if some data is not available, we also developed an optimization model that could be used in vaccine stock management, and this created an opportunity for collaboration in future vaccination rollouts in state level organizations. The work developed in Chapter 4 was able to deliver specific results that were used to advise public policies regarding vaccinating with AZD1222. We had the opportunity to present these results to policymakers at Fiocruz, the local producers of AZD1222 in Brazil, incentivizing an increase in vaccine procurement.

In the same fashion, the work in Chapter 5 has shown the considerable impact of expedited vaccination of children against COVID-19. This work was also presented to policymakers to supply them with information to reduce vaccine hesitancy. For the same purpose, the study was disseminated to the public through many media formats.

Whilst these works had good reception in technical committees, they are always barred when going to be implemented as actual policies. This is not due to a fault of the committees, but because the last word in these situations is given to political actors and not scientists. This is a symptom of the organizational structure of the Brazilian government (in every level) and is not restricted to modelling studies, but any technical recommendation. Therefore, we should elect politicians that make science-guided decisions and select properly prepared professionals to key positions in the Brazilian government, if we expect to have a functional society.

Unfortunately, the objectives and limitations of this type of work are not always properly understood by policymakers. One of the reasons may be the lack of quantitative methods' knowledge in health science courses in Brazil. Another

reason may be the lack of integration of modelers and researchers with health policymakers. While a lot of research is done inside academia, many policymakers, specially in lower levels of the Brazilian government, are not updated to the best practices in public health. This led to wrong recommendations to the public, that may have led to excess deaths during this pandemic.

While Brazil has some statistics in epidemiology groups inside governmental institutions with the objective of disease forecasting, such as InfoGripe and InfoDengue, we lack groups with a focus in other than academic research in mathematical epidemiology. This should be addressed by the government if we want to achieve international standards, such as done in the United States and Europe, as this type of work requires a certain level of investment and access to epidemiologic data that academic institutions may not have available.

Nevertheless, the pandemic may have sparkled interest in the area, and we expect a growth in the number of groups dedicated to mathematical epidemiology in Brazil in the future.

Appendix A

Supplementary material for Chapter 3

This supplementary material describes more thoroughly our model. In section A.1 We have the equations that describe the model. A.2 contains the epidemiological parameters of the model (the vaccination parameters are described in the main text), together with our mathematical approach to vaccine efficacies in A.2.1. Finally, in section A.3 we describe the mathematical approach to calculate Rt and the initial conditions of the model. The code is available at https://github.com/covid19br/VaxModel-paper.

A.1 Model Equations

To model the virus dispersal in the population, we assume that asymptomatic individuals have equal infectiousness compared to symptomatic ones, while pre-symptomatics have reduced infectiousness given by ω. To model behavior, we assume that symptomatic individuals isolate themselves at some degree, reducing their contacts by ξ, individuals with severe disease have greater isolation ξ_{sev} due to hospitalization. The daily contacts between each age class is given by the matrix $\hat{C}$ and the force of infection λ is given below:

$$\begin{aligned}\lambda = \hat{C}[&A + \omega E + (1-\xi)I + (1-\xi_{sev})H + \\ &A_v + \omega E_v + (1-\xi)I_v + (1-\xi_{sev})H_v + \\ &A_w + \omega E_w + (1-\xi)I_w + (1-\xi_{sev})H_w]\end{aligned} \tag{A.1}$$

Our model does not assume a reduction in infectiousness by vaccination, given the lack of data[1].

[1] We expect that this would not change the results qualitatively.

Unvaccinated

$$\frac{dS}{dt} = -\beta\lambda\frac{S}{N} - v(t)\frac{S}{S+R} \tag{A.2a}$$

$$\frac{dE}{dt} = \beta\lambda\frac{S}{N} - \frac{E}{\gamma} \tag{A.2b}$$

$$\frac{dA}{dt} = \frac{\alpha(1-\sigma)E}{\gamma} - \frac{A}{\nu_i} \tag{A.2c}$$

$$\frac{dI}{dt} = \frac{(1-\alpha)(1-\sigma)E}{\gamma} - \frac{I}{\nu_i} \tag{A.2d}$$

$$\frac{dH}{dt} = \frac{\sigma E}{\gamma} - \frac{H}{\nu_s} \tag{A.2e}$$

$$\frac{dR}{dt} = \frac{A}{\nu_i} + \frac{I}{\nu_i} + \frac{(1-\mu)H}{\nu_s} - v(t)\frac{R}{S+R} \tag{A.2f}$$

$$\frac{dD}{dt} = \frac{\mu H}{\nu_s} \tag{A.2g}$$

Vaccinated once

$$\frac{dS_v}{dt} = -\beta_v\lambda\frac{S_v}{N} + v(t)\frac{S}{S+R} - (1-\theta)v(t-a)\frac{S(t-a)}{S(t-a)+R(t-a)} \tag{A.2h}$$

$$\frac{dE_v}{dt} = \beta_v\lambda\frac{S_v}{N} - \frac{E_v}{\gamma} \tag{A.2i}$$

$$\frac{dA_v}{dt} = \frac{\alpha_v(1-\sigma_v)E_v}{\gamma} - \frac{A_v}{\nu_i} \tag{A.2j}$$

$$\frac{dI_v}{dt} = \frac{(1-\alpha_v)(1-\sigma_v)E_v}{\gamma} - \frac{I_v}{\nu_i} \tag{A.2k}$$

$$\frac{dH_v}{dt} = \frac{\sigma_v E_v}{\gamma} - \frac{H_v}{\nu_s} \tag{A.2l}$$

$$\frac{dR_v}{dt} = \frac{A_v}{\nu_i} + \frac{I_v}{\nu_i} + \frac{(1-\mu_v)H_v}{\nu_s} + v(t)\frac{R}{S+R} - (1-\theta)v(t-a)\frac{R(t-a)}{S(t-a)+R(t-a)} \tag{A.2m}$$

$$\frac{dD_v}{dt} = \frac{\mu_v H_v}{\nu_s} \tag{A.2n}$$

Vaccinated twice

$$\frac{dS_w}{dt} = -\beta_w \lambda \frac{S_w}{N} + (1-\theta)v(t-a)\frac{S(t-a)}{S(t-a)+R(t-a)} \tag{A.2o}$$

$$\frac{dE_w}{dt} = \beta_w \lambda \frac{S_w}{N} - \frac{E_v}{\gamma} \tag{A.2p}$$

$$\frac{dA_w}{dt} = \frac{\alpha_w(1-\sigma_w)E_w}{\gamma} - \frac{A_w}{\nu_i} \tag{A.2q}$$

$$\frac{dI_w}{dt} = \frac{(1-\alpha_w)(1-\sigma_w)E_w}{\gamma} - \frac{I_w}{\nu_i} \tag{A.2r}$$

$$\frac{dH_w}{dt} = \frac{\sigma_w E_w}{\gamma} - \frac{H_w}{\nu_s} \tag{A.2s}$$

$$\frac{dR_w}{dt} = \frac{A_w}{\nu_i} + \frac{I_w}{\nu_i} + \frac{(1-\mu_w)H_w}{\nu_s} + (1-\theta)v(t-a)\frac{R(t-a)}{S(t-a)+R(t-a)} \tag{A.2t}$$

$$\frac{dD_w}{dt} = \frac{\mu_w H_w}{\nu_s} \tag{A.2u}$$

The equations were numerically solved by the R package developed by FitzJohn and Hinsley [228].

A.2 Parameterization of the model

The parameters that do not depend on vaccination are given in Table A.1.

Table A.1: Epidemiological parameters

Parameter	Description	Value	Source
γ	Average time in days between being infected and developing symptoms	5.8	Wei et al. [229]
ν_i	Average time in days between being infectious and recovering for asymptomatic and mild cases	9.0	Cevik et al. [230]
ν_s	Average time between being infectious and recovering/dying for severe cases	8.4	SIVEP-Gripe for São Paulo State [73, 74]
ξ	Reduction on the exposure of symptomatic cases (due to symptoms/quarantining)	0.1	Assumed
ξ_{sev}	Reduction on the exposure of severe cases (due to hospitalization)	0.9	Assumed
ω	Relative infectiousness of pre-symptomatic individuals	1.0	Assumed
α	Proportion of asymptomatic cases	[0.67,0.44,0.31]	Juvenile [231] Adult and Elderly [232]
σ	Proportion of infectious cases that require hospitalization	[0.001, 0.014, 0.099]	Salje et al. [233]
μ	In-hospital mortality ratio	[0.417,0.188,0.754]	Portella et al. [234]

A.2.1 Efficacy parameters computation from observed efficacies

The vaccinated classes parameters are combined with vaccine efficacies as:

$$\begin{aligned} \beta_v &= (1-\epsilon_{\beta,v})\beta & \alpha_v &= 1-(1-\epsilon_{\alpha,v})(1-\alpha) \\ \beta_w &= (1-\epsilon_{\beta,w})\beta & \alpha_w &= 1-(1-\epsilon_{\alpha,w})(1-\alpha) \\ \sigma_v &= (1-\epsilon_{\sigma,v})\sigma & \mu_v &= (1-\epsilon_{\mu,v})\mu \\ \sigma_w &= (1-\epsilon_{\sigma,w})\sigma & \mu_w &= (1-\epsilon_{\mu,w})\mu \end{aligned} \tag{A.3}$$

To avoid multiplicative effects in vaccine efficacies, we need to calculate the efficacy parameters from the reported values. Let us start with the risk of infection. In our model, this is given by β. Thus, the observed efficacy against infection E_β is given by:

$$E_\beta = 1 - \frac{(1-\epsilon_\beta)\beta}{\beta} = \epsilon_\beta \tag{A.4}$$

Therefore, the protection against infection parameter is simply the observed efficacy. Note that we dropped the dose index as these expressions are valid for both first and second dose efficacies.

The risk of individuals being hospitalized is given by $\beta\sigma$, therefore, the observed efficacy in reducing hospitalized cases E_σ is then given by:

$$E_\sigma = 1 - \frac{(1-\epsilon_\beta)\beta(1-\epsilon_\sigma)\sigma}{\beta\sigma} = 1-(1-\epsilon_\beta)(1-\epsilon_\sigma) \tag{A.5}$$

In terms of known values, the protection against hospitalization is given by:

$$\epsilon_\sigma = 1 - \frac{1-E_\sigma}{1-E_\beta} \tag{A.6}$$

Being μ the proportion of hospitalized individuals that die, we have that the risk of an individual being infected and die is given by $\beta\sigma\mu$, therefore the observed efficacy against death E_μ is given by:

$$E_\mu = 1 - \frac{(1-\epsilon_\beta)\beta(1-\epsilon_\sigma)\sigma(1-\epsilon_\mu)\mu}{\beta\sigma\mu} = 1-(1-\epsilon_\beta)(1-\epsilon_\sigma)(1-\epsilon_\mu) \tag{A.7}$$

We then can obtain ε_μ in terms of known values:

$$\varepsilon_\mu = 1 - \frac{1 - E_\mu}{(1-\epsilon_\beta)(1-\epsilon_\sigma)} = 1 - \frac{1 - E_\mu}{(1-E_\beta)\frac{(1-E_\sigma)}{(1-E_\beta)}} = 1 - \frac{1-E_\mu}{1-E_\sigma} \tag{A.8}$$

In our model, symptomatic cases are given by severe (hospitalized) and mild cases, the risk of becoming a symptomatic individual is given by $\beta[\sigma + (1-\sigma)(1-\alpha)]$, then the observed efficacy E_{symp} is given by:

$$E_{symp} = 1 - \frac{(1-\epsilon_\beta)\beta\{(1-\varepsilon_\sigma)\sigma + [1-(1-\varepsilon_\sigma)\sigma][(1-\varepsilon_\alpha)(1-\alpha)]\}}{\beta[\sigma + (1-\sigma)(1-\alpha)]} \tag{A.9}$$

Thus

$$\frac{(1-E_{symp})[\sigma + (1-\sigma)(1-\alpha)]}{1-\epsilon_\beta} = (1-\epsilon_\sigma)\sigma + [1-(1-\epsilon_\sigma)\sigma][(1-\epsilon_\alpha)(1-\alpha)] \tag{A.10}$$

Then

$$1 - \epsilon_\alpha = \frac{\frac{(1-E_{symp})}{(1-\epsilon_\beta)}[\sigma + (1-\sigma)(1-\alpha)] - (1-\epsilon_\sigma)\sigma}{[1-(1-\epsilon_\sigma)\sigma](1-\alpha)} \tag{A.11}$$

Therefore, ε_α is given in terms of known variables as:

$$\varepsilon_\alpha = 1 - \frac{(1-E_{symp})[\sigma + (1-\sigma)(1-\alpha)] - (1-E_\sigma)\sigma}{(1-E_\beta)\left[1 - \frac{(1-E_\sigma)}{(1-E_\beta)}\sigma\right](1-\alpha)} \tag{A.12}$$

Note that $1 - E_{symp}$ does not multiply the whole expression.

A.3 Effective reproduction number and initial conditions estimation

Both initial conditions estimation and effective reproduction number calculations go through rewriting the model in a different notation. It is a system of equations for two different groups, infected ($\mathbf{y}$) and non-infected ($\mathbf{z}$) populations, being $\mathbf{y} = (E,\ A,\ I,\ H)^T$, and $\mathbf{z} = (S,\ R,\ D)^T$. Note that none of the vaccinated classes are considered since at the initial condition no vaccine has been applied yet.

We write the system

$$\dot{\mathbf{y}} = F(\mathbf{y}, \mathbf{z}) - G(\mathbf{y}, \mathbf{z}), \tag{A.13}$$

$$\dot{\mathbf{z}} = J(\mathbf{y}, \mathbf{z}), \tag{A.14}$$

where F are all entries of new Infected, coming from classes $\mathbf{z}$, whilst G accounts for the transitions within infected classes and also recovery and death from the disease. J accounts for the exits of the susceptible population to exposed classes, and the entrance of recovered and deceased in their respective compartments. Consider a linearization around a fixed vector $\mathbf{z} = \tilde{\mathbf{z}}$, the equation for $\mathbf{y}$ becomes

$$\dot{\mathbf{y}} = (\hat{F} - \hat{G})\mathbf{y}, \tag{A.15}$$

where $\hat{F}$ and $\hat{G}$ are matrices that appear from linearizing functions F and G, respectively. Remembering that each of the compartments is divided into three age sub-compartments, that is $\mathbf{S} = (S_{young}, S_{adult}, S_{elderly})$ and that the only entrance of new infected comes from the $\beta \mathbf{S} \lambda / N$ terms in the $\dot{E}$ equations, we write

$$\hat{F} = \frac{\beta}{N} \begin{bmatrix} \omega\hat{b} & \hat{b} & (1-\xi)\hat{b} & (1-\xi_{sev})\hat{b} \\ & & 0_{9,12} & \end{bmatrix}, \tag{A.16}$$

where

$$\hat{b} = \text{diag}(\mathbf{S})\hat{C}, \tag{A.17}$$

being $\hat{C}$ the contact matrices, from [136], ω the relative infectiousness of exposed individuals and ξ and ξ_{sev} the reductions in contacts of people that are symptomatic and hospitalized, respectively.

Now, $\hat{G}$ contains the terms of Exposed, E, developing the possible forms of disease considered in the model as the terms in its first 3 rows, while it's main diagonal contains terms of recovery and death, writing

$$\hat{G} = \begin{bmatrix} \gamma^{-1} & & & \\ -\alpha(1-\sigma)\gamma^{-1} & \nu_i^{-1} & & \\ -(1-\alpha)(1-\sigma)\gamma^{-1} & & \nu_i^{-1} & \\ -\sigma\gamma^{-1} & & & \nu_s^{-1} \end{bmatrix}. \tag{A.18}$$

Now, F and G are important for both R_t calculation and initial conditions estimation. Note that for the linear problem, assuming, $\mathbf{y}(t) = \sum_i \mathbf{a}_i e^{r_i t}$, $\mathbf{a}_i$ constant vectors, yields

$$\sum_i r_i \mathbf{a}_i e^{r_i t} = (\hat{F} - \hat{G}) \sum_i \mathbf{a}_i e^{r_i t}. \tag{A.19}$$

Defining $r^* = \max r_i$, $\mathbf{a}^*$ the vector associated with the exponential coefficient r^*, and dividing the above equation by $e^{r^* t}$, we get

$$\sum_i r_i \mathbf{a}_i e^{(r_i - r^*)t} = (\hat{F} - \hat{G}) \sum_i \mathbf{a}_i e^{(r_i - r^*)t}\ , \tag{A.20}$$

so after some time t elapses, the tuple $(\mathbf{a}^*, r^*)$ dominate the dynamics, and we're left with

$$r^* \mathbf{a}^* = (\hat{F} - \hat{G}) \mathbf{a}^* \tag{A.21}$$

The main eigenvector of $\hat{F} - \hat{G}$, $\mathbf{a}^*$, gives a distribution of infected individuals among different classes. With hospitalizations per day data, we can fit a re-scaling factor for the eigenvector to match the term of hospital entrances ($\sigma\gamma^{-1}E$).

Notably, the effective reproduction calculation can be performed with $\hat{F}$ and $\hat{G}$ as

$$R_t = \rho(FG^{-1})\ , \tag{A.22}$$

where $\rho(FG^{-1})$ is the spectral radius of FG^{-1}, which may be seen as the dominant eigenvalue of FG^{-1} in the simplest cases. The derivation of said result can be checked in multiple textbooks, see, for instance, chapter 6 in Driessche and Watmough [115].

Appendix B

Supplementary material for Chapter 4

In this material, we describe the methodology used in the paper. The code is available at https://github.com/covid19br/paper_markov. In section B.1.1 we describe the basic epidemiological model. In section B.1.2 we describe how we add vaccination to the model. In section B.1.3 we describe the optimization model for vaccine doses allocation. In section B.1.4 we describe how we allocate vaccine doses between ages. Finally, in section B.2 we describe the parameters used in the model, together with sources. In section B.3 we show the tabulated results.

B.1 Model

B.1.1 Epidemiological model

We construct a discrete-time SEIR-like model with constant probabilities. We assume that a susceptible individual (S) has a probability p of being infected. If a infection occurs, the individual transits to the exposed (E), pre-symptomatic, compartment. After the incubation period, the individual can transit to hospitalized (H), mildly symptomatic (I) or asymptomatic (A) compartments. If the individual is hospitalized, the possible outcomes are recovery (R) or death (D), with the respective compartments. In the case of asymptomatic and mildly symptomatic we assume recovery as the only possibility.

As some parameters can be described as rates $(1/t)$, we assume (as in typical SEIR-like models) an exponential distribution of time to transition. For example, the incubation period γ, can be written as the probability of a pre-symptomatic individual exiting the Exposed compartment after one day, given by $1 - \exp(-1/\gamma)$, as follows from the Gillespie algorithm. Ignoring age structure and vaccination, the model can be written by:

$$S^{t+1} = (1-p)S^t \tag{B.1}$$
$$E^{t+1} = pS^t + \exp(-1/\gamma)E^t \tag{B.2}$$
$$I^{t+1} = (1-\sigma)(1-\alpha)(1-\exp(-1/\gamma))E^t + \exp(-1/\nu)I^t \tag{B.3}$$
$$A^{t+1} = (1-\sigma)\alpha(1-\exp(-1/\gamma))E^t + \exp(-1/\nu)A^t \tag{B.4}$$
$$H^{t+1} = \sigma(1-\exp(-1/\gamma))E^t + \exp(-1/\nu)H^t \tag{B.5}$$
$$\begin{aligned} R^{t+1} &= R^t + (1-\mu)(1-\exp(-1/\nu))H^t \\ &\quad + (1-\exp(-1/\nu))A^t + (1-\exp(-1/\nu))I^t \end{aligned} \tag{B.6}$$
$$D^{t+1} = D^t + \mu(1-\exp(-1/\nu))H^t \tag{B.7}$$

Or in the form of a transition matrix:

$$\mathbf{P} = \begin{pmatrix} 1-p & p & 0 & 0 & 0 & 0 & 0 \\ 0 & e^{-1/\gamma} & (1-\sigma)(1-\alpha)(1-e^{-1/\gamma}) & (1-\sigma)\alpha(1-e^{-1/\gamma}) & \sigma(1-e^{-1/\gamma}) & 0 & 0 \\ 0 & 0 & e^{-1/\nu} & 0 & 0 & 1-e^{-1/\nu} & 0 \\ 0 & 0 & 0 & e^{-1/\nu} & 0 & 1-e^{-1/\nu} & 0 \\ 0 & 0 & 0 & 0 & e^{-1/\nu} & (1-\mu)(1-e^{-1/\nu}) & \mu(1-e^{-1/\nu}) \\ 0 & 0 & 0 & 0 & 0 & 1 & 0 \\ 0 & 0 & 0 & 0 & 0 & 0 & 1 \end{pmatrix} \tag{B.8}$$

where the evolution of the system is given by the Chapman-Kolmogorov equation [235]:

$$\mathbf{x^{t+1}} = \mathbf{P}\mathbf{x^t} \tag{B.9}$$

where $\mathbf{x^t}$ is a column vector given by:

$$\mathbf{x^t} = (S^t,\, E^t,\, I^t,\, A^t,\, H^t,\, R^t,\, D^t) \tag{B.10}$$

Notice that we now can write the compartments as vector quantities describing age structure. We divide our population in 10-year age bins, thus, for example S, is written as $S = (S_1, S_2, \ldots, S_{10})$ and the transition matrix has the probabilities rewritten as diagonal matrices, giving different values for each age bin, if necessary (see Tables B.4 and B.5).

B.1.2 Vaccination Model

To account for vaccination we duplicate the model for first and second dose vaccinated individuals for each vaccine (AZD1222, CoronaVac, BNT162b2), as

they are simulated at the same time. The equations for these compartments are given by:

$$S_{j,v}^{t+1} = (1 - p_{j,v})S_{j,v}^{t} \tag{B.11}$$
$$E_{j,v}^{t+1} = p_{j,v}S_{j,v}^{t} + \exp(-1/\gamma)E_{j,v}^{t} \tag{B.12}$$
$$I_{j,v}^{t+1} = (1 - \sigma_{j,v})(1 - \alpha_{j,v})(1 - \exp(-1/\gamma))E_{j,v}^{t} + \exp(-1/\nu)I_{j,v}^{t} \tag{B.13}$$
$$A_{j,v}^{t+1} = (1 - \sigma_{j,v})\alpha_{j,v}(1 - \exp(-1/\gamma))E_{j,v}^{t} + \exp(-1/\nu)A_{j,v}^{t} \tag{B.14}$$
$$H_{j,v}^{t+1} = \sigma_{j,v}(1 - 1/\exp(-\gamma))E_{j,v}^{t} + \exp(-1/\nu)H_{j,v}^{t} \tag{B.15}$$
$$\begin{aligned} R_{j,v}^{t+1} &= R_{j,v}^{t} + (1 - \mu_{j,v})(1 - \exp(-\nu))H_{j,v}^{t} \\ &\quad + (1 - \exp(-1/\nu))A_{j,v}^{t} + (1 - \exp(-1/\nu))I_{j,v}^{t} \end{aligned} \tag{B.16}$$
$$D_{j,v}^{t+1} = D_{j,v}^{t} + \mu_{j,v}(1 - \exp(-1/\nu))H_{j,v}^{t} \tag{B.17}$$

where j accounts for number of doses and v accounts for vaccine type. And the parameters are written as done by Ferreira et al. [118]:

$$\begin{aligned} p_{j,v} &= (1 - \epsilon_{p,j,v})p \\ \alpha_{j,v} &= 1 - (1 - \epsilon_{\alpha,j,v})(1 - \alpha) \\ \sigma_{j,v} &= (1 - \epsilon_{\sigma,j,v})\sigma \\ \mu_{j,v} &= (1 - \epsilon_{\mu,j,w})\mu \end{aligned} \tag{B.18}$$

Where ϵ is the protection parameter that depends on outcome, dose number, vaccine used and also might depend on age (but the expression holds for age-dependent parameters). Notice the different expression for α because the related efficacy parameter reduces the number of symptomatic cases (therefore increasing asymptomatic cases) and comes from considering:

$$1 - \alpha_v = (1 - \epsilon)(1 - \alpha)$$

Also notice that the protection parameters are different than efficacies, since we follow the mathematical approach to remove multiplicative effects of efficacies done in Ferreira et al. [118] (notice that our p is equivalent to β in their model). We thus get the values of efficacy from the tables in the main text (p is related to infection, α is related to symptomatic infections, σ is related to hospitalizations and μ is related to deaths), and then use the mathematical approach in Ferreira

et al. [118], calculating the respective values of ϵ.

We have now to specify how the transitions from unvaccinated to vaccinated individuals happen. Since the vaccination rates can change in time, it is not trivial to modify the transition matrix. We then transfer the individuals to the vaccinated classes using an external vector $\mathbf{v}$, thus we have

$$\mathbf{x}^* = \mathbf{P}\mathbf{x}^{\mathbf{t}} \tag{B.19}$$

$$\mathbf{x}^{\mathbf{t+1}} = \mathbf{x}^* + \mathbf{v} \tag{B.20}$$

where $\mathbf{v}$ is vaccine and age stratified. $\mathbf{v}$ contains the number of individuals that will leave the unvaccinated (or single vaccinated) as negative entries, whereas the number of individuals that will enter vaccinated (or doubly vaccinated) compartments are positive entries (also considering the number that enter, but also leave single vaccinated compartments). Compartments that are not vaccinated receive "zero" entries. We still need to calculate $\mathbf{v}$, and this is done in the next sections.

B.1.3 Optimization model

What is left to us is to calculate the values of $\mathbf{v}$ in time. We follow a similar fashion of Ferreira et al. [118], where we use an optimization model to allocate doses to first and second inoculations, guaranteeing the availability of doses for the second shot, while keeping the number of doses in stock to a minimum. In this work, we generalize the work by Ferreira et al. [118] by assuming that the production/deployment rate of vaccine doses can vary in time, and also that individuals could have been vaccinated previously with the first dose.

We write a dynamical equation for the vaccine stock $V(t)$ assuming a previously defined production rate $\rho(t)$ and a varying withdrawal rate given by the vaccination rate, which can be chosen, that is, it is the control variable. We impose that a constant fraction $\theta' = 1 - \theta$ of the people who take the first dose will receive the second one after a period a (in this work, 8, 10 or 12 weeks, that is 56, 70 or 84 days, respectively), so we must be careful that the total vaccination rate is the sum of both first and second dose vaccination rates, but the control variable $v(t)$ is the vaccination rate of first doses only. We also assume that there's an initial stock of vaccines V_0, and an initial history of people who have already received the first dose, which show up as a rate $g(t)$ of second doses in the beginning of the roll-out (that is, for $t \in [0, a)$). The equation for $V(t)$ then is:

$$\begin{cases} \frac{dV}{dt} & = \rho(t) - v(t) - \theta' v(t-a) - g(t) \\ V(0) & = V_0\,, \qquad v(t) = 0 \,\forall\, t < 0 \end{cases} \tag{B.21}$$

We note already that we can solve this equation, obtaining

$$V(t) = V_0 + \int_0^t \rho(t')dt' - \int_0^t v(t')dt' - \theta' \int_0^{t-a} v(t')dt' - \int_0^t g(t')dt' \tag{B.22}$$

We define the optimization problem by stating the objective function to be minimized and restrictions that the solution must obey. Since we want to use vaccine doses as quickly as possible, a reasonable goal is to minimize the stock of vaccines $V(t)$. With that, we impose that total vaccination rate is limited by a certain maximum value, and of course it is positive; also, the vaccine stock $V(t)$ is always positive. Finally, we must ensure that, in the period after the simulation ends ($t > T$) there will be enough doses left to apply the second doses on those who have already taken the first dose, here assuming that the production rate after the simulation interval will be the same as the value in the end of the simulation.

These considerations lead to the following optimization problem:

$$\begin{aligned} &\text{find } \min_f J = \int_0^T V(t)dt \text{ subject to} \\ &v(t) \geq 0 \\ &v(t) + \theta' v(t-a) + g(t) \leq v_{max} \\ &V(t) \geq 0 \\ &V(T) \geq \theta' \int_{T-a}^{T} v(t')dt' - \rho(T)a \end{aligned} \tag{B.23}$$

Solution

We can solve the problem defined by Eqs. (B.22, B.23) using linear programming. This is feasible because the objective function and all constraints are linear functions of the control variable f and state variable V and, as Eq.(B.22) shows, V is linear on the control variable.

We first discretize the time in n intervals of length $\Delta t = \frac{T}{n}$, each interval ending at t_i, $i = 1, \ldots, n$, and assume that the production rate, the initial second-dose rate, and the control function will be constant over each interval (that is, a step function), with values $\vec{\rho} = (\rho(t_1), \rho(t_2), \ldots, \rho(t_n))$, $\vec{g} = (g(t_1), g(t_2), \ldots, g(t_n))$,

and $\vec{x} = (v(t_1), v(t_2), \ldots, v(t_n))$, with $g(t) = 0$ when $t > a$. Eq.(B.22) then becomes

$$V(t_i) = V_0 + \sum_{j=1}^{i} \rho_i - \sum_{j=1}^{i} x_j - \theta' \sum_{j=1}^{i-\hat{a}} x_j - \sum_{j=1}^{i} g_i \,,$$

and we seek to minimize the objective function (given by Eq.(B.23), up to a constant) that is a linear function of $\vec{x}$, subject to the (linear) restrictions.

The discrete version of the problem becomes:

$$\begin{aligned}
\min_{\vec{x}} J = \min_{\vec{x}} - \sum_{j=1}^{n} \left[\sum_{i=1}^{j} x_i + \theta' \sum_{i=1}^{j-\hat{a}} x_i \right] \quad & \text{subject to} \\
\vec{x} \geq 0 & \\
x_i + \theta' x_{i-\hat{a}} + g_i \leq v_{max} \,, \text{for } i = 1, \ldots, n & \\
\sum_{i=1}^{j} x_i + \theta' \sum_{i=1}^{j-\hat{a}} x_i \leq V_0 + \sum_{i=1}^{j} \rho_i - \sum_{i=1}^{j} g_i \,, \text{for } j = 1, \ldots, n & \\
(1 + \theta') \sum_{i=1}^{n} x_i \leq V_0 + \sum_{i=1}^{n} \rho_i + p_n a \,, &
\end{aligned} \tag{B.24}$$

where $\hat{a} = \frac{a}{\Delta t}$ (chosen so that $\hat{a}$ is integer), and, to simplify notation, x_i is taken to be zero over values of i below 1. Moreover, some care must be taken with the function g for the system to be feasible: we have to guarantee that $g_j \leq v_{max}$ and $\sum_{i=1}^{j} g_i \leq V_0 + \sum_{i=1}^{j} \rho_i$ for $j = 1, 2 \ldots \hat{a}$.

These conditions can readily be written in matrix form and solved using standard linear programming algorithms. We implemented them in R using the package `lpSolve` [140] to solve the linear programming problem. Each vaccine is run independently.

B.1.4 Dose allocation by age and vaccine

The solution of the optimization problem gives us the number of shots given for first and second doses by day, without differentiating between classes of the model. We consider two scenarios, the first assumes that all available shots will be used in the oldest age-bin before making vaccines available to younger ones. The second scenario assumes that vaccines will be available to younger individuals if a coverage threshold is reached by the older age bins.

First Scenario

For the first scenario, we have for the first dose:

$$v^t_{S,a,j,1} = \min\left(\sum_i V^t_{i,1}, S^t_a + R^t_a\right) \frac{S^t_a}{S^t_a + R^t_a} \frac{V^t_{j,1}}{\sum_i V^t_{i,1}} \tag{B.25}$$

$$v^t_{R,a,j,1} = \min\left(\sum_i V^t_{i,1}, S^t_a + R^t_a\right) \frac{R^t_a}{S^t_a + R^t_a} \frac{V^t_{j,1}}{\sum_i V^t_{i,1}} \tag{B.26}$$

where $V^t_{j,1}$ accounts for all vaccine doses of type j available to first inoculation at time t and a gives the age bin being currently vaccinated. The first term accounts for not vaccinating more than available individuals. The first ratio accounts for proportionality between unvaccinated populations of susceptible and recovered individuals and the second ratio accounts for proportionality of number of doses in stock for each vaccine (thus we not consider rational choice of vaccine type). Notice also that we only vaccinate susceptible or recovered individuals since the epidemiologic dynamics is much faster than protection building generated by vaccination.

Second dose vaccination follows the same idea, with the difference of not having to be proportional to vaccine stock since we do not model interchangeability of vaccines, Setting $V^t_{j,a,1} = v^t_{S,a,j,1} + v^t_{R,a,j,1}$, i.e. the vaccine doses of type j used for first dose in age bin a at time t, we have:

$$v^t_{S,a,j,2} = \min\left(\theta' V^{t-\omega_j}_{j,a,1}, S^t_{a,j,1} + R^t_{a,j,1}\right) \frac{S^t_{a,j,1}}{S^t_{a,j,1} + R^t_{a,j,1}} \tag{B.27}$$

$$v^t_{R,a,j,2} = \min\left(\theta' V^{t-\omega_j}_{j,a,1}, S^t_{a,j,1} + R^t_{a,j,1}\right) \frac{R^t_{a,j,1}}{S^t_{a,j,1} + R^t_{a,j,1}} \tag{B.28}$$

where θ' accounts for the proportion of individuals that appears for second dose inoculation and ω_j is the time interval between doses assumed for vaccine j (28 days for CoronaVac, for example). By using the “delayed" vaccination rate, we ensure that the same quantity of individuals that receive the first dose ω days before receive the second dose. If there is any vaccine dose available to younger ages, the procedure is repeated until total consumption of vaccine doses (or unvaccinated population). $\mathbf{v}$ is then written appropriately to transfer the individuals between compartments.

Second Scenario

The second scenario consider making vaccine doses available to younger ages before total coverage of older individuals. Considering a preset coverage threshold T, at each iteration of the model, we calculate beforehand the age classes that have coverage equal or greater than T. Then, the "open" age bins are one lower than the calculated and the index is given by D. For the first dose, the distribution of doses is weighted by the number of unvaccinated individuals in each age bin. Thus, we have:

$$v^t_{S,a,j,1} = \min\left(\sum_i V^t_{i,1}, S^t_a + R^t_a\right) \frac{S^t_a}{\sum_{i=D}^{N} S^t_i + R^t_i} \frac{V^t_{j,1}}{\sum_i V^t_{i,1}} \tag{B.29}$$

$$v^t_{R,a,j,1} = \min\left(\sum_i V^t_{i,1}, S^t_a + R^t_a\right) \frac{R^t_a}{\sum_{i=D}^{N} S^t_i + R^t_i} \frac{V^t_{j,1}}{\sum_i V^t_{i,1}} \tag{B.30}$$

and for the second dose:

$$v^t_{S,a,j,2} = \min\left(\theta' V^{t-\omega_j}_{j,a,1}, S^t_{a,j,1} + R^t_{a,j,1}\right) \frac{S^t_{a,j,1}}{S^t_{a,j,1} + R^t_{a,j,1}} \tag{B.31}$$

$$v^t_{R,a,j,2} = \min\left(\theta' V^{t-\omega_j}_{j,a,1}, S^t_{a,j,1} + R^t_{a,j,1}\right) \frac{R^t_{a,j,1}}{S^t_{a,j,1} + R^t_{a,j,1}} \tag{B.32}$$

following the same idea of the first scenario. If there is any vaccine dose available to younger ages, the procedure is repeated until total consumption of vaccine doses (or unvaccinated population). $\mathbf{v}$ is then written appropriately to transfer the individuals between compartments.

B.2 Parameterization

Table B.4 comprises the parameters used in the model. Table B.5 comprises the values of age dependent parameters of the model. Table B.6 comprises projected vaccine quantities by the Ministry of Health (from [236]), thus giving us the deployment/production rate by vaccine. We distribute the quantities described in the table in daily rates, given the quantity and time interval expected for the vaccine to be used. Fig B.1 illustrates the deployment rate of vaccines as function

of time.

Table B.1: CoronaVac vaccine effectiveness against Gamma Variant of Concern, by outcome, age group, and vaccine dose.

Outcome	Age group	One-dose effectiveness (% and 95% CI)	Two-doses effectiveness (% and 95% CI)	Source
Infection	All	0[a]	0[a]	Assumed
Symptomatic disease	All	16 (14-18)	67 (65-69)	Jara et al. [141]
Hospitalization	<60	33.7 (27.1-39.7)	84.2 (81.3-86.7)	Cerqueira-Silva et al. [43]
Hospitalization	60-69	29.5 (25.8-33.0)	78.2 (76.3-79.8)	Cerqueira-Silva et al. [43]
Hospitalization	70-79	32.5 (29.9-35.1)	74.0 (72.6-75.4)	Cerqueira-Silva et al. [43]
Hospitalization	80-89	8.2 (2.1-13.8)	63.0 (59.9-66.0)	Cerqueira-Silva et al. [43]
Hospitalization	>90	0[a]	32.7 (22.8-41.3)	Cerqueira-Silva et al. [43]
Death	<60	41.7 (26.4-53.9)	70.5 (51.4-82.1)	Cerqueira-Silva et al. [43]
Death	60-69	35.7 (30.3-40.7)	76.5 (66.9-83.3)	Cerqueira-Silva et al. [43]
Death	70-79	38.2 (34.7-41.5)	78.7 (76.6-80.0)	Cerqueira-Silva et al. [43]
Death	80-89	10.1 (2.7-10.7)	67.3 (63.6-70.6)	Cerqueira-Silva et al. [43]
Death	>90	0[a]	35.4 (23.8-45.1)	Cerqueira-Silva et al. [43]

[a] CoronaVac effectiveness for infections is considered zero in this model.
[b] Confidence intervals including zero or negative results were considered zero (0) in this table.

Table B.2: AZD1222 Vaccine Effectiveness against Gamma Variant of Concern, by outcome, age-group, and vaccine dose.

Outcome	Age group	One-dose effectiveness (% and 95% CI)	Two-doses effectiveness (% and 95% CI)	Source
Infection	All	63.9 (46-75.9)	59.9 (35.8-75.0)	Voysey et al. [123]
Symptomatic disease	<60	50 (27-66)	100[b]	Nasreen et al. [237]
Symptomatic disease	>60	33.4 (26.4-39.7)	77.9 (69.2-84.2)	Hitchings et al. [238]
Hospitalization	<60	64.1 (62.6-65.5)	94.2 (89.8-96.6)	Cerqueira-Silva et al. [43]
Hospitalization	60-69	44.9 (42.4-47.4)	91.7 (84.3-95.6)	Cerqueira-Silva et al. [43]
Hospitalization	70-79	32.9 (25.2-39.8)	88.4 (84.6-91.2)	Cerqueira-Silva et al. [43]
Hospitalization	80-89	32.9 (28.0-37.4)	86.9 (84.9-88.7)	Cerqueira-Silva et al. [43]
Hospitalization	>90	0[a]	54.9 (35.4-68.5)	Cerqueira-Silva et al. [43]
Death	<60	64.8 (61.8-67.6)	93.3 (72.1-98.4)	Cerqueira-Silva et al. [43]
Death	60-69	45.4 (41.0-49.4)	89.6 (71.8-96.2)	Cerqueira-Silva et al. [43]
Death	70-79	37.1 (26.9-45.8)	92.5 (88.1-95.3)	Cerqueira-Silva et al. [43]
Death	80-89	38.1 (32.2-43.4)	91.2 (89.1-92.9)	Cerqueira-Silva et al. [43]
Death	>90	0[a]	70.5 (51.4-82.1)	Cerqueira-Silva et al. [43]

[a] Negative results were considered zero (0) in this table.
[b] Considered 99% in this model.

Table B.3: BNT162b2 vaccine effectiveness against Gamma Variant of Concern, by outcome, age-group and vaccine dose.

Outcome	Age group	One-dose effectiveness (% and 95% CI)	Two-doses effectiveness (% and 95% CI)	Source
Infection	All	60 (53-66)	92 (88-95)	Dagan et al. [137]
Symptomatic disease	All	65 (56-71)	85 (70-93)	Nasreen et al. [237]
Hospitalization/Deaths	All	83 (75-88)	98 (82-100)	Nasreen et al. [237]

Table B.4: Parameters used in the model with sources.

Parameter	Description	Value	Source
p	Probability of infection of susceptible individual per day	see main text	Assumed
age dist	Estimated age distribution of Brazil as 2020	Table B.5	IBGE [177]
γ	Incubation period of the disease	5.8	Wei et al. [229]
σ	Infection hospitalization rate	Table B.5	Salje et al. [233]
α	Proportion of asymptomatic individuals	Table B.5	[0-20)[231] [20-120)[232]
ν	Time to recovery/death (assumed equal for any disease severity)	Table B.5	SIVEP-Gripe [73, 74]
μ	Proportion of hospitalized individuals that die	Table B.5	SIVEP-Gripe [73, 74]
θ	Proportion of individuals that not appear to the second dose	0.10	Assumed

Table B.5: Age dependent parameters separated by age bins.

Age bin	age dist	σ	μ	α	$1-\alpha$	ν (days)
[0-10)	29,380,622	0.001	0.071	0.695	0.305	9.27
[10-20)	30,596,341	0.001	0.11	0.695	0.305	9.9
[20-30)	34,219,132	0.005	0.131	0.44	0.56	8.96
[30-40)	34,231,961	0.011	0.155	0.44	0.56	9.45
[40-50)	29,255,478	0.014	0.208	0.44	0.56	10.41
[50-60)	23,875,081	0.029	0.287	0.44	0.56	11.61
[60-70)	16,732,972	0.058	0.408	0.31	0.69	12.71
[70-80)	9,023,052	0.093	0.516	0.31	0.69	12.79
[80-90)	3,625,888	0.262	0.602	0.31	0.69	11.69
[90-120)	815,165	0.262	0.678	0.31	0.69	10.31

Table B.6: Projected number of doses by vaccine and month.

Month	AZD1222	BNT162b2	CoronaVac
August	11,600,000	33,300,000	20,000,000
September	11,951,500	37,495,530	17,115,672
Oct to Dec	55,919,600	99,999,900	0

B.3 Results

In this section we show the results in table format. Table B.7 comprises the results concerning coverage threshold and excess of deaths. Table B.8 comprises the reduction in deaths by reducing interval between doses of AZD1222 in an ideal vaccination program. Table B.9 comprises the reduction in deaths by reducing interval between doses of AZD1222 with the current projected doses by the Ministry of Health (Table B.6). Finally, Tables B.10 and B.11 comprises the results concerning the reduction in deaths caused by increase of production of AZD1222.

Table B.7: Excess of deaths caused by premature vaccination of younger individuals. Results appear in Fig. 4.2 of the main text.

Probability of infection	Coverage threshold (%)	Excess of deaths	95% CI
Very low	10	212.97	214.12-256.90
	20	212.97	214.12-256.90
	30	212.97	214.12-256.90
	40	201.04	202.07-242.57
	50	191.5	192.48-231.48
	60	167.93	169.00-203.32
	70	137.84	138.56-167.57
	80	83.42	84.02-102.58
	90	10.57	10.60-13.43
Low	10	4780.72	4817.59-5788.25
	20	4780.72	4817.59-5788.25
	30	4780.72	4817.59-5788.25
	40	4509.89	4544.69-5461.25
	50	4290.55	4324.54-5202.03
	60	3757.32	3787.30-4563.93
	70	3073.25	3098.22-3753.94
	80	1871.93	1881.89-2304.52
	90	232.05	232.64-291.15
Medium	10	8587.94	8665.31-10442.08
	20	8587.94	8665.31-10442.08
	30	8587.94	8665.31-10442.08
	40	8095.57	8166.75-9844.54
	50	7692.68	7765.54-9365.58
	60	6727.47	6786.80-8201.17
	70	5484.90	5518.52-6705.85
	80	3315.35	3331.87-4088.31
	90	400.67	400.72-501.53
High	10	14048.19	14105.32-17182.06
	20	14048.19	14105.32-17182.06
	30	14048.19	14105.32-17182.06
	40	13225.35	13276.29-16176.70
	50	12542.13	12589.76-15366.06
	60	10945.61	10985.07-13408.18
	70	8883.86	8917.38-10906.72
	80	5306.95	5325.87-6542.27
	90	620.21	617.35-774.56

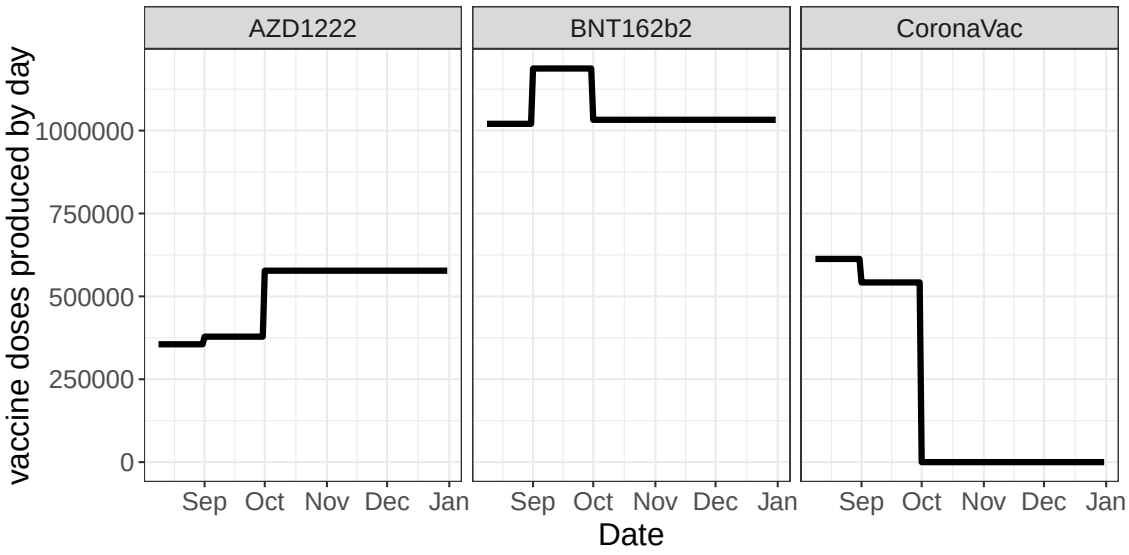

Figure B.1: Vaccine doses projected to be produced by type of vaccine.

Table B.8: Reduction in deaths caused by reducing interval between doses of AZD1222 without limitation of number of doses. Results appear in Fig. 4.3 of the main text.

Probability of infection	Interval between doses (weeks)	Reduction in deaths	95% CI
Very Low	8	99.56	64.17-133.82
	9	79.34	50.40-107.54
	10	55.83	35.23-76.23
	11	32.96	21.31-44.55
Low	8	2451.48	1598.06-3273.52
	9	1947.00	1255.87-2620.37
	10	1355.21	854.36-1837.43
	11	781.16	502.75-1050.65
Medium	8	4799.96	3155.86-6398.54
	9	3806.35	2493.27-5103.71
	10	2621.67	1658.09-3530.17
	11	1478.42	943.62-1987.47
High	8	9146.34	5941.56-12298.09
	9	7211.36	4595.12-9817.33
	10	4887.34	3015.67-6712.7
	11	2655.41	1665.4-3602.38

Table B.9: Reduction in deaths caused by reducing interval between doses of AZD1222 with the current number of projected doses. Results appear in Fig. 4.4 of the main text.

Probability of infection	Interval between doses (weeks)	Reduction in deaths	95% CI
Very Low	8	0.00	0.00-0.01
	9	0.00	0.00-0.00
	10	0.00	0.00-0.00
	11	0.00	0.00-0.00
Low	8	0.09	0.02-0.16
	9	0.07	0.00-0.13
	10	0.07	0.00-0.13
	11	0.07	0.00-0.13
Medium	8	0.19	0.05-0.31
	9	0.16	0.03-0.26
	10	0.16	0.03-0.26
	11	0.16	0.03-0.26
High	8	0.38	0.13-0.58
	9	0.34	0.11-0.53
	10	0.34	0.11-0.53
	11	0.34	0.11-0.53

Table B.10: Reduction in deaths caused by reducing interval between doses of AZD1222 and increasing the number of doses produced, for very low and low probabilities of infection. Results appear in Fig. 4.5 of the main text.

Probability of infection	Interval between doses (weeks)	Increase in production (%)	Reduction in deaths	95% CI
Very Low	8	0	0.01	0.00-0.01
		25	0.82	0.36-1.22
		50	4.36	1.84-6.51
		75	13.61	7.45-19.40
		100	20.56	11.3-29.03
	9	0	0.01	0.00-0.01
		25	0.74	0.32-1.10
		50	4.10	1.70-6.14
		75	13.14	7.20-18.74
		100	19.77	10.88-27.90
	10	0	0.01	0.00-0.01
		25	0.71	0.31-1.07
		50	3.90	1.62-5.84
		75	12.52	6.97-17.75
		100	18.53	10.33-26.03
	11	0	0.01	0.00-0.01
		25	0.50	0.14-0.79
		50	3.12	1.25-4.72
		75	11.03	6.44-15.38
		100	14.56	8.25-20.38
Low	8	0	0.13	0.06-0.19
		25	16.64	6.25-25.70
		50	105.82	44.36-157.39
		75	310.59	169.15-441.57
		100	496.11	280.81-703.06
	9	0	0.13	0.06-0.19
		25	15.07	5.41-23.50
		50	100.50	41.56-149.98
		75	300.63	163.88-427.57
		100	478.02	268.29-675.22
	10	0	0.13	0.06-0.19
		25	14.59	5.17-22.83
		50	95.94	39.55-143.26
		75	285.32	156.96-404.34
		100	444.13	248.71-622.53
	11	0	0.13	0.06-0.19
		25	13.77	5.27-21.18
		50	79.50	32.53-118.85
		75	248.32	144.05-347.72
		100	376.10	224.31-518.26

Table B.11: Reduction in deaths caused by reducing interval between doses of AZD1222 and increasing the number of doses produced, for medium and high probabilities of infection. Results appear in Fig. 4.5 of the main text.

Probability of infection	Interval between doses (weeks)	Increase in production (%)	Reduction in deaths	95% CI
Medium	8	0	0.25	0.11-0.36
		25	38.44	17.72-56.41
		50	205.05	86.60-301.85
		75	620.25	341.31-882.8
		100	1009.33	587.16-1429.56
	9	0	0.24	0.11-0.35
		25	36.13	16.56-53.18
		50	196.94	82.00-290.75
		75	604.18	332.31-861.06
		100	975.44	568.78-1370.74
	10	0	0.24	0.11-0.35
		25	35.40	16.18-52.14
		50	186.54	76.73-271.63
		75	574.96	320.94-817.50
		100	911.22	533.01-1278.87
	11	0	0.24	0.11-0.35
		25	33.23	15.40-48.43
		50	157.86	65.45-233.44
		75	500.26	294.94-702.29
		100	769.53	460.20-1063.99
High	8	0	0.43	0.18-0.63
		25	67.91	33.96-98.89
		50	375.75	158.83-551.02
		75	1213.50	677.49-1723.24
		100	2018.58	1167.27-2823.14
	9	0	0.43	0.18-0.62
		25	65.36	32.86-95.43
		50	366.36	154.68-538.26
		75	1191.99	666.74-1691.30
		100	1966.14	1138.37-2746.82
	10	0	0.43	0.18-0.62
		25	64.47	32.48-94.18
		50	353.23	149.18-521.67
		75	1133.36	637.63-1602.48
		100	1847.51	1089.35-2565.96
	11	0	0.43	0.18-0.62
		25	58.81	29.94-85.16
		50	304.72	132.46-445.86
		75	991.74	579.41-1379.72
		100	1566.21	931.57-2142.29

Appendix C

Supplementary material for chapter 5

In this material, we describe the methodology used in the paper. The code is available at https://github.com/covid19br/child_vac_omicron. In section C.1.1 we describe how we account two strains in the model. In section C.1.2 we describe the basic epidemiological model. In section C.2 we describe how we calculate the Effective Reproduction Number, growth rate and initial conditions from hospitalization data. In section C.3 we describe the parameters used in the model, together with sources. Finally, in section C.4 we show additional results concerning the sensitivity analysis.

C.1 Model

C.1.1 Modelling competition between variants

For simplicity, suppose that we have a simple SIR model with two strains named D and O. Then the probability of a susceptible individual not being infected between t and $t+1$ is given by:

$$P(S|I_D, I_O) = \exp\left(-\beta_D I_D - \beta_O I_O\right) \tag{C.1}$$

where β is the probability of infection given a contact.

Conversely, the probability of becoming infected by ANY of the strains is given by:

$$P(I|I_D, I_O) = 1 - \exp\left(-\beta_D I_D - \beta_O I_O\right) \tag{C.2}$$

Since being infected by one strain precludes infection by the other strain, the probability of being infected by an specific strain is given by the rate of events of

infection of each strain, as given by the Gillespie algorithm. Thus, we have:

$$P(I_D|I_D,\, I_O) = \frac{\beta_D I_D}{\beta_D I_D + \beta_O I_O}(1 - \exp\left(-\beta_D I_D - \beta_O I_O\right)) \tag{C.3}$$

$$P(I_O|I_D,\, I_O) = \frac{\beta_O I_O}{\beta_D I_D + \beta_O I_O}(1 - \exp\left(-\beta_D I_D - \beta_O I_O\right)) \tag{C.4}$$

Therefore, a complete two-strain SIR discrete time model would be given by:

$$S^{t+1} = \exp\left(-\beta_D I_D - \beta_O I_O\right) S^t \tag{C.5}$$

$$I_D^{t+1} = \frac{\beta_D I_D}{\beta_D I_D + \beta_O I_O}(1 - \exp\left(-\beta_D I_D - \beta_O I_O\right)) S^t + (1-\nu) I_D^t \tag{C.6}$$

$$I_O^{t+1} = \frac{\beta_O I_O}{\beta_D I_D + \beta_O I_O}(1 - \exp\left(-\beta_D I_D - \beta_O I_O\right)) S^t + (1-\nu) I_O^t \tag{C.7}$$

$$R_D^{t+1} = \nu I_D^t + R_D^T \tag{C.8}$$

$$R_O^{t+1} = \nu I_O^t + R_O^T \tag{C.9}$$

C.1.2 Epidemiological model

Following Allen and Van Den Driessche [116], we construct a discrete-time SEIR-like model. We assume that a susceptible individual (S) has a probability p of being infected. If a infection occurs, the individual transits to the exposed (E), pre-symptomatic, compartment. After the incubation period, the individual can transit to hospitalized (H), mildly symptomatic (I) or asymptomatic (A) compartments. If the individual is hospitalized, the possible outcomes are recovery (R) or death (D), with the respective compartments. In the case of asymptomatic and mildly symptomatic we assume recovery as the only possibility.

As some parameters can be described as rates $(1/t)$, we assume (as in typical SEIR-like models) an exponential distribution of time to transition. For example, the incubation period γ, can be rewritten as the probability of a pre-symptomatic individual exiting the Exposed compartment, given by $1 - \exp\left(-1/\gamma\right)$, as follows from the Gillespie algorithm.

Our model is age-structured. Since we aim to evaluate vaccination in children, we use specific age bins, those being $S = (S_{0-4},\, S_{5-11},\, S_{12-17},\, S_{18-29},\, S_{30-39},\, S_{40-49}, \ldots,\, S_{80+})^T$, and for other classes in this way as well, but we drop those indexes for readability. Besides the age indexes, this model possess three more indexes, $j = \{u = \text{ unvaccinated}, v = \text{ vaccinated with one dose}, w = \text{ vaccinated with two doses}, b = \text{vaccinated with booster dose}\}$, $k = \{A = \text{ AZD1222}, P = \text{ BNT16b2}, C = \text{ CoronaVac}\}$

and $x = \{d = \text{Delta}, o = \text{Omicron}\}$. Since we assume that vaccinated individuals have equal transmissibility compared to unvaccinated individuals, consider $E := \sum_{j,k} E_{j,k,x}$ (not summed over ages), as well as the other classes. Thus, number of (alive) individuals is given by $N = S + E + I + A + H + R$. We use contact matrices between ages from Prem et al. [136]. The total number of contacts with infectious individuals per age and variant is then given by:

$$C_d = \hat{c}(I_d + \omega E_d + \omega_a A_d + \omega_s H_d)/N \tag{C.10}$$

$$C_o = \hat{c}(I_o + \omega E_o + \omega_a A_o + \omega_s H_o)/N \tag{C.11}$$

Finally, our model is given by:

Unvaccinated

$$S_u^{t+1} = \exp(-\beta_d C_d - \beta_o C_o)\left(1 - \sum_k V_{svk}^t\right) S_u^t \tag{C.12}$$

$$\begin{aligned} E_{ux}^{t+1} = {} & \frac{\beta_x C_x}{\beta_d C_d + \beta_o C_o}(1 - \exp(-\beta_d C_d - \beta_o C_o))\left(1 - \sum_k V_{svkx}^t\right) S_u^t \\ & + \frac{\rho_{dx}\beta_x C_x}{\rho_{dd}\beta_d C_d + \rho_{do}\beta_o C_o}(1 - \exp(-\rho_{dd}\beta_d C_d - \rho_{do}\beta_o C_o))\left(1 - \sum_k V_{rvkx}^t\right) R_{ud}^t \end{aligned} \tag{C.13}$$

$$\begin{aligned} & + \frac{\rho_{ox}\beta_x C_x}{\rho_{od}\beta_d C_d + \rho_{oo}\beta_o C_o}(1 - \exp(-\rho_{od}\beta_d C_d - \rho_{oo}\beta_o C_o))\left(1 - \sum_k V_{rvkx}^t\right) R_{uo}^t \\ & + (1 - \gamma_{ux}) E_{ux}^t \end{aligned}$$

$$I_{ux}^{t+1} = (1 - \sigma_{ux})(1 - \alpha_{ux})\gamma_x E_{ux}^t + (1 - \nu) I_{ux}^t \tag{C.14}$$

$$A_{ux}^{t+1} = (1 - \sigma_{ux})\alpha_{ux}\gamma_x E_{ux}^t + (1 - \nu) A_{ux}^t \tag{C.15}$$

$$H_{ux}^{t+1} = \sigma_{ux}\gamma_x E_{ux}^t + (1 - \nu_s) H_{ux}^t \tag{C.16}$$

$$R_{ux}^{t+1} = \exp(-\rho_{dd}\beta_d C_d - \rho_{do}\beta_o C_o)\left(1 - \sum_k V_{rvkx}^t\right) R_{ux}^t \tag{C.17}$$

$$+ (1 - \mu)\nu_s H_{ux}^t + \nu A_{ux}^t + \nu I_{ux}^t \tag{C.18}$$

$$D_{ux}^{t+1} = D_{ux}^t + \mu_{ux}\nu_s H_{ux}^t \tag{C.19}$$

1 Dose

$$
\begin{aligned}
S_{vk}^{t+1} &= \exp(-\beta_d C_d - \beta_o C_o) V_{svk}^t S_u^t && \text{(C.20)}\\
&+ \exp(-\beta_{vkd} C_d - \beta_{vko} C_o) \left(1 - V_{swk}^t\right) S_{vk}^t && \text{(C.21)}\\
E_{vkx}^{t+1} &= \frac{\beta_x C_x}{\beta_d C_d + \beta_o C_o}(1 - \exp(-\beta_d C_d - \beta_o C_o)) V_{svk}^t S_u^t \\
&+ \frac{\rho_{dx}\beta_x C_x}{\rho_{dd}\beta_d C_d + \rho_{do}\beta_o C_o}(1 - \exp(-\rho_{dd}\beta_d C_d - \rho_{do}\beta_o C_o)) V_{rvkx}^t R_{ud}^t \\
&+ \frac{\rho_{ox}\beta_x C_x}{\rho_{od}\beta_d C_d + \rho_{oo}\beta_o C_o}(1 - \exp(-\rho_{od}\beta_d C_d - \rho_{oo}\beta_o C_o)) V_{rvkx}^t R_{uo}^t && \text{(C.22)}\\
&+ \frac{\beta_{vkx}\beta_x C_x}{\beta_{vkd} C_d + \beta_{vko} C_o}(1 - \exp(-\beta_{vkd} C_d - \beta_{vko} C_o)) \left(1 - V_{swkx}^t\right) S_{vk}^t \\
&+ \frac{\rho_{dx}\beta_{vkx} C_x}{\rho_{dd}\beta_{vkd} C_d + \rho_{do}\beta_{vko} C_o}(1 - \exp(-\rho_{dd}\beta_{vkd} C_d - \rho_{do}\beta_{vko} C_o)) \left(1 - V_{rwkd}^t\right) R_{vkd}^t \\
&+ \frac{\rho_{ox}\beta_{vkx} C_x}{\rho_{od}\beta_{vkd} C_d + \rho_{oo}\beta_{vko} C_o}(1 - \exp(-\rho_{od}\beta_{vkd} C_d - \rho_{oo}\beta_{vko} C_o)) \left(1 - V_{rwko}^t\right) R_{vko}^t \\
&+ (1 - \gamma_x) E_{vkx}^t \\
I_{vkx}^{t+1} &= (1 - \sigma_{vkx})(1 - \alpha_{vkx})\gamma_x E_{vkx}^t + (1 - \nu) I_{vkx}^t && \text{(C.23)}\\
A_{vkx}^{t+1} &= (1 - \sigma_{vkx})\alpha_{vkx}\gamma_x E_{vkx}^t + (1 - \nu) A_{vkx}^t && \text{(C.24)}\\
H_{vkx}^{t+1} &= \sigma_{vkx}\gamma_x E_{vkx}^t + (1 - \nu_s) H_{vkx}^t && \text{(C.25)}\\
R_{vkx}^{t+1} &= (1 - \mu_{vkx})\nu_s H_{vkx}^t + \nu A_{vkx}^t + \nu I_{vkx}^t && \text{(C.26)}\\
&+ \exp(-\rho_{dd}\beta_{vkd} C_d - \rho_{do}\beta_{vko} C_o)(1 - V_{rwkx}^t) R_{vkx} && \text{(C.27)}\\
&+ \exp(-\rho_{dd}\beta_d C_d - \rho_{do}\beta_o C_o) V_{rvkx}^t R_{ux} && \text{(C.28)}\\
D_{vkx}^{t+1} &= D_{vkx}^t + \mu_{vkx}\nu_s H_{vkx}^t && \text{(C.29)}
\end{aligned}
$$

2 Doses

$$
\begin{aligned}
S_{wk}^{t+1} &= \exp(-\beta_{vkd}C_d - \beta_{vko}C_o)V_{wk}^t S_{vk}^t \\
&+ \exp(-\beta_{wkd}C_d - \beta_{wko}C_o)(1 - V_{bp}^t)S_{wk}^t && \text{(C.30)} \\
E_{wkx}^{t+1} &= \frac{\beta_{vkx}C_x}{\beta_{vkd}C_d + \beta_{vko}C_o}(1 - \exp(-\beta_{vkd}C_d - \beta_{vko}C_o))V_{swk}^t S_{vk}^t \\
&+ \frac{\rho_{dx}\beta_{vkx}C_x}{\rho_{dd}\beta_{vkd}C_d + \rho_{do}\beta_{vko}C_o}(1 - \exp(-\rho_{dd}\beta_{vkd}C_d - \rho_{do}\beta_{vko}C_o))V_{rwkd}^t R_{vkd}^t \\
&+ \frac{\rho_{ox}\beta_{vkx}C_x}{\rho_{od}\beta_{vkd}C_d + \rho_{oo}\beta_{vko}C_o}(1 - \exp(-\rho_{od}\beta_{vkd}C_d - \rho_{oo}\beta_{vko}C_o))V_{rwko}^t R_{vko}^t \\
&+ \frac{\beta_{wkx}\beta_x C_x}{\beta_{wkd}C_d + \beta_{wko}C_o}(1 - \exp(-\beta_{wkd}C_d - \beta_{wko}C_o))\left(1 - V_{sbp}^t\right)S_{wk}^t && \text{(C.31)} \\
&+ \frac{\rho_{dx}\beta_{wkx}C_x}{\rho_{dd}\beta_{wkd}C_d + \rho_{do}\beta_{wko}C_o}(1 - \exp(-\rho_{dd}\beta_{wkd}C_d - \rho_{do}\beta_{wko}C_o))\left(1 - V_{rbpd}^t\right)R_{wkd}^t \\
&+ \frac{\rho_{ox}\beta_{wkx}C_x}{\rho_{od}\beta_{wkd}C_d + \rho_{oo}\beta_{wko}C_o}(1 - \exp(-\rho_{od}\beta_{wkd}C_d - \rho_{oo}\beta_{wko}C_o))\left(1 - V_{rbpd}^t\right)R_{wko}^t \\
&+ (1 - \gamma_d)E_{wkx}^t \\
I_{wkx}^{t+1} &= (1 - \sigma_{wkx})(1 - \alpha_{wkx})\gamma_x E_{wkx}^t + (1 - \nu)I_{wkx}^t && \text{(C.32)} \\
A_{wkx}^{t+1} &= (1 - \sigma_{wkx})\alpha_{wkx}\gamma_x E_{wkx}^t + (1 - \nu)A_{wkx}^t && \text{(C.33)} \\
H_{wkx}^{t+1} &= \sigma_{wkx}\gamma_x E_{wkx}^t + (1 - \nu_s)H_{wkx}^t && \text{(C.34)} \\
R_{wkx}^{t+1} &= (1 - \mu_{wkx})\nu_s H_{wkx}^t + \nu A_{wkx}^t + \nu I_{wkx}^t && \text{(C.35)} \\
&+ \exp(-\rho_{dd}\beta_{wkd}C_d - \rho_{do}\beta_{wko}C_o)(1 - V_{rbpx}^t)R_{wkd} && \text{(C.36)} \\
&+ \exp(-\rho_{dd}\beta_{vkd}C_d - \rho_{do}\beta_{vko}C_o)V_{rwkx}^t R_{vkd} && \text{(C.37)} \\
D_{wkx}^{t+1} &= D_{wkx}^t + \mu_{wkx}\nu_s H_{wkx}^t && \text{(C.38)}
\end{aligned}
$$

Booster Doses

$$S_{bp}^{t+1} = \sum_k \exp(-\beta_{wkd}C_d - \beta_{wko}C_o)V_{sbp}^t S_{wk}^t \tag{C.39}$$
$$+ \exp(-\beta_{bpd}C_d - \beta_{bpo}C_o)S_{bp}^t$$
$$E_{bpx}^{t+1} = \sum_k \frac{\beta_{wkxC_x}}{\beta_{wkd}C_d + \beta_{wko}C_o}(1 - \exp(-\beta_{wkd}C_d - \beta_{wko}C_o))V_{sbp}^t S_{wk}^t$$
$$+ \sum_k \frac{\rho_{dx}\beta_{wkx}C_x}{\rho_{dd}\beta_{wkd}C_d + \rho_{do}\beta_{wko}C_o}(1 - exp(-\rho_{dd}\beta_{wkd}C_d - \rho_{do}\beta_{wko}C_o))V_{rbpd}^t R_{wkd}^t$$
$$+ \sum_k \frac{\rho_{ox}\beta_{wkx}C_x}{\rho_{od}\beta_{wkd}C_d + \rho_{oo}\beta_{wko}C_o}(1 - exp(-\rho_{od}\beta_{wkd}C_d - \rho_{oo}\beta_{wko}C_o))V_{rbpo}^t R_{wko}^t$$
$$+ \frac{\beta_{bpx}C_x}{\beta_{bpd}C_d + \beta_{bpo}C_o}(1 - \exp(-\beta_{bpd}C_d - \beta_{bpo}C_o))S_{bp} \tag{C.40}$$
$$+ \frac{\rho_{dx}\beta_{bpx}C_x}{\rho_{dd}\beta_{bpd}C_d + \rho_{do}\beta_{bpo}C_o}(1 - \exp(-\rho_{dd}\beta_{bpd}C_d - \rho_{do}\beta_{bpo}C_o))R_{bpd}$$
$$+ \frac{\rho_{ox}\beta_{bpx}C_x}{\rho_{od}\beta_{bpd}C_d + \rho_{oo}\beta_{bpo}C_o}(1 - \exp(-\rho_{od}\beta_{bpd}C_d - \rho_{oo}\beta_{bpo}C_o))R_{bpo}$$
$$+ (1 - \gamma_x)E_{bpx}$$
$$I_{bpx}^{t+1} = (1 - \sigma_{bpx})(1 - \alpha_{bpx})\gamma_x E_{bpx}^t + (1 - \nu)I_{bpx}^t \tag{C.41}$$
$$A_{bpx}^{t+1} = (1 - \sigma_{bpx})\alpha_{bpx}\gamma_x E_{bpx}^t + (1 - \nu)A_{bpx}^t \tag{C.42}$$
$$H_{bpx}^{t+1} = \sigma_{bpx}\gamma_x E_{bpx}^t + (1 - \nu_s)H_{bpx}^t \tag{C.43}$$
$$R_{bpx}^{t+1} = (1 - \mu_{bpx})\nu_s H_{bpx}^t + \nu A_{bpx}^t + \nu I_{bpx}^t \tag{C.44}$$
$$+ \sum_k \exp(-\rho_{dd}\beta_{wkd}C_d - \rho_{do}\beta_{wko}C_o)V_{rbpd}^t R_{wkd} \tag{C.45}$$
$$+ \exp(-\rho_{dd}\beta_{wkd}C_d - \rho_{do}\beta_{wko}C_o)R_{bpd} \tag{C.46}$$
$$D_{bpx}^{t+1} = D_{bpx}^t + \mu_{bpx}\nu_s H_{bpx}^t \tag{C.47}$$

where k accounts for vaccine type and V_{jkx}^t is the proportion of individuals that have (or have not) been infected by variant x that receive the j dose of the said vaccine (Notice that V is proportional to S and R, but it is not written explicitly). The quantity of doses that are allocated for first or second dose are done as in [118]. Usually, the vaccine allocation would also depend on the age of the individuals, but since we only vaccinate children from 5 to 11 years old, this is not necessary (but the model is flexible enough to deal with this). And the parameters are written

as done by Ferreira et al. [118]:

$$\begin{aligned}
\beta_{jkx} &= (1-\epsilon_{\beta,jkx})\beta_x \\
\alpha_{jkx} &= 1-(1-\epsilon_{\alpha,jkx})(1-\alpha_x) \\
\sigma_{jkx} &= (1-\epsilon_{\sigma,jkx})\sigma_x \\
\mu_{jkx} &= (1-\epsilon_{\sigma,jkx})\mu_x
\end{aligned} \tag{C.48}$$

Notice that the protection parameters are different than efficacies, since we follow the mathematical approach to remove multiplicative effects of efficacies done in Ferreira et al. [118].

C.2 Next Generation Matrix and Initial Conditions

In order to calculate the basic and effective reproduction numbers of the model, we follow Allen and Van Den Driessche [116] work. For that, we define $\mathbf{x}^t$ as the vector containing all infected classes, that is, all of $E_{a,j,k,x}$, $I_{a,j,k,x}$, $A_{a,j,k,x}$ and $H_{a,j,k,x}$, at time t and $\mathbf{y}^t$ as the vector containing the susceptible, recovered and deceased at time t. With it, we write our model as

$$\begin{cases} \mathbf{x}^{t+1} &= \mathbf{G}(\mathbf{x}^t, \mathbf{y}^t) \\ \mathbf{y}^{t+1} &= \mathbf{M}(\mathbf{x}^t, \mathbf{y}^t). \end{cases} \tag{C.49}$$

Suppose now that $\mathbf{G}$ can be written as a sum of two main processes, one given by $\mathbf{F}$, the new infections that survive from t to $t+1$ and the other one given by $\mathbf{T}$, the transitions between different infected classes, and also recoveries and deaths that happen from t to $t+1$. This is a classic decomposition in matrix population models, see, for instance, chapter five in Caswell [239]. Let $\hat{F}(\bar{\mathbf{x}}, \bar{\mathbf{y}})$ be the linearized matrix of $\mathbf{F}$ around a given equilibrium $(\bar{\mathbf{x}}, \bar{\mathbf{y}})$, and the same for $\hat{T}(\bar{\mathbf{x}}, \bar{\mathbf{y}})$ and $\hat{M}(\bar{\mathbf{x}}, \bar{\mathbf{y}})$. the system linearized around $(\bar{\mathbf{x}}, \bar{\mathbf{y}})$ is

$$\begin{cases} \mathbf{x}^{t+1} &= \mathbf{G}(\bar{\mathbf{x}}, \bar{\mathbf{y}}) + (\hat{F}(\bar{\mathbf{x}}, \bar{\mathbf{y}}) + \hat{T}(\bar{\mathbf{x}}, \bar{\mathbf{y}}))\mathbf{x}^t \\ \mathbf{y}^{t+1} &= \mathbf{H}(\bar{\mathbf{x}}, \bar{\mathbf{y}}) + \hat{H}(\bar{\mathbf{x}}, \bar{\mathbf{y}})\mathbf{y}^t \end{cases} \tag{C.50}$$

Note that around the given equilibrium, the number of new infections is given by the the $(\hat{F}(\bar{\mathbf{x}}, \bar{\mathbf{y}}) + \hat{T}(\bar{\mathbf{x}}, \bar{\mathbf{y}}))$ terms. If the equilibrium we linearize around is the disease free equilibrium (DFE), that is $(\bar{\mathbf{x}}, \bar{\mathbf{y}}) = (\mathbf{0}, \mathbf{y}_0)$, $\mathbf{y}_0$ the non-infected populations at DFE, we have $\mathbf{G}(0, \mathbf{y}_0) = 0$. With it, we define the basic reproduction number, R_0, as

$$R_0 = \rho\left\{\hat{F}(\mathbf{0}, \mathbf{y}_0)(\mathbb{1} + \hat{T}(\mathbf{0}, \mathbf{y}_0))^{-1}\right\}, \tag{C.51}$$

where $\rho(.)$ is the notation for the dominant eigenvalue, and $\hat{F}(\mathbf{0}, \mathbf{y}_0)(\mathbb{1} + \hat{T}(\mathbf{0}, \mathbf{y}_0))^{-1}$ is the next generation matrix (NGM).

Note now that the problem for $\mathbf{x}^t$ at DFE is

$$\mathbf{x}^{t+1} = (\hat{F}(\mathbf{0}, \mathbf{y_0}) + \hat{T}(\mathbf{0}, \mathbf{y_0}))\mathbf{x}^t, \tag{C.52}$$

and we write a solution as a linear combination of the eigenvectors, $\mathbf{q}_i$, and correspondent eigenvalues, r_i, of $(\hat{F}(\mathbf{0}, \mathbf{y_0}) + \hat{T}(\mathbf{0}, \mathbf{y_0}))$ as

$$\mathbf{x}^t = \sum_i \phi_i r_i^t \mathbf{q}_i. \tag{C.53}$$

The r_i can be ordered, that is $r^* = r_1 > r_2 > ... > r_D$, D the total number of infected classes. This way, for large t, $(r_i/r^*)^t \approx 0$ for $i > 2$ and we can write

$$\mathbf{x}^t = r^{*t} \sum_i \phi_i \left(\frac{r_i}{r^*}\right)^t \mathbf{q}_i \approx \phi^* r^{*t} \mathbf{q}^*. \tag{C.54}$$

To estimate proper values for the β_i coefficients we use a minimizing algorithm for r^*, the dominant eigenvalue in equation (C.54). Say that the observed growth coefficient is r_{obs} and for a given set of β_i, let's call it $B_j = (\beta_d^{(j)}, \beta_o^{(j)}, ...)$, we find $r^*(B_j)$, the dominant eigenvalue of $\hat{F} + \hat{T}$ calculated with set B_j, and also $R_0(B_j)$, the basic reproduction number calculated with this same set. We then minimize the quantity $\|r(B_j) - r_{obs}\|$ by iterating the set B_j such that

$$B_j = \frac{R_0(B_{j-2})}{R_0(B_{j-1})} B_{j-1}, \tag{C.55}$$

where B_1 and $R_0(B_0)$ are our initial guesses for the iterative process.

The dominant eigenvector $\mathbf{q}^*$ in equation (C.54) is the infected population distribution. We use that alongside the factor ϕ^*, to fit our initial infected population distribution based on hospitalization data. Let $H_{T,obs}$ be the number of new hospitalizations observed on our data-set (SIVEP-Gripe) at a given date T, to find proper initial conditions, we need the total number of new hospitalizations given by the model to be equal to $H_{T,obs}$. For that, we'll need the terms $\sigma\gamma E$ in each of the H_{jkx}^{t+1}. Let each index d in the interval (n_l, n_h) correspond to an exposed class set of indexes, that is, $\phi^* q_d^* = E_{j,k,x}^0$ for all $n_l \leq d \leq n_h$ and (j, k, x). We have

$$\phi^* \sum_{d=n_l}^{n_h} q_d^* \sigma_d \gamma_d = H_{T,obs} \implies \phi^* = \frac{H_{T,obs}}{\sum_{d=n_l}^{n_h} q_d^* \sigma_d \gamma_d} \tag{C.56}$$

That way, our initial condition for infected individuals is given by $\phi^* \mathbf{q}^*$.

C.3 Parameterization

We consider that Omicron has a 50% reduced risk of hospitalization compared to Delta, whereas we use the data from Salje et al. [233] to obtain age-specific infection-hospitalization rate. Due to the short time interval, we consider that it is not possible to have reinfections by Omicron in Omicron-recovered individuals (i.e. $\rho_{oo} = 0$). And since we do not have Delta circulating in this model, we assume that ρ_{dd}, $\rho_{od} = 0$ also. Finally, we assume a Beta-distributed cross immunity given by Delta against Omicron infections (ρ_{do}) from Ferguson [175]. Tables C.1 and C.2 describe the basic epidemiological parameters. Figures C.1, C.2, C.3 and C.4 describe vaccine effectiveness parameters in forest plot format.

Table C.1: Parameters used in the model with sources.

Parameter	Description	Value	Source
age dist	Estimated age distribution of Brazilian states as 2020	-	IBGE [177]
γ	Incubation period of the disease	3.2 days	Gozzi et al. [240]
σ	Infection hospitalization rate	Table B.5	Salje et al. [233]
α	Proportion of asymptomatic individuals	Table B.5	[0-20)[231] [20-120)[232]
ν	Time to recovery for asymptomatic/mild symptomatic	11 days	-
ν_s	Time to recovery/death for hospitalized individuals	Table B.5	SIVEP-Gripe [73, 74]
μ	Proportion of hospitalized individuals that die	Table B.5	SIVEP-Gripe [73, 74]

Table C.2: Age dependent parameters.

Age Group	σ	μ	α	$1-\alpha$	ν_s
0-4	0.0005	0.0712	0.6950	0.3050	9.2700
5-11	0.0005	0.0822	0.6950	0.3050	9.4464
12-17	0.0005	0.1104	0.6950	0.3050	9.9000
18-29	0.0022	0.1276	0.4788	0.5212	9.1032
30-39	0.0055	0.1552	0.4400	0.5600	9.4500
40-49	0.0070	0.2085	0.4400	0.5600	10.410
50-59	0.0145	0.2874	0.4400	0.5600	11.610
60-69	0.0290	0.4077	0.3100	0.6900	12.710
70-79	0.0465	0.5165	0.3100	0.6900	12.790
80+	0.1310	0.6162	0.3100	0.6900	11.426

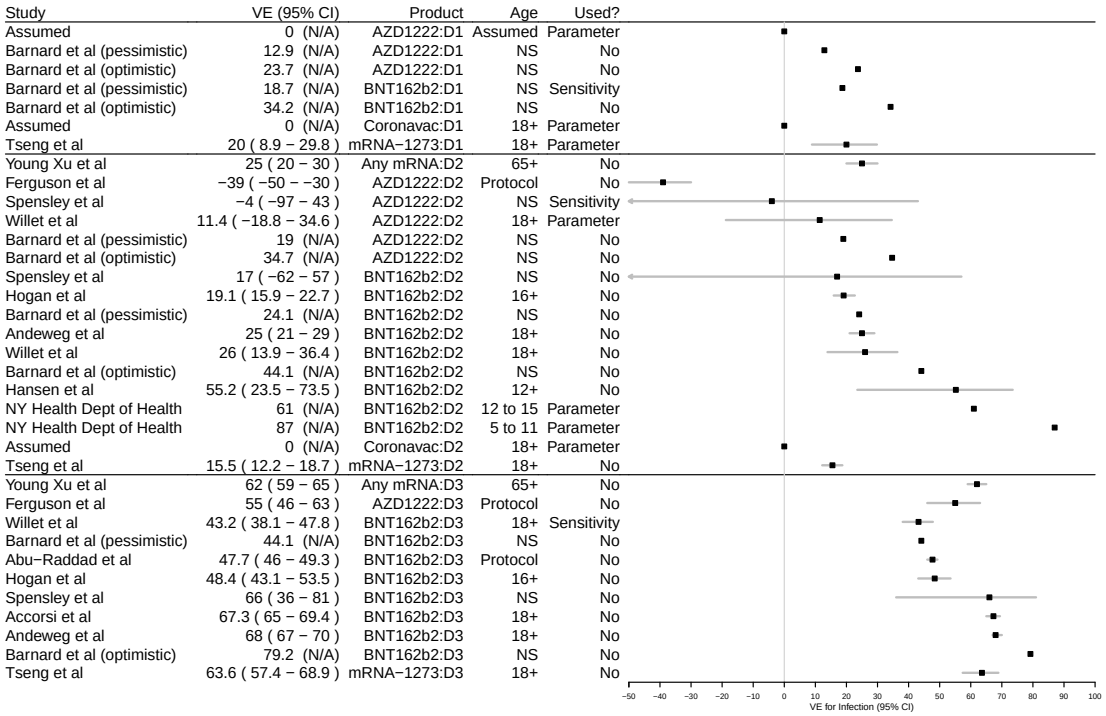

Figure C.1: Forest plot of effectiveness studies regarding protection against COVID-19 infection. The studies are organized per dose and alphabetical order of vaccine name (See Product column). Used? column describes which studies were used in the main results (Parameter), sensitivity analysis (Sensitivity) or not used at all (No), but considered in the literature review. The studies are, in order of appearance: Barnard et al. [188], Tseng et al. [186], Young-Xu et al. [190], Ferguson [175], Spensley et al. [241], Willett et al. [187], Hogan et al. [242], Andeweg et al. [243], Hansen et al. [244], New York State Department of Health [184], Abu-Raddad et al. [245], Accorsi et al. [246].

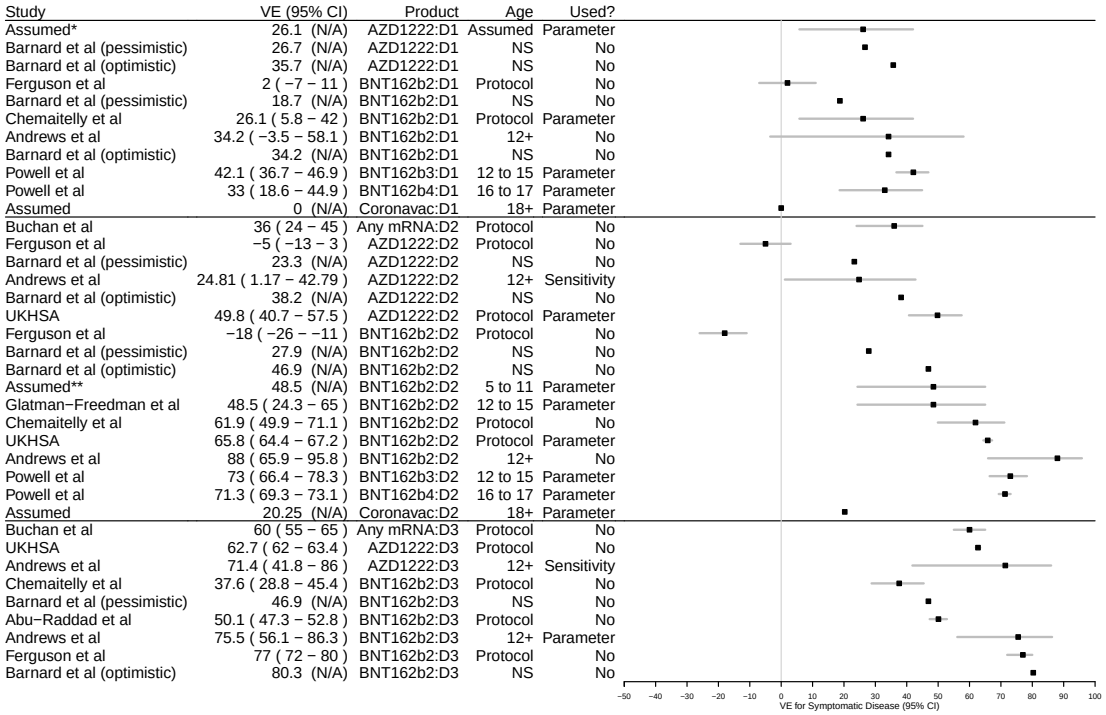

Figure C.2: Forest plot of effectiveness studies regarding protection against COVID-19 symptomatic disease. The studies are organized per dose and alphabetical order of vaccine name (See Product column). Used? column describes which studies were used in the main results (Parameter), sensitivity analysis (Sensitivity) or not used at all (No), but considered in the literature review. The studies are, in order of appearance: Barnard et al. [188], Ferguson [175], Chemaitelly et al. [247], Andrews et al. [176], Powell et al. [185], Buchan et al. [248], UK Health Security Agency [249], Powell et al. [185], Glatman-Freedman et al. [180], Abu-Raddad et al. [245].

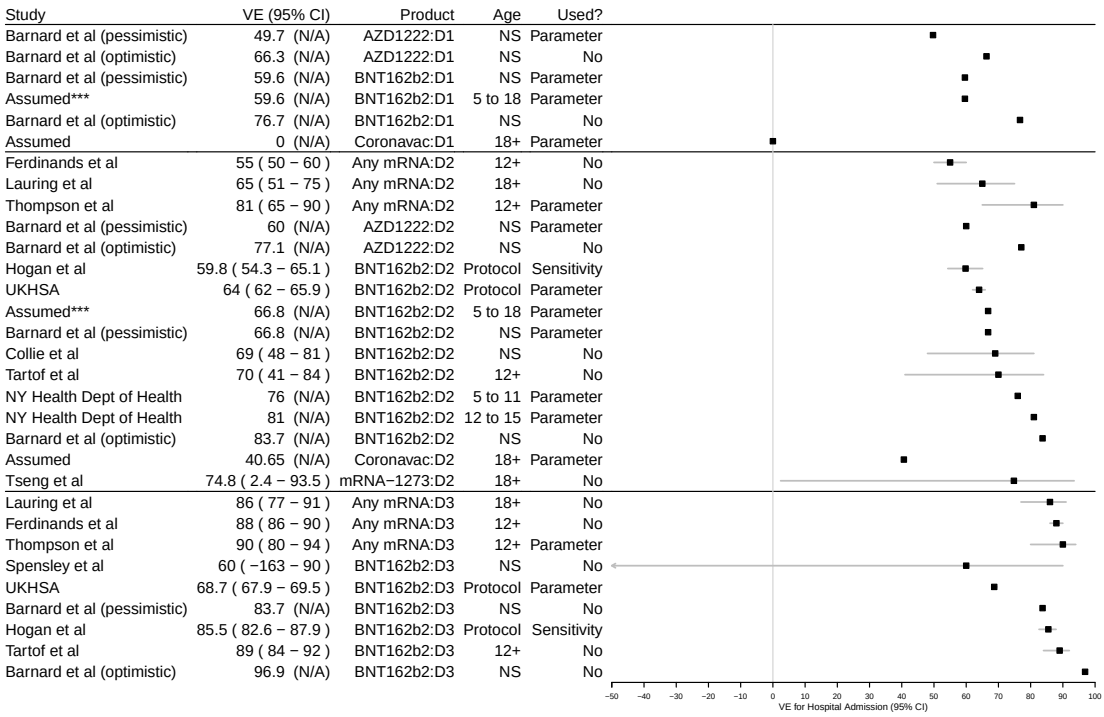

Figure C.3: Forest plot of effectiveness studies regarding protection against COVID-19 hospital admission. The studies are organized per dose and alphabetical order of vaccine name (See Product column). Used? column describes which studies were used in the main results (Parameter), sensitivity analysis (Sensitivity) or not used at all (No), but considered in the literature review. The studies are, in order of appearance: Barnard et al. [188], Ferdinands et al. [250], Lauring et al. [251], Thompson et al. [252], Hogan et al. [242], UK Health Security Agency [249], Collie et al. [253], Tartof et al. [254], New York State Department of Health [184], Tseng et al. [186], Spensley et al. [241].

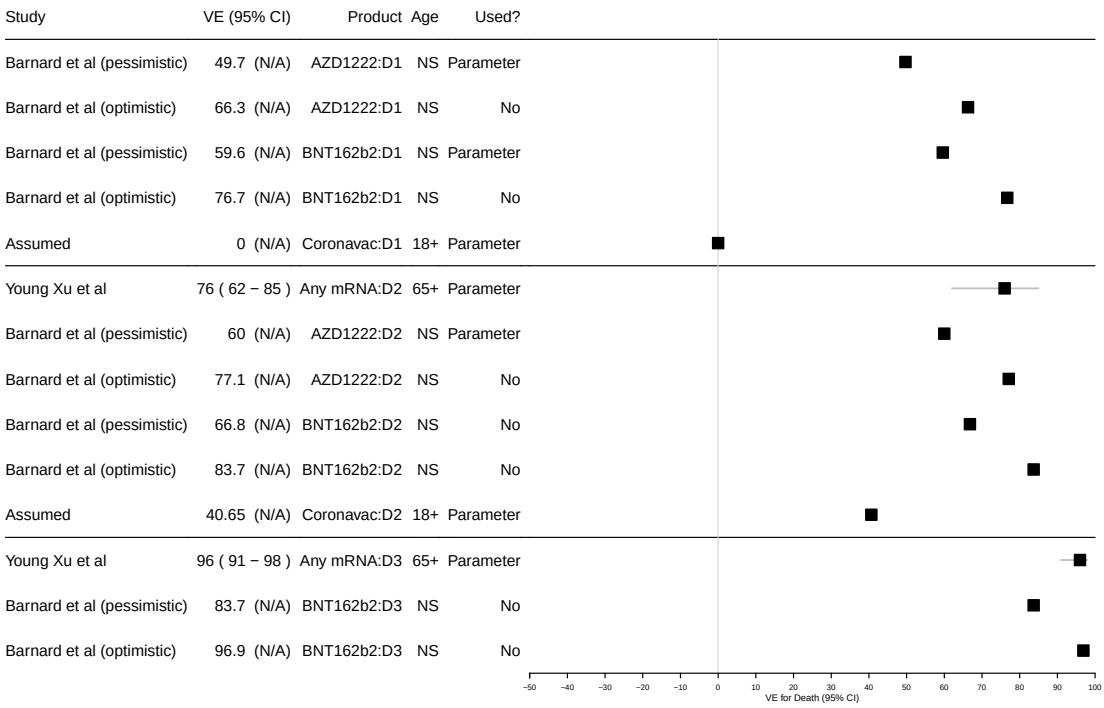

Figure C.4: Forest plot of effectiveness studies regarding protection against COVID-19 death. The studies are organized per dose and alphabetical order of vaccine name (See Product column). Used? column describes which studies were used in the main results (Parameter), sensitivity analysis (Sensitivity) or not used at all (No), but considered in the literature review. The studies are, in order of appearance: Barnard et al. [188], Young-Xu et al. [190].

C.4 Additional results

We do a sensitivity analysis of the results changing vaccine parameterization to other sources (see Figs C.1, C.2, C.3 and C.4). The number of deaths and hospitalizations avoided are described in Table C.3. In Figures C.5 and C.6, we see the heterogeneity of the outcomes between states. Fig C.7 describes a possible explanation for such heterogeneity.

Table C.3: Number of outcome averted by age group and vaccination pace, in thousands, with 95% Confidence Interval.

Outcome	Age Group	Current Pace	Ideal Pace
Hospitalization	All	6.16 (5.35 – 7.17)	15.3 (13.09 – 18.44)
Death	All	1.54 (1.31 – 1.86)	4.31 (3.64 – 5.27)
Hospitalization	5-11	2.39 (2.25 – 2.55)	5.40 (5.07 – 5.74)
Death	5-11	0.18 (0.17 – 0.19)	0.41 (0.38 – 0.44)

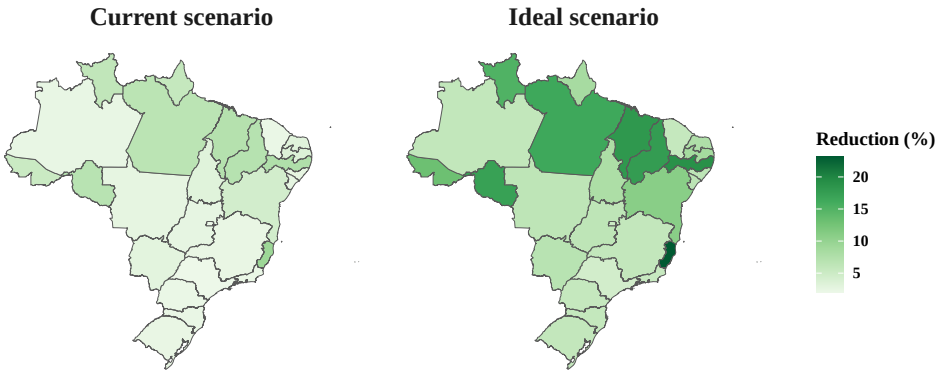

Figure C.5: Mean number of percentage of hospitalizations reduced by vaccination in 5-11 age group, by state.

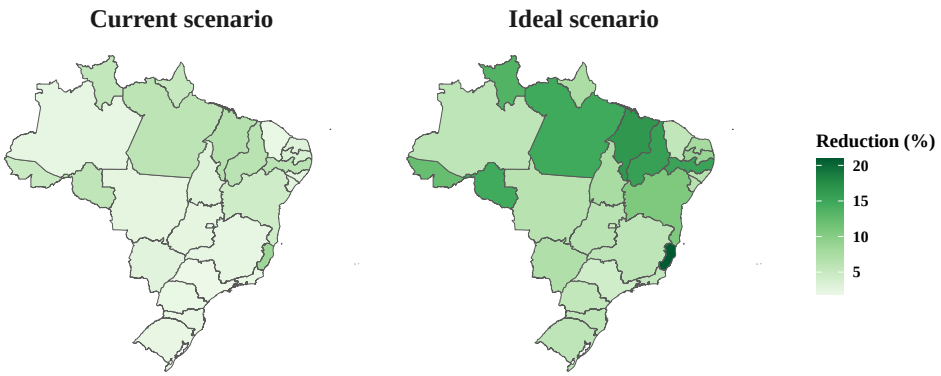

Figure C.6: Mean number of percentage of deaths reduced by vaccination in 5-11 age group, by state.

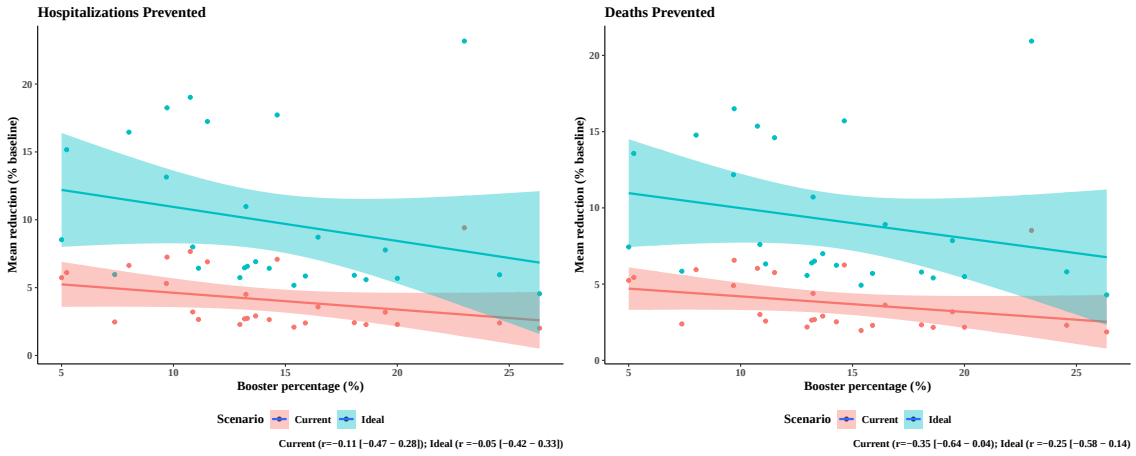

Figure C.7: Linear regression of the mean number of percentage of hospitalizations reduced by vaccination in 5-11 age group, by state, versus coverage of booster doses in the whole population.

Appendix D

Supplementary material for chapter 7

This supplementary material contains a graphical measurement of fitting quality,a figure showing the timing when vaccination reached perceptible coverage in each state and age group, a figure of vaccine coverage during the period analysed and the graphical results for individual states. The tabulated results for each state is available in our repository at https://github.com/covid19br/bayes-vacina-paper together with the code used to generate the results.

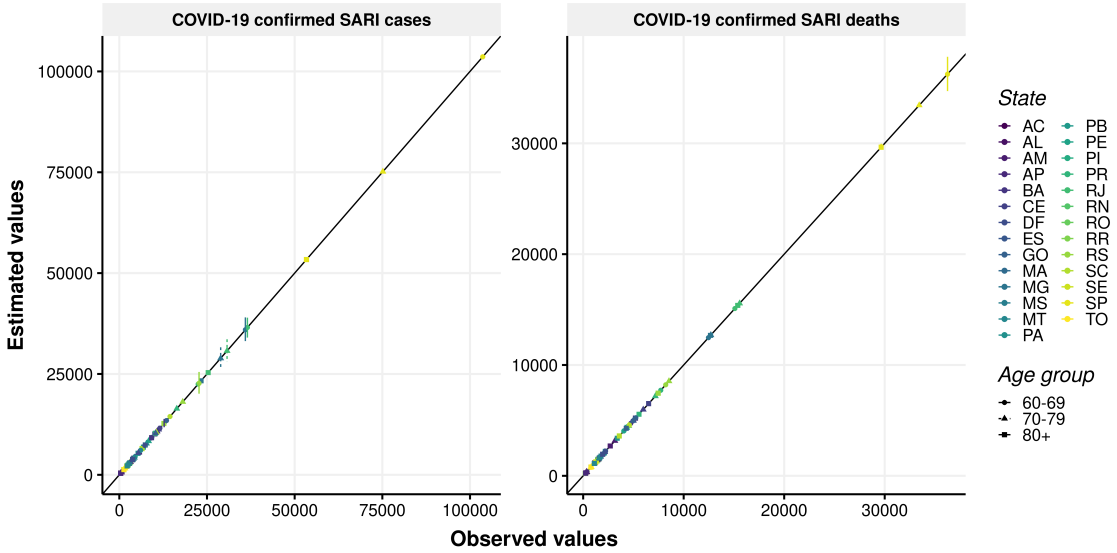

Figure D.1: Estimated value of outcome (hospitalisation on the left and deaths on the right) as a function of the observed value, per state (color) and age group (point type). A black line with 1:1 relationship is plotted for reference.

Table D.1: Name codes and their respective states

Name Code	State
North Region	
AC	Acre
AM	Amazonas
AP	Amapá
PA	Pará
RR	Roraima
RO	Rondônia
TO	Tocantins
Northeast Region	
AL	Alagoas
BA	Bahia
CE	Ceará
MA	Maranhão
PB	Paraíba
PE	Pernambuco
PI	Piauí
RN	Rio Grande do Norte
SE	Sergipe
Southeast Region	
ES	Espírito Santo
MG	Minas Gerais
RJ	Rio de Janeiro
SP	São Paulo
Center-West Region	
DF	Distrito Federal
GO	Goiás
MS	Mato Grosso do Sul
MT	Mato Grosso
South Region	
PR	Paraná
RS	Rio Grande do Sul
SC	Santa Catarina

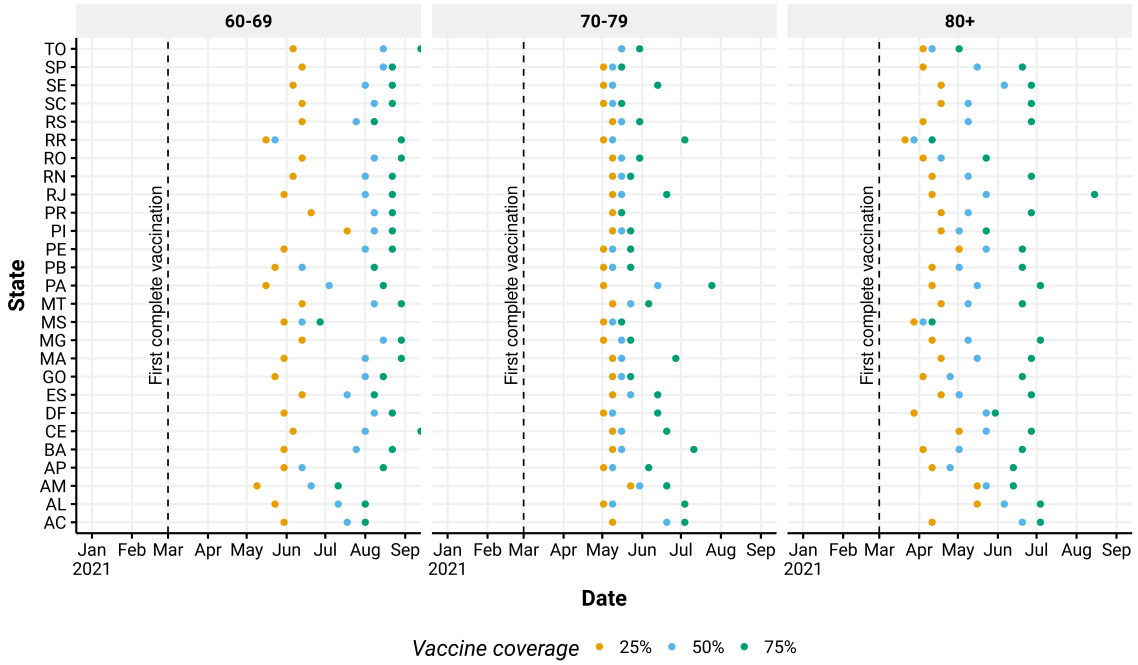

Figure D.2: Week (x-axis) in which different vaccine coverage thresholds were reached (colors), by state (y axis) for the analysed age groups (panels). The dashed line denotes the day that the first vaccination could be completed considering the official start as January 17, 2021 (first dose + 28 days + second dose + 14 days, as the first vaccines were CoronaVac).

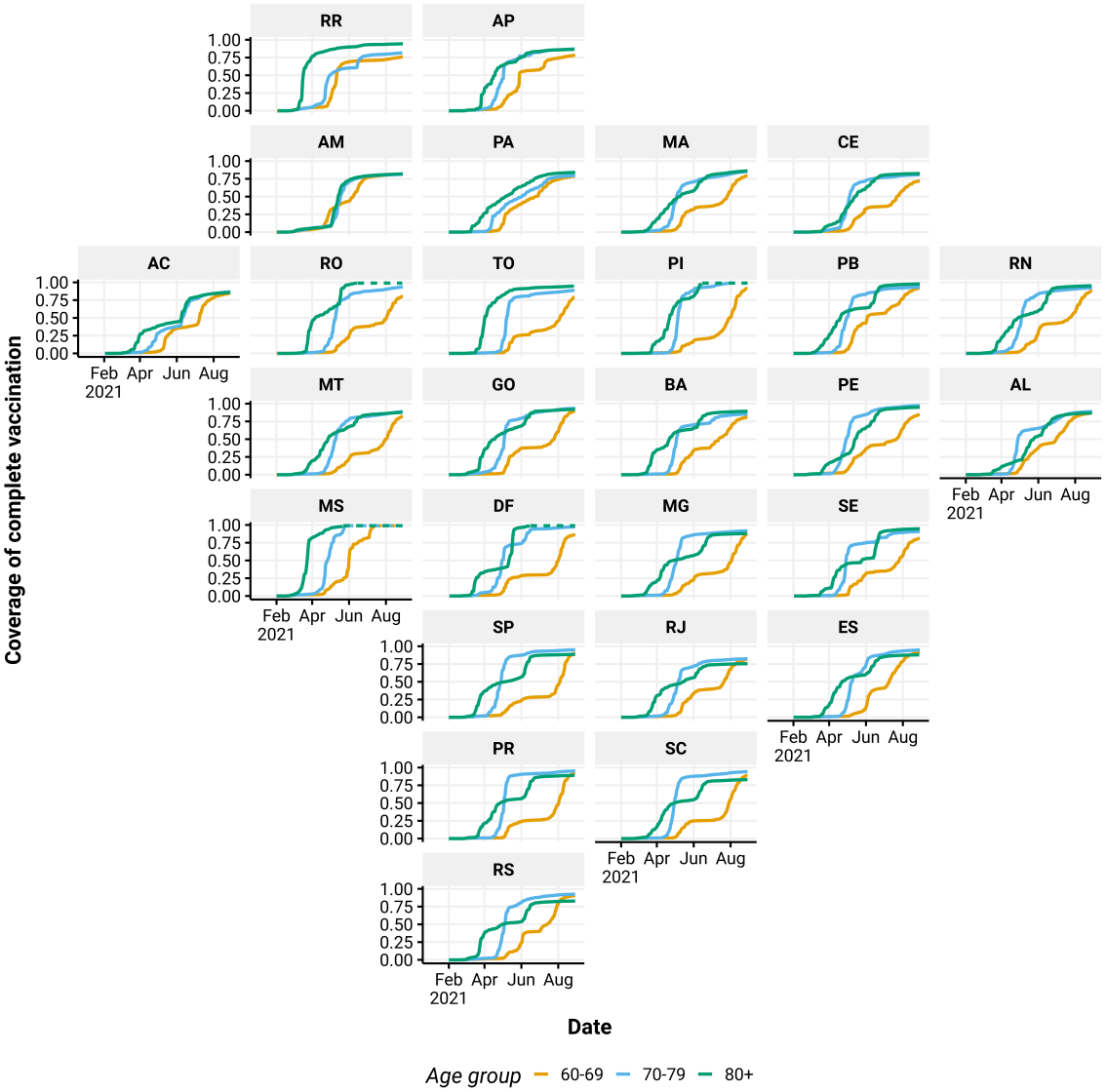

Figure D.3: Vaccine coverage per age group. Due to imprecise estimates of population size, some age groups surpassed 100% coverage and these cases are denoted with a dashed line.

Table D.2: Number of hospitalisations and deaths averted by COVID-19 vaccination, by state, by timing of vaccination rollout.

			Vaccination		
State	Outcome	Age group	Realized	4 weeks earlier	8 weeks earlier
AC	Hospitalisations	60-69	52 (15-92)	81 (26-140)	120 (42-199)
		70-79	44 (-6-93)	63 (1-126)	91 (-1-183)
		80+	39 (-2-79)	59 (2-115)	81 (4-154)
	Deaths	60-69	21 (6-37)	27 (4-52)	39 (0-80)
		70-79	14 (-5-33)	20 (-9-48)	29 (-13-69)
		80+	21 (5-38)	28 (6-52)	33 (6-62)
AL	Hospitalisations	60-69	345 (24-671)	585 (29-1,135)	883 (-11-1,762)
		70-79	329 (40-619)	497 (24-936)	677 (-10-1,358)
		80+	128 (-157-413)	95 (-281-478)	56 (-410-532)
	Deaths	60-69	120 (17-216)	193 (8-375)	271 (-23-553)
		70-79	76 (-42-183)	109 (-81-279)	140 (-130-381)
		80+	14 (-94-113)	24 (-114-152)	35 (-127-187)
AM	Hospitalisations	60-69	519 (-149-1,280)	722 (-118-1,677)	966 (-148-2,222)
		70-79	660 (9-1,325)	878 (11-1,748)	1,194 (-23-2,426)
		80+	509 (65-964)	680 (88-1,290)	931 (71-1,784)
	Deaths	60-69	350 (161-555)	514 (234-809)	737 (340-1,163)
		70-79	288 (113-458)	422 (160-675)	661 (266-1,047)
		80+	209 (49-370)	314 (78-553)	501 (127-887)
AP	Hospitalisations	60-69	60 (-50-172)	104 (-88-308)	160 (-150-487)
		70-79	-10 (-83-74)	-21 (-133-104)	-33 (-196-138)
		80+	43 (-39-125)	46 (-68-164)	48 (-92-197)
	Deaths	60-69	11 (-14-39)	18 (-19-56)	26 (-28-79)
		70-79	4 (-21-28)	5 (-29-38)	6 (-41-52)
		80+	-13 (-37-11)	-18 (-50-16)	-22 (-64-21)
BA	Hospitalisations	60-69	2,377 (1,632-3,160)	3,657 (2,665-4,674)	4,838 (3,288-6,398)
		70-79	954 (172-1,679)	1,256 (-30-2,496)	1,541 (-463-3,454)
		80+	1,468 (605-2,344)	1,902 (772-3,041)	2,292 (889-3,698)
	Deaths	60-69	297 (44-561)	530 (52-1,012)	837 (15-1,661)
		70-79	206 (-90-512)	283 (-212-761)	340 (-358-1,038)
		80+	379 (20-740)	415 (-70-887)	396 (-221-965)
CE	Hospitalisations	60-69	1,154 (224-2,052)	2,072 (227-3,897)	3,130 (-312-6,644)
		70-79	1,093 (12-2,063)	1,676 (-163-3,428)	2,247 (-620-4,864)
		80+	921 (-215-2,046)	1,259 (-551-3,127)	1,555 (-1,161-4,300)
	Deaths	60-69	609 (342-875)	1,030 (582-1,473)	1,456 (740-2,141)
		70-79	898 (473-1,314)	1,341 (706-1,975)	1,703 (860-2,542)
		80+	1,275 (758-1,755)	1,744 (1,011-2,445)	2,077 (1,109-2,991)
DF	Hospitalisations	60-69	1,572 (1,152-1,982)	2,037 (1,434-2,583)	2,630 (1,773-3,413)
		70-79	1,050 (644-1,483)	1,371 (826-1,947)	1,752 (1,060-2,484)
		80+	658 (366-997)	836 (467-1,262)	962 (534-1,436)
	Deaths	60-69	277 (116-427)	416 (171-646)	558 (224-870)
		70-79	310 (144-469)	456 (213-693)	553 (249-853)
		80+	219 (19-441)	235 (0-490)	221 (-55-506)
ES	Hospitalisations	60-69	78 (-88-235)	112 (-125-348)	166 (-198-528)
		70-79	151 (-29-322)	225 (-39-489)	327 (-61-714)
		80+	190 (64-325)	273 (87-465)	341 (112-589)
	Deaths	60-69	74 (-7-155)	130 (-29-296)	193 (-47-444)
		70-79	98 (21-178)	151 (33-278)	195 (44-363)
		80+	215 (116-324)	270 (147-407)	283 (130-445)
GO	Hospitalisations	60-69	3,232 (2,195-4,233)	4,208 (2,818-5,551)	5,216 (3,375-6,993)
		70-79	2,850 (1,883-3,718)	3,389 (2,151-4,423)	4,017 (2,525-5,268)
		80+	2,216 (1,521-2,943)	2,595 (1,764-3,484)	2,908 (1,976-3,899)
	Deaths	60-69	761 (409-1,138)	1,047 (491-1,621)	1,492 (638-2,379)
		70-79	674 (273-1,083)	908 (346-1,508)	1,208 (432-2,030)
		80+	736 (384-1,084)	962 (482-1,426)	1,023 (413-1,554)
MA	Hospitalisations	60-69	723 (385-1,063)	1,054 (266-1,799)	1,386 (-394-3,120)
		70-79	500 (57-895)	699 (10-1,376)	902 (-112-1,964)
		80+	588 (138-1,049)	718 (125-1,364)	821 (95-1,617)
	Deaths	60-69	138 (-14-299)	182 (-50-402)	248 (-126-604)
		70-79	408 (216-596)	519 (262-769)	651 (298-968)
		80+	329 (92-568)	425 (103-742)	501 (119-886)
MG	Hospitalisations	60-69	10,941 (8,768-13,164)	14,930 (12,157-17,645)	18,154 (14,432-22,146)
		70-79	9,628 (7,636-11,779)	11,839 (9,202-14,269)	13,821 (10,867-16,955)
		80+	6,080 (3,237-8,656)	7,518 (3,634-11,011)	8,672 (3,875-12,991)
	Deaths	60-69	3,000 (2,095-3,919)	4,376 (2,812-5,838)	6,055 (3,520-8,527)
		70-79	4,287 (3,366-5,127)	5,762 (4,538-6,911)	7,166 (5,601-8,642)
		80+	3,658 (2,071-5,232)	4,639 (2,702-6,601)	5,244 (2,968-7,450)
MS	Hospitalisations	60-69	418 (-48-867)	668 (-154-1,430)	827 (-405-2,018)
		70-79	361 (-64-811)	434 (-150-1,030)	488 (-511-1,543)

		80+	161 (-197-519)	102 (-378-566)	66 (-1,108-1,164)
	Deaths	60-69	171 (46-300)	269 (32-508)	363 (-4-736)
		70-79	255 (68-435)	269 (39-493)	281 (1-570)
		80+	151 (-51-365)	151 (-76-390)	138 (-178-442)
MT	Hospitalisations	60-69	227 (-264-700)	595 (-437-1,600)	1,139 (-661-2,901)
		70-79	-27 (-362-338)	-65 (-698-585)	-116 (-1,145-920)
		80+	104 (-189-409)	126 (-296-556)	147 (-396-714)
	Deaths	60-69	73 (-60-213)	45 (-209-309)	7 (-414-441)
		70-79	37 (-88-162)	42 (-126-218)	42 (-172-261)
		80+	100 (-27-222)	105 (-48-250)	89 (-76-250)
PA	Hospitalisations	60-69	1,319 (541-2,096)	1,906 (567-3,195)	2,602 (513-4,600)
		70-79	1,714 (1,084-2,301)	2,238 (1,547-2,900)	2,708 (1,742-3,549)
		80+	1,456 (907-2,015)	1,917 (1,120-2,712)	2,256 (1,239-3,316)
	Deaths	60-69	374 (-14-774)	552 (-48-1,153)	748 (-97-1,622)
		70-79	665 (173-1,114)	941 (204-1,594)	1,163 (209-2,007)
		80+	355 (-42-802)	484 (-75-1,075)	594 (-120-1,326)
PB	Hospitalisations	60-69	393 (144-642)	640 (192-1,086)	891 (69-1,666)
		70-79	561 (162-938)	748 (157-1,300)	933 (34-1,752)
		80+	470 (80-847)	599 (79-1,102)	724 (26-1,427)
	Deaths	60-69	115 (-20-249)	197 (-49-427)	309 (-106-689)
		70-79	107 (-114-320)	141 (-142-405)	171 (-167-488)
		80+	187 (-40-443)	262 (-9-568)	316 (11-658)
PE	Hospitalisations	60-69	413 (2-829)	726 (-9-1,499)	1,084 (-303-2,485)
		70-79	292 (-233-800)	454 (-516-1,393)	606 (-901-2,144)
		80+	205 (-293-698)	337 (-344-1,021)	468 (-428-1,381)
	Deaths	60-69	240 (57-433)	408 (107-733)	601 (125-1,140)
		70-79	389 (73-686)	584 (110-1,032)	746 (134-1,342)
		80+	637 (365-915)	837 (452-1,225)	981 (488-1,478)
PI	Hospitalisations	60-69	364 (137-607)	615 (201-1,040)	921 (194-1,657)
		70-79	299 (126-484)	459 (178-767)	645 (161-1,142)
		80+	220 (-2-468)	334 (-38-738)	446 (-104-1,038)
	Deaths	60-69	8 (-41-54)	14 (-80-102)	23 (-160-204)
		70-79	37 (-27-108)	66 (-47-193)	87 (-66-254)
		80+	64 (-19-149)	89 (-27-205)	95 (-33-224)
PR	Hospitalisations	60-69	5,414 (4,110-6,832)	7,169 (5,375-9,106)	8,482 (6,283-10,785)
		70-79	3,419 (2,112-4,684)	4,347 (2,674-6,130)	5,219 (3,111-7,535)
		80+	3,972 (3,069-4,891)	4,767 (3,678-5,885)	5,514 (4,202-6,820)
	Deaths	60-69	1,216 (553-1,826)	1,582 (694-2,420)	2,017 (793-3,191)
		70-79	1,795 (1,219-2,357)	2,163 (1,482-2,839)	2,588 (1,747-3,437)
		80+	1,782 (1,331-2,231)	2,167 (1,611-2,718)	2,423 (1,779-3,071)
RJ	Hospitalisations	60-69	6,457 (4,456-8,455)	8,254 (6,026-10,488)	10,013 (7,210-12,647)
		70-79	5,269 (3,255-7,237)	6,268 (4,003-8,581)	7,173 (4,712-9,582)
		80+	2,819 (213-5,217)	3,414 (11-6,626)	3,714 (-521-7,600)
	Deaths	60-69	2,629 (1,724-3,504)	3,611 (2,291-4,814)	4,575 (2,797-6,189)
		70-79	2,423 (1,390-3,439)	3,298 (1,911-4,709)	3,911 (2,188-5,654)
		80+	2,492 (898-4,120)	2,949 (933-4,907)	3,256 (684-5,669)
RN	Hospitalisations	60-69	286 (96-455)	556 (152-910)	895 (86-1,666)
		70-79	375 (153-615)	533 (177-923)	703 (126-1,333)
		80+	433 (161-707)	601 (166-1,054)	777 (146-1,465)
	Deaths	60-69	17 (-45-80)	51 (-65-165)	140 (-89-382)
		70-79	130 (28-228)	177 (30-331)	226 (16-443)
		80+	193 (49-328)	249 (42-441)	278 (12-523)
RO	Hospitalisations	60-69	138 (-8-284)	228 (-51-495)	322 (-185-811)
		70-79	204 (71-344)	327 (109-551)	501 (152-855)
		80+	165 (56-276)	251 (84-417)	331 (110-549)
	Deaths	60-69	79 (29-129)	111 (32-185)	191 (55-316)
		70-79	75 (22-124)	120 (30-197)	211 (56-346)
		80+	44 (-3-88)	69 (-3-140)	79 (-15-165)
RR	Hospitalisations	60-69	6 (-41-55)	7 (-61-78)	5 (-92-103)
		70-79	66 (27-104)	77 (25-132)	90 (19-169)
		80+	6 (-34-43)	10 (-44-62)	15 (-56-86)
	Deaths	60-69	13 (-15-42)	13 (-20-47)	13 (-29-59)
		70-79	-26 (-52–2)	-32 (-66–1)	-38 (-81-1)
		80+	6 (-12-22)	6 (-16-27)	7 (-20-34)
RS	Hospitalisations	60-69	5,153 (3,026-7,210)	7,920 (5,319-10,504)	9,715 (5,714-13,287)
		70-79	3,945 (2,407-5,430)	4,898 (2,407-7,536)	5,910 (2,338-9,704)
		80+	3,565 (2,272-4,826)	4,617 (2,784-6,440)	5,560 (3,258-7,960)
	Deaths	60-69	914 (276-1,571)	1,487 (382-2,589)	2,234 (350-4,109)
		70-79	1,794 (1,015-2,544)	2,477 (1,367-3,514)	3,424 (1,895-4,835)
		80+	2,717 (2,082-3,429)	3,619 (2,733-4,605)	4,001 (2,932-5,102)
SC	Hospitalisations	60-69	3,792 (2,845-4,654)	5,069 (3,835-6,244)	6,450 (4,827-8,080)
		70-79	2,470 (1,513-3,431)	3,206 (1,969-4,464)	4,088 (2,515-5,740)
		80+	1,954 (1,161-2,743)	2,442 (1,415-3,439)	2,945 (1,696-4,173)
	Deaths	60-69	526 (132-924)	740 (161-1,313)	994 (160-1,820)

		70-79	631 (148-1,146)	890 (201-1,612)	1,105 (224-2,010)
		80+	1,254 (724-1,814)	1,593 (917-2,317)	1,810 (1,033-2,649)
SE	Hospitalisations	60-69	202 (52-351)	359 (71-660)	635 (-105-1,357)
		70-79	207 (34-369)	389 (47-735)	632 (10-1,235)
		80+	164 (-8-326)	308 (-2-616)	443 (-18-923)
	Deaths	60-69	35 (-5-74)	61 (-11-132)	89 (-109-285)
		70-79	56 (8-107)	92 (1-188)	114 (-45-280)
		80+	-16 (-76-47)	26 (-79-135)	79 (-92-260)
SP	Hospitalisations	60-69	25,183 (21,396-29,046)	34,936 (28,393-41,287)	44,275 (32,947-55,943)
		70-79	19,517 (15,716-23,448)	23,549 (18,236-29,076)	28,553 (21,499-35,829)
		80+	11,156 (8,761-13,712)	13,828 (10,647-17,181)	15,556 (11,872-19,448)
	Deaths	60-69	10,390 (9,153-11,742)	14,150 (12,600-15,797)	18,819 (16,494-21,280)
		70-79	10,965 (9,662-12,258)	14,257 (12,536-15,957)	17,169 (15,012-19,287)
		80+	10,245 (8,229-12,228)	12,281 (9,865-14,751)	13,326 (10,687-16,078)
TO	Hospitalisations	60-69	177 (53-293)	219 (23-410)	240 (-72-548)
		70-79	33 (-93-145)	45 (-132-204)	56 (-194-279)
		80+	145 (-10-298)	171 (-17-356)	189 (-28-395)
	Deaths	60-69	59 (23-95)	93 (40-147)	130 (52-210)
		70-79	40 (-3-82)	54 (-4-112)	69 (-6-147)
		80+	97 (43-151)	122 (54-191)	134 (59-210)

D.1 Results

D.1.1 North Region

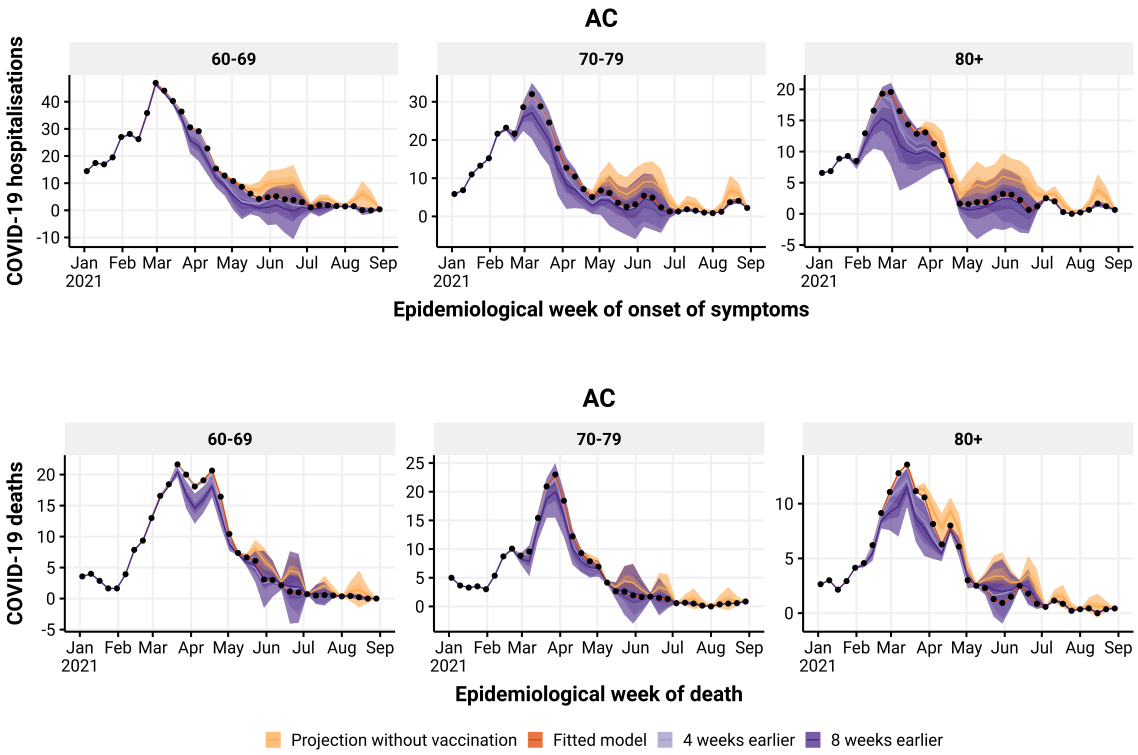

Figure D.4: Estimated number of hospitalisations (top) and deaths (bottom) by epidemiological week with the realized (dark orange), no vaccination (light orange), 4 (light purple) and 8 (dark purple) weeks earlier vaccination rollout, by age group (panels), in AC state. The observed number of hospitalisations and deaths are given by the black points.

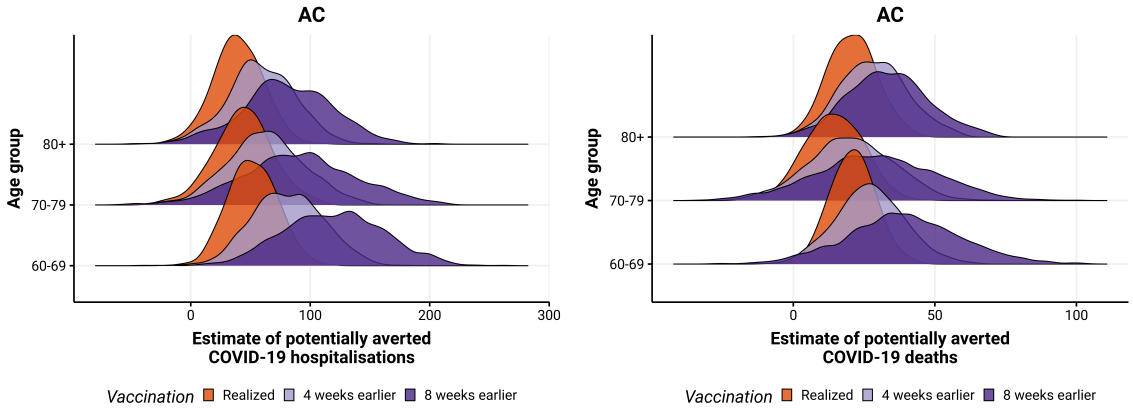

Figure D.5: Posterior distribution of hospitalisations (left) and deaths (right) potentially averted by vaccination between 2021-01-01 and 2021-08-29 by age group, with the realized (orange), 4 (light purple) and 8 weeks earlier (dark purple) vaccination rollout in AC state.

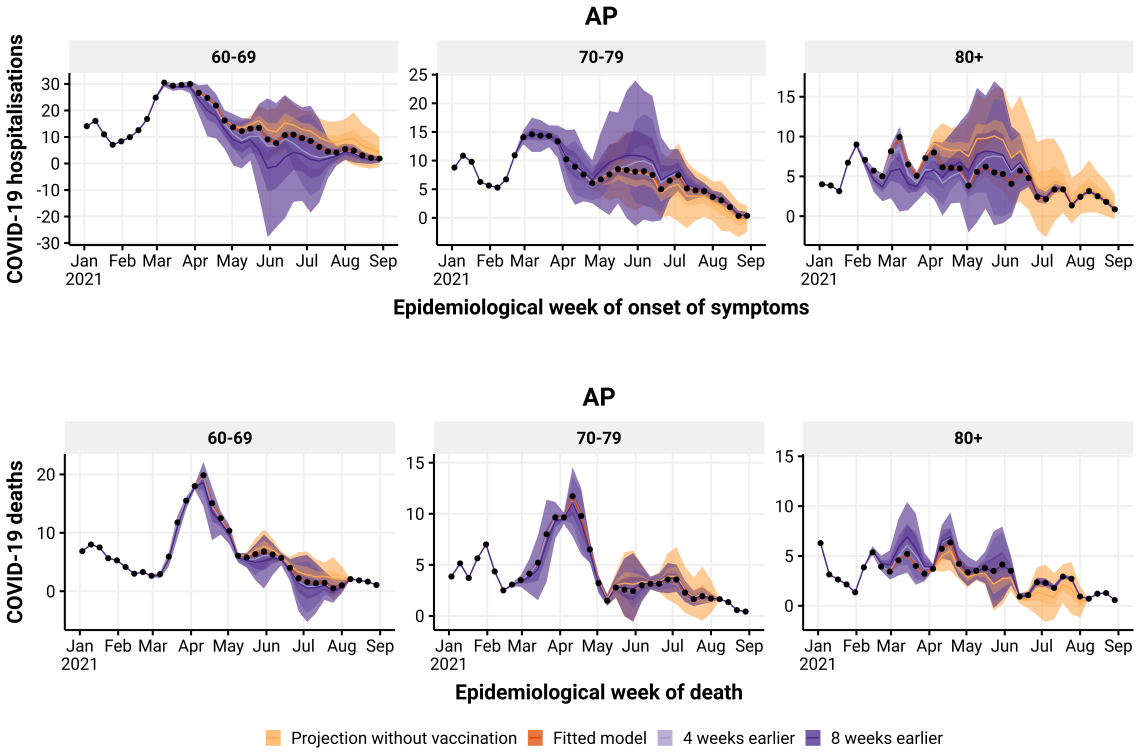

Figure D.6: Estimated number of hospitalisations (top) and deaths (bottom) by epidemiological week with the realized (dark orange), no vaccination (light orange), 4 (light purple) and 8 (dark purple) weeks earlier vaccination rollout, by age group (panels), in AP state. The observed number of hospitalisations and deaths are given by the black points.

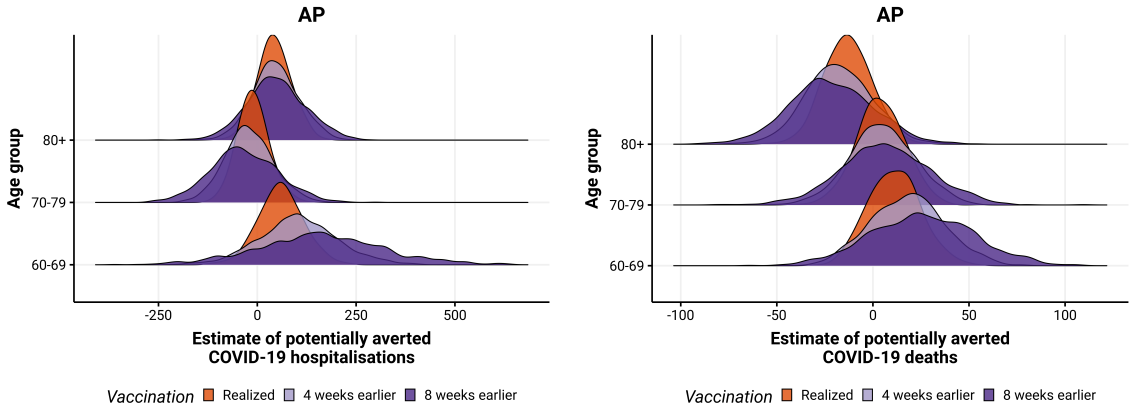

Figure D.7: Posterior distribution of hospitalisations (left) and deaths (right) potentially averted by vaccination between 2021-01-01 and 2021-08-29 by age group, with the realized (orange), 4 (light purple) and 8 weeks earlier (dark purple) vaccination rollout in AP state.

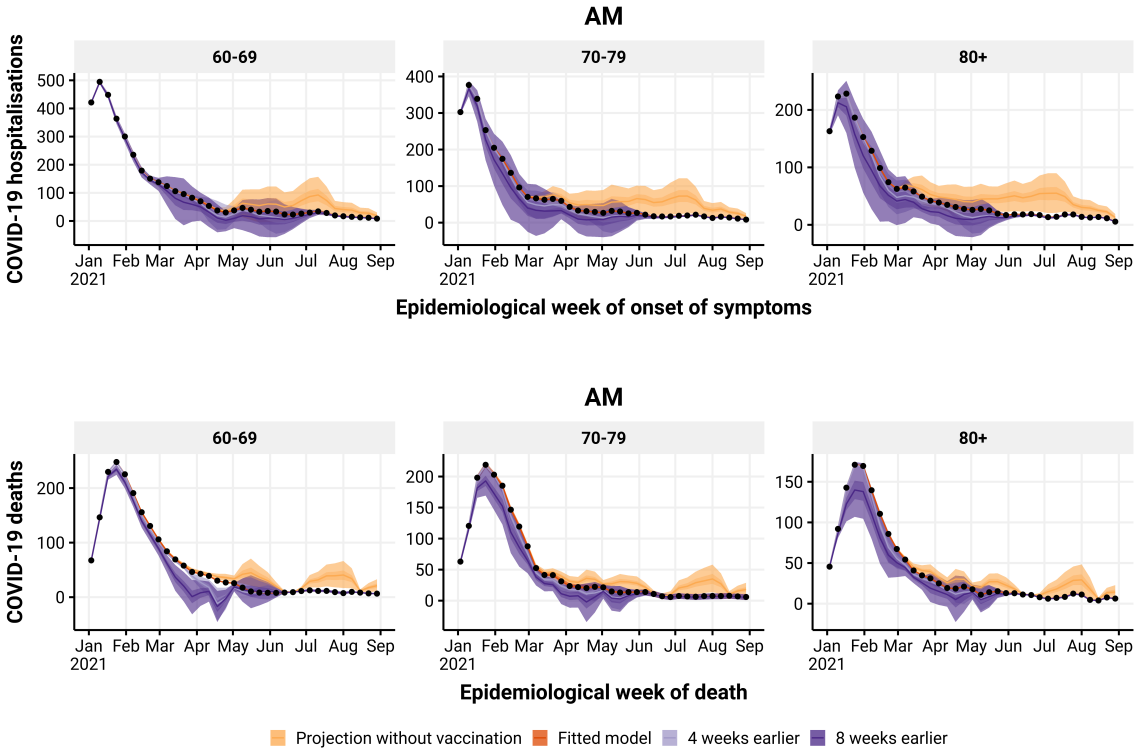

Figure D.8: Estimated number of hospitalisations (top) and deaths (bottom) by epidemiological week with the realized (dark orange), no vaccination (light orange), 4 (light purple) and 8 (dark purple) weeks earlier vaccination rollout, by age group (panels), in AM state. The observed number of hospitalisations and deaths are given by the black points.

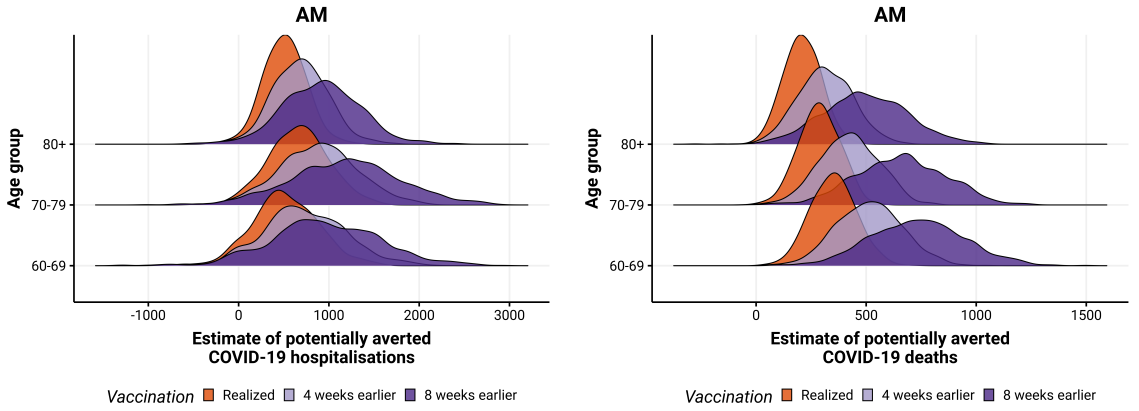

Figure D.9: Posterior distribution of hospitalisations (left) and deaths (right) potentially averted by vaccination between 2021-01-01 and 2021-08-29 by age group, with the realized (orange), 4 (light purple) and 8 weeks earlier (dark purple) vaccination rollout in AM state.

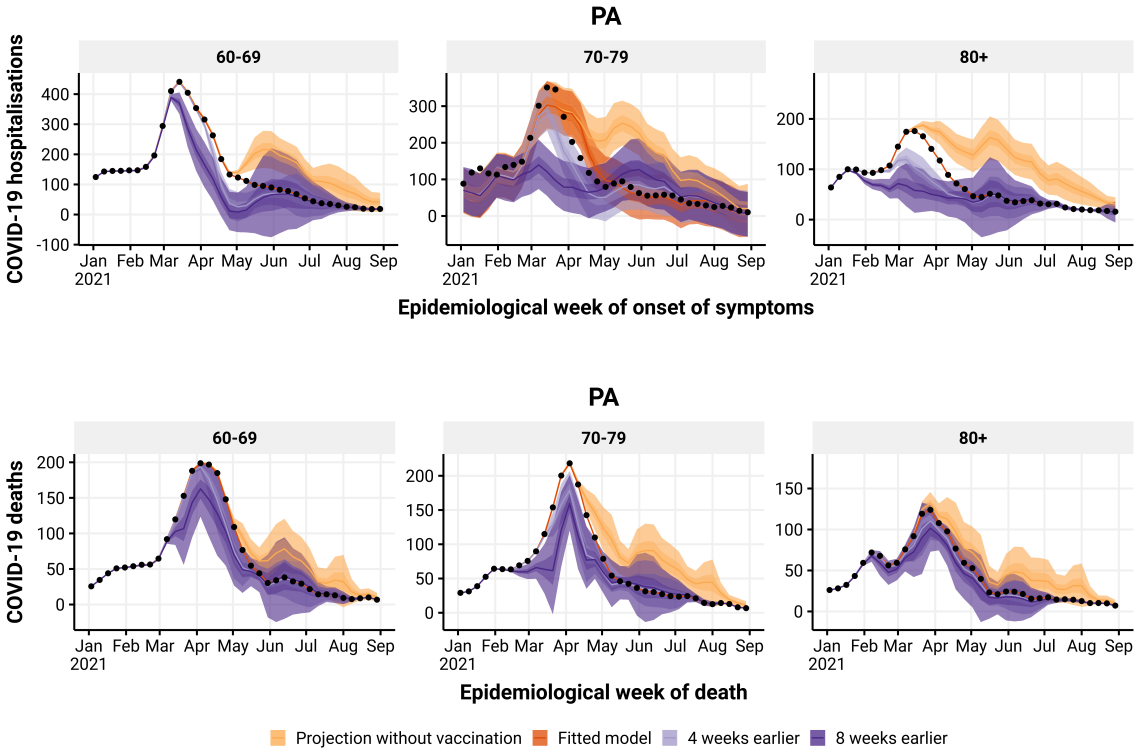

Figure D.10: Estimated number of hospitalisations (top) and deaths (bottom) by epidemiological week with the realized (dark orange), no vaccination (light orange), 4 (light purple) and 8 (dark purple) weeks earlier vaccination rollout, by age group (panels), in PA state. The observed number of hospitalisations and deaths are given by the black points.

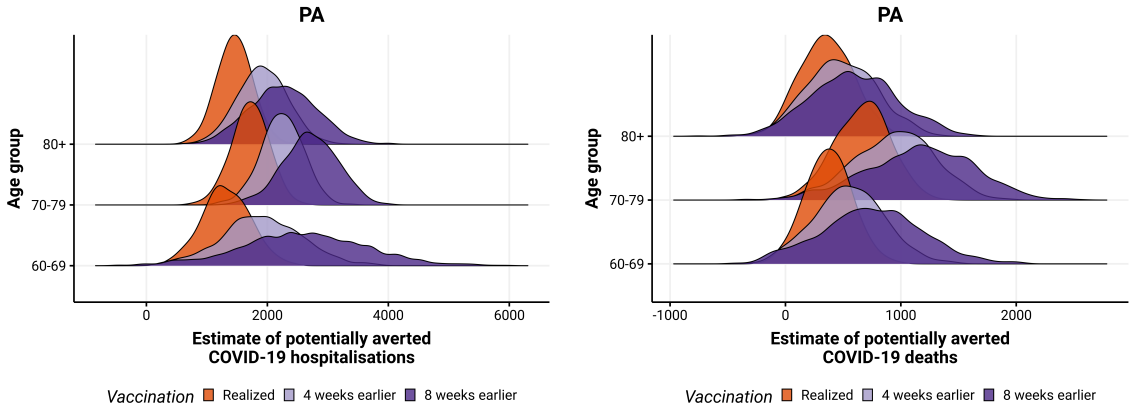

Figure D.11: Posterior distribution of hospitalisations (left) and deaths (right) potentially averted by vaccination between 2021-01-01 and 2021-08-29 by age group, with the realized (orange), 4 (light purple) and 8 weeks earlier (dark purple) vaccination rollout in PA state.

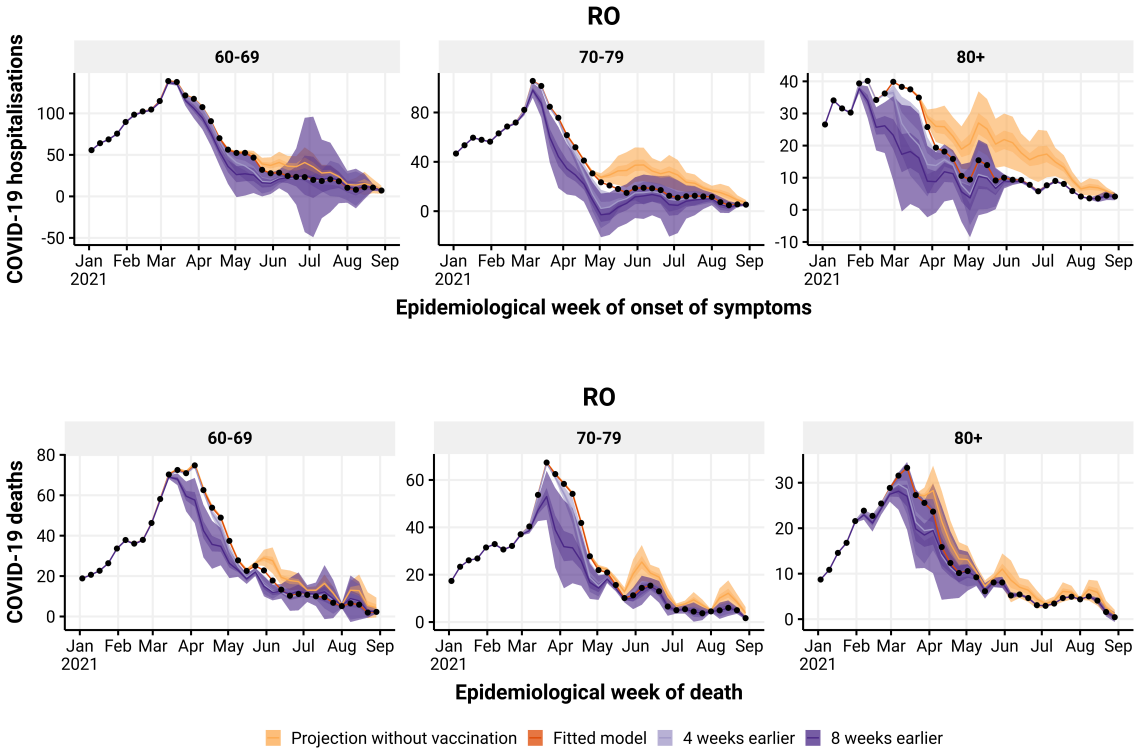

Figure D.12: Estimated number of hospitalisations (top) and deaths (bottom) by epidemiological week with the realized (dark orange), no vaccination (light orange), 4 (light purple) and 8 (dark purple) weeks earlier vaccination rollout, by age group (panels), in RO state. The observed number of hospitalisations and deaths are given by the black points.

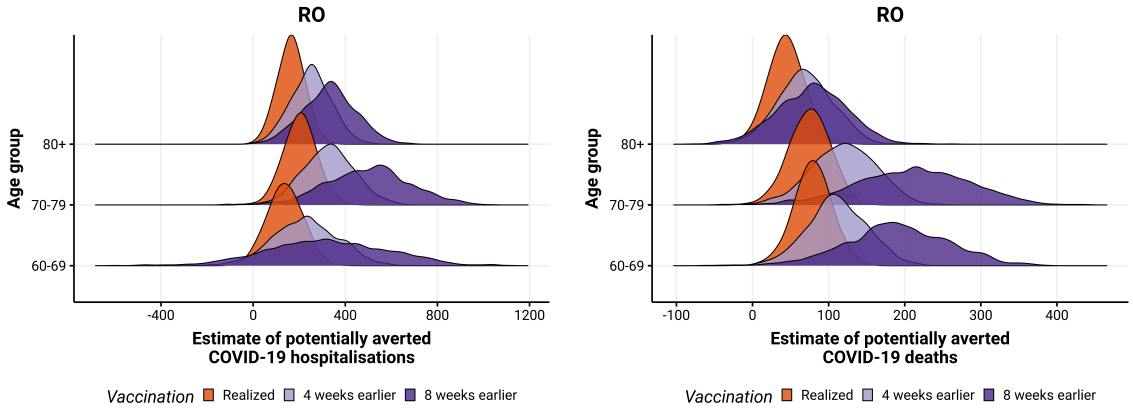

Figure D.13: Posterior distribution of hospitalisations (left) and deaths (right) potentially averted by vaccination between 2021-01-01 and 2021-08-29 by age group, with the realized (orange), 4 (light purple) and 8 weeks earlier (dark purple) vaccination rollout in RO state.

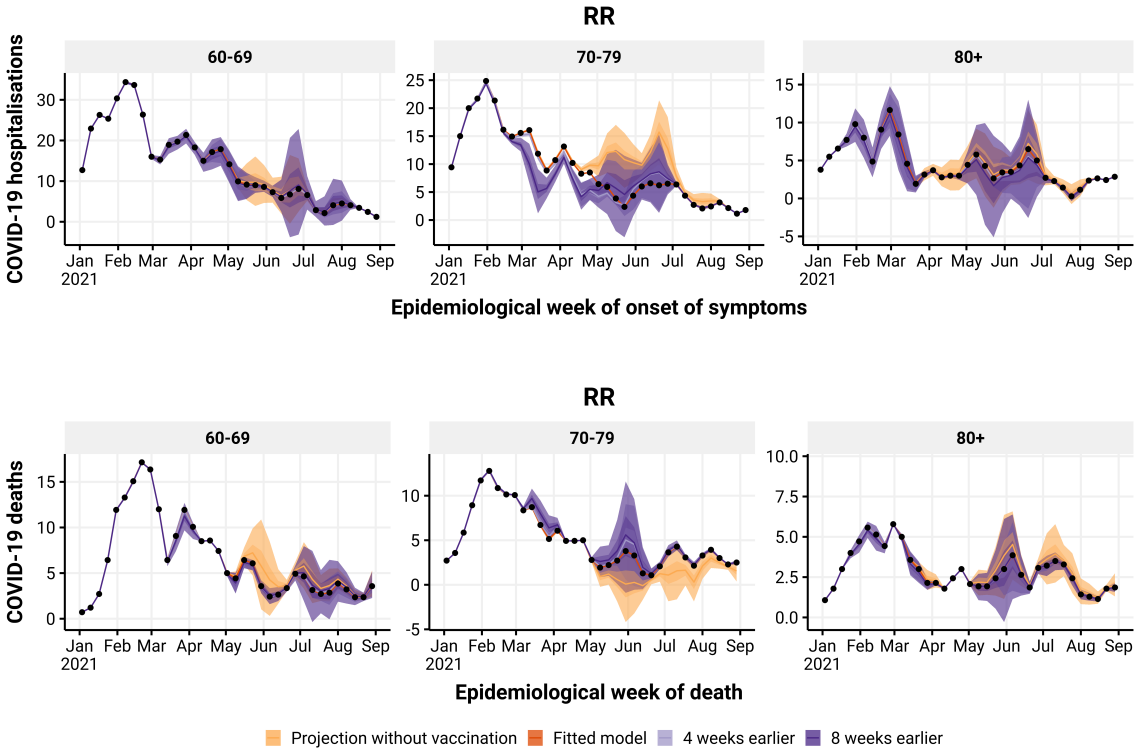

Figure D.14: Estimated number of hospitalisations (top) and deaths (bottom) by epidemiological week with the realized (dark orange), no vaccination (light orange), 4 (light purple) and 8 (dark purple) weeks earlier vaccination rollout, by age group (panels), in RR state. The observed number of hospitalisations and deaths are given by the black points.

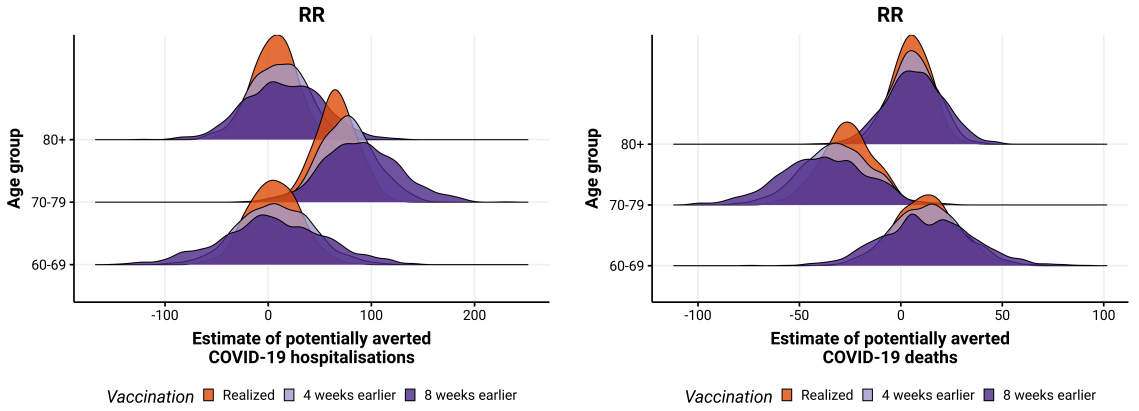

Figure D.15: Posterior distribution of hospitalisations (left) and deaths (right) potentially averted by vaccination between 2021-01-01 and 2021-08-29 by age group, with the realized (orange), 4 (light purple) and 8 weeks earlier (dark purple) vaccination rollout in RR state.

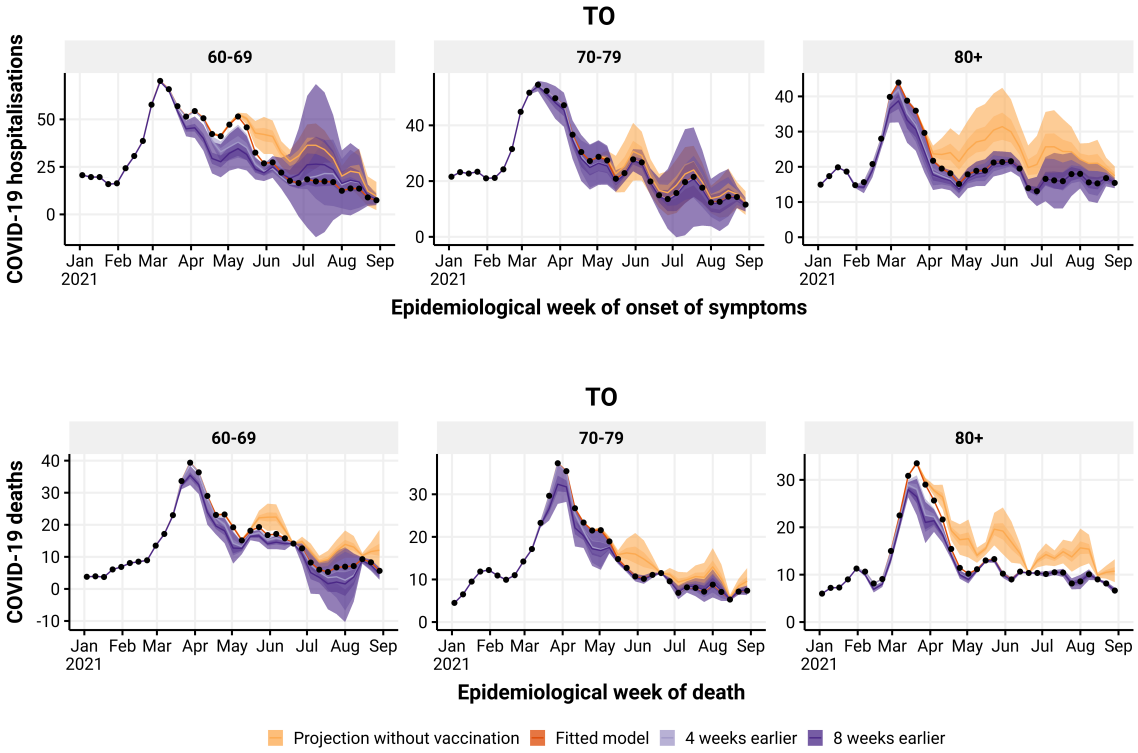

Figure D.16: Estimated number of hospitalisations (top) and deaths (bottom) by epidemiological week with the realized (dark orange), no vaccination (light orange), 4 (light purple) and 8 (dark purple) weeks earlier vaccination rollout, by age group (panels), in TO state. The observed number of hospitalisations and deaths are given by the black points.

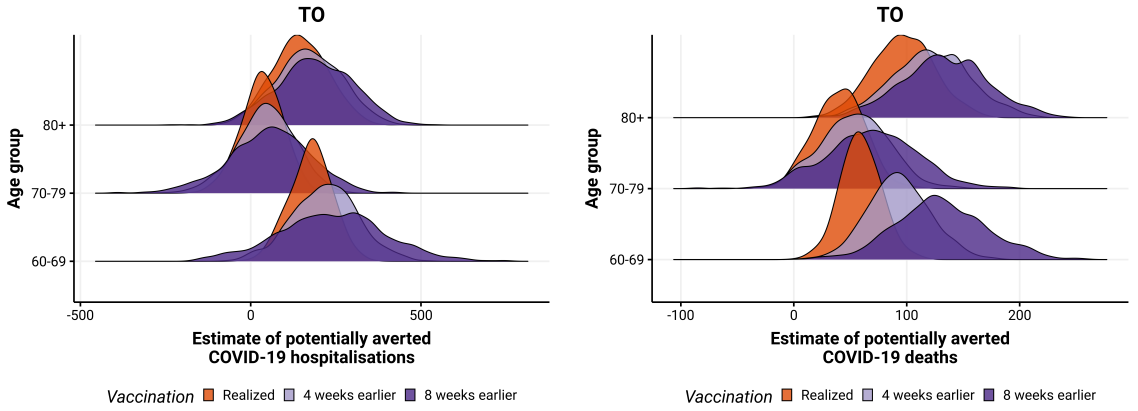

Figure D.17: Posterior distribution of hospitalisations (left) and deaths (right) potentially averted by vaccination between 2021-01-01 and 2021-08-29 by age group, with the realized (orange), 4 (light purple) and 8 weeks earlier (dark purple) vaccination rollout in TO state.

D.1.2 Northeast Region

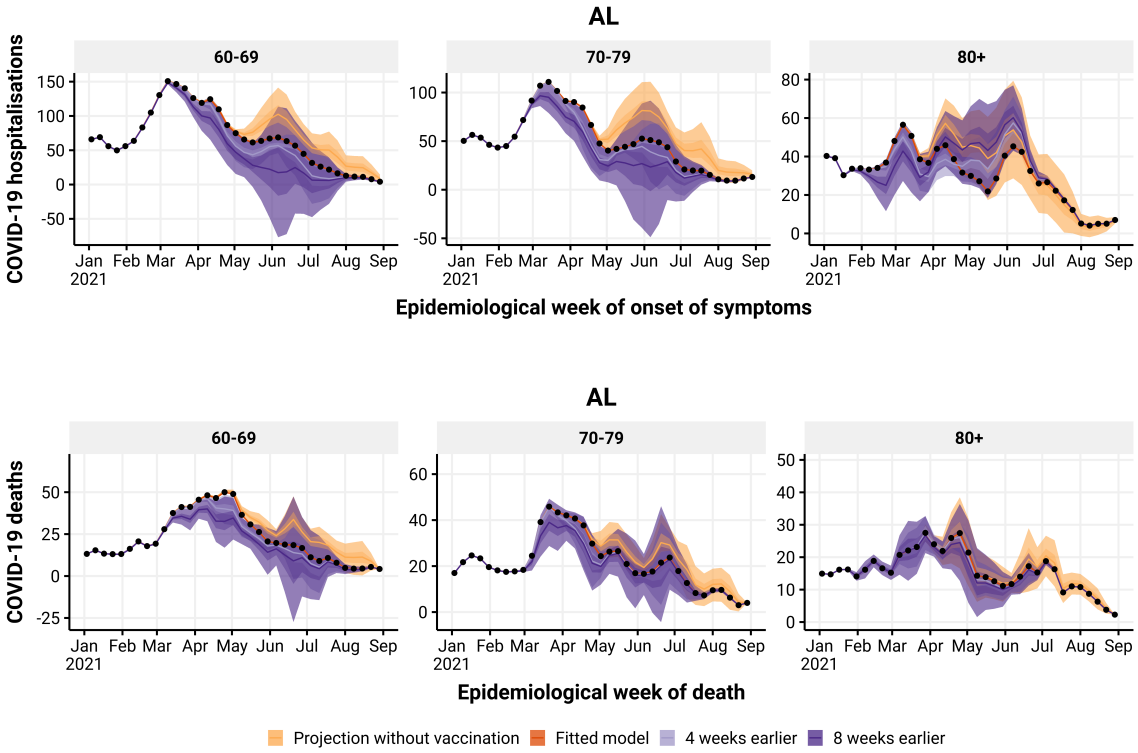

Figure D.18: Estimated number of hospitalisations (top) and deaths (bottom) by epidemiological week with the realized (orange), no vaccination (blue), 4 (green) and 8 (yellow) weeks earlier vaccination rollout, by age group (panels), in AL state. The observed number of hospitalisations and deaths are given by the black points.

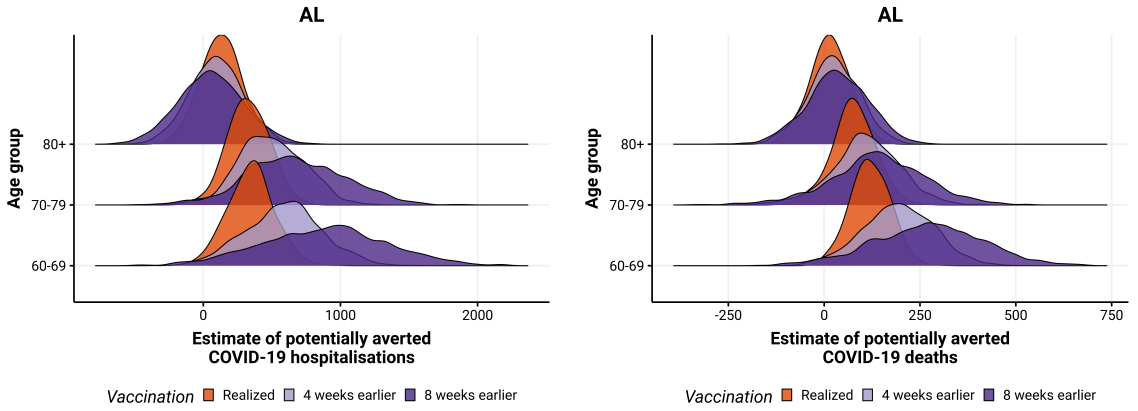

Figure D.19: Posterior distribution of hospitalisations (left) and deaths (right) potentially averted by vaccination between 2021-01-01 and 2021-08-29 by age group, with the realized (orange), 4 (blue) and 8 weeks earlier (green) vaccination rollout in AL state.

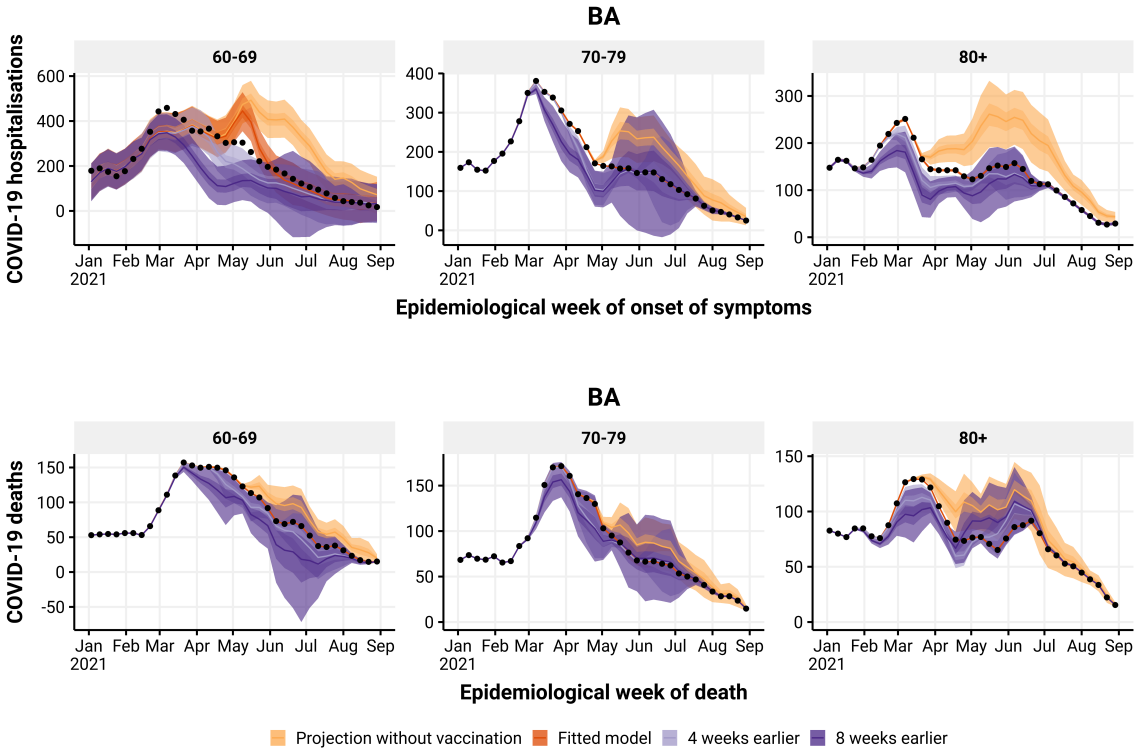

Figure D.20: Estimated number of hospitalisations (top) and deaths (bottom) by epidemiological week with the realized (orange), no vaccination (blue), 4 (green) and 8 (yellow) weeks earlier vaccination rollout, by age group (panels), in BA state. The observed number of hospitalisations and deaths are given by the black points.

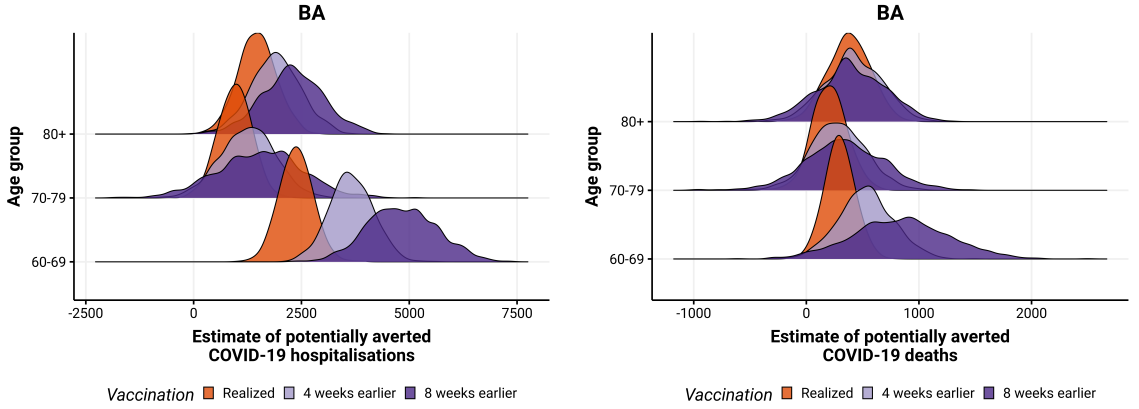

Figure D.21: Posterior distribution of hospitalisations (left) and deaths (right) potentially averted by vaccination between 2021-01-01 and 2021-08-29 by age group, with the realized (orange), 4 (blue) and 8 weeks earlier (green) vaccination rollout in BA state.

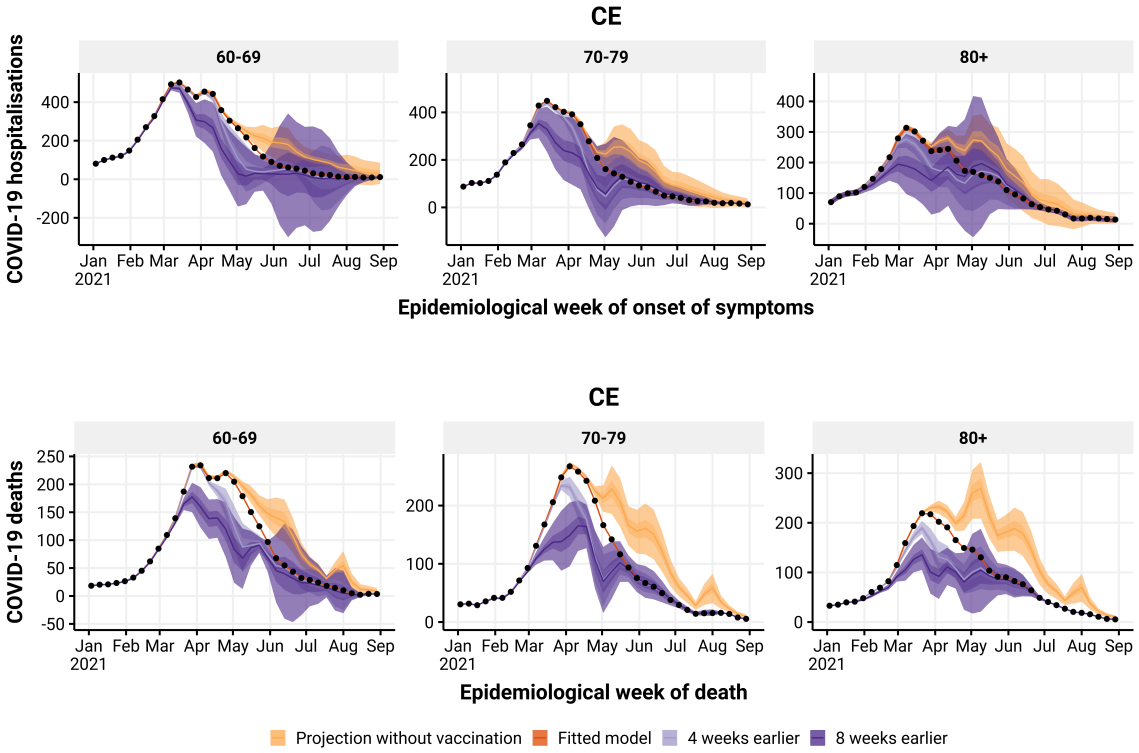

Figure D.22: Estimated number of hospitalisations (top) and deaths (bottom) by epidemiological week with the realized (orange), no vaccination (blue), 4 (green) and 8 (yellow) weeks earlier vaccination rollout, by age group (panels), in CE state. The observed number of hospitalisations and deaths are given by the black points.

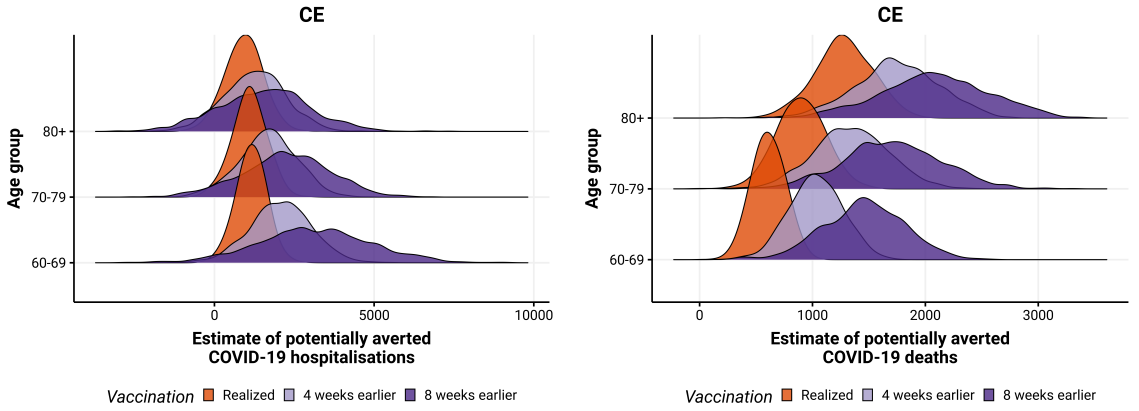

Figure D.23: Posterior distribution of hospitalisations (left) and deaths (right) potentially averted by vaccination between 2021-01-01 and 2021-08-29 by age group, with the realized (orange), 4 (blue) and 8 weeks earlier (green) vaccination rollout in CE state.

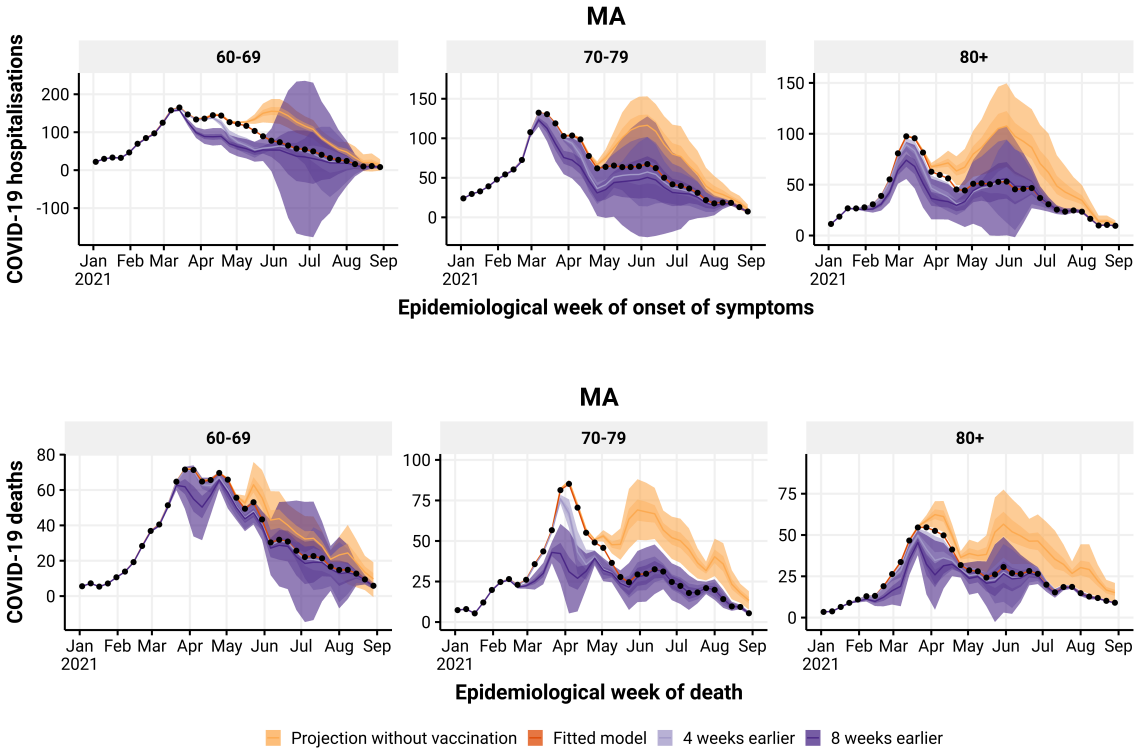

Figure D.24: Estimated number of hospitalisations (top) and deaths (bottom) by epidemiological week with the realized (orange), no vaccination (blue), 4 (green) and 8 (yellow) weeks earlier vaccination rollout, by age group (panels), in MA state. The observed number of hospitalisations and deaths are given by the black points.

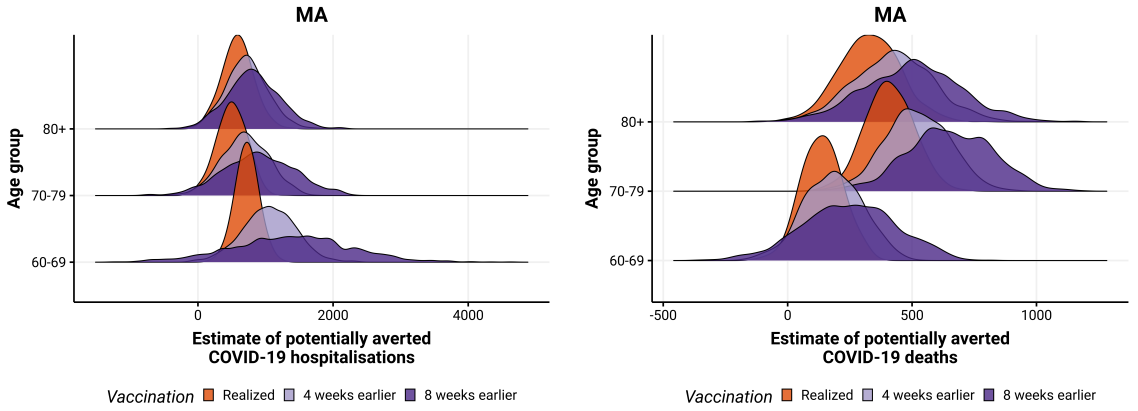

Figure D.25: Posterior distribution of hospitalisations (left) and deaths (right) potentially averted by vaccination between 2021-01-01 and 2021-08-29 by age group, with the realized (orange), 4 (blue) and 8 weeks earlier (green) vaccination rollout in MA state.

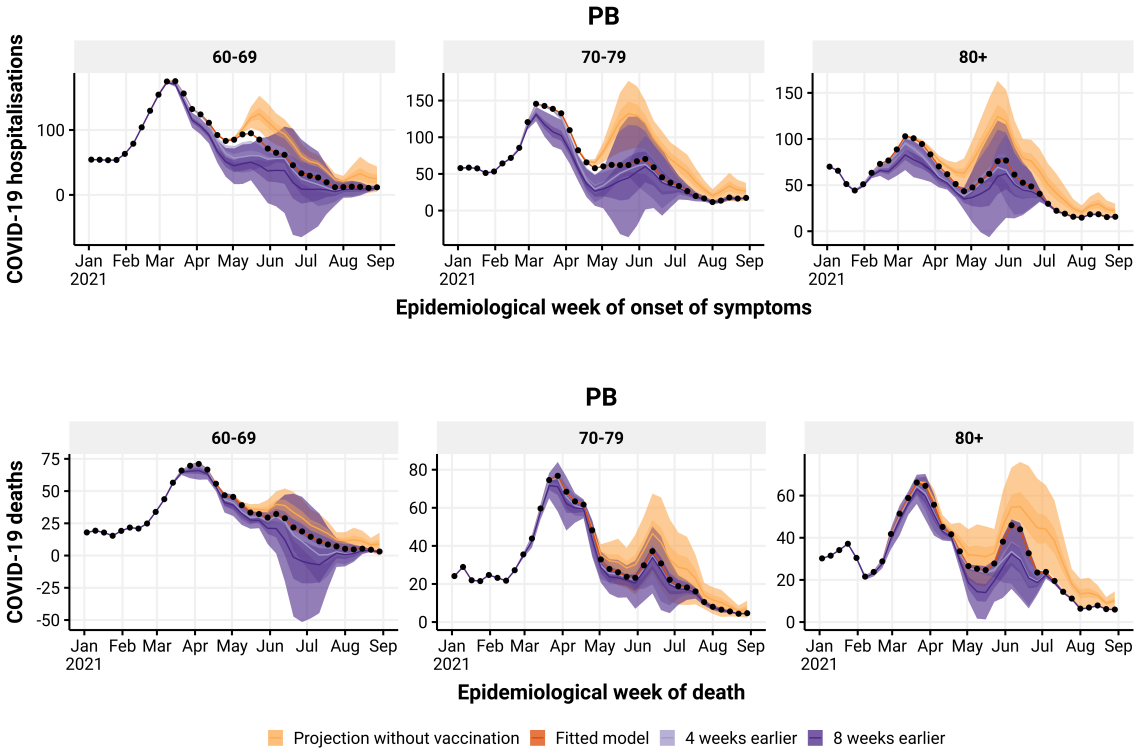

Figure D.26: Estimated number of hospitalisations (top) and deaths (bottom) by epidemiological week with the realized (orange), no vaccination (blue), 4 (green) and 8 (yellow) weeks earlier vaccination rollout, by age group (panels), in PB state. The observed number of hospitalisations and deaths are given by the black points.

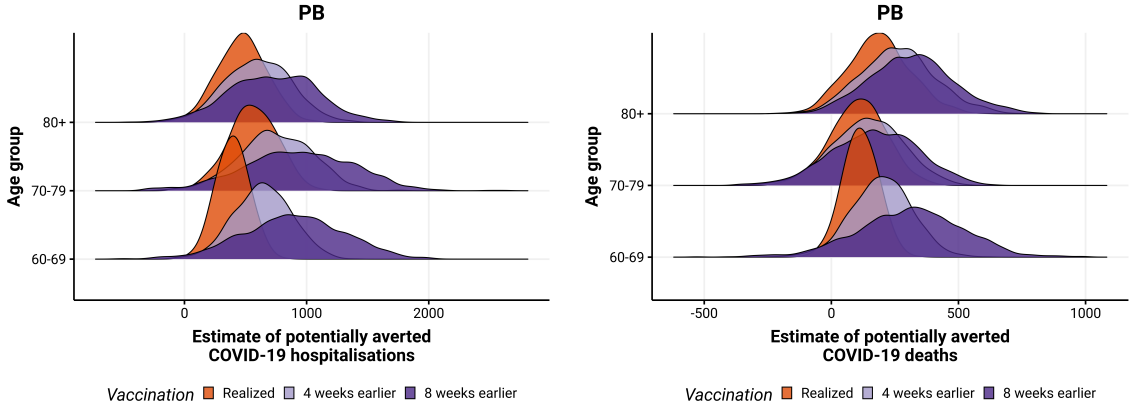

Figure D.27: Posterior distribution of hospitalisations (left) and deaths (right) potentially averted by vaccination between 2021-01-01 and 2021-08-29 by age group, with the realized (orange), 4 (blue) and 8 weeks earlier (green) vaccination rollout in PB state.

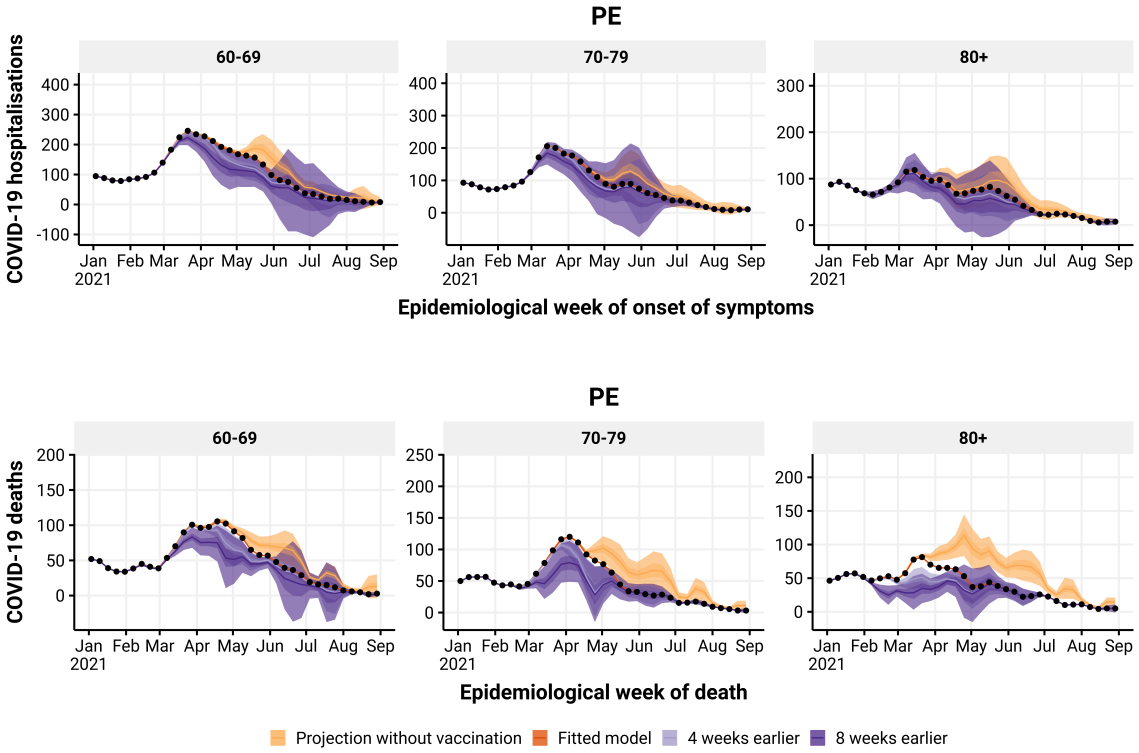

Figure D.28: Estimated number of hospitalisations (top) and deaths (bottom) by epidemiological week with the realized (orange), no vaccination (blue), 4 (green) and 8 (yellow) weeks earlier vaccination rollout, by age group (panels), in PE state. The observed number of hospitalisations and deaths are given by the black points.

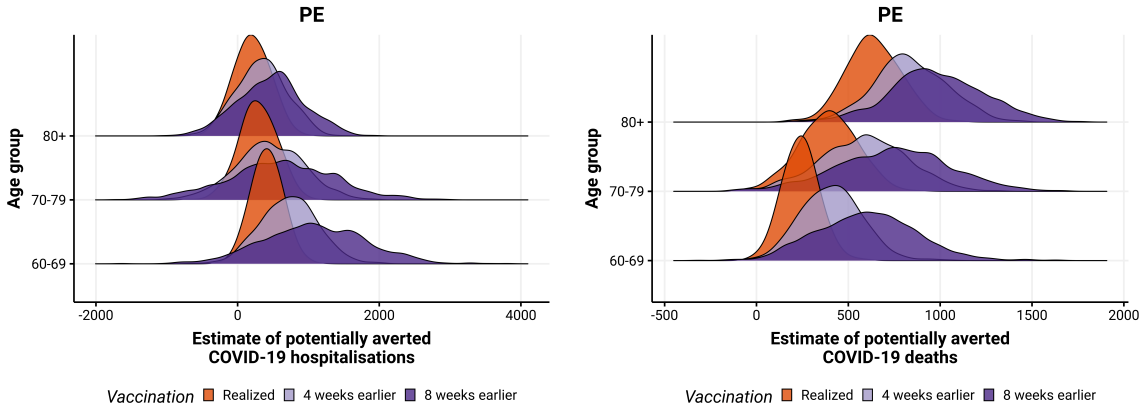

Figure D.29: Posterior distribution of hospitalisations (left) and deaths (right) potentially averted by vaccination between 2021-01-01 and 2021-08-29 by age group, with the realized (orange), 4 (blue) and 8 weeks earlier (green) vaccination rollout in PE state.

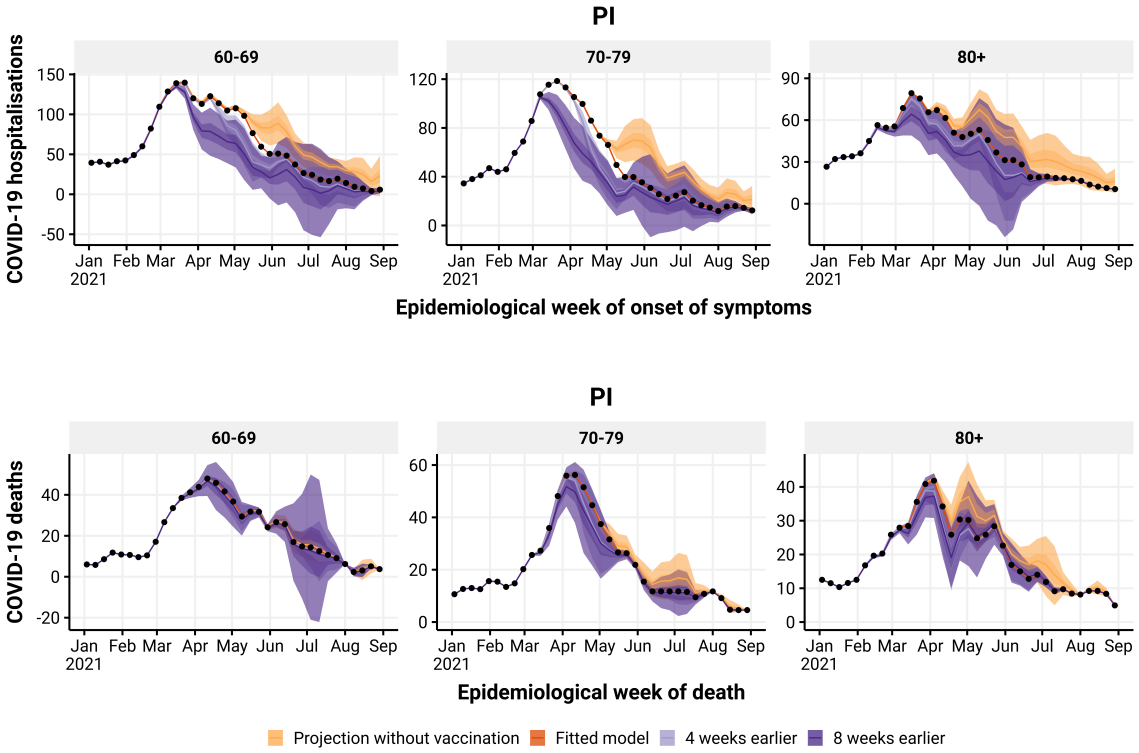

Figure D.30: Estimated number of hospitalisations (top) and deaths (bottom) by epidemiological week with the realized (orange), no vaccination (blue), 4 (green) and 8 (yellow) weeks earlier vaccination rollout, by age group (panels), in PI state. The observed number of hospitalisations and deaths are given by the black points.

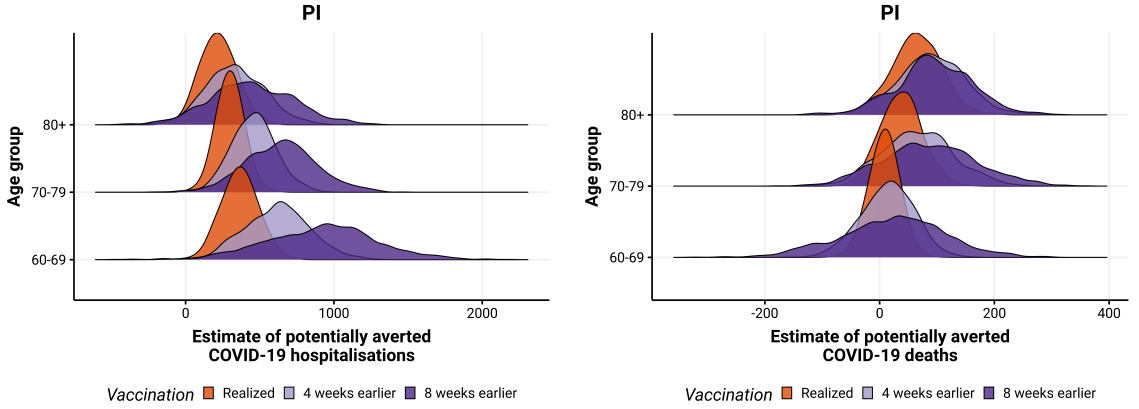

Figure D.31: Posterior distribution of hospitalisations (left) and deaths (right) potentially averted by vaccination between 2021-01-01 and 2021-08-29 by age group, with the realized (orange), 4 (blue) and 8 weeks earlier (green) vaccination rollout in PI state.

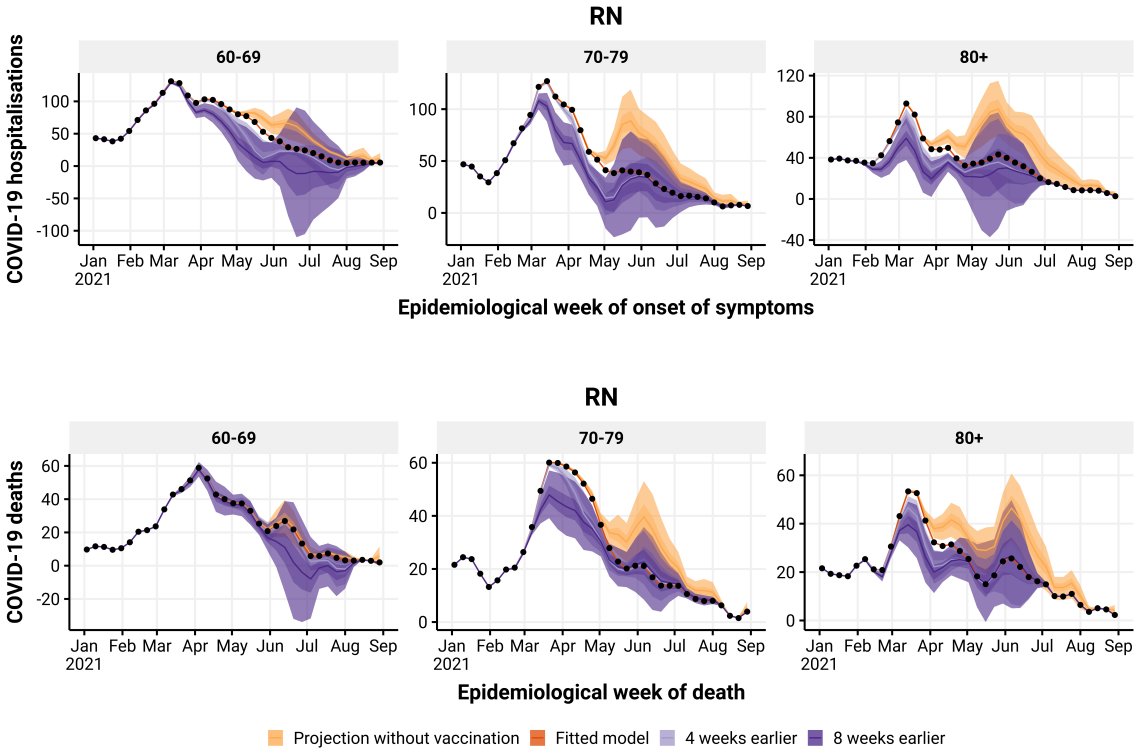

Figure D.32: Estimated number of hospitalisations (top) and deaths (bottom) by epidemiological week with the realized (orange), no vaccination (blue), 4 (green) and 8 (yellow) weeks earlier vaccination rollout, by age group (panels), in RN state. The observed number of hospitalisations and deaths are given by the black points.

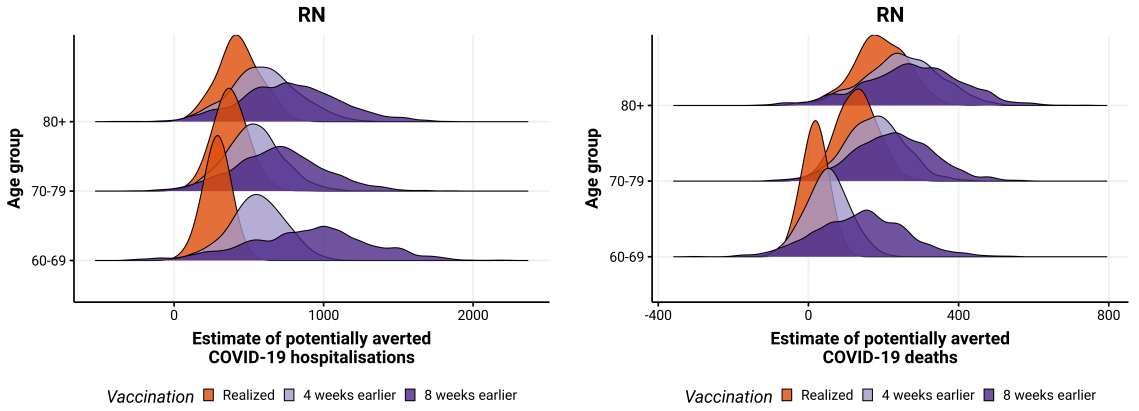

Figure D.33: Posterior distribution of hospitalisations (left) and deaths (right) potentially averted by vaccination between 2021-01-01 and 2021-08-29 by age group, with the realized (orange), 4 (blue) and 8 weeks earlier (green) vaccination rollout in RN state.

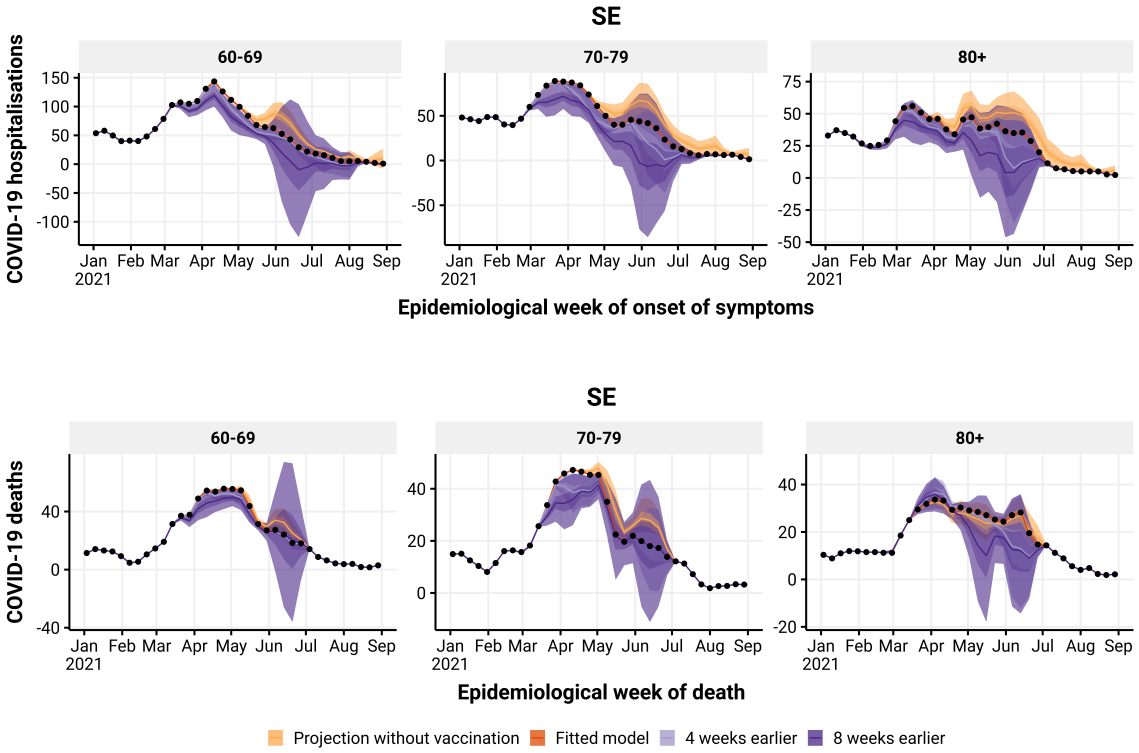

Figure D.34: Estimated number of hospitalisations (top) and deaths (bottom) by epidemiological week with the realized (orange), no vaccination (blue), 4 (green) and 8 (yellow) weeks earlier vaccination rollout, by age group (panels), in SE state. The observed number of hospitalisations and deaths are given by the black points.

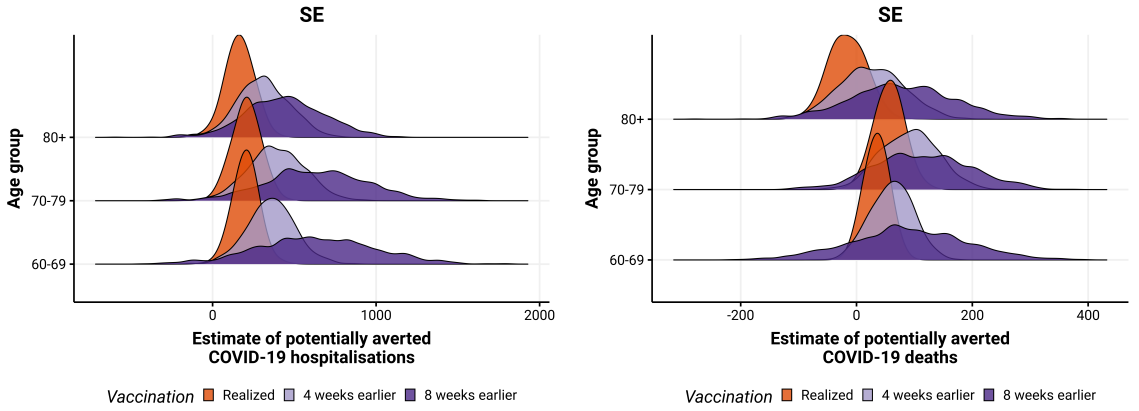

Figure D.35: Posterior distribution of hospitalisations (left) and deaths (right) potentially averted by vaccination between 2021-01-01 and 2021-08-29 by age group, with the realized (orange), 4 (blue) and 8 weeks earlier (green) vaccination rollout in SE state.

D.1.3 Southeast Region

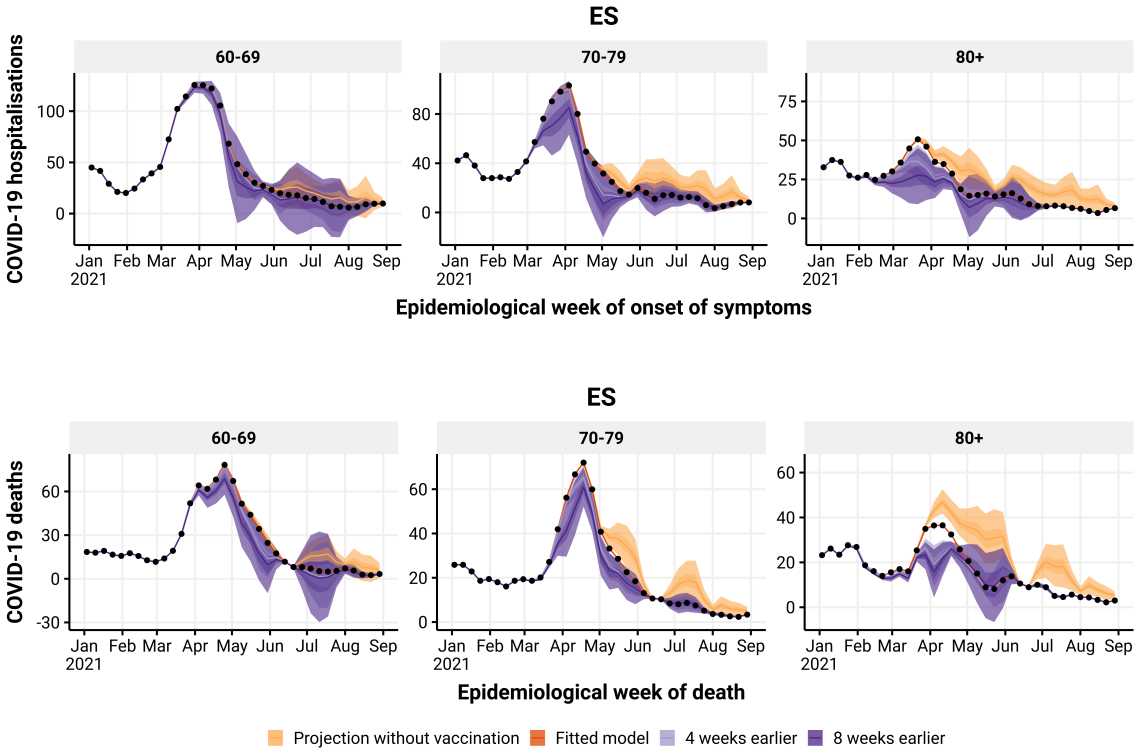

Figure D.36: Estimated number of hospitalisations (top) and deaths (bottom) by epidemiological week with the realized (orange), no vaccination (blue), 4 (green) and 8 (yellow) weeks earlier vaccination rollout, by age group (panels), in ES state. The observed number of hospitalisations and deaths are given by the black points.

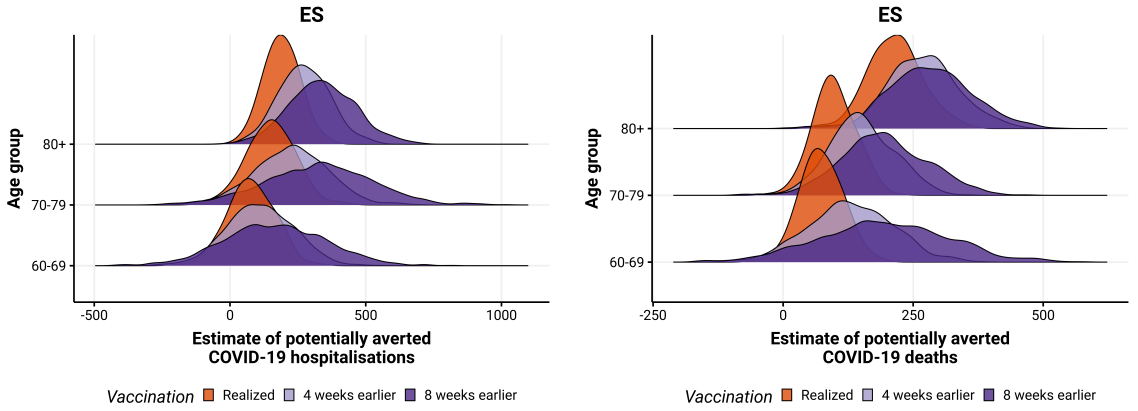

Figure D.37: Posterior distribution of hospitalisations (left) and deaths (right) potentially averted by vaccination between 2021-01-01 and 2021-08-29 by age group, with the realized (orange), 4 (blue) and 8 weeks earlier (green) vaccination rollout in ES state.

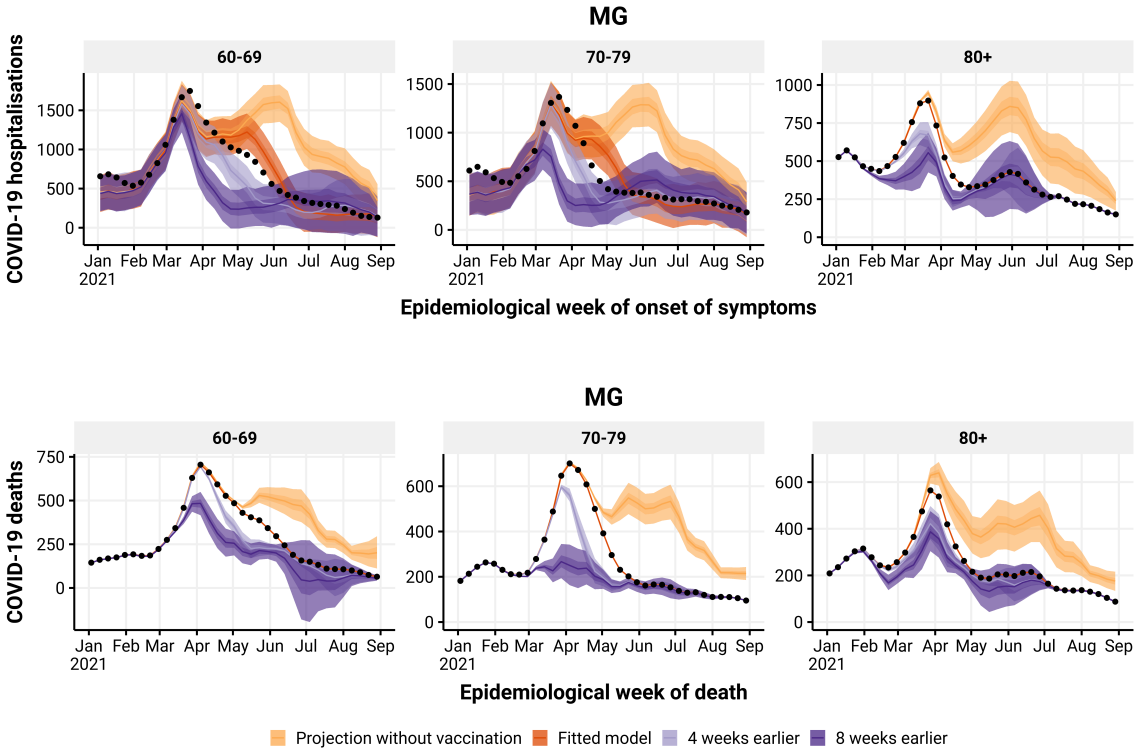

Figure D.38: Estimated number of hospitalisations (top) and deaths (bottom) by epidemiological week with the realized (orange), no vaccination (blue), 4 (green) and 8 (yellow) weeks earlier vaccination rollout, by age group (panels), in MG state. The observed number of hospitalisations and deaths are given by the black points.

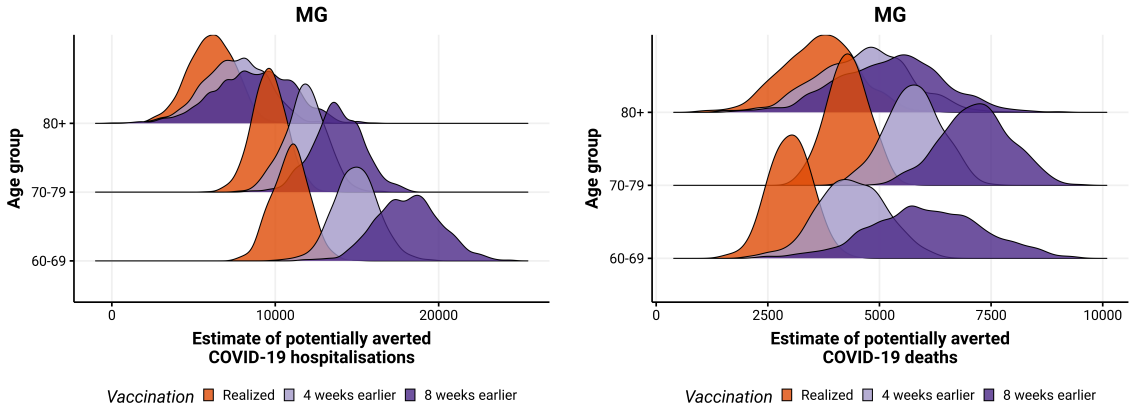

Figure D.39: Posterior distribution of hospitalisations (left) and deaths (right) potentially averted by vaccination between 2021-01-01 and 2021-08-29 by age group, with the realized (orange), 4 (blue) and 8 weeks earlier (green) vaccination rollout in MG state.

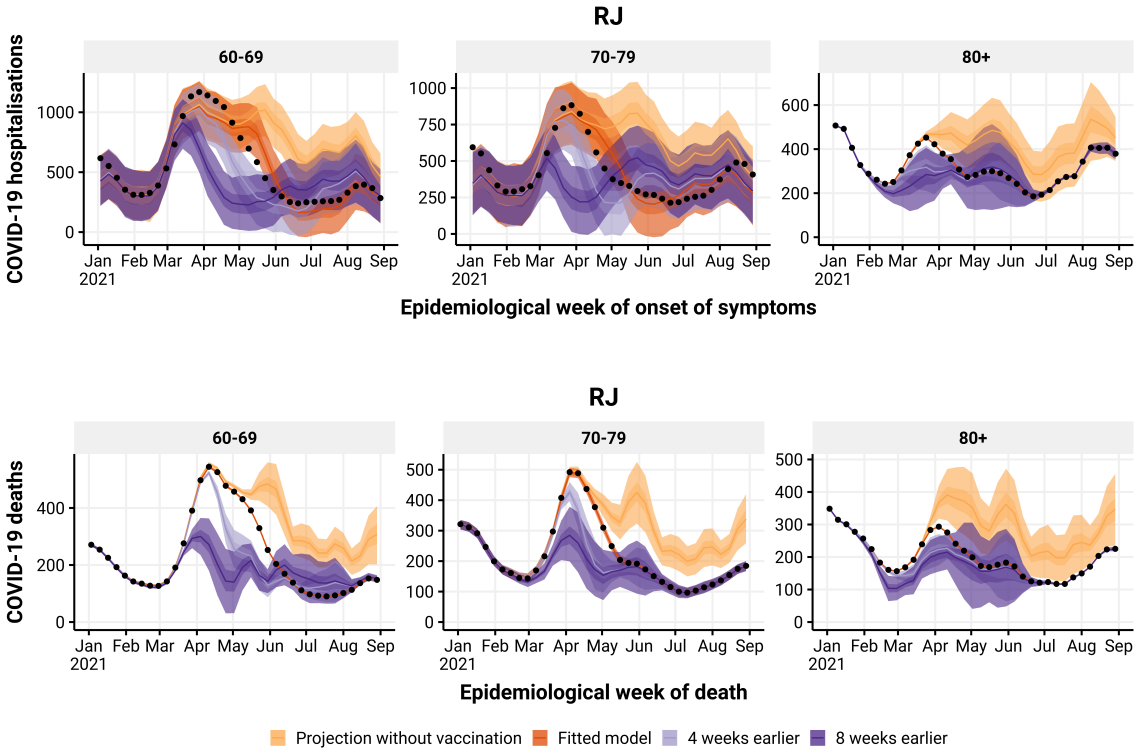

Figure D.40: Estimated number of hospitalisations (top) and deaths (bottom) by epidemiological week with the realized (orange), no vaccination (blue), 4 (green) and 8 (yellow) weeks earlier vaccination rollout, by age group (panels), in RJ state. The observed number of hospitalisations and deaths are given by the black points.

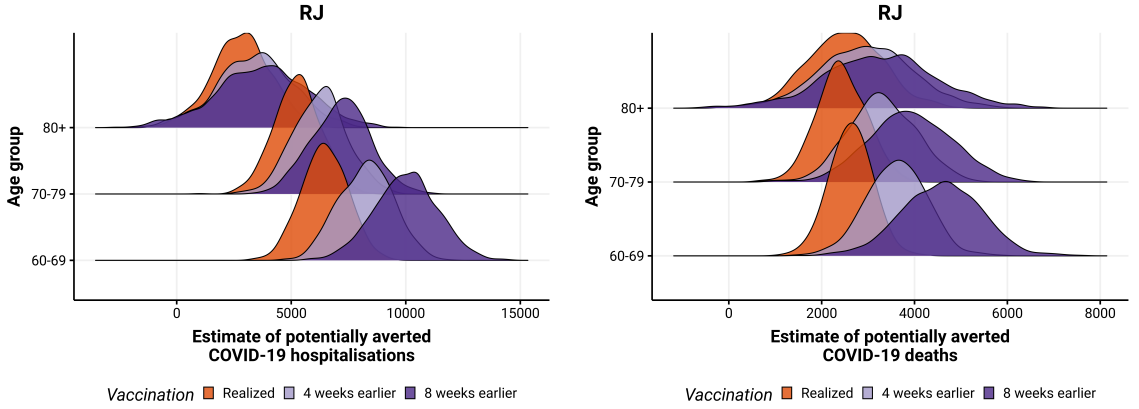

Figure D.41: Posterior distribution of hospitalisations (left) and deaths (right) potentially averted by vaccination between 2021-01-01 and 2021-08-29 by age group, with the realized (orange), 4 (blue) and 8 weeks earlier (green) vaccination rollout in RJ state.

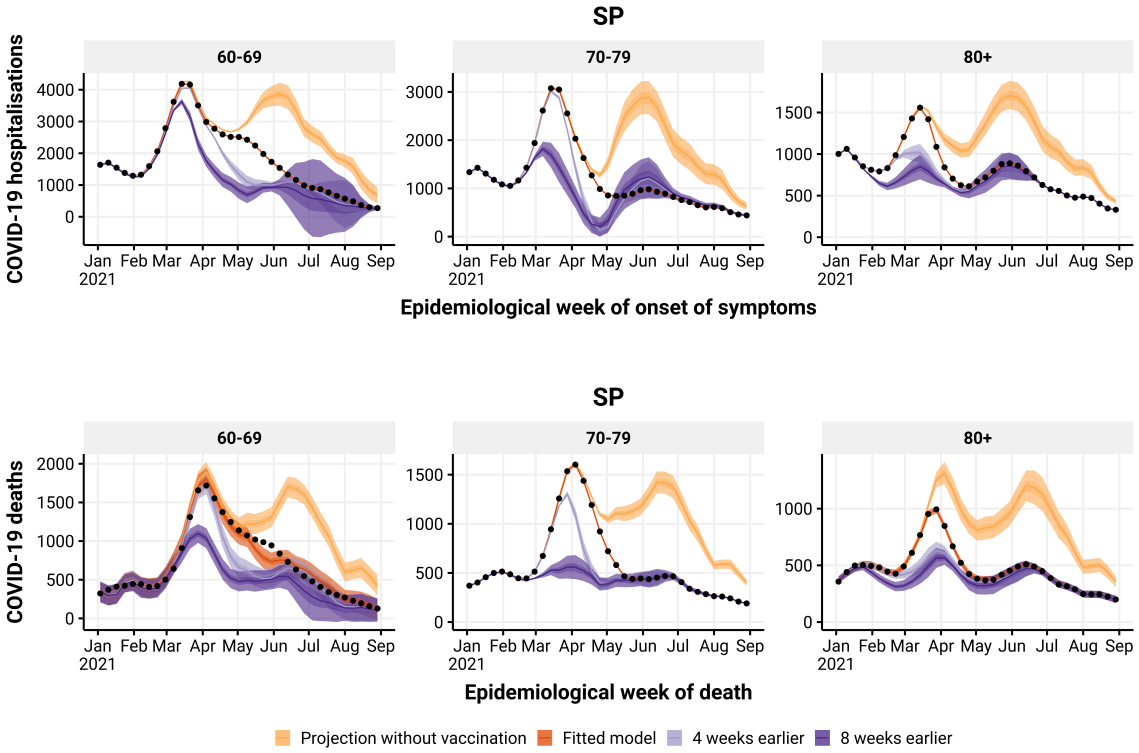

Figure D.42: Estimated number of hospitalisations (top) and deaths (bottom) by epidemiological week with the realized (orange), no vaccination (blue), 4 (green) and 8 (yellow) weeks earlier vaccination rollout, by age group (panels), in SP state. The observed number of hospitalisations and deaths are given by the black points.

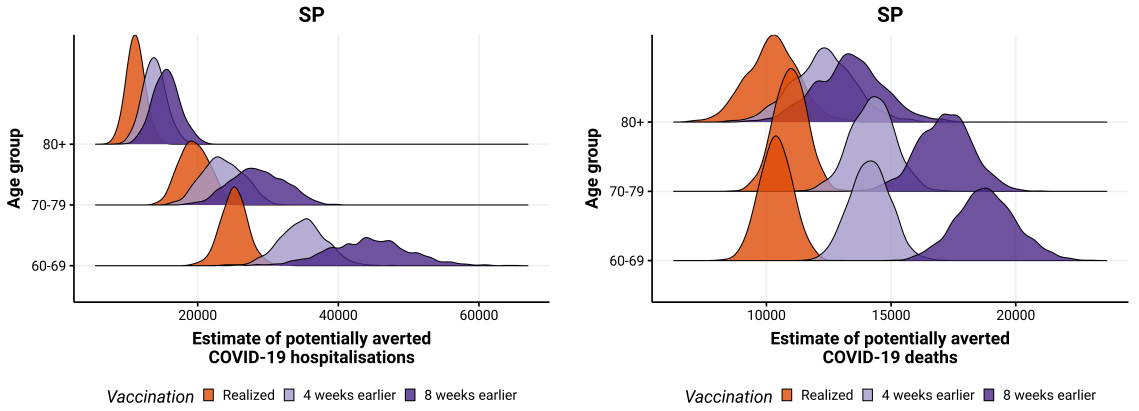

Figure D.43: Posterior distribution of hospitalisations (left) and deaths (right) potentially averted by vaccination between 2021-01-01 and 2021-08-29 by age group, with the realized (orange), 4 (blue) and 8 weeks earlier (green) vaccination rollout in SP state.

D.1.4 South Region

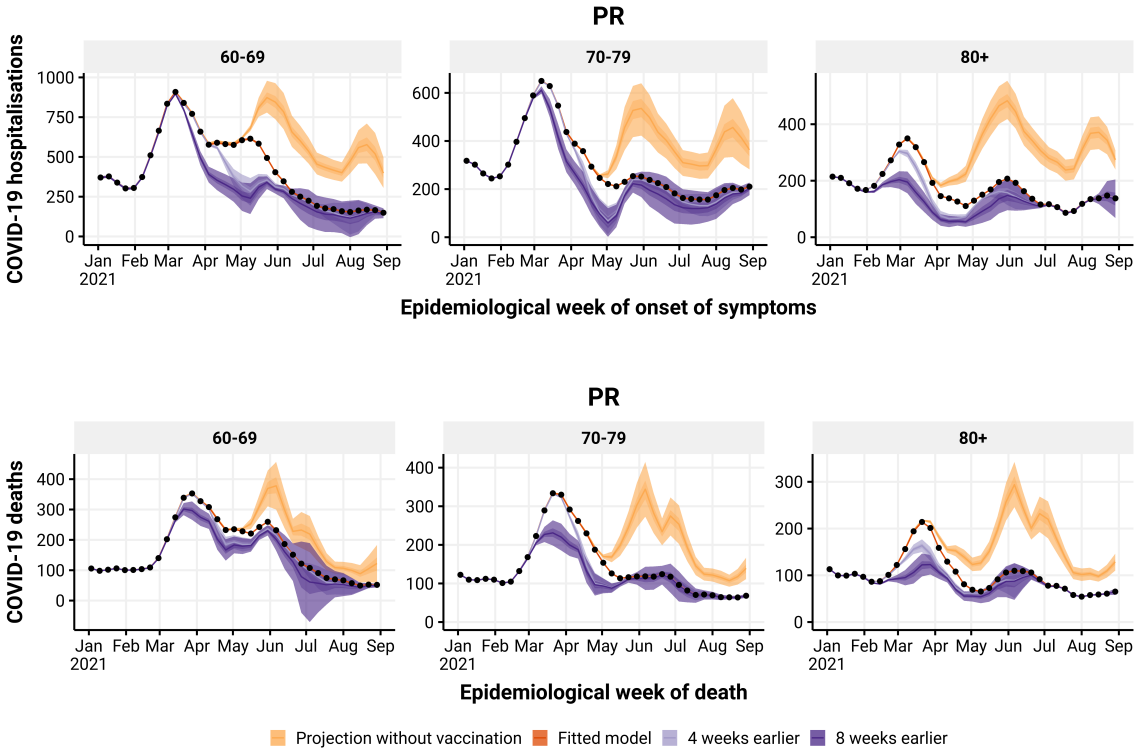

Figure D.44: Estimated number of hospitalisations (top) and deaths (bottom) by epidemiological week with the realized (orange), no vaccination (blue), 4 (green) and 8 (yellow) weeks earlier vaccination rollout, by age group (panels), in PR state. The observed number of hospitalisations and deaths are given by the black points.

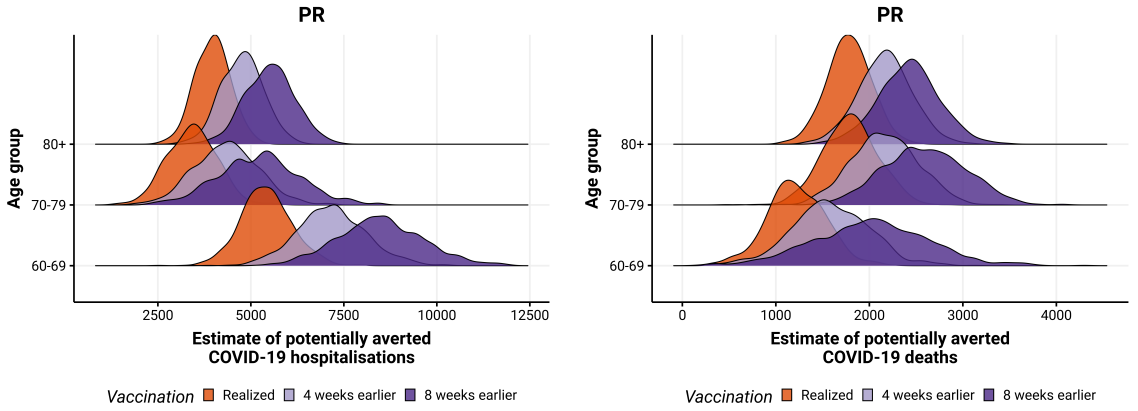

Figure D.45: Posterior distribution of hospitalisations (left) and deaths (right) potentially averted by vaccination between 2021-01-01 and 2021-08-29 by age group, with the realized (orange), 4 (blue) and 8 weeks earlier (green) vaccination rollout in PR state.

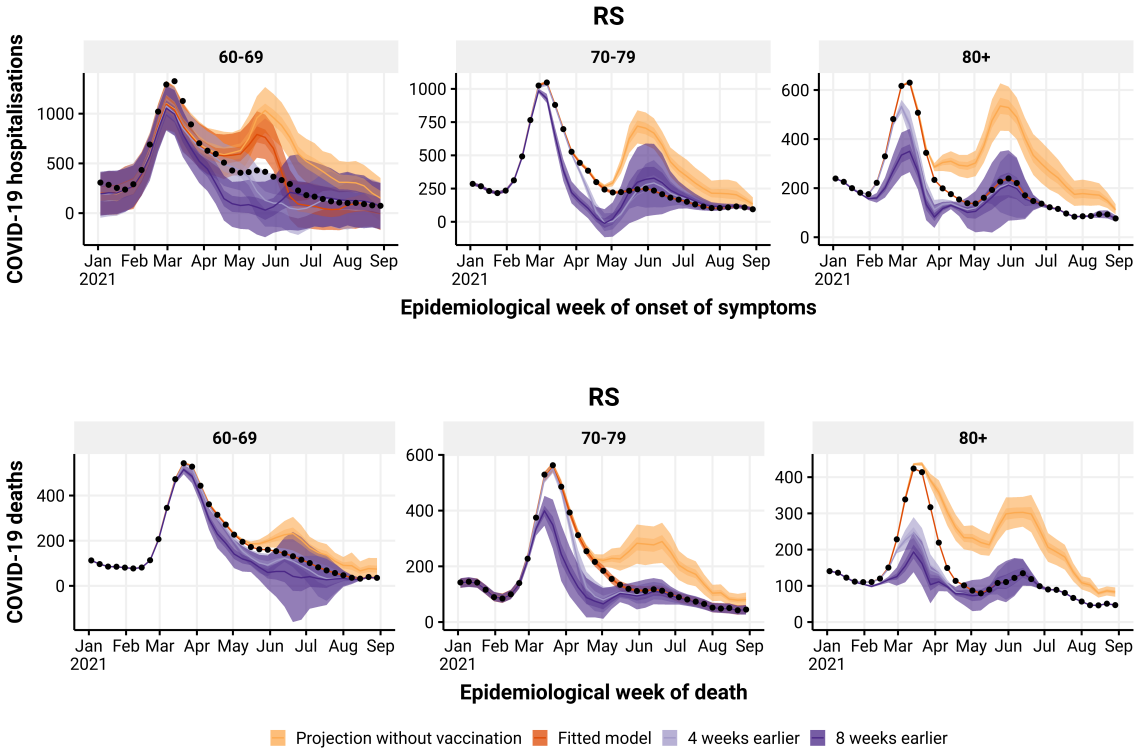

Figure D.46: Estimated number of hospitalisations (top) and deaths (bottom) by epidemiological week with the realized (orange), no vaccination (blue), 4 (green) and 8 (yellow) weeks earlier vaccination rollout, by age group (panels), in RS state. The observed number of hospitalisations and deaths are given by the black points.

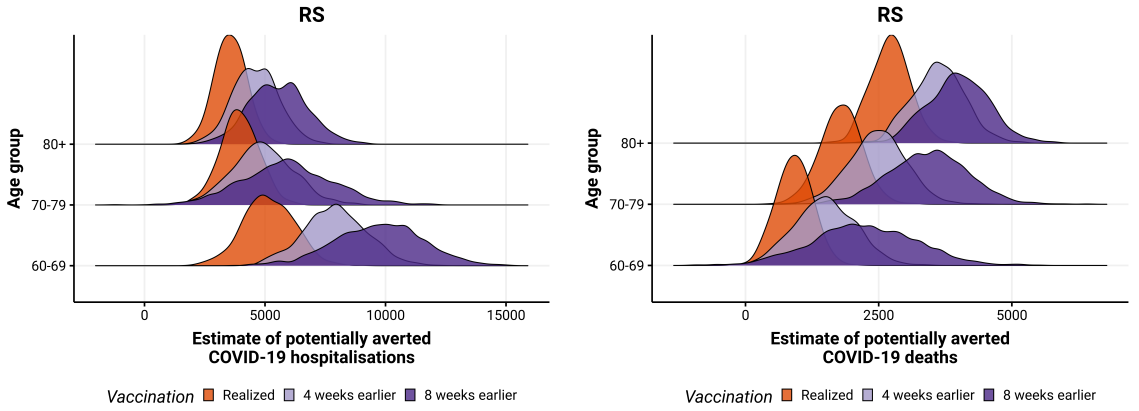

Figure D.47: Posterior distribution of hospitalisations (left) and deaths (right) potentially averted by vaccination between 2021-01-01 and 2021-08-29 by age group, with the realized (orange), 4 (blue) and 8 weeks earlier (green) vaccination rollout in RS state.

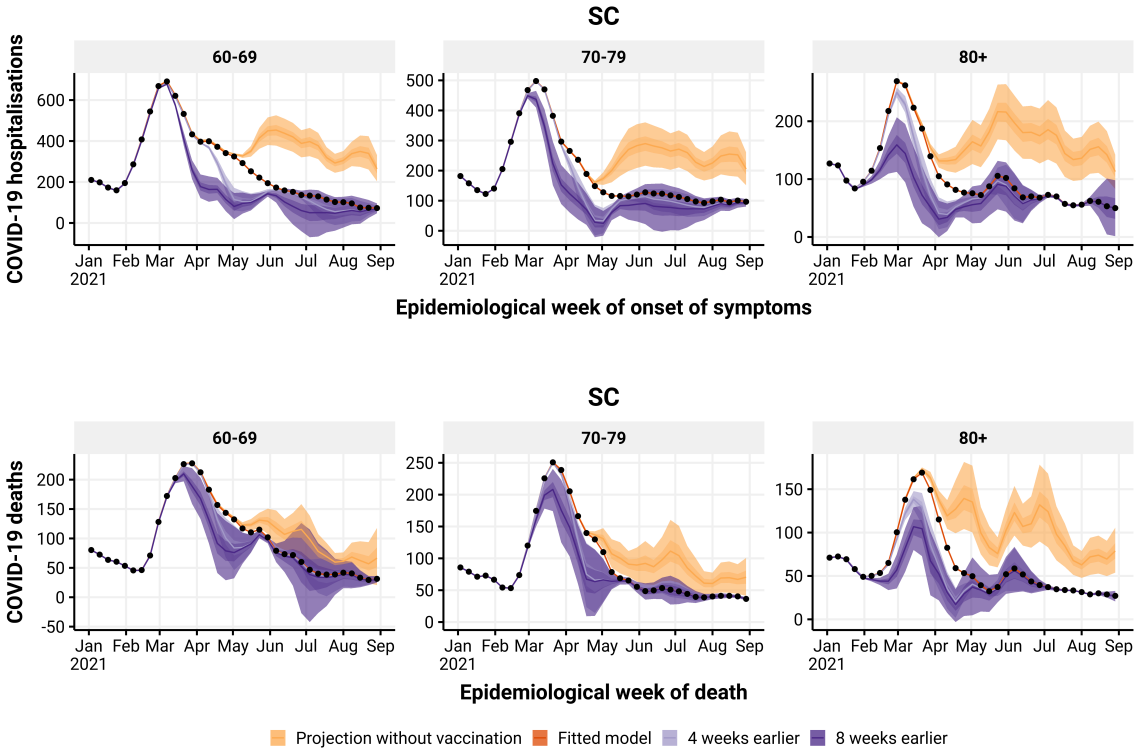

Figure D.48: Estimated number of hospitalisations (top) and deaths (bottom) by epidemiological week with the realized (orange), no vaccination (blue), 4 (green) and 8 (yellow) weeks earlier vaccination rollout, by age group (panels), in SC state. The observed number of hospitalisations and deaths are given by the black points.

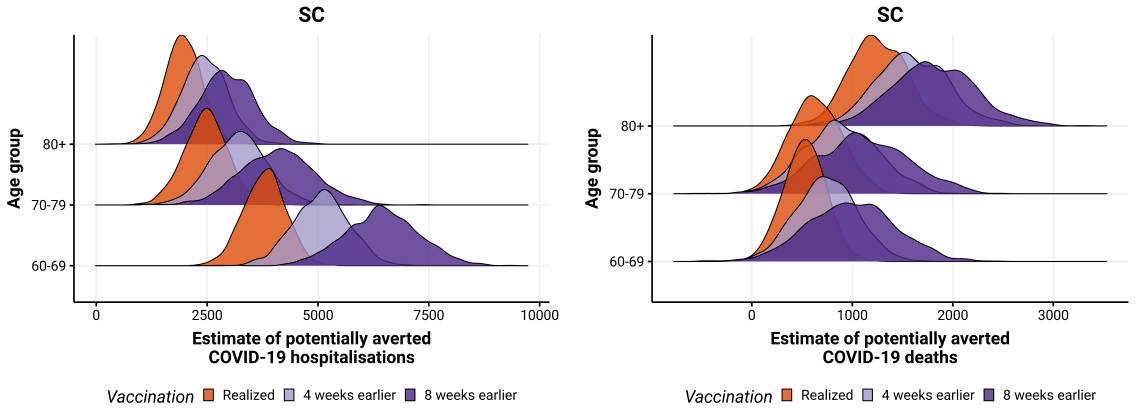

Figure D.49: Posterior distribution of hospitalisations (left) and deaths (right) potentially averted by vaccination between 2021-01-01 and 2021-08-29 by age group, with the realized (orange), 4 (blue) and 8 weeks earlier (green) vaccination rollout in SC state.

D.1.5 Center-west Region

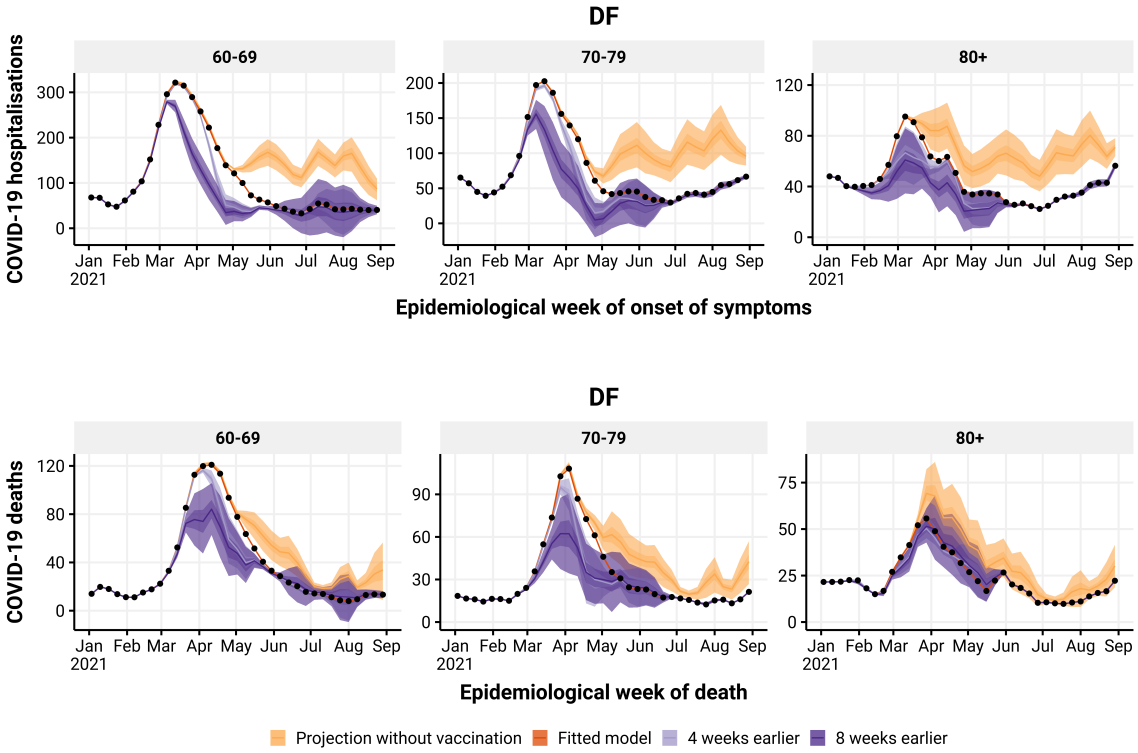

Figure D.50: Estimated number of hospitalisations (top) and deaths (bottom) by epidemiological week with the realized (orange), no vaccination (blue), 4 (green) and 8 (yellow) weeks earlier vaccination rollout, by age group (panels), in DF state. The observed number of hospitalisations and deaths are given by the black points.

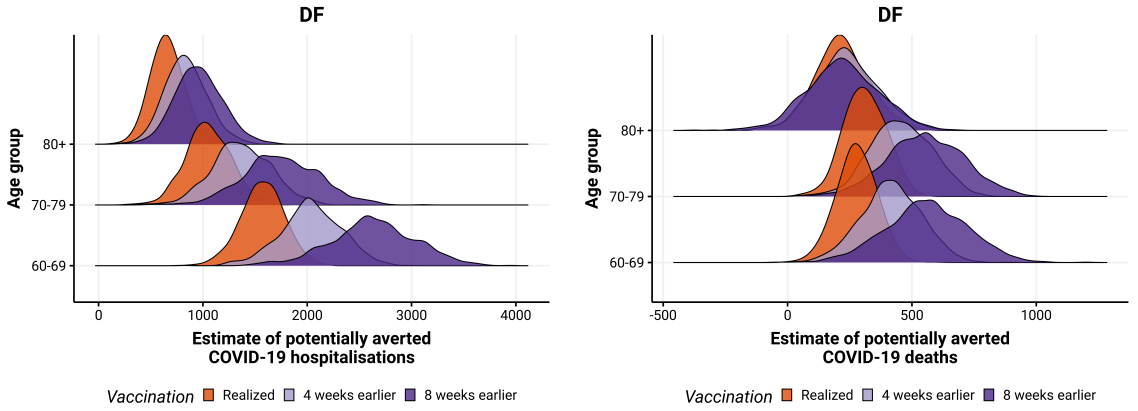

Figure D.51: Posterior distribution of hospitalisations (left) and deaths (right) potentially averted by vaccination between 2021-01-01 and 2021-08-29 by age group, with the realized (orange), 4 (blue) and 8 weeks earlier (green) vaccination rollout in DF state.

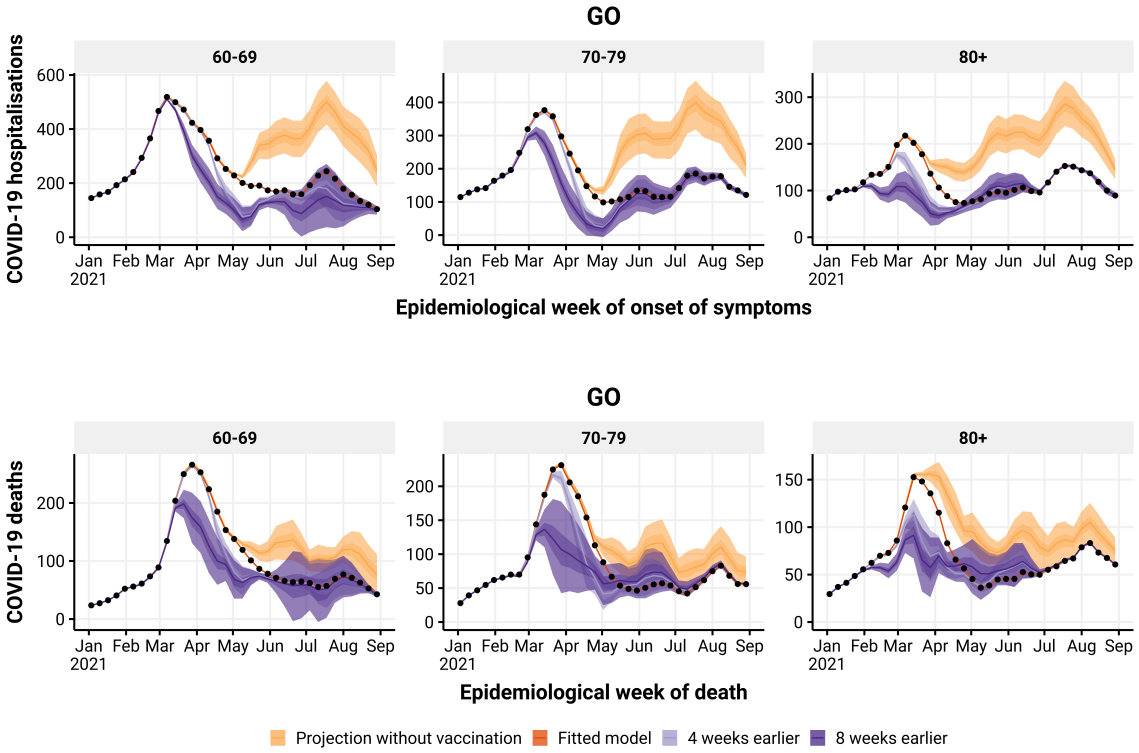

Figure D.52: Estimated number of hospitalisations (top) and deaths (bottom) by epidemiological week with the realized (orange), no vaccination (blue), 4 (green) and 8 (yellow) weeks earlier vaccination rollout, by age group (panels), in GO state. The observed number of hospitalisations and deaths are given by the black points.

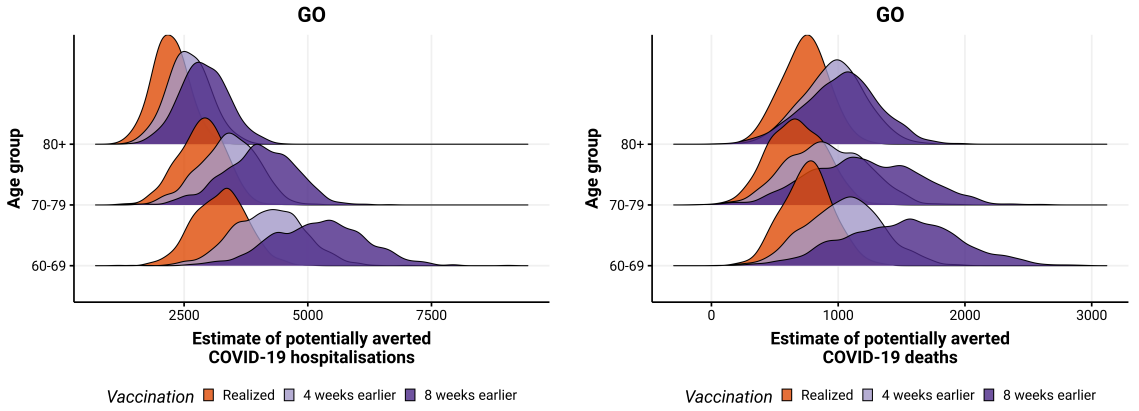

Figure D.53: Posterior distribution of hospitalisations (left) and deaths (right) potentially averted by vaccination between 2021-01-01 and 2021-08-29 by age group, with the realized (orange), 4 (blue) and 8 weeks earlier (green) vaccination rollout in GO state.

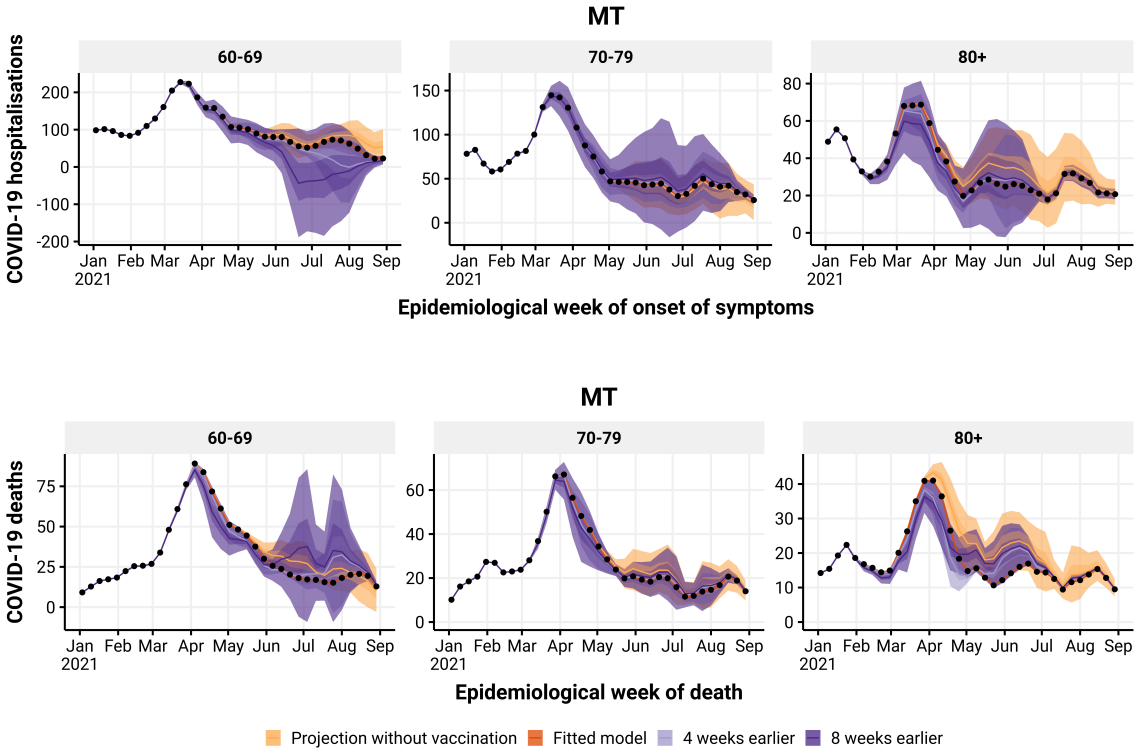

Figure D.54: Estimated number of hospitalisations (top) and deaths (bottom) by epidemiological week with the realized (orange), no vaccination (blue), 4 (green) and 8 (yellow) weeks earlier vaccination rollout, by age group (panels), in MT state. The observed number of hospitalisations and deaths are given by the black points.

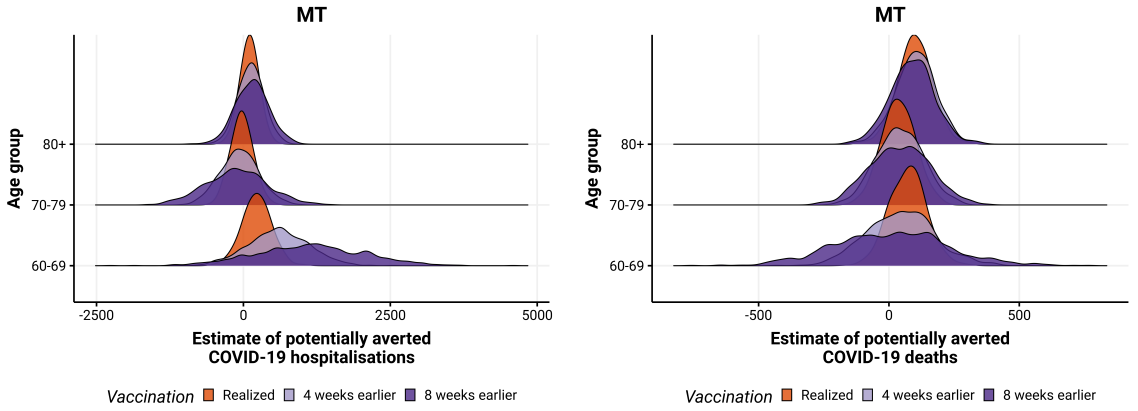

Figure D.55: Posterior distribution of hospitalisations (left) and deaths (right) potentially averted by vaccination between 2021-01-01 and 2021-08-29 by age group, with the realized (orange), 4 (blue) and 8 weeks earlier (green) vaccination rollout in MT state.

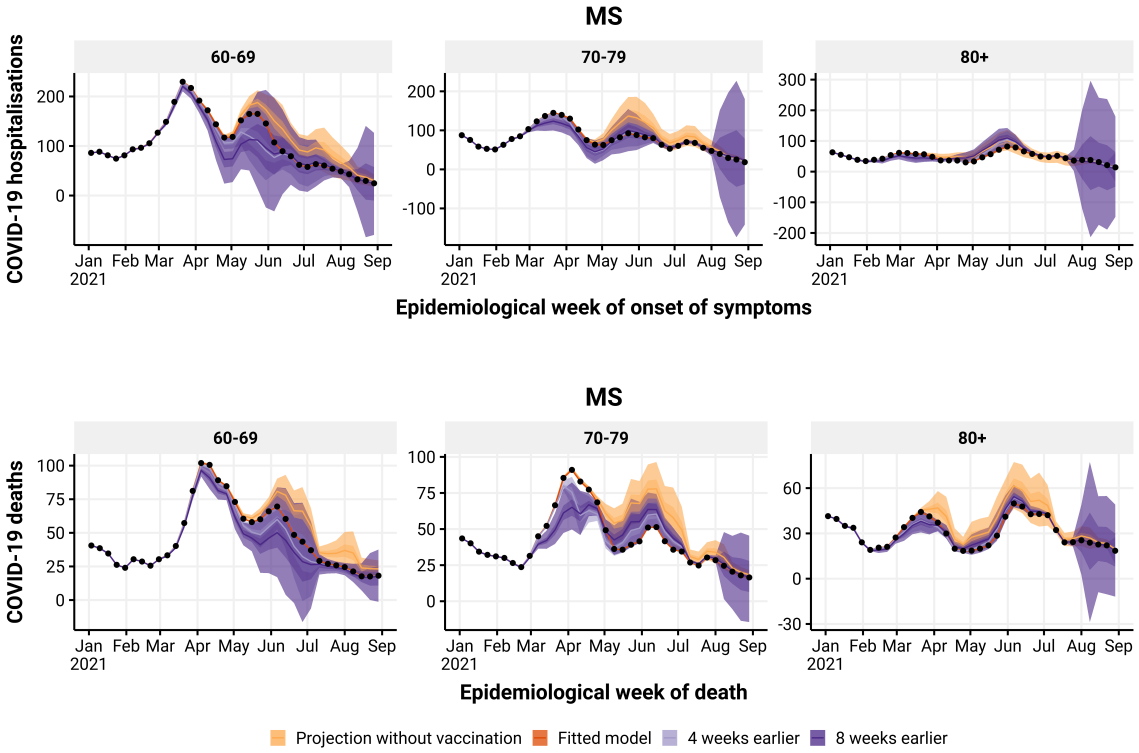

Figure D.56: Estimated number of hospitalisations (top) and deaths (bottom) by epidemiological week with the realized (orange), no vaccination (blue), 4 (green) and 8 (yellow) weeks earlier vaccination rollout, by age group (panels), in MS state. The observed number of hospitalisations and deaths are given by the black points.

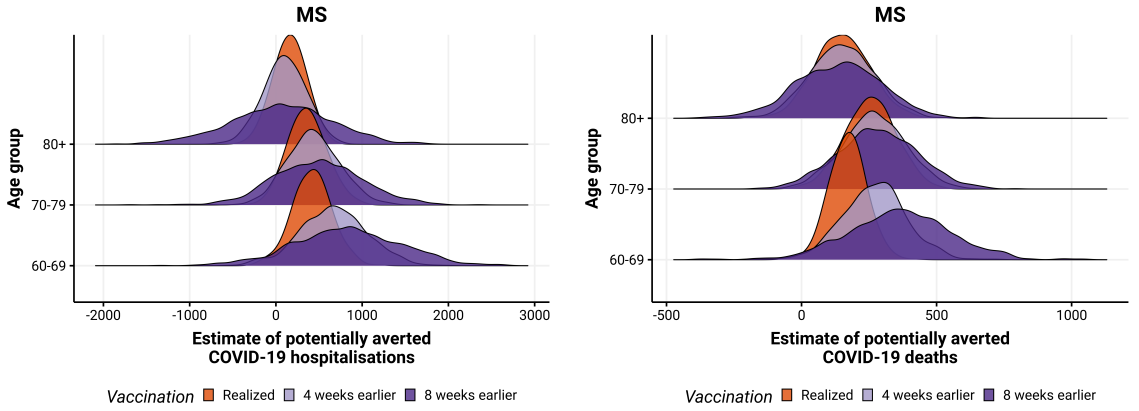

Figure D.57: Posterior distribution of hospitalisations (left) and deaths (right) potentially averted by vaccination between 2021-01-01 and 2021-08-29 by age group, with the realized (orange), 4 (blue) and 8 weeks earlier (green) vaccination rollout in MS state.

Bibliography

[1] Chaolin Huang et al. "Clinical features of patients infected with 2019 novel coronavirus in Wuhan, China". In: *The Lancet* 395.10223 (2020), pp. 497–506. ISSN: 1474547X. DOI: 10.1016/S0140-6736(20)30183-5 (cit. on p. 1).

[2] World Health Organization. *WHO Director-General's opening remarks at the media briefing on COVID-19 - 11 March 2020*. 2020. URL: https://www.who.int/director-general/speeches/detail/who-director-general-s-opening-remarks-at-the-media-briefing-on-covid-19---11-march-2020 (visited on 04/20/2022) (cit. on p. 1).

[3] Hannah Ritchie et al. *Coronavirus Pandemic (COVID-19)*. 2022. URL: https://ourworldindata.org/coronavirus (visited on 04/20/2022) (cit. on p. 1).

[4] Roujian Lu et al. "Genomic characterisation and epidemiology of 2019 novel coronavirus: implications for virus origins and receptor binding". In: *The Lancet* 395.10224 (2020). Publisher: Elsevier Ltd, pp. 565–574. ISSN: 1474547X. DOI: 10.1016/S0140-6736(20)30251-8. URL: http://dx.doi.org/10.1016/S0140-6736(20)30251-8 (cit. on p. 1).

[5] J. S.M. Peiris, Y. Guan, and K. Y. Yuen. "Severe acute respiratory syndrome". In: *Nature Medicine* 10.12S (2004), S88–S97. ISSN: 1546170X. DOI: 10.1038/nm1143 (cit. on p. 1).

[6] Alimuddin Zumla, David S. Hui, and Stanley Perlman. "Middle East respiratory syndrome". In: *The Lancet* 386.9997 (2015). Publisher: Elsevier Ltd, pp. 995–1007. ISSN: 1474547X. DOI: 10.1016/S0140-6736(15)60454-8. URL: http://dx.doi.org/10.1016/S0140-6736(15)60454-8 (cit. on p. 1).

[7] Ben Hu et al. "Characteristics of SARS-CoV-2 and COVID-19". In: *Nature Reviews Microbiology* 19.3 (2021). Publisher: Springer US, pp. 141–154. ISSN: 17401534. DOI: 10.1038/s41579-020-00459-7 (cit. on p. 1).

[8] Yuefei Jin et al. "Virology, epidemiology, pathogenesis, and control of covid-19". In: *Viruses* 12.4 (2020), pp. 1–17. ISSN: 19994915. DOI: 10.3390/v12040372 (cit. on p. 1).

[9] Barak Mizrahi et al. "Longitudinal symptom dynamics of COVID-19 infection". In: *Nature Communications* 11.1 (2020). Publisher: Springer US, pp. 1–10. ISSN: 20411723. DOI: 10.1038/s41467-020-20053-y. URL: http://dx.doi.org/10.1038/s41467-020-20053-y (cit. on p. 1).

[10] Koichi Yuki, Miho Fujiogi, and Sophia Koutsogiannaki. "COVID-19 pathophysiology: A review". In: *Clinical Immunology* 215.April (2020). ISSN: 15217035. DOI: 10.1016/j.clim.2020.108427 (cit. on p. 1).

[11] Jantien A. Backer, Don Klinkenberg, and Jacco Wallinga. "Incubation period of 2019 novel coronavirus (2019- nCoV) infections among travellers from Wuhan, China, 20 28 January 2020". In: *Eurosurveillance* 25.5 (2020). Publisher: European Centre for Disease Control and Prevention (ECDC), pp. 1–6. ISSN: 15607917. DOI: 10.2807/1560-7917.ES.2020.25.5.2000062. URL: http://dx.doi.org/10.2807/1560-7917.ES.2020.25.5.2000062 (cit. on p. 2).

[12] Tadesse Tolossa et al. "Time to recovery from COVID-19 and its predictors among patients admitted to treatment center of Wollega University Referral Hospital (WURH), Western Ethiopia: Survival analysis of retrospective cohort study". In: *PLoS ONE* 16.6 June (2021). ISBN: 1111111111, pp. 1–12. ISSN: 19326203. DOI: 10.1371/journal.pone.0252389. URL: http://dx.doi.org/10.1371/journal.pone.0252389 (cit. on p. 2).

[13] Harry Crook et al. "Long covid - Mechanisms, risk factors, and management". In: *The BMJ* 374 (2021), pp. 1–18. ISSN: 17561833. DOI: 10.1136/bmj.n1648 (cit. on p. 2).

[14] Pratha Sah et al. "Asymptomatic SARS-CoV-2 infection: A systematic review and meta-analysis". In: *Proceedings of the National Academy of Sciences of the United States of America* 118.34 (2021), pp. 1–12. ISSN: 10916490. DOI: 10.1073/pnas.2109229118 (cit. on p. 2).

[15] Zhaohai Zheng et al. "Risk factors of critical & mortal COVID-19 cases: A systematic literature review and meta-analysis". In: *Journal of Infection* 81.2 (2020). Publisher: Elsevier Ltd, e16–e25. ISSN: 15322742. DOI: 10.1016/j.jinf.2020.04.021 (cit. on p. 2).

[16] Du Juan. "Wuhan wet market closes amid pneumonia outbreak". In: (2020). URL: https://www.chinadaily.com.cn/a/202001/01/WS5e0c6a49a310cf3e3html (cit. on p. 2).

[17] Barda. "Vietnam: Two cases of 2019-nCoV confirmed January 23". In: *Barda* (2020). URL: https://crisis24.garda.com/alerts/2020/01/vietnam-two-cases-of-2019-ncov-confirmed-january-23 (cit. on p. 2).

[18] Zaheer Allam. *Surveying the Covid-19 Pandemic and its Implications: Urban Health, Data Technology and Political Economy*. Elsevier, 2020. ISBN: 978-0-12-824313-8. DOI: 10.1016/C2020-0-01743-3. URL: https://linkinghub.elsevier.com/retrieve/pii/C20200017433 (cit. on pp. 2, 4).

[19] Jose Jimenez et al. "What Were the Historical Reasons for the Resistance to Recognizing Airborne Transmission during the COVID-19 Pandemic?" In: *SSRN Electronic Journal* (2021). ISBN: 1477529688306. ISSN: 1556-5068. DOI: 10.2139/ssrn.3904176. URL: https://www.ssrn.com/abstract=3904176 (cit. on pp. 2, 3).

[20] World Health Organization. *Coronavirus disease 2019 (COVID-19) Situation Report - 66*. Tech. rep. Publication Title: World Health Organization. 2020 (cit. on p. 3).

[21] Anthea L. Katelaris et al. "Epidemiologic Evidence for Airborne Transmission of SARS-CoV-2 during Church Singing, Australia, 2020". In: *Emerging infectious diseases* 27.6 (2021), pp. 1677–1680. ISSN: 10806059. DOI: 10.3201/eid2706.210465 (cit. on p. 3).

[22] Nick Eichler et al. "Transmission of severe acute respiratory syndrome coronavirus 2 during border quarantine and air travel, New Zealand (Aotearoa)". In: *Emerging Infectious Diseases* 27.5 (2021), pp. 1274–1278. ISSN: 10806059. DOI: 10.3201/eid2705.210514 (cit. on p. 3).

[23] Shuk Ching Wong et al. "Transmission of Omicron (B.1.1.529) - SARS-CoV-2 Variant of Concern in a designated quarantine hotel for travelers: a challenge of elimination strategy of COVID-19". In: *The Lancet Regional Health - Western Pacific* 18.December 2021 (2022). Publisher: Elsevier Ltd, p. 100360. ISSN: 26666065. DOI: 10.1016/j.lanwpc.2021.100360. URL: https://doi.org/10.1016/j.lanwpc.2021.100360 (cit. on p. 3).

[24] Andrew Fox-Lewis et al. "Airborne Transmission of SARS-CoV-2 Delta Variant within Tightly Monitored Isolation Facility, New Zealand (Aotearoa)".

In: *Emerging Infectious Diseases* 28.3 (2022), pp. 501–509. ISSN: 10806059. DOI: 10.3201/eid2803.212318 (cit. on p. 3).

[25] Trisha Greenhalgh et al. "Ten scientific reasons in support of airborne transmission of SARS-CoV-2". In: *The Lancet* 397.10285 (2021), pp. 1603–1605. ISSN: 1474547X. DOI: 10.1016/S0140-6736(21)00869-2 (cit. on p. 3).

[26] Chia C. Wang et al. "Airborne transmission of respiratory viruses". In: *Science* 373.6558 (2021). ISSN: 10959203. DOI: 10.1126/science.abd9149 (cit. on p. 3).

[27] Dyani Lewis. "Why the WHO took two years to say COVID is airborne." In: *Nature* 604.7904 (2022), pp. 26–31. ISSN: 1476-4687. DOI: 10.1038/d41586-022-00925-7. URL: http://www.ncbi.nlm.nih.gov/pubmed/35388203 (cit. on p. 3).

[28] Siobain Duffy, Laura A. Shackelton, and Edward C. Holmes. "Rates of evolutionary change in viruses: Patterns and determinants". In: *Nature Reviews Genetics* 9.4 (2008), pp. 267–276. ISSN: 14710056. DOI: 10.1038/nrg2323 (cit. on p. 3).

[29] World Health Organization. *Tracking SARS-CoV-2 variants*. 2020. URL: https://www.who.int/en/activities/tracking-SARS-CoV-2-variants/ (cit. on p. 3).

[30] Erik Volz et al. "Assessing transmissibility of SARS-CoV-2 lineage B.1.1.7 in England". In: *Nature* 593.7858 (2021), pp. 266–269. ISSN: 14764687. DOI: 10.1038/s41586-021-03470-x (cit. on pp. 3, 11).

[31] Nicholas G. Davies et al. "Increased mortality in community-tested cases of SARS-CoV-2 lineage B.1.1.7". In: *Nature* 593.7858 (2021), pp. 270–274. ISSN: 14764687. DOI: 10.1038/s41586-021-03426-1 (cit. on p. 3).

[32] Xiaoying Shen et al. "SARS-CoV-2 variant B.1.1.7 is susceptible to neutralizing antibodies elicited by ancestral spike vaccines". In: *Cell Host and Microbe* 29.4 (2021), 529–539.e3. ISSN: 19346069. DOI: 10.1016/j.chom.2021.03.002 (cit. on p. 3).

[33] Houriiyah Tegally et al. "Detection of a SARS-CoV-2 variant of concern in South Africa". In: *Nature* 592.7854 (2021). Publisher: Springer US, pp. 438–443. ISSN: 14764687. DOI: 10.1038/s41586-021-03402-9. URL: http://dx.doi.org/10.1038/s41586-021-03402-9 (cit. on p. 4).

[34] Bénédicte Roquebert et al. "The SARS-CoV-2 B.1.351 lineage (VOC Beta) is outgrowing the B.1.1.7 lineage (VOC Alpha) in some French regions in April 2021". In: *Eurosurveillance* 26.23 (2021). Publisher: European Centre for Disease Prevention and Control (ECDC), pp. 1–6. ISSN: 15607917. DOI: 10.2807/1560-7917.ES.2021.26.23.2100447. URL: http://dx.doi.org/10.2807/1560-7917.ES.2021.26.23.2100447 (cit. on p. 4).

[35] Finlay Campbell et al. "Increased transmissibility and global spread of SARSCoV- 2 variants of concern as at June 2021". In: *Eurosurveillance* 26.24 (2021). Publisher: European Centre for Disease Prevention and Control (ECDC), pp. 1–6. ISSN: 15607917. DOI: 10.2807/1560-7917.ES.2021.26.24.2100509. URL: http://dx.doi.org/10.2807/1560-7917.ES.2021.26.24.2100509 (cit. on p. 4).

[36] Kaiming Tao et al. "The biological and clinical significance of emerging SARS-CoV-2 variants". In: *Nature Reviews Genetics* 22.12 (2021). Publisher: Springer US ISBN: 0123456789, pp. 757–773. ISSN: 14710064. DOI: 10.1038/s41576-021-00408-x (cit. on p. 4).

[37] Ester C. Sabino et al. "Resurgence of COVID-19 in Manaus, Brazil, despite high seroprevalence". In: *The Lancet* 397.10273 (2021), pp. 452–455. ISSN: 1474547X. DOI: 10.1016/S0140-6736(21)00183-5 (cit. on pp. 4, 6, 52, 53, 89, 90).

[38] Renato Mendes Coutinho et al. "Model-based estimation of transmissibility and reinfection of SARS-CoV-2 P.1 variant". In: *Communications Medicine* 1.1 (2021). Publisher: Springer US, pp. 1–8. DOI: 10.1038/s43856-021-00048-6 (cit. on pp. 4, 6, 11, 22, 37, 40, 90).

[39] Nuno R. Faria et al. "Genomics and epidemiology of the P.1 SARS-CoV-2 lineage in Manaus, Brazil". In: *Science* 372.6544 (May 2021), pp. 815–821. ISSN: 0036-8075. DOI: 10.1126/science.abh2644. URL: https://www.science.org/doi/10.1126/science.abh2644 (cit. on pp. 4, 11).

[40] Felipe Gomes Naveca et al. "COVID-19 in Amazonas, Brazil, was driven by the persistence of endemic lineages and P.1 emergence". In: *Nature Medicine* 27.7 (2021). Publisher: Springer US ISBN: 4159102101378, pp. 1230–1238. ISSN: 1546170X. DOI: 10.1038/s41591-021-01378-7. URL: http:

//dx.doi.org/10.1038/s41591-021-01378-7 (cit. on pp. 4, 11, 90, 94).

[41] Carlos A. Prete et al. "Reinfection by the SARS-CoV-2 Gamma variant in blood donors in Manaus, Brazil". In: *BMC Infectious Diseases* 22.1 (2022). Publisher: BioMed Central, pp. 1–8. ISSN: 14712334. DOI: 10.1186/s12879-022-07094-y. URL: https://doi.org/10.1186/s12879-022-07094-y (cit. on p. 4).

[42] Otavio T. Ranzani et al. "Effectiveness of the CoronaVac vaccine in older adults during a gamma variant associated epidemic of covid-19 in Brazil: Test negative case-control study". In: *The BMJ* 374 (2021). ISSN: 17561833. DOI: 10.1136/bmj.n2015 (cit. on pp. 4, 94).

[43] Thiago Cerqueira-Silva et al. "Influence of age on the effectiveness and duration of protection of Vaxzevria and CoronaVac vaccines: A population-based study". In: *The Lancet Regional Health - Americas* 6 (2022), p. 100154. ISSN: 2667193X. DOI: 10.1016/j.lana.2021.100154 (cit. on pp. 4, 57, 73, 98, 118).

[44] Rebecca Earnest et al. "Comparative transmissibility of SARS-CoV-2 variants Delta and Alpha in New England, USA". In: *Cell Reports Medicine* 3.4 (2022), p. 100583. ISSN: 26663791. DOI: 10.1016/j.xcrm.2022.100583 (cit. on p. 4).

[45] Adeel A. Butt et al. "Severity of Illness in Persons Infected With the SARS-CoV-2 Delta Variant vs Beta Variant in Qatar". In: *JAMA Internal Medicine* 182.2 (2022), pp. 197–205. ISSN: 21686114. DOI: 10.1001/jamainternmed.2021.7949 (cit. on p. 4).

[46] Aziz Sheikh et al. "SARS-CoV-2 Delta VOC in Scotland: demographics, risk of hospital admission, and vaccine effectiveness". In: *The Lancet* 397.10293 (2021). Publisher: Elsevier Ltd ISBN: 4159102101408, pp. 2461–2462. ISSN: 1474547X. DOI: 10.1016/S0140-6736(21)01358-1. URL: http://dx.doi.org/10.1016/S0140-6736(21)01358-1 (cit. on p. 4).

[47] Timothy Farinholt et al. "Transmission event of SARS-CoV-2 delta variant reveals multiple vaccine breakthrough infections". In: *BMC Medicine* 19.1 (2021). Publisher: BMC Medicine ISBN: 1291602102103, pp. 1–6. ISSN: 17417015. DOI: 10.1186/s12916-021-02103-4 (cit. on p. 4).

[48] Hester Allen et al. "Comparative transmission of {SARS}-{CoV}-2 Omicron (B.1.1.529) and Delta (B.1.617.2) variants and the impact of vaccination: national cohort study, England". In: *medRxiv* (2022). Publisher: Cold Spring Harbor Laboratory. DOI: 10.1101/2022.02.15.22271001. URL: https://doi.org/10.1101%2F2022.02.15.22271001 (cit. on p. 4).

[49] Heba N. Altarawneh et al. "Protection against the Omicron Variant from Previous SARS-CoV-2 Infection". In: *New England Journal of Medicine* 386.13 (Mar. 2022), pp. 1288–1290. ISSN: 0028-4793. DOI: 10.1056/NEJMc2200133. URL: http://www.nejm.org/doi/10.1056/NEJMc2200133 (cit. on p. 4).

[50] Olha Puhach et al. "Infectious viral load in unvaccinated and vaccinated individuals infected with ancestral, Delta or Omicron SARS-CoV-2". In: *Nature Medicine* (Apr. 2022). ISSN: 1078-8956. DOI: 10.1038/s41591-022-01816-0. URL: https://www.nature.com/articles/s41591-022-01816-0 (cit. on p. 4).

[51] Juliet R. C. Pulliam et al. "Increased risk of SARS-CoV-2 reinfection associated with emergence of Omicron in South Africa". In: *Science* 4947.8.5.2017 (Mar. 2022), pp. 2003–2005. ISSN: 0036-8075. DOI: 10.1126/science.abn4947. URL: https://www.science.org/doi/10.1126/science.abn4947 (cit. on pp. 4, 11).

[52] Frederik Plesner Lyngse et al. "SARS-CoV-2 Omicron VOC Transmission in Danish Households". In: *medRxiv* (2021), p. 2021.12.27.21268278. URL: https://www.medrxiv.org/content/10.1101/2021.12.27.21268278v1%0Ahttps://www.medrxiv.org/content/10.1101/2021.12.27.21268278v1.abstract (cit. on p. 4).

[53] Ana Cecilia Ulloa et al. "Early estimates of SARS-CoV-2 Omicron variant severity based on a matched cohort study, Ontario, Canada". In: *medRxiv* (2022). DOI: 10.1101/2021.12.24.21268382. URL: https://www.medrxiv.org/content/10.1101/2021.12.24.21268382v2%0Ahttps://www.medrxiv.org/content/10.1101/2021.12.24.21268382v2.abstract (cit. on p. 4).

[54] Jin Su Song et al. "Serial Intervals and Household Transmission of SARS-CoV-2 Omicron Variant, South Korea, 2021". In: *Emerging Infectious Diseases*

28.3 (2022), pp. 756–759. ISSN: 10806059. DOI: 10.3201/eid2803.212607 (cit. on p. 4).

[55] Annette B. Vogel et al. "BNT162b vaccines protect rhesus macaques from SARS-CoV-2". In: *Nature* 592.7853 (2021). Publisher: Springer US, pp. 283–289. ISSN: 14764687. DOI: 10.1038/s41586-021-03275-y. URL: http://dx.doi.org/10.1038/s41586-021-03275-y (cit. on p. 4).

[56] Kizzmekia S. Corbett et al. "Evaluation of the mRNA-1273 Vaccine against SARS-CoV-2 in Nonhuman Primates". In: *New England Journal of Medicine* 383.16 (2020), pp. 1544–1555. ISSN: 0028-4793. DOI: 10.1056/nejmoa2024671 (cit. on p. 4).

[57] Nicole E. Basta and Erica E. M Moodie. *COVID-19 Vaccine Tracker*. 2020. URL: https://covid19.trackvaccines.org/ (visited on 05/17/2022) (cit. on p. 4).

[58] Ewen Callaway. "The race for coronavirus vaccines: a graphical guide". In: *Nature* 580.7805 (Apr. 2020), pp. 576–577. DOI: 10.1038/d41586-020-01221-y. URL: http://www.nature.com/articles/d41586-020-01221-y (cit. on p. 4).

[59] Cheryl Keech et al. "Phase 1–2 Trial of a SARS-CoV-2 Recombinant Spike Protein Nanoparticle Vaccine". In: *New England Journal of Medicine* 383.24 (2020), pp. 2320–2332. ISSN: 0028-4793. DOI: 10.1056/nejmoa2026920 (cit. on p. 4).

[60] Edward E. Walsh et al. "Safety and Immunogenicity of Two RNA-Based Covid-19 Vaccine Candidates". In: *New England Journal of Medicine* 383.25 (2020), pp. 2439–2450. ISSN: 0028-4793. DOI: 10.1056/nejmoa2027906 (cit. on p. 5).

[61] Lisa A. Jackson et al. "An mRNA Vaccine against SARS-CoV-2 — Preliminary Report". In: *New England Journal of Medicine* 383.20 (2020), pp. 1920–1931. ISSN: 0028-4793. DOI: 10.1056/nejmoa2022483 (cit. on p. 5).

[62] Jerald Sadoff et al. "Interim Results of a Phase 1–2a Trial of Ad26.COV2.S Covid-19 Vaccine". In: *New England Journal of Medicine* 384.19 (2021), pp. 1824–1835. ISSN: 0028-4793. DOI: 10.1056/nejmoa2034201 (cit. on p. 5).

[63] Pedro M. Folegatti et al. "Safety and immunogenicity of the ChAdOx1 nCoV-19 vaccine against SARS-CoV-2: a preliminary report of a phase 1/2, single-blind, randomised controlled trial". In: *The Lancet* 396.10249 (2020), pp. 467–478. ISSN: 1474547X. DOI: 10.1016/S0140-6736(20)31604-4 (cit. on p. 5).

[64] Raches Ella et al. "Safety and immunogenicity of an inactivated SARS-CoV-2 vaccine, BBV152: a double-blind, randomised, phase 1 trial". In: *The Lancet Infectious Diseases* 21.5 (2021). Publisher: Elsevier Ltd, pp. 637–646. ISSN: 14744457. DOI: 10.1016/S1473-3099(20)30942-7. URL: http://dx.doi.org/10.1016/S1473-3099(20)30942-7 (cit. on p. 5).

[65] Shengli Xia et al. "Safety and immunogenicity of an inactivated SARS-CoV-2 vaccine, BBIBP-CorV: a randomised, double-blind, placebo-controlled, phase 1/2 trial". In: *The Lancet Infectious Diseases* 21.1 (2021). Publisher: Elsevier Ltd, pp. 39–51. ISSN: 14744457. DOI: 10.1016/S1473-3099(20)30831-8. URL: http://dx.doi.org/10.1016/S1473-3099(20)30831-8 (cit. on p. 5).

[66] Zhiwei Wu et al. "Safety, tolerability, and immunogenicity of an inactivated SARS-CoV-2 vaccine (CoronaVac) in healthy adults aged 60 years and older: a randomised, double-blind, placebo-controlled, phase 1/2 clinical trial". In: *The Lancet Infectious Diseases* 21.6 (2021). Publisher: Elsevier Ltd, pp. 803–812. ISSN: 14744457. DOI: 10.1016/S1473-3099(20)30987-7. URL: http://dx.doi.org/10.1016/S1473-3099(20)30987-7 (cit. on p. 5).

[67] World Health Organization. *COVID-19 Public Health Emergency of International Concern (PHEIC) Global research and innovation forum*. 2021. URL: https://www.who.int/publications/m/item/covid-19-public-health-emergency-of-international-concern-(pheic)-global-research-and-innovation-forum (visited on 05/18/2022) (cit. on p. 5).

[68] Ministério da Saúde. *PORTARIA Nº 188, DE 3 DE FEVEREIRO DE 2020*. 2021. URL: https://www.in.gov.br/en/web/dou/-/portaria-n-188-de-3-de-fevereiro-de-2020-241408388 (visited on 05/18/2022) (cit. on p. 5).

[69] Universidade Aberta do Sistema Único de Saúde. *Coronavírus: Brasil confirma primeiro caso da doença*. 2021. URL: https://www.unasus.gov.br/noticia/coronavirus-brasil-confirma-primeiro-caso-da-doenca (cit. on p. 5).

[70] G1. "Primeira morte por coronavírus no Brasil aconteceu em 12 de março, diz Ministério da Saúde". In: *G1* (2021). URL: https://g1.globo.com/bemestar/coronavirus/noticia/2020/06/27/primeira-morte-por-coronavirus-no-brasil-aconteceu-em-12-de-marco-diz-ministerio-da-saude.ghtml (cit. on p. 5).

[71] Marcia C. Castro et al. "Spatiotemporal pattern of COVID-19 spread in Brazil". In: *Science* 372.6544 (2021), pp. 821–826. ISSN: 10959203. DOI: 10.1126/science.abh1558 (cit. on pp. 5, 68, 89, 99).

[72] Rudi Rocha et al. "Effect of socioeconomic inequalities and vulnerabilities on health-system preparedness and response to COVID-19 in Brazil: a comprehensive analysis". In: *The Lancet Global Health* 9.6 (2021), e782–e792. ISSN: 2214109X. DOI: 10.1016/S2214-109X(21)00081-4 (cit. on p. 5).

[73] Ministério da Saúde. *SRAG 2020 - Banco de Dados de Síndrome Respiratória Aguda Grave - incluindo dados da COVID-19*. 2022. URL: https://opendatasus.saude.gov.br/dataset/srag-2020 (visited on 05/18/2022) (cit. on pp. 5–7, 9, 69, 77, 91, 100, 105, 119, 133).

[74] Ministério da Saúde. *SRAG 2021 e 2022 - Banco de Dados de Síndrome Respiratória Aguda Grave - incluindo dados da COVID-19*. 2022. URL: https://opendatasus.saude.gov.br/dataset/srag-2021-e-2022 (visited on 05/18/2022) (cit. on pp. 6, 7, 9, 69, 77, 91, 100, 105, 119, 133).

[75] Fundação Oswaldo Cruz. *Rede Genômica Fiocruz*. 2022. URL: http://www.genomahcov.fiocruz.br/ (visited on 05/25/2022) (cit. on pp. 8, 90).

[76] Agência Nacional de Vigilância Sanitária. *Anvisa aprova por unanimidade uso emergencial das vacinas*. 2021. URL: https://www.gov.br/anvisa/pt-br/assuntos/noticias-anvisa/2021/anvisa-aprova-por-unanimidade-uso-emergencial-das-vacinas (visited on 05/25/2022) (cit. on p. 7).

[77] Agência Nacional de Vigilância Sanitária. *Guia sobre os requisitos mínimos para submissão de solicitação de autorização temporária de uso emergencial, em caráter experimental, de vacinas Covid-19*. Tech. rep. 2020, p. 15. URL: https://www.gov.br/anvisa/pt-br/centraisdeconteudo/publicacoes/medicamentos/publicacoes-sobre-medicamentos/guia-sobre-os-requisitos-minimos-para-submissao-de-solicitacao-de-autorizacao-temporaria-de-uso-emergencial-em-carater-experimental-de-vacinas-covid (cit. on p. 8).

[78] Agência Nacional de Vigilância Sanitária. *Anvisa aprova uso emergencial da vacina da Janssen*. 2021. URL: https://www.gov.br/anvisa/pt-br/assuntos/noticias-anvisa/2021/anvisa-aprova-uso-emergencial-da-vacina-da-janssen (visited on 05/25/2022) (cit. on p. 8).

[79] Agência Nacional de Vigilância Sanitária. *Anvisa aprova registro da vacina da Fiocruz/AstraZeneca e de medicamento contra o coronavírus*. 2021. URL: https://www.gov.br/anvisa/pt-br/assuntos/noticias-anvisa/2021/anvisa-aprova-registro-da-vacina-da-fiocruz-astrazeneca-e-de-medicamento-contra-o-coronavirus (visited on 05/25/2022) (cit. on p. 8).

[80] Agência Nacional de Vigilância Sanitária. *Anvisa aprova registro definitivo da vacina Covid-19 da Janssen*. 2021. URL: https://www.gov.br/anvisa/pt-br/assuntos/noticias-anvisa/2022/anvisa-aprova-registro-definitivo-da-vacina-covid-19-da-janssen (visited on 05/25/2022) (cit. on p. 8).

[81] Agência Nacional de Vigilância Sanitária. *Informe à população brasileira*. 2021. URL: https://www.gov.br/anvisa/pt-br/assuntos/noticias-anvisa/2021/informe-a-populacao-brasileira (visited on 05/25/2022) (cit. on p. 8).

[82] Agência Nacional de Vigilância Sanitária. *Aprovada ampliação de uso da CoronaVac para crianças e adolescentes de 6 a 17 anos*. 2022. URL: https://www.gov.br/anvisa/pt-br/assuntos/noticias-anvisa/2022/aprovada-ampliacao-de-uso-da-vacina-coronavac-para-criancas-de-6-a-17-anos (visited on 05/25/2022) (cit. on p. 8).

[83] Agência Nacional de Vigilância Sanitária. *Anvisa autoriza vacina da Pfizer para crianças com mais de 12 anos*. 2021. URL: https://www.gov.br/anvisa/pt-br/assuntos/noticias-anvisa/2021/anvisa-autoriza-vacina-da-pfizer-para-criancas-com-mais-de-12-anos (visited on 05/25/2022) (cit. on p. 8).

[84] Agência Nacional de Vigilância Sanitária. *Anvisa aprova vacina da Pfizer contra Covid para crianças de 5 a 11 anos*. 2021. URL: https://www.gov.br/anvisa/pt-br/assuntos/noticias-anvisa/2021/anvisa-aprova-vacina-da-pfizer-contra-covid-para-criancas-de-5-a-11-anos (visited on 05/25/2022) (cit. on pp. 8, 100).

[85] Carla Magda Allan S. Domingues and Wanderson Kleber de Oliveira. "Uptake of pandemic influenza (H1N1)-2009 vaccines in Brazil, 2010". In: *Vaccine* 30.32 (2012), pp. 4744–4751. ISSN: 0264410X. DOI: 10.1016/j.vaccine.2012.05.007 (cit. on pp. 8, 90, 98, 99).

[86] Elize Massard da Fonseca, Kenneth C. Shadlen, and Francisco I. Bastos. "The politics of COVID-19 vaccination in middle-income countries: Lessons from Brazil". In: *Social Science and Medicine* 281.May (2021). Publisher: Elsevier Ltd, p. 114093. ISSN: 18735347. DOI: 10.1016/j.socscimed.2021.114093. URL: https://doi.org/10.1016/j.socscimed.2021.114093 (cit. on p. 8).

[87] Ministério da Saúde. *Campanha Nacional de Vacinação contra Covid-19*. 2022. URL: https://opendatasus.saude.gov.br/dataset/covid-19-vacinacao (visited on 05/25/2022) (cit. on pp. 9, 10, 69, 70, 78, 90–92, 98, 99).

[88] Ministério da Saúde. *Saiba como é feita a definição de casos suspeitos de Covid-19 no Brasil*. 2021. URL: https://www.gov.br/saude/pt-br/coronavirus/artigos/definicao-e-casos-suspeitos (visited on 05/25/2022) (cit. on p. 9).

[89] Ministério da Saúde. *Notificações de Síndrome Gripal - 2020*. 2022. URL: https://opendatasus.saude.gov.br/dataset/notificacoes-de-sindrome-gripal-leve-2020 (visited on 05/25/2022) (cit. on p. 10).

[90] Ministério da Saúde. *Notificações de Síndrome Gripal - 2021*. 2022. URL: https://opendatasus.saude.gov.br/dataset/notificacoes-de-sindrome-gripal-leve-2021 (visited on 05/25/2022) (cit. on p. 10).

[91] Ministério da Saúde. *Notificações de Síndrome Gripal - 2022*. 2022. URL: https://opendatasus.saude.gov.br/dataset/notificacoes-de-sindrome-gripal-leve-2022 (visited on 05/25/2022) (cit. on p. 10).

[92] Patrick GT T Walker et al. "Report 12: TheThe Global Impact of COVID-19 and Strategies for Mitigation and Suppression". In: *Imperial College COVID-19 Response Team* March.June (2020), p. 19. URL: https://doi.org/10.25561/77735%0Ahttps://doi.org/10.25561/77735%0Adoi.org/10.25561/77735 (cit. on p. 11).

[93] Leonardo S. Bastos et al. "A modelling approach for correcting reporting delays in disease surveillance data". In: *Statistics in Medicine* 38.22 (2019), pp. 4363–4377. ISSN: 10970258. DOI: 10.1002/sim.8303 (cit. on p. 11).

[94] Seth Flaxman et al. "Estimating the effects of non-pharmaceutical interventions on COVID-19 in Europe". In: *Nature* 584.7820 (2020). ISBN: 4158602024057, pp. 257–261. ISSN: 14764687. DOI: 10.1038/s41586-020-2405-7 (cit. on p. 11).

[95] Laura Di Domenico et al. "Impact of lockdown on COVID-19 epidemic in Île-de-France and possible exit strategies". In: *BMC Medicine* 18.1 (2020). Publisher: BMC Medicine, pp. 1–13. ISSN: 17417015. DOI: 10.1186/s12916-020-01698-4 (cit. on p. 11).

[96] James D. Munday et al. "Estimating the impact of reopening schools on the reproduction number of SARS-CoV-2 in England, using weekly contact survey data". In: *BMC Medicine* 19.1 (2021). Publisher: BMC Medicine, pp. 1–13. ISSN: 17417015. DOI: 10.1186/s12916-021-02107-0 (cit. on p. 11).

[97] Marcelo Eduardo Borges et al. "Modeling the impact of school reopening and contact tracing strategies on COVID-19 dynamics in different epidemiologic settings in Brazil". In: *medRxiv* (2021), p. 2021.10.22.21264706. URL: https://www.medrxiv.org/content/10.1101/2021.10.22.21264706v2 (cit. on pp. 11, 65).

[98] Andrea Brizzi et al. "Spatial and temporal fluctuations in COVID-19 fatality rates in Brazilian hospitals". In: *Nature Medicine* (May 2022). ISSN: 1078-8956. DOI: 10.1038/s41591-022-01807-1. URL: http://www.ncbi.nlm.nih.gov/pubmed/34751273%0Ahttp://www.pubmedcentral.nih.gov/articlerender.fcgi?artid=PMC8575144 (cit. on p. 11).

[99] Kevin C. Ma et al. "Modeling the impact of racial and ethnic disparities on covid-19 epidemic dynamics". In: *eLife* 10 (2021), pp. 1–16. ISSN: 2050084X. DOI: 10.7554/eLife.66601 (cit. on p. 11).

[100] Paolo Bosetti et al. "Impact of mass testing during an epidemic rebound of SARS-CoV-2: A modelling study using the example of France". In: *Eurosurveillance* 26.1 (2020). Publisher: European Centre for Disease Prevention and Control (ECDC), pp. 1–7. ISSN: 15607917. DOI: 10.2807/1560-7917.ES.2020.26.1.2001978. URL: http://dx.doi.org/10.2807/1560-7917.ES.2020.26.1.2001978 (cit. on p. 11).

[101] Caroline E. Wagner, Chadi M. Saad-Roy, and Bryan T. Grenfell. "Modelling vaccination strategies for COVID-19". In: *Nature Reviews Immunology* 22.3 (2022). Publisher: Springer US ISBN: 0123456789, pp. 139–141. ISSN: 14741741. DOI: 10.1038/s41577-022-00687-3 (cit. on p. 11).

[102] Laura Matrajt et al. "Vaccine optimization for COVID-19: Who to vaccinate first?" In: *Science Advances* 7.6 (2021). ISSN: 23752548. DOI: 10.1126/sciadv.abf1374 (cit. on p. 11).

[103] Kate M. Bubar et al. "Model-informed COVID-19 vaccine prioritization strategies by age and serostatus". In: *Science* (Jan. 2021), eabe6959. ISSN: 0036-8075. DOI: 10.1126/science.abe6959. URL: https://www.sciencemag.org/lookup/doi/10.1126/science.abe6959 (cit. on pp. 11, 33, 39, 48, 65).

[104] Caroline E. Wagner et al. "Vaccine nationalism and the dynamics and control of SARS-CoV-2". In: *Science* 373.6562 (2021). ISSN: 10959203. DOI: 10.1126/science.abj7364 (cit. on p. 11).

[105] Sally Blower and Daniel Bernoulli. "An attempt at a new analysis of the mortality caused by smallpox and of the advantages of inoculation to prevent it. 1766." In: *Reviews in medical virology* 14.5 (2004), pp. 275–288. ISSN: 10529276. DOI: 10.1002/rmv.443 (cit. on p. 13).

[106] BY W H Hamer and FRCP Lond. "The Milroy Lectures ON EPIDEMIC DISEASE IN ENGLAND—THE EVIDENCE OF VARIABILITY AND OF PERSISTENCY OF TYPE." In: *The Lancet* 167.4306 (Mar. 1906), pp. 655–662. ISSN: 01406736. DOI: 10.1016/S0140-6736(01)80264-6. URL: https://linkinghub.elsevier.com/retrieve/pii/S0140673601802646 (cit. on p. 13).

[107] R Ross. *The Prevention of malaria*. J. Murray, 1910. URL: https://books.google.com.br/books?id=0jRaWNX--s0C (cit. on p. 13).

[108] W. O. Kermack and A. G. McKendrick. "A contribution to the mathematical theory of epidemics". In: *Proceedings of the Royal Society of London. Series A, Containing Papers of a Mathematical and Physical Character* 115.772 (Aug. 1927), pp. 700–721. ISSN: 0950-1207. DOI: 10.1098/rspa.1927.0118. URL: https://royalsocietypublishing.org/doi/10.1098/rspa.1927.0118 (cit. on p. 13).

[109] W O Kermack and a G Mckendrick. "CONTRIBUTIONS TO THE MATHEMATICAL THEORY OF EPIDEMICS–II . THE PROBLEM OF ENDEMICITY * Laboratory of the Royal College of Physicians , Edinburgh , U . K . 1 . Introduction . In a previous communication (Kermack and McKendrick , 1927) an attempt was mad". In: *Bulletin of Mathematical Biology* 53.1 (1991), pp. 57–87 (cit. on p. 13).

[110] W. O. Kermack and A. G. McKendrick. "Contributions to the mathematical theory of epidemics—III. Further studies of the problem of endemicity". In: *Bulletin of Mathematical Biology* 53.1-2 (Mar. 1991), pp. 89–118. ISSN: 0092-8240. DOI: 10.1007/BF02464425. URL: http://link.springer.com/10.1007/BF02464425 (cit. on p. 13).

[111] Edwin B. Wilson and Jane Worcester. "The Law of Mass Action in Epidemiology". In: *Proceedings of the National Academy of Sciences* 31.1 (1945), pp. 24–34. ISSN: 0027-8424. DOI: 10.1073/pnas.31.1.24 (cit. on p. 14).

[112] Fred Brauer. "Compartmental Models in Epidemiology". In: 2008, pp. 19–79. DOI: 10.1007/978-3-540-78911-6_2. URL: http://link.springer.com/10.1007/978-3-540-78911-6_2 (cit. on p. 14).

[113] Junling Ma and David J.D. Earn. "Generality of the final size formula for an epidemic of a newly invading infectious disease". In: *Bulletin of*

Mathematical Biology 68.3 (2006), pp. 679–702. ISSN: 00928240. DOI: 10.1007/s11538-005-9047-7 (cit. on p. 17).

[114] L. J.S. Allen, M. A. Jones, and C. F. Martin. "A discrete-time model with vaccination for a measles epidemic". In: *Mathematical Biosciences* 105.1 (1991), pp. 111–131. ISSN: 00255564. DOI: 10.1016/0025-5564(91)90051-J (cit. on p. 18).

[115] P van den Driessche and James Watmough. "Further Notes on the Basic Reproduction Number". In: *Mathematical Epidemiology*. Ed. by Fred Brauer, Pauline van den Driessche, and Jianhong Wu. Berlin, Heidelberg: Springer Berlin Heidelberg, 2008, pp. 159–178. ISBN: 978-3-540-78911-6. DOI: 10.1007/978-3-540-78911-6_6. URL: https://doi.org/10.1007/978-3-540-78911-6_6 (cit. on pp. 23, 25, 109).

[116] Linda J.S. Allen and P. Van Den Driessche. "The basic reproduction number in some discrete-time epidemic models". In: *Journal of Difference Equations and Applications* 14.10-11 (2008), pp. 1127–1147. ISSN: 10236198. DOI: 10.1080/10236190802332308 (cit. on pp. 23, 27, 74, 126, 131).

[117] Chi Kwong Li and Hans Schneider. "Applications of Perron-Frobenius theory to population dynamics". In: *Journal of Mathematical Biology* 44.5 (2002). arXiv: math/0109008, pp. 450–462. ISSN: 03036812. DOI: 10.1007/s002850100132 (cit. on p. 28).

[118] Leonardo Souto Ferreira et al. "Assessing the best time interval between doses in a two-dose vaccination regimen to reduce the number of deaths in an ongoing epidemic of SARS-CoV-2". In: *PLoS Computational Biology* 18.3 (2022). ISBN: 1111111111, pp. 1–15. ISSN: 15537358. DOI: 10.1371/journal.pcbi.1009978 (cit. on pp. 34, 55, 66, 112, 113, 130, 131).

[119] Joint Committee on Vaccination and Immunization. *Optimising the COVID-19 vaccination programme for maximum short-term impact*. Tech. rep. 2021 (cit. on pp. 35, 48).

[120] Ministério da Saúde. *Décimo Quinto Informe Técnico - Orientações Técnicas Relativas à Continuidade da Campanha Nacional de Vacinação Contra a COVID-19*. Tech. rep. 2021 (cit. on p. 35).

[121] Public Health England. *COVID-19 vaccination programme - Information for healthcare practitioners*. 2021 (cit. on p. 35).

[122] Julia Stowe et al. *Effectiveness of COVID-19 vaccines against hospital admission with the Delta (B.1.617.2) variant*. Tech. rep. 2021 (cit. on p. 36).

[123] Merryn Voysey et al. "Single-dose administration and the influence of the timing of the booster dose on immunogenicity and efficacy of ChAdOx1 nCoV-19 (AZD1222) vaccine: a pooled analysis of four randomised trials". In: *The Lancet* 397.10277 (2021), pp. 881–891. ISSN: 1474547X. DOI: 10.1016/S0140-6736(21)00432-3 (cit. on pp. 36, 39, 47–49, 118).

[124] Ricardo Palacios et al. "Efficacy and Safety of a COVID-19 Inactivated Vaccine in Healthcare Professionals in Brazil: The PROFISCOV Study". In: *SSRN Electronic Journal* (2021). ISSN: 1556-5068. DOI: 10.2139/ssrn.3822780. URL: https://www.ssrn.com/abstract=3822780 (cit. on pp. 36, 39, 48).

[125] Fernando P. Polack et al. "Safety and Efficacy of the BNT162b2 mRNA Covid-19 Vaccine". In: *New England Journal of Medicine* 383.27 (2020), pp. 2603–2615. ISSN: 0028-4793. DOI: 10.1056/nejmoa2034577 (cit. on pp. 36, 53).

[126] Jamie Lopez Bernal et al. "Effectiveness of Covid-19 Vaccines against the B.1.617.2 (Delta) Variant". In: *New England Journal of Medicine* 385.7 (2021), pp. 585–594. ISSN: 0028-4793. DOI: 10.1056/nejmoa2108891 (cit. on p. 36).

[127] Robert Koch Institute. *Epidemiologisches Bulletin 2/2021*. Tech. rep. 2021. URL: https://www.rki.de/DE/Content/Infekt/EpidBull/Archiv/2021/Ausgaben/02_21.html (cit. on p. 36).

[128] Ministério da Saúde. *Plano Nacional de Operacionalização da Vacinação contra Covid-19*. 2021. URL: https://www.gov.br/saude/pt-br/coronavirus/publicacoes-tecnicas/guias-e-planos/plano-nacional-de-vacinacao-covid-19/view (cit. on pp. 36, 40, 90, 98).

[129] Julien Arino et al. "A model for influenza with vaccination and antiviral treatment". In: *Journal of Theoretical Biology* 253.1 (2008), pp. 118–130. ISSN: 00225193. DOI: 10.1016/j.jtbi.2008.02.026 (cit. on p. 36).

[130] Matthias Ehrhardt, Ján Gašper, and Soňa Kilianová. "SIR-based mathematical modeling of infectious diseases with vaccination and waning immunity". In: *Journal of Computational Science* 37 (2019), pp. 1–10. ISSN: 18777503. DOI: 10.1016/j.jocs.2019.101027 (cit. on p. 36).

[131] Elamin H. Elbasha and Alison P. Galvani. "Vaccination against multiple HPV types". In: *Mathematical Biosciences* 197.1 (2005), pp. 88–117. ISSN: 00255564. DOI: 10.1016/j.mbs.2005.05.004 (cit. on p. 36).

[132] David Greenhalgh. "Vaccination campaigns for common childhood diseases". In: *Mathematical Biosciences* 100.2 (1990), pp. 201–240. ISSN: 00255564. DOI: 10.1016/0025-5564(90)90040-6 (cit. on p. 36).

[133] Shoujun Zhao, Zhiyi Xu, and Ying Lu. "A mathematical model of hepatitis B virus transmission and its application for vaccination strategy in China". In: *International Journal of Epidemiology* 29.4 (2000), pp. 744–752. ISSN: 03005771. DOI: 10.1093/ije/29.4.744 (cit. on p. 36).

[134] Laura Matrajt et al. "One versus two doses: What is the best use of vaccine in an influenza pandemic?" In: *Epidemics* 13 (2015). Publisher: Elsevier B.V., pp. 17–27. ISSN: 18780067. DOI: 10.1016/j.epidem.2015.06.001. URL: http://dx.doi.org/10.1016/j.epidem.2015.06.001 (cit. on p. 36).

[135] Alicia N M Kraay et al. "Modeling the use of SARS-CoV-2 vaccination to safely relax non-pharmaceutical interventions". In: *medRxiv* (2021). URL: https://www.medrxiv.org/content/10.1101/2021.03.12.21253481v1 (cit. on p. 36).

[136] Kiesha Prem et al. "Projecting contact matrices in 177 geographical regions: An update and comparison with empirical data for the COVID-19 era". In: *PLoS Computational Biology* 17.7 (2021). ISBN: 1111111111, 1DUMMUY. ISSN: 15537358. DOI: 10.1371/journal.pcbi.1009098. URL: http://dx.doi.org/10.1371/journal.pcbi.1009098 (cit. on pp. 37, 108, 127).

[137] Noa Dagan et al. "BNT162b2 mRNA Covid-19 Vaccine in a Nationwide Mass Vaccination Setting". In: *New England Journal of Medicine* 384.15 (2021), pp. 1412–1423. ISSN: 0028-4793. DOI: 10.1056/nejmoa2101765 (cit. on pp. 39, 118).

[138] Nicholas G. Davies et al. "Estimated transmissibility and impact of SARS-CoV-2 lineage B.1.1.7 in England". In: *Science* 372.6538 (2021), pp. 1–11. ISSN: 0036-8075. DOI: 10.1126/science.abg3055 (cit. on p. 40).

[139] Agência Nacional de Vigilância Sanitária. *Avaliação do Uso Emergencial da Vacina CoronaVac - Apresentação*. Tech. rep. 2021 (cit. on p. 41).

[140] Michel Berkelaar, Kjell Eikland, and Peter Notebaert. *lpSolve: Interface to 'Lp_solve' v. 5.5 to Solve Linear/Integer Programs*. 2020. URL: https://cran.r-project.org/package=lpSolve (cit. on pp. 43, 115).

[141] Alejandro Jara et al. "Effectiveness of an Inactivated SARS-CoV-2 Vaccine in Chile". In: *New England Journal of Medicine* 385.10 (2021), pp. 875–884. ISSN: 0028-4793. DOI: 10.1056/nejmoa2107715 (cit. on pp. 47, 118).

[142] B. Afrough, S. Dowall, and R. Hewson. "Emerging viruses and current strategies for vaccine intervention". In: *Clinical and Experimental Immunology* 196.2 (2019), pp. 157–166. ISSN: 13652249. DOI: 10.1111/cei.13295 (cit. on pp. 47, 58).

[143] Rachel L. Roper and Kristina E. Rehm. "SARS vaccines: Where are we?" In: *Expert Review of Vaccines* 8.7 (2009), pp. 887–898. ISSN: 14760584. DOI: 10.1586/erv.09.43 (cit. on p. 47).

[144] Emma Pritchard et al. "Impact of vaccination on new SARS-CoV-2 infections in the United Kingdom". In: *Nature Medicine* 27.8 (2021). Publisher: Springer US, pp. 1370–1378. ISSN: 1546170X. DOI: 10.1038/s41591-021-01410-w. URL: http://dx.doi.org/10.1038/s41591-021-01410-w (cit. on pp. 47–49).

[145] John F.R. Robertson, Herb F. Sewell, and Marcia Stewart. "Delayed second dose of the BNT162b2 vaccine: innovation or misguided conjecture?" In: *The Lancet* 397.10277 (2021). Publisher: Elsevier Ltd, pp. 879–880. ISSN: 1474547X. DOI: 10.1016/S0140-6736(21)00455-4. URL: http://dx.doi.org/10.1016/S0140-6736(21)00455-4 (cit. on p. 48).

[146] Rebecca P. Payne et al. "Immunogenicity of standard and extended dosing intervals of BNT162b2 mRNA vaccine". In: *Cell* 184.23 (2021), 5699–5714.e11. ISSN: 10974172. DOI: 10.1016/j.cell.2021.10.011 (cit. on p. 48).

[147] Peter C. Jentsch, Madhur Anand, and Chris T. Bauch. "Prioritising COVID-19 vaccination in changing social and epidemiological landscapes: a mathematical modelling study". In: *The Lancet Infectious Diseases* 21.8 (2021). Publisher: Elsevier Ltd, pp. 1097–1106. ISSN: 14744457. DOI: 10.1016/S1473-3099(21)00057-8. URL: http://dx.doi.org/10.1016/S1473-3099(21)00057-8 (cit. on p. 48).

[148] Sam Moore et al. "Vaccination and non-pharmaceutical interventions for COVID-19: a mathematical modelling study". In: *The Lancet Infectious Diseases* 21.6 (2021). Publisher: The Author(s). Published by Elsevier Ltd. This is an Open Access article under the CC BY-NC-ND 4.0 license, pp. 793–802. ISSN: 14744457. DOI: 10.1016/S1473-3099(21)00143-2. URL: http://dx.doi.org/10.1016/S1473-3099(21)00143-2 (cit. on p. 48).

[149] Seyed M. Moghadas et al. "Evaluation of COVID-19 vaccination strategies with a delayed second dose". In: *PLoS Biology* 19.4 (2021). ISBN: 1111111111, pp. 1–13. ISSN: 15457885. DOI: 10.1371/journal.pbio.3001211. URL: http://dx.doi.org/10.1371/journal.pbio.3001211 (cit. on pp. 48, 49, 65).

[150] Santiago Romero-Brufau et al. "Public health impact of delaying second dose of BNT162b2 or mRNA-1273 covid-19 vaccine: Simulation agent based modeling study". In: *The BMJ* 373 (2021). ISSN: 17561833. DOI: 10.1136/bmj.n1087 (cit. on pp. 48, 65).

[151] Ho-Yin Mak, Tinglong Dai, and Christopher S. Tang. "Managing Two-Dose COVID-19 Vaccine Rollouts with Limited Supply". In: *SSRN Electronic Journal* (2021). DOI: 10.2139/ssrn.3790836 (cit. on p. 48).

[152] Madhumita Shrotri et al. "Vaccine effectiveness of the first dose of ChAdOx1 nCoV-19 and BNT162b2 against SARS-CoV-2 infection in residents of long-term care facilities in England (VIVALDI): a prospective cohort study". In: *The Lancet Infectious Diseases* 21.11 (2021). Publisher: The Author(s). Published by Elsevier Ltd. This is an Open Access article under the CC BY-NC-ND 4.0 license, pp. 1529–1538. ISSN: 14744457. DOI: 10.1016/S1473-3099(21)00289-9. URL: http://dx.doi.org/10.1016/S1473-3099(21)00289-9 (cit. on p. 49).

[153] Leonardo Souto Ferreira et al. *Modelling optimal vaccination strategies against Covid-19 in a context of Gamma variant predominance in Brazil*. en. preprint. Nov. 2021. DOI: 10.1101/2021.11.19.21266590. URL: http://medrxiv.org/lookup/doi/10.1101/2021.11.19.21266590 (visited on 07/11/2022) (cit. on p. 51).

[154] Ministério da Saúde. *Boletim epidemiológico especial – Doença pelo Novo Coronavírus – COVID-19. Semana Epidemiológica 35*. Tech. rep. 2021 (cit. on pp. 52, 100).

[155] Tatiana Aline Carvalho, Matheus Negri Boschiero, and Fernando Augusto Lima Marson. "COVID-19 in Brazil: 150,000 deaths and the Brazilian underreporting". In: *Diagnostic Microbiology and Infectious Disease* 99.3 (2021). Publisher: Elsevier Inc., p. 115258. ISSN: 18790070. DOI: 10.1016/j.diagmicrobio.2020.115258. URL: https://doi.org/10.1016/j.diagmicrobio.2020.115258 (cit. on p. 52).

[156] Leonardo SL Bastos et al. "COVID-19 hospital admissions: Brazil's first and second waves compared". In: *The Lancet Respiratory Medicine* 9.8 (2021). Publisher: Elsevier Ltd, e82–e83. ISSN: 22132619. DOI: 10.1016/S2213-2600(21)00287-3. URL: http://dx.doi.org/10.1016/S2213-2600(21)00287-3 (cit. on p. 53).

[157] World Health Organization. *WHO SAGE Roadmap For Prioritizing Uses Of COVID-19 Vaccines In The Context Of Limited Supply*. Tech. rep. 2021. URL: https://www.who.int/publications-detail-redirect/who-sage-roadmap-for-prioritizing-uses-of-covid-19-vaccines-in-the-context-of-limited-supply (cit. on p. 53).

[158] Governo do Brasil. *Vacinação contra a Covid-19 no Brasil - #PÁTRIAVACINADA*. 2021. URL: https://www.gov.br/saude/pt-br/vacinacao (cit. on pp. 53, 55).

[159] Mine Durusu Tanriover et al. "Efficacy and safety of an inactivated whole-virion SARS-CoV-2 vaccine (CoronaVac): interim results of a double-blind, randomised, placebo-controlled, phase 3 trial in Turkey". In: *The Lancet* 398.10296 (2021), pp. 213–222. ISSN: 1474547X. DOI: 10.1016/S0140-6736(21)01429-X (cit. on p. 53).

[160] Ann R. Falsey et al. "Phase 3 Safety and Efficacy of AZD1222 (ChAdOx1 nCoV-19) Covid-19 Vaccine". In: *New England Journal of Medicine* 385.25 (2021), pp. 2348–2360. ISSN: 0028-4793. DOI: 10.1056/nejmoa2105290 (cit. on p. 53).

[161] World Health Organization. *Interim recommendations for use of the Pfizer–BioNTech COVID-19 vaccine, BNT162b2, under Emergency Use Listing*. Tech. rep. 2021. URL: https://www.who.int/publications-detail-redirect/WHO-2019-nCoV-vaccines-SAGE_recommendation-BNT162b2-2021.1 (cit. on p. 53).

[162] World Health Organization. *Interim recommendations for use of the ChAdOx1-S [recombinant] vaccine against COVID-19 (AstraZeneca COVID-19 vaccine AZD1222 VaxzevriaTM, SII COVISHIELDTM)*. Tech. rep. 2021. URL: https://www.who.int/publications-detail-redirect/WHO-2019-nCoV-vaccines-SAGE_recommendation-AZD1222-2021.1 (cit. on pp. 53, 57).

[163] Samuel Karlin. *An introduction to stochastic modeling*. Ed. by H M Taylor. San Diego, CA: Academic Press, 1998 (cit. on p. 55).

[164] Matt J Keeling and Pejman Rohani. *Modeling infectious diseases in humans and animals*. Princeton, NJ: Princeton University Press, 2007 (cit. on p. 55).

[165] Lewis F. Buss et al. "Three-quarters attack rate of SARS-CoV-2 in the Brazilian Amazon during a largely unmitigated epidemic". In: *Science* 371.6526 (2021), pp. 288–292. ISSN: 10959203. DOI: 10.1126/science.abe9728 (cit. on p. 57).

[166] João Luiz Miraglia et al. "A seroprevalence survey of anti-SARS-CoV-2 antibodies among individuals 18 years of age or older living in a vulnerable region of the city of São Paulo, Brazil". In: *PLoS ONE* 16.7 July (2021). ISBN: 1111111111, pp. 1–9. ISSN: 19326203. DOI: 10.1371/journal.pone.0255412 (cit. on p. 57).

[167] Flavia Maria Darcie Marquitti et al. "Brazil in the face of new SARS-CoV-2 variants: emergencies and challenges in public health". en. In: *Revista Brasileira de Epidemiologia* 24 (2021), e210022. ISSN: 1980-5497, 1415-790X. DOI: 10.1590/1980-549720210022. URL: http://www.scielo.br/scielo.php?script=sci_arttext&pid=S1415-790X2021000100204&tlng=en (visited on 07/04/2022) (cit. on p. 63).

[168] Francisco Ortega and Michael Orsini. "Governing COVID-19 without government in Brazil: Ignorance, neoliberal authoritarianism, and the collapse of public health leadership". en. In: *Global Public Health* 15.9 (Sept. 2020), pp. 1257–1277. ISSN: 1744-1692, 1744-1706. DOI: 10.1080/17441692.2020.1795223. URL: https://www.tandfonline.com/doi/full/10.1080/17441692.2020.1795223 (visited on 07/04/2022) (cit. on p. 63).

[169] José Gomes Temporão. "O Programa Nacional de Imunizações (PNI): origens e desenvolvimento". pt. In: *História, Ciências, Saúde-Manguinhos* 10.suppl 2 (2003), pp. 601–617. ISSN: 0104-5970. DOI: 10.1590/S0104-59702003000500008. URL: http://www.scielo.br/scielo.php?script=sci_arttext&pid=S0104-59702003000500008&lng=pt&tlng=pt (visited on 07/04/2022) (cit. on p. 64).

[170] Nick Andrews et al. "Covid-19 Vaccine Effectiveness against the Omicron (B.1.1.529) Variant". en. In: *New England Journal of Medicine* 386.16 (Apr. 2022), pp. 1532–1546. ISSN: 0028-4793, 1533-4406. DOI: 10.1056/NEJMoa2119451. URL: http://www.nejm.org/doi/10.1056/NEJMoa2119451 (visited on 07/04/2022) (cit. on p. 65).

[171] João Viana et al. "Controlling the pandemic during the SARS-CoV-2 vaccination rollout". en. In: *Nature Communications* 12.1 (Dec. 2021), p. 3674. ISSN: 2041-1723. DOI: 10.1038/s41467-021-23938-8. URL: http://www.nature.com/articles/s41467-021-23938-8 (visited on 07/04/2022) (cit. on p. 65).

[172] Sam Moore et al. "Modelling optimal vaccination strategy for SARS-CoV-2 in the UK". en. In: *PLOS Computational Biology* 17.5 (May 2021). Ed. by Alex Perkins, e1008849. ISSN: 1553-7358. DOI: 10.1371/journal.pcbi.1008849. URL: https://dx.plos.org/10.1371/journal.pcbi.1008849 (visited on 07/04/2022) (cit. on p. 65).

[173] Paulo J. S. Silva et al. "Optimized delay of the second COVID-19 vaccine dose reduces ICU admissions". en. In: *Proceedings of the National Academy of Sciences* 118.35 (Aug. 2021), e2104640118. ISSN: 0027-8424, 1091-6490. DOI: 10.1073/pnas.2104640118. URL: https://pnas.org/doi/full/10.1073/pnas.2104640118 (visited on 07/04/2022) (cit. on p. 65).

[174] UK Health Security Agency. *Investigation of SARS-COV-2 variants: Technical briefings*. Publication Title: GOV.UK. June 2022. URL: https://www.gov.uk/government/publications/investigation-of-sars-cov-2-variants-technical-briefings (cit. on p. 69).

[175] N Ferguson. *Report 49: Growth and immune escape of the Omicron SARS-CoV-2 variant of concern in England*. en. Tech. rep. Imperial College London, Dec. 2021. DOI: 10.25561/93038. URL: http://spiral.imperial.ac.uk/handle/10044/1/93038 (visited on 07/04/2022) (cit. on pp. 69, 133–135).

[176] Nick Andrews et al. "Effectiveness of COVID-19 booster vaccines against COVID-19-related symptoms, hospitalization and death in England". en. In: *Nature Medicine* 28.4 (Apr. 2022), pp. 831–837. ISSN: 1078-8956, 1546-170X. DOI: 10.1038/s41591-022-01699-1. URL: https://www.nature.com/articles/s41591-022-01699-1 (visited on 07/04/2022) (cit. on pp. 69, 73, 78, 135).

[177] Instituto Brasileiro de Geografia e Estatística. *Projeções da população*. 2021. URL: https://www.ibge.gov.br/estatisticas/sociais/populacao/9109-projecao-da-populacao.html (visited on 10/01/2021) (cit. on pp. 69, 70, 74, 119, 133).

[178] Centers for Disease Control and Prevention. *CDC Covid Data tracker*. Publication Title: Centers for Disease Control and Prevention. URL: https://covid.cdc.gov/covid-data-tracker/#covidnet-hospitalization-network (cit. on pp. 69, 77).

[179] Secretaria Estadual de Saúde do Rio Grande do Sul. *Boletim de hospitalizações - RS, Macrorregiões e Regiões - COVID-19*. Publication Title: Boletim de hospitalizações - RS, Macrorregiões e Regiões - COVID-19. URL: https://app.powerbi.com/view?r=eyJrIjoiMjg2MWVkMDMtNjZlYy00NjIzLWI1MDQtYzQ5N
MmQ2IiwidCI6IjRmZjE0NWRhLThkZWYtNGI3Zi05YTlkLTFiZjRjZDI3MzViYSJ9
(cit. on p. 69).

[180] Aharona Glatman-Freedman et al. "Effectiveness of BNT162b2 Vaccine in Adolescents during Outbreak of SARS-CoV-2 Delta Variant Infection, Israel, 2021". en. In: *Emerging Infectious Diseases* 27.11 (Nov. 2021), pp. 2919–2922. ISSN: 1080-6040, 1080-6059. DOI: 10.3201/eid2711.211886. URL: https://wwwnc.cdc.gov/eid/article/27/11/21-1886_article.htm (visited on 07/06/2022) (cit. on pp. 69, 135).

[181] Emmanuel B. Walter et al. "Evaluation of the BNT162b2 Covid-19 Vaccine in Children 5 to 11 Years of Age". en. In: *New England Journal of Medicine* 386.1 (Jan. 2022), pp. 35–46. ISSN: 0028-4793, 1533-4406. DOI: 10.1056/NEJMoa2116298. URL: http://www.nejm.org/doi/10.1056/NEJMoa2116298 (visited on 07/06/2022) (cit. on p. 69).

[182] Sarah F. McGough et al. "Nowcasting by Bayesian Smoothing: A flexible, generalizable model for real-time epidemic tracking". en. In: *PLOS Computational Biology* 16.4 (Apr. 2020). Ed. by Bryan Lewis, e1007735. ISSN: 1553-7358. DOI: 10.1371/journal.pcbi.1007735. URL: https:

//dx.plos.org/10.1371/journal.pcbi.1007735 (visited on 07/06/2022) (cit. on p. 70).

[183] Ministério da Saúde. *Produção Hospitalar (SIH/SUS) - Sistema de Informação Hospitalar - DATASUS*. Publication Title: Datasus. URL: https://datasus.saude.gov.br/acesso-a-informacao/producao-hospitalar-sih-sus/ (cit. on p. 70).

[184] New York State Department of Health. *Full Report - Pediatric COVID-19 update: January 7, 2022*. en. Tech. rep. Jan. 2022, p. 15 (cit. on pp. 73, 134, 136).

[185] Annabel A Powell et al. "Effectiveness of BNT162b2 against COVID-19 in adolescents". en. In: *The Lancet Infectious Diseases* 22.5 (May 2022), pp. 581–583. ISSN: 14733099. DOI: 10.1016/S1473-3099(22)00177-3. URL: https://linkinghub.elsevier.com/retrieve/pii/S1473309922001773 (visited on 07/06/2022) (cit. on pp. 73, 135).

[186] Hung Fu Tseng et al. "Effectiveness of mRNA-1273 against SARS-CoV-2 Omicron and Delta variants". en. In: *Nature Medicine* 28.5 (May 2022), pp. 1063–1071. ISSN: 1078-8956, 1546-170X. DOI: 10.1038/s41591-022-01753-y. URL: https://www.nature.com/articles/s41591-022-01753-y (visited on 07/06/2022) (cit. on pp. 73, 134, 136).

[187] Brian J. Willett et al. *The hyper-transmissible SARS-CoV-2 Omicron variant exhibits significant antigenic change, vaccine escape and a switch in cell entry mechanism*. en. preprint. Jan. 2022. DOI: 10.1101/2022.01.03.21268111. URL: http://medrxiv.org/lookup/doi/10.1101/2022.01.03.21268111 (visited on 07/06/2022) (cit. on pp. 73, 134).

[188] Rosanna C. Barnard et al. *Projected epidemiological consequences of the Omicron SARS-CoV-2 variant in England, December 2021 to April 2022*. en. preprint. Epidemiology, Dec. 2021. DOI: 10.1101/2021.12.15.21267858. URL: http://medrxiv.org/lookup/doi/10.1101/2021.12.15.21267858 (visited on 07/06/2022) (cit. on pp. 73, 134–137).

[189] UK Health Security Agency. *COVID-19 vaccine surveillance report - week 48*. en. Tech. rep. Nov. 2021, p. 47. URL: https://assets.publishing.service.gov.uk/government/uploads/system/uploads/attachment_data/file/1037987/Vaccine-surveillance-report-week-48.pdf (cit. on pp. 73, 78).

[190] Yinong Young-Xu et al. *Effectiveness of mRNA COVID-19 Booster Vaccines against Omicron and Delta Variants among US Veterans*. en. preprint. Jan. 2022. DOI: 10.1101/2022.01.15.22269360. URL: http://medrxiv.org/lookup/doi/10.1101/2022.01.15.22269360 (visited on 07/06/2022) (cit. on pp. 73, 134, 137).

[191] Carlos Prete Junior et al. *SARS-CoV-2 antibody dynamics in blood donors and COVID-19 epidemiology in eight Brazilian state capitals*. en. preprint. Feb. 2022. DOI: 10.21203/rs.3.rs-1363260/v1. URL: https://www.researchsquare.com/article/rs-1363260/v1 (visited on 07/06/2022) (cit. on p. 73).

[192] Ruprecht Schmidt-Ott et al. "Assessing direct and indirect effects of pediatric influenza vaccination in Germany by individual-based simulations". en. In: *Human Vaccines & Immunotherapeutics* 16.4 (Apr. 2020), pp. 836–845. ISSN: 2164-5515, 2164-554X. DOI: 10.1080/21645515.2019.1682843. URL: https://www.tandfonline.com/doi/full/10.1080/21645515.2019.1682843 (visited on 07/06/2022) (cit. on p. 77).

[193] Anna Miethke-Morais et al. "COVID-19-related hospital cost-outcome analysis: The impact of clinical and demographic factors". en. In: *The Brazilian Journal of Infectious Diseases* 25.4 (July 2021), p. 101609. ISSN: 14138670. DOI: 10.1016/j.bjid.2021.101609. URL: https://linkinghub.elsevier.com/retrieve/pii/S1413867021000787 (visited on 07/06/2022) (cit. on pp. 78, 97).

[194] Edson Zangiacomi Martinez, Davi Casale Aragon, and Altacílio Aparecido Nunes. "Long-term forecasts of the COVID-19 epidemic: a dangerous idea". en. In: *Revista da Sociedade Brasileira de Medicina Tropical* 53 (2020), e20200481. ISSN: 1678-9849, 0037-8682. DOI: 10.1590/0037-8682-0481-2020. URL: http://www.scielo.br/scielo.php?script=sci_arttext&pid=S0037-86822020000100658&tlng=en (visited on 07/06/2022) (cit. on p. 78).

[195] Jeffrey Shaman and Marta Galanti. "Will SARS-CoV-2 become endemic?" en. In: *Science* 370.6516 (Oct. 2020), pp. 527–529. ISSN: 0036-8075, 1095-9203. DOI: 10.1126/science.abe5960. URL: https://www.science.org/doi/10.1126/science.abe5960 (visited on 07/06/2022) (cit. on pp. 78, 79).

[196] Rm Stuart et al. *The role of masks in reducing the risk of new waves of COVID-19 in low transmission settings: a modeling study*. en. preprint. Sept. 2020. DOI: 10.1101/2020.09.02.20186742. URL: http://medrxiv.org/lookup/doi/10.1101/2020.09.02.20186742 (visited on 07/06/2022) (cit. on p. 79).

[197] Nicholas Lewin-Koh, Mark L. Taper, and Subhash R. Lele. "A brief tour of statistical concepts". In: *The Nature of Scientific Evidence*. Mark L. Taper and Subhash R. Lele, 2004. ISBN: 0-226-78957-8 (cit. on p. 80).

[198] Thomas Bayes. "LII. An essay towards solving a problem in the doctrine of chances. By the late Rev. Mr. Bayes, F. R. S. communicated by Mr. Price, in a letter to John Canton, A. M. F. R. S". In: *Philosophical Transactions of the Royal Society of London* 53 (Dec. 1763), pp. 370–418. ISSN: 0261-0523. DOI: 10.1098/rstl.1763.0053. URL: https://royalsocietypublishing.org/doi/10.1098/rstl.1763.0053 (cit. on p. 80).

[199] Andrew Gelman et al. *Bayesian Data Analysis*. 3rd ed. Chapman & Hall/CRC Texts in Statistical Science. Philadelphia, PA: Chapman & Hall/CRC, Nov. 2013 (cit. on pp. 82, 83).

[200] Matthew D Hoffman and Andrew Gelman. "The No-U-Turn Sampler: Adaptively Setting Path Lengths in Hamiltonian Monte Carlo". In: *J. Mach. Learn. Res.* 15.1 (Jan. 2014). Publisher: JMLR.org, pp. 1593–1623. ISSN: 1532-4435 (cit. on p. 84).

[201] Stan Development Team. *RStan: the R interface to Stan*. 2022. URL: https://mc-stan.org/ (cit. on p. 84).

[202] Håvard Rue, Sara Martino, and Nicolas Chopin. "Approximate Bayesian inference for latent Gaussian models by using integrated nested Laplace approximations". In: *Journal of the Royal Statistical Society. Series B: Statistical Methodology* 71.2 (2009), pp. 319–392. ISSN: 13697412. DOI: 10.1111/j.1467-9868.2008.00700.x (cit. on pp. 84–87, 93).

[203] Håvard Rue et al. "Bayesian Computing with INLA: A Review". en. In: *Annual Review of Statistics and Its Application* 4.1 (Mar. 2017), pp. 395–421. ISSN: 2326-8298, 2326-831X. DOI: 10.1146/annurev-statistics-060116-054045. URL: https://www.annualreviews.org/doi/10.1146/annurev-statistics-060116-054045 (visited on 07/08/2022) (cit. on pp. 84, 93).

[204] HÅvard Rue and Leonhard Held. *Gaussian Markov Random Fields: Theory and Applications*. Chapman and Hall/CRC, Feb. 2005 (cit. on p. 85).

[205] HÅvard Rue and Sara Martino. "Approximate Bayesian inference for hierarchical Gaussian Markov random field models". In: *Journal of Statistical Planning and Inference* 137.10 (2007), pp. 3177–3192. ISSN: 03783758. DOI: 10.1016/j.jspi.2006.07.016 (cit. on pp. 86, 87).

[206] Luke Tierney and Joseph B. Kadane. "Accurate Approximations for Posterior Moments and Marginal Densities". en. In: *Journal of the American Statistical Association* 81.393 (Mar. 1986), pp. 82–86. ISSN: 0162-1459, 1537-274X. DOI: 10.1080/01621459.1986.10478240. URL: http://www.tandfonline.com/doi/abs/10.1080/01621459.1986.10478240 (visited on 07/08/2022) (cit. on p. 87).

[207] Virgilio Gomez-Rubio. *Bayesian inference with INLA*. London, England: Taylor & Francis, Sept. 2021 (cit. on p. 87).

[208] Paula Moraga. *Geospatial health data*. Chapman & Hall/CRC Biostatistics Series. London, England: CRC Press, Nov. 2019 (cit. on p. 87).

[209] Leonardo Souto Ferreira et al. *Estimating the impact of implementation and timing of COVID-19 vaccination programme in Brazil: a counterfactual analysis*. en. preprint. Dec. 2021. DOI: 10.1101/2021.12.24.21268384. URL: http://medrxiv.org/lookup/doi/10.1101/2021.12.24.21268384 (visited on 07/12/2022) (cit. on p. 88).

[210] William Marciel de Souza et al. "Epidemiological and clinical characteristics of the COVID-19 epidemic in Brazil". In: *Nature Human Behaviour* 4.8 (2020). Publisher: Springer US, pp. 856–865. ISSN: 23973374. DOI: 10.1038/s41562-020-0928-4. URL: http://dx.doi.org/10.1038/s41562-020-0928-4 (cit. on p. 89).

[211] Felipe Naveca et al. "Phylogenetic relationship of SARS-CoV-2 sequences from Amazonas with emerging Brazilian variants harboring mutations E484K and N501Y in the Spike protein". In: *Virological* ~ (2021). URL: https://virological.org/t/phylogenetic-relationship-of-sars-cov-2-sequences-from-amazonas-with-emerging-brazilian-variants-harboring-mutations-e484k-and-n501y-in-the-spike-protein/585 (cit. on p. 89).

[212] Renata T.C. Yokota et al. "Risk factors for death from pandemic (H1N1) 2009, southern Brazil". In: *Emerging Infectious Diseases* 17.8 (2011), pp. 1467–1471. ISSN: 10806040. DOI: 10.3201/eid1708.101233 (cit. on pp. 90, 98, 99).

[213] Flávia C. Pacheco et al. "Decrease in the coverage of measles-containing vaccines and the risk of reestablishing endemic transmission of measles in Brazil". In: *International Journal of Infectious Diseases* 82 (2019), pp. 51–53. ISSN: 18783511. DOI: 10.1016/j.ijid.2019.03.014 (cit. on p. 90).

[214] Elize Massard da Fonseca, Kenneth C. Shadlen, and Francisco I. Bastos. "The politics of COVID-19 vaccination in middle-income countries: Lessons from Brazil". In: *Social Science and Medicine* 281.June (2021). Publisher: Elsevier Ltd, p. 114093. ISSN: 18735347. DOI: 10.1016/j.socscimed.2021.114093. URL: https://doi.org/10.1016/j.socscimed.2021.114093 (cit. on p. 90).

[215] Raquel Martins Lana et al. "Identificação de grupos prioritários para a vacinação contra COVID-19 no Brasil". In: *Cadernos de saude publica* 37.10 (2021), e00049821. ISSN: 16784464. DOI: 10.1590/0102-311X00049821 (cit. on p. 90).

[216] Rafael Izbicki et al. "How many hospitalizations has the covid-19 vaccination already prevented in são paulo?" In: *Clinics* 76 (2021), pp. 3–4. ISSN: 18075932. DOI: 10.6061/clinics/2021/e3250 (cit. on p. 90).

[217] Leonardo Soares Bastos et al. "COVID-19 and hospitalizations for SARI in Brazil: A comparison up to the 12th epidemiological week of 2020". In: *Cadernos de Saude Publica* 36.4 (2020), pp. 1–8. ISSN: 16784464. DOI: 10.1590/0102-311X00070120 (cit. on p. 91).

[218] R Core Team. *R: A Language and Environment for Statistical Computing*. Vienna, Austria, 2021. URL: https://www.R-project.org/ (cit. on p. 93).

[219] Ministério da Economia do Brasil. *Gastos da União com Combate à COVID-19*. 2021. URL: https://www.tesourotransparente.gov.br/visualizacao/painel-de-monitoramentos-dos-gastos-com-covid-19 (visited on 01/28/2022) (cit. on p. 97).

[220] M.Elizabeth Halloran et al. "Direct and Indirect Effects in Vaccine Efficacy and Effectiveness". In: *American Journal of Epidemiology* 133.4 (Feb. 1991), pp. 323–331. ISSN: 1476-6256. DOI: 10.1093/oxfordjournals.aje.a115884. URL: https://academic.oup.com/aje/article/166589/Direct (cit. on p. 98).

[221] Carla D.Scarbrough Lefebvre, Augustin Terlinden, and Baudouin Standaert. "Dissecting the indirect effects caused by vaccines into the basic elements". In: *Human Vaccines and Immunotherapeutics* 11.9 (2015), pp. 2142–2157. ISSN: 2164554X. DOI: 10.1080/21645515.2015.1052196 (cit. on p. 98).

[222] Susana Monge et al. "Direct and indirect eff ectiveness of mrna vaccination against severe acute respiratory syndrome coronavirus 2 in long-term care facilities, spain". In: *Emerging Infectious Diseases* 27.10 (2021), pp. 2595–2603. ISSN: 10806059. DOI: 10.3201/eid2710.211184 (cit. on p. 98).

[223] J. Baptista Risi. "The control of poliomyelitis in Brazil." In: *Reviews of Infectious Diseases* 6 Suppl 2.June (1984). ISSN: 01620886. DOI: 10.1093/clinids/6.supplement_2.s400 (cit. on p. 99).

[224] Jean Marc Olivé, Joao Baptista Risi, and Ciro A. De Quadros. "National immunization days: Experience in Latin America". In: *Journal of Infectious Diseases* 175.2 SUPPL. (1997), pp. 189–193. ISSN: 00221899. DOI: 10.1093/infdis/175.supplement_1.s189 (cit. on p. 99).

[225] Poliana de Oliveira Figueiredo et al. "Re-emergence of yellow fever in brazil during 2016–2019: Challenges, lessons learned, and perspectives". In: *Viruses* 12.11 (2020). ISSN: 19994915. DOI: 10.3390/v12111233 (cit. on p. 99).

[226] Governo do Estado de São Paulo. *Indígena de 8 anos que faz tratamento de saúde em SP é 1a. criança vacinada do Brasil*. 2022. URL: https://www.saopaulo.sp.gov.br/spnoticias/indigena-de-8-anos-que-faz-tratamento-de-saude-em-sp-e-1a-crianca-vacinada-do-brasil-2/ (visited on 01/14/2022) (cit. on p. 100).

[227] Ministério da Saúde. *Banco de dados do Sistema Único de Saúde - DATASUS. Informações de Saúde, Sistema de Informações sobre Mortalidade*. 2021. URL: http://tabnet.datasus.gov.br/cgi/tabcgi.exe?sim/cnv/obt10uf.def (visited on 12/21/2021) (cit. on p. 100).

[228] Rich FitzJohn and Wes Hinsley. *dde: Solve Delay Differential Equations*. 2020. URL: https://cran.r-project.org/package=dde (cit. on p. 105).

[229] Yongyue Wei et al. "A systematic review and meta-analysis reveals long and dispersive incubation period of COVID-19". In: *medRxiv* (2020), p. 2020.06.20.20134387. URL: https://doi.org/10.1101/2020.06.20.20134387 (cit. on pp. 105, 119).

[230] Muge Cevik et al. "SARS-CoV-2, SARS-CoV, and MERS-CoV viral load dynamics, duration of viral shedding, and infectiousness: a systematic review and meta-analysis". In: *The Lancet Microbe* 2.1 (2021). Publisher: The Author(s). Published by Elsevier Ltd. This is an Open Access article under the CC BY-NC-ND 4.0 license, e13–e22. ISSN: 26665247. DOI: 10.1016/S2666-5247(20)30172-5. URL: http://dx.doi.org/10.1016/S2666-5247(20)30172-5 (cit. on p. 105).

[231] Secretaria Municipal de Saúde - Município de São Paulo. *Inquérito sorológico para Sars-Cov-2: Prevalência da infecção em escolares das redes públicas e privada da cidade de São Paulo*. Tech. rep. 2021 (cit. on pp. 105, 119, 133).

[232] W. W. Sun et al. "Epidemiological characteristics of COVID-19 family clustering in Zhejiang Province". In: *Zhonghua yu fang yi xue za zhi [Chinese journal of preventive medicine]* 54.6 (2020), pp. 625–629. ISSN: 02539624. DOI: 10.3760/cma.j.cn112150-20200227-00199 (cit. on pp. 105, 119, 133).

[233] Henrik Salje et al. "Estimating the burden of SARS-CoV-2 in France". In: *Science* 369.6500 (July 2020), pp. 208–211. ISSN: 0036-8075. DOI: 10.1126/science.abc3517. URL: https://www.science.org/doi/10.1126/science.abc3517 (cit. on pp. 105, 119, 133).

[234] Tatiana Pineda Portella et al. "Temporal and geographical variation of COVID-19 in-hospital fatality rate in Brazil". In: *medRxiv* (2021), p. 2021.02.19.21251949. URL: https://www.medrxiv.org/content/10.1101/2021.02.19.21251949v1%0Ahttps://www.medrxiv.org/content/10.1101/2021.02.19.21251949v1.abstract (cit. on p. 105).

[235] Sheldon M. Ross. *Introduction to probability models*. Eleventh edition. Amsterdam ; Boston: Elsevier, 2014. ISBN: 978-0-12-407948-9 (cit. on p. 111).

[236] Ministério da Saúde. *Vacinas da COVID-19 disponíveis*. 2021. URL: https://web.archive.org/web/20210930213825/https://www.gov.br/saude/pt-br/vacinacao/ (visited on 09/30/2021) (cit. on p. 117).

[237] Sharifa Nasreen et al. *Effectiveness of mRNA and ChAdOx1 COVID-19 vaccines against symptomatic SARS-CoV-2 infection and severe outcomes with variants of concern in Ontario*. en. preprint. Public and Global Health, July 2021. DOI: 10.1101/2021.06.28.21259420. URL: http://medrxiv.org/lookup/doi/10.1101/2021.06.28.21259420 (visited on 07/04/2022) (cit. on p. 118).

[238] Matt D. T. Hitchings et al. "Effectiveness of ChAdOx1 vaccine in older adults during SARS-CoV-2 Gamma variant circulation in São Paulo". en. In: *Nature Communications* 12.1 (Dec. 2021), p. 6220. ISSN: 2041-1723. DOI: 10.1038/s41467-021-26459-6. URL: https://www.nature.com/articles/s41467-021-26459-6 (visited on 07/04/2022) (cit. on p. 118).

[239] Hal Caswell. *Matrix population models*. Vol. 1. Sinauer Sunderland, MA, 2000 (cit. on p. 131).

[240] Nicolò Gozzi et al. *Preliminary modeling estimates of the relative transmissibility and immune escape of the Omicron SARS-CoV-2 variant of concern in South Africa*. en. preprint. Jan. 2022. DOI: 10.1101/2022.01.04.22268721. URL: http://medrxiv.org/lookup/doi/10.1101/2022.01.04.22268721 (visited on 07/07/2022) (cit. on p. 133).

[241] Katrina J. Spensley et al. "Comparison of Vaccine Effectiveness Against the Omicron (B.1.1.529) Variant in Hemodialysis Patients". en. In: *Kidney International Reports* 7.6 (June 2022), pp. 1406–1409. ISSN: 24680249. DOI: 10.1016/j.ekir.2022.04.005. URL: https://linkinghub.elsevier.com/retrieve/pii/S246802492201261X (visited on 07/07/2022) (cit. on pp. 134, 136).

[242] A Hogan et al. *Report 48: The value of vaccine booster doses to mitigate the global impact of the Omicron SARS-CoV-2 variant*. en. Tech. rep. Imperial College London, Dec. 2021. DOI: 10.25561/93034. URL: http://spiral.imperial.ac.uk/handle/10044/1/93034 (visited on 07/07/2022) (cit. on pp. 134, 136).

[243] Stijn P. Andeweg et al. *Protection of COVID-19 vaccination and previous infection against Omicron BA.1, BA.2 and Delta SARS-CoV-2 infections*. en. preprint. Epidemiology, Feb. 2022. DOI: 10.1101/2022.02.06.22270457. URL: http://medrxiv.org/lookup/doi/10.1101/2022.02.06.22270457 (visited on 07/07/2022) (cit. on p. 134).

[244] Christian Holm Hansen et al. *Vaccine effectiveness against SARS-CoV-2 infection with the Omicron or Delta variants following a two-dose or booster BNT162b2 or mRNA-1273 vaccination series: A Danish cohort study*. en. preprint. Dec. 2021. DOI: 10.1101/2021.12.20.21267966. URL: http://medrxiv.org/lookup/doi/10.1101/2021.12.20.21267966 (visited on 07/07/2022) (cit. on p. 134).

[245] Laith J. Abu-Raddad et al. "Effect of mRNA Vaccine Boosters against SARS-CoV-2 Omicron Infection in Qatar". en. In: *New England Journal of Medicine* 386.19 (May 2022), pp. 1804–1816. ISSN: 0028-4793, 1533-4406. DOI: 10.1056/NEJMoa2200797. URL: http://www.nejm.org/doi/10.1056/NEJMoa2200797 (visited on 07/07/2022) (cit. on pp. 134, 135).

[246] Emma K. Accorsi et al. "Association Between 3 Doses of mRNA COVID-19 Vaccine and Symptomatic Infection Caused by the SARS-CoV-2 Omicron and Delta Variants". en. In: *JAMA* 327.7 (Feb. 2022), p. 639. ISSN: 0098-7484. DOI: 10.1001/jama.2022.0470. URL: https://jamanetwork.com/journals/jama/fullarticle/2788485 (visited on 07/07/2022) (cit. on p. 134).

[247] Hiam Chemaitelly et al. *Duration of mRNA vaccine protection against SARS-CoV-2 Omicron BA.1 and BA.2 subvariants in Qatar*. en. preprint. Mar. 2022. DOI: 10.1101/2022.03.13.22272308. URL: http://medrxiv.org/lookup/doi/10.1101/2022.03.13.22272308 (visited on 07/07/2022) (cit. on p. 135).

[248] Sarah A. Buchan et al. *Effectiveness of COVID-19 vaccines against Omicron or Delta symptomatic infection and severe outcomes*. en. preprint. Jan. 2022. DOI: 10.1101/2021.12.30.21268565. URL: http://medrxiv.org/lookup/doi/10.1101/2021.12.30.21268565 (visited on 07/07/2022) (cit. on p. 135).

[249] UK Health Security Agency. *COVID-19 vaccine surveillance report, Week 5, 3 February 2022*. Tech. rep. 2022. URL: https://assets.publishing.service.gov.uk/government/uploads/system/uploads/attachment_

data/file/1052353/Vaccine_surveillance_report_-_week_5.pdf (visited on 02/03/2022) (cit. on pp. 135, 136).

[250] Jill M. Ferdinands et al. "Waning 2-Dose and 3-Dose Effectiveness of mRNA Vaccines Against COVID-19–Associated Emergency Department and Urgent Care Encounters and Hospitalizations Among Adults During Periods of Delta and Omicron Variant Predominance — VISION Network, 10 States, August 2021–January 2022". en. In: *MMWR. Morbidity and Mortality Weekly Report* 71.7 (Feb. 2022), pp. 255–263. ISSN: 0149-2195, 1545-861X. DOI: 10.15585/mmwr.mm7107e2. URL: http://www.cdc.gov/mmwr/volumes/71/wr/mm7107e2.htm?s_cid=mm7107e2_w (visited on 07/07/2022) (cit. on p. 136).

[251] Adam S. Lauring et al. *Clinical Severity and mRNA Vaccine Effectiveness for Omicron, Delta, and Alpha SARS-CoV-2 Variants in the United States: A Prospective Observational Study*. en. preprint. Feb. 2022. DOI: 10.1101/2022.02.06.22270558. URL: http://medrxiv.org/lookup/doi/10.1101/2022.02.06.22270558 (visited on 07/07/2022) (cit. on p. 136).

[252] Mark G. Thompson et al. "Effectiveness of a Third Dose of mRNA Vaccines Against COVID-19–Associated Emergency Department and Urgent Care Encounters and Hospitalizations Among Adults During Periods of Delta and Omicron Variant Predominance — VISION Network, 10 States, August 2021–January 2022". en. In: *MMWR. Morbidity and Mortality Weekly Report* 71.4 (Jan. 2022), pp. 139–145. ISSN: 0149-2195, 1545-861X. DOI: 10.15585/mmwr.mm7104e3. URL: http://www.cdc.gov/mmwr/volumes/71/wr/mm7104e3.htm?s_cid=mm7104e3_w (visited on 07/07/2022) (cit. on p. 136).

[253] Shirley Collie et al. "Effectiveness of BNT162b2 Vaccine against Omicron Variant in South Africa". en. In: *New England Journal of Medicine* 386.5 (Feb. 2022), pp. 494–496. ISSN: 0028-4793, 1533-4406. DOI: 10.1056/NEJMc2119270. URL: http://www.nejm.org/doi/10.1056/NEJMc2119270 (visited on 07/07/2022) (cit. on p. 136).

[254] Sara Y Tartof et al. "Durability of BNT162b2 vaccine against hospital and emergency department admissions due to the omicron and delta variants in a large health system in the USA: a test-negative case–control study". en. In: *The Lancet Respiratory Medicine* 10.7 (July 2022), pp. 689–699. ISSN:

22132600. DOI: 10.1016/S2213-2600(22)00101-1. URL: https://linkinghub.elsevier.com/retrieve/pii/S2213260022001011 (visited on 07/07/2022) (cit. on p. 136).